TESE DE DOUTORAMENTO

PRECIPITATION RECYCLING AND THE IMPORTANCE OF THE LAND-ATMOSPHERE INTERACTIONS OVER THE EUROPEAN CONTINENT

Sabela Regueiro Sanfiz

ESCOLA DE DOUTORAMENTO INTERNACIONAL

PROGRAMA DE DOUTORAMENTO EN ENERXÍAS RENOVABLES E SUSTENTABILIDADE ENERXÉTICA

SANTIAGO DE COMPOSTELA

2020

USC
UNIVERSIDADE
DE SANTIAGO
DE COMPOSTELA

DECLARACIÓN DO AUTOR/A DA TESE

Precipitation recycling and the importance of the land-atmosphere interactions over the European continent.

Dna Sabela Regueiro Sanfiz

Presento a miña tese, seguindo o procedemento axeitado ao Regulamento, e declaro que:

1) A tese abarca os resultados da elaboración do meu traballo.
2) De selo caso, na tese faise referencia ás colaboracións que tivo este traballo.
3) A tese é a versión definitiva presentada para a súa defensa e coincide coa versión enviada en formato electrónico.
4) Confirmo que a tese non incorre en ningún tipo de plaxio doutros autores nin de traballos presentados por min para a obtención doutros títulos.

En Santiago de Compostela, 24 de Febreiro de 2020

Asdo Sabela Regueiro Sanfiz

USC
UNIVERSIDADE
DE SANTIAGO
DE COMPOSTELA

AUTORIZACIÓN DO DIRECTOR / TITOR DA TESE

Precipitation recycling and the importance of the land-atmosphere interactions over the European continent.

D. Gonzalo Míguez Macho

INFORMA/N:

Que a presente tese, correspóndese co traballo realizado por Dna. Sabela Regueiro Sanfiz, baixo a miña dirección, e autorizo a súa presentación, considerando que reúne os requisitos esixidos no Regulamento de Estudos de Doutoramento da USC, e que como director desta non incorre nas causas de abstención establecidas na Lei 40/2015.

En Santiago de Compostela, 24 de Febreiro de 2020

Asdo Gonzalo Míguez Macho

USC
UNIVERSIDADE
DE SANTIAGO
DE COMPOSTELA

Aos meus pais, María Isabel e Ramón

USC
UNIVERSIDADE
DE SANTIAGO
DE COMPOSTELA

“They told me it was totally inappropriate for a woman to be a meteorologist”

Joanne Simpson, née Gerould

The first woman in the United States to receive a PhD in Meteorology

USC
UNIVERSIDADE
DE SANTIAGO
DE COMPOSTELA

Contents

Acknowledgments **15**

Summary **17**

Preface **21**

1 Introduction and State of the Art **29**
1.1 The Water Cycle: Precipitation and Evapotranspiration 30
1.2 Water Recycling 32
1.2.1 Review of the Recycling Computation Methods 32
1.2.2 Indirect Recycling or Amplification Processes 37
1.3 The Role of Groundwater 39
1.3.1 The Water Table and Soil Moisture 40
1.3.2 A Short Review of the Land Surface Models 41
1.4 Climates in the Areas of Study 43
1.4.1 Iberian Peninsula Climate 43
1.4.2 European Climate 47
1.5 Climate modelling 51

2 Objectives and Structure of this Thesis **53**

3 Methodology **55**
3.1 The WRF model. Setup of Numerical Experiments 56
3.1.1 First WRF Simulations Setup 57
3.1.2 Second WRF Simulations Setup 59
3.1.3 Third WRF Simulations Setup 59
3.2 Bulk Precipitation Recycling Models 64
3.2.1 Numerical Recycling Model: Eltahir and Bras (1994) 67
3.2.2 Analytical Recycling Model: Schär et al. (1999) 69
3.2.3 Dynamical Recycling Model: Dominguez et al. (2006) 70
3.3 Water Vapour Tracers Method (WVTM) 72
3.4 Relative Change in Precipitation 78
3.5 WRF-LEAFHYDRO Land-Atmospheric Model 79
3.5.1 LEAFHYDRO Land Surface Model 79
3.5.2 Coupling LEAFHYDRO to WRF 82

4 A Study with a Water Vapour Tracer Method **85**
4.1 Vertical Structure of the Tagged Moisture Field . . . 86
4.2 Daily Moisture Cycle . . . 91
4.3 Precipitation and Recycling Interannual Variability . . . 94
4.4 Spatial Distribution of the Moisture . . . 98
4.5 Comparison between WVTM and Bulk Recycling Models . . . 104
4.6 Conclusions Chapter 4 . . . 111

5 A Study of the Amplification Processes in the Iberian Peninsula **115**
5.1 The Impact of ET Fluxes in Spring Precipitation . . . 116
5.1.1 Precipitation interannual Variability . . . 116
5.1.2 Diurnal Cycle . . . 122
5.2 Recycling or Amplification of Precipitation Dynamics . . . 124
5.3 Conclusions Chapter 5 . . . 126

6 A Study of the European Climate with a Coupled Land-Atmospheric Model **129**
6.1 The Dynamic Water Table . . . 130
6.1.1 Spatial and Seasonal Variability of the European Water Table Depth . . . 130
6.1.2 Impact of the Water Table on the Soil Wetness . . . 134
6.2 Influence of the Water Table on the Atmospheric Forcings . . . 138
6.2.1 Enhanced Evapotranspiration . . . 138
6.2.2 Effects on Temperatures . . . 141
6.2.3 Effects on Precipitation . . . 153
6.3 Conclusions Chapter 6 . . . 159

7 General Conclusions **163**

Long Summary in Galician **167**

List of Figures **177**

List of Tables **179**

List of Acronyms **181**

Bibliography **183**

Related Publications **195**

USC
UNIVERSIDADE
DE SANTIAGO
DE COMPOSTELA

USC
UNIVERSIDADE
DE SANTIAGO
DE COMPOSTELA

Acknowledgments

En primer lugar, muchas gracias a Gonzalo Míguez Macho, el director de esta tesis. Gracias por la dirección de este trabajo, por el trato cercano y por sus brillantes aportaciones. Pero sobre todo, gracias por haberme dado esta oportunidad, que considero tan valiosa.

Quero exprimir o meu sincero agradecimento aos professores Rita M. Cardoso e Pedro M. Matos Soares, baixo a sua supervisão realizei um estágio de cinco meses no Instituto Dom Luiz da Universidade de Lisboa. Muito obrigada pelo caloroso acolhimento no seu bonito país.

Gracias a Breogán Gómez del Met Office y a Pedro Soares de la Universidad de Lisboa, por su labor como revisores, que ha contribuído a la obtención de la mención internacional.

Gracias al Centro de Supercomputación de Galicia por el soporte técnico y computacional. Gracias al proyecto Earth2Observe por haber financiado esta tesis durante tres años.

Gracias a los profesores y compañeros del Grupo de Física No Lineal, he aprendido mucho de todos ellos. Gracias a Dani, por su buena disposición y ayuda. Muchisisímas gracias a Miguel Prósper, por haber sido un súper compañero de doctorado, pero lo que es mucho más importante, gracias por ser un amigo insuperable.

Gracias a todos mis compañeros de Meteogalicia y al coordinador de numérico Juan Taboada, por su buena acogida. Gracias en especial a Swen Brands, por sus valiosos consejos de experto en clima y por su constante ayuda.

Grazas ás tres mulleres bravas que fixeron correccións linguísticas nesta tese: María Isabel Sanfiz Pena (castelán), Merche Espiño Amil (galego), Lucía Puebla González (inglés).

Grazas aos amigos, á familia Regueiro e á familia Sanfiz-Penilla.

Mil millóns de grazas aos verdadeiros artífices desta tese, Ramón e María Isabel, meus pais. Grazas polo voso apoio e pola vosa comprensión. Grazas por ser familia, refuxio e enorme exemplo. Grazas por axudarme a facer maletas, primeiro rumbo a Lisboa e despois a Londres, pero sobre todo grazas por terdes sido partícipes nas dúas aventuras. Isto nunca tería sido bonito nin posíbel sen vós.

USC
UNIVERSIDADE
DE SANTIAGO
DE COMPOSTELA

Short Summaries in English, Galician and Spanish

Summary in English

The experimental motivation of this thesis is to improve the knowledge and understanding of the climatic system, through the study of land-atmosphere interactions. We mainly, focus on the fundamental role played by the moisture coming from the evapotranspiration terrestrial fluxes on the atmospheric forcings. We intend to investigate in detail the precipitation recycling processes over some areas of the European continent.

Currently, atmospheric models represent the most accurate technique to forecast the meteorological conditions or to reconstruct the past climatic conditions. For that reason, in this thesis, we employ as a primary tool the widely known regional meteorological model WRF-ARW. A new water vapour tagging technique has been embedded in the model, allowing us to track the evapotranspired moisture from a source region. With this methodology, we can quantify the intensity of the recycling processes in any area of the planet. We compare the recycling values obtained with the tagging technique with those obtained with classic recycling models. To better understand the precipitation regime over the Iberian Peninsula, we have employed a method able to quantify the contribution of the indirect or amplification precipitation processes. Furthermore in this research, LEAFHYDRO Land Surface Model is used, coupled to the atmospheric model WRF. LEAFHYDRO includes a groundwater parameterisation fully coupling the water table to the soil-vegetation and surface waters via two-way fluxes and, it calculates river routing and discharges.

The water vapour tracer method allows us to obtain a more detailed picture of the European water cycle. The results obtained with this technique suggests that moisture from local evapotranspiration is often not well-mixed throughout the atmospheric column, varying through the day and with the synoptic situation. The recycling values obtained with classical models are not able to reflect the temporal variations with the same accuracy as the tagging technique, because they do not show the seasonal or daily changes, tending to overestimate or underestimate the results.

The results of this investigation show the impact on the climatic system of using a fully coupled hydrology-atmospheric modelling system. The role of the water table in controlling soil moisture during the growing season in Europe is very significant. At long timescales, the groundwater induces a buffering effect on soil moisture in regions with a relatively shallow water table. We also show that enhanced evapotranspiration due to the presence of more soil wetness affects atmospheric forcings, like temperature and precipitation.

Summary in Galician (Resumo)

A motivación experimental desta tese é a de mellorar o entendimento do sistema climático a través do estudo das interaccións terra-atmosfera. Centrámonos principalmente no rol que xoga a humidade que provén dos fluxos de evapotranspiración terrestres nos forzamentos atmosféricos. Preténdese investigar en detalle os procesos de reciclaxe de precipitación nalgunhas áreas do continente europeo.

Os modelos atmosféricos representan hoxe en día unha das técnicas máis precisas para predicir as condicións meteorolóxicas ou reconstruír o clima pasado. Por iso aquí empregamos como ferramenta principal o coñecido modelo meteorolóxico rexional WRF-ARW. Introduciuse unha innovadora técnica de etiquetado de vapor de agua, que nos permite seguir a humidade evapotranspirada dunha rexión fonte. Con esta metodoloxía é posíbel cuantificar a intensidade dos procesos de reciclaxe en calquera área do planeta. Comparamos os resultados obtidos con esta técnica cos dos modelos clásicos de reciclaxe. Para comprender mellor o réxime de precipitacións sobre a Península Ibérica, utilizamos un método que permite cuantificar a contribución dos procesos indirectos ou de amplificación da precipitación. Ademais desta investigación, emprégase o modelo de solos LEAFHYDRO acoplado ao modelo atmosférico WRF. LEAFHYDRO inclúe unha parametrización das augas subterráneas que une completamente a capa freática á vexetación do solo e ás augas subterráneas a través dos fluxos, e ademais ten en conta os leitos e desembocaduras fluviais.

O método de trazadores permitiunos obter unha representación detallada do ciclo hidrolóxico en Europa. Os resultados acadados con esta técnica suxiren que a humidade que provén da evapotranspiración local a miúdo non está ben mesturada ao longo da columna atmosférica, variando ao longo do día e coa situación sinóptica. Os valores de reciclaxe obtidos cos modelos clásicos non son capaces de reflectir as variacións temporais coa mesma precisión que a técnica dos trazadores, porque non amosan as variacións estacionais ou diarias, e acostuman sobrevalorar ou infravalorar os resultados.

As conclusións desta investigación amosan o impacto que supón o empregar un modelo que acopla totalmente hidroloxía e atmosfera no sistema climático. O rol da capa freática, controlando a humidade do solo durante a temporada de crecemento das plantas, é moi significativo. En escalas temporais grandes, as augas subterráneas inducen un efecto coador nas rexións en que a capa freática é superficial. Mostramos tamén como unha evapotranspiración incrementada debido á humidade do solo afecta os forzamentos atmosféricos, como a temperatura e humidade.

Summary in Spanish (Resumen)

La motivación experimental de esta tesis es la de mejorar el conocimiento y entendimiento del sistema climático, a través del estudio de las interacciones tierra-atmósfera. Para ello nos hemos centrado principalmente en el rol que juega la humedad proveniente de los flujos de evapotranspiración terrestres en los forzamientos atmosféricos. Se pretende investigar en detalle los procesos de reciclaje de precipitación en algunas áreas del continente europeo.

Los modelos atmosféricos representan en la actualidad una de las técnicas más precisas para predecir las condiciones meteorológicas o reconstruir el clima pasado. Por ello en esta tesis, hemos empleado como herramienta principal el conocido modelo meteorológico regional WRF-ARW. Además se ha introducido en el modelo una innovadora técnica de etiquetado de vapor de agua, que nos permite seguir la humedad evapotranspirada de una seguir fuente hasta que sale del dominio o precipita. Esta metodología posibilita la cuantificación de la intensidad de los procesos de reciclaje en cualquier área del planeta. Los resultados obtenidos con esta técnica se han comparado con los obtenidos con los modelos clásicos de reciclaje. Para comprender mejor el régimen de precipitaciones sobre la Península Ibérica, hemos empleado un método capaz de cuantificar la contribución de los procesos de precipitación indirectos o de amplificación. Además en esta investigación, se ha empleado el modelo de suelo LEAFHYDRO, acoplado al modelo atmosférico WRF. LEAFHYDRO incluye una parametrización de aguas subterráneas, que acopla completamente la capa freática a la vegetación del suelo y a las aguas superficiales a través de flujos y calcula los cauces y desembocaduras de los ríos.

El método de trazadores nos ha permitido obtener una representación detallada del ciclo hidrológico europeo. Los resultados obtenidos con esta técnica, sugieren que la humedad proveniente de la evapotranspiración local, a menudo, no está bien mezclada a lo largo de la columna atmosférica, variando a lo largo del día y con la situación sinóptica. Los valores de reciclaje obtenidos con los modelos clásicos, no son capaces de reflejar las variaciones temporales con la misma precisión que la técnica de trazadores, ya que no muestran las variaciones estacionales o diarias, y tienden a sobreestimar o infraestimar los resultados.

Las conclusiones de esta investigación muestran el impacto en el sistema climático de usar un modelo completamente acoplado tierra-atmósfera. El rol de la capa freática de controlar la humedad del suelo durante la temporada de crecimiento de las plantas es muy significativo. En escalas temporales grandes, las aguas subterráneas inducen un efecto colador en las regiones en las que la capa freática es relativamente poco profunda. Mostramos también una evapotranspiración incrementada debido a la demás humedad en el suelo, afecta los forzamientos atmosféricos, como la temperatura y la precipitación.

USC
UNIVERSIDADE
DE SANTIAGO
DE COMPOSTELA

Preface

This PhD dissertation is focused on the study of atmospheric sciences. However, the reader should not be surprised if in the following pages, corresponding to the preface, she or he finds a historical overview, that initially might seem to be wholly separate from the main topic of the thesis.
We believe that first, it is necessary to take a look at the past and to acquaint ourselves with the achievements, scientific contributions and lives of some pioneer climatologists, meteorologists and scientists of the last two centuries. Most of them had to overcome exceptional circumstances during difficult times in history, and yet, they made incredible contributions to meteorology and science. The work of these scientists contributed and promoted the development of the atmospheric sciences as we know it today. For this reason, we believe the lives and works of these prominent scientists should be known to any person interested in, or conversant with, atmospheric sciences.

We would like to begin by referring to the life and achievements of an American scientist called ***Eunice Newton Foote***. In 1856, she presented the results of a simple experiment at the annual meeting of the American Association for the Advancement of Science. Because she was a woman, she was not allowed to present her own work "Circumstances Affecting the Heat of the Sun's Rays" (Foote 1856). This work reported the results of an experiment whose primary purpose was to study the response of different types of gases after being heated. To that end, Newton Foote filled up glass containers with various gases and exposed them to the sun's heating effect. Her results showed that the carbonic acid gas, later named carbon dioxide or CO2, heated up faster than any other gas. She even speculated that owing to the heat-trapping properties of the CO2, if there were more of this gas in the atmosphere, the earth temperature would be warmer.
At the time that Eunice carried out her experiment, average CO2 levels were about 290 parts per million in the atmosphere. She probably would never have imagined that by 2016, they would be at the blood-curdling rate of approximately 400 parts per million. Her conclusions could have been the basis for the discovery of the actual theory about the harmful greenhouse effect resulting from increased CO2 emissions. Her work goes unnoticed because it was never published. Three years later the famous Irish physicist John Tyndall published similar results, demonstrating the greenhouse effect in some particular gases, including the carbonic acid gas. Consequently, he took the credit for this groundbreaking discovery, and he is usually recognised as the first person to prove the greenhouse effect. In contrast, Newton Foote was not recognised as such.
Despite her unacknowledged finding of the role of CO2 in the Earth's greenhouse effect, Eunice Newton Foote is known for her research in physics and chemistry, and for inventing and patenting several discoveries. She also took part in the so-called Seneca Falls convention, a congress in

which several American illustrated persons came together to discuss and fight for women's rights.

Ten years after the death of Eunice Newton Foote, a child who was meant to be the very first woman in AEMET, the Spanish national weather service, was born. ***Felisa Martín Bravo*** (1898-1979) was not only one of the first female meteorologists in Spain but also the first woman to earn a PhD in physics in the country. As a result of her PhD thesis, she published the first paper about crystallography written in Spanish.

Like many other physicists of her generation, Dr Martín Bravo took the Spanish public examinations to enter AEMET. In 1931, when she passed the exams, she became the first Spanish female meteorologist, and the only one until 1935. Felisa worked as an assistant during her early years in the weather agency, and she even obtained a fellowship from AEMET to study for a short period at Cambridge University. There, she had the chance to collaborate with the renowned scientist Charles Thomson Rees Wilson, who had won the Nobel Prize for Physics in 1927 for his invention of the cloud chamber. Felisa came back to Spain in 1934, and she worked at AEMET until the Spanish civil war began in 1936.

The Spanish war meant a significant and sad turning point in the course of Spanish science, and of course in the career paths of the majority of the scientists and professors. Unfortunately, for so many young female scientists, the war led to the end of their professional careers. Felisa was luckier than others, and the civil war only caused a halt of a few years in her working life at AEMET. Still, it took some years for this to happen, and in the meantime, Felisa kept trying to research and work in the field of Atmospheric Sciences.

From 1937 to 1940, Felisa was hired as a director of the Igeldo Meteorological Observatory, located in the north of Spain. There she focused her research in the study of the atmospheric event named "Galernas", this is a sudden and violent thunderstorm occurring in a small area of the northern coast of the Iberian Peninsula.

At the end of the military conflict, a dictatorial political regime was established in Spain, and the new government embarked on a tough adjustment and reform programme of the ministries and governmental agencies. Because of these changes, AEMET was attached to the Spanish Air Force. Within this political environment, all the civil servants (which included the meteorologists of AEMET) were purge, to prove their loyalty to the new dictatorial regime. Not to have demonstrated their affinity with the new government caused a temporary or definitive disqualification of their employment. Furthermore, throughout the dictatorship period, women were forbidden to work at any governmental service. Only those who had obtained their jobs in previous years to the war were allowed to keep their positions. Felisa Martín Bravo was one of the lucky few, and she was allowed to rejoin the weather agency, becoming one of only six women employed in AEMET until the sixties. Between 1973 and 1974 she acted as president of the Spanish Association of Meteorology, another first for a woman.

The biography of Felisa Martín Bravo is brilliant in its first pages, but from the end of the Spanish war onward there is barely any information about her. What is known is that she was promoted in AEMET, reaching the highest professional category and that she spent the rest of her working life in the national weather service. This pioneering meteorologist passed away on October 29th, 1979, in Madrid.

Five were the Spanish women that follow Felisa Martín Bravo in joining the Spanish Meteorological Service. Mercè Potau Gili, Josefina Ricart, Antonia Roldán Fernández, Maria Cristina González Pintor and Pilar Martínez Díez-Canedo entered the agency in the class of 1935. All these women were part of AEMET in the years before the war and, luckily, they were allowed to rejoin the agency after the military action. There is a lack of information about their career paths after the war; still, some details are known.

Antonia Roldán rejoined AEMET in 1941, and she pursued her professional career in the Climatology Department. She carried out several studies that gave rise to publications about climate. In 1973, she became the oldest member of AEMET, and she kept working until she retired in 1982.

Mercè Potau Gili was born in Spain in 1912, and she took the second position in the national exams to join AEMET as an assistant meteorologist in 1935. She worked in the agency from the end of the war until 1955. Then, she rejoined the service for one year in 1981. Besides this, Mercè did the translations from foreign languages to Spanish of several physics books. She passed away in 2005.

Josefina Ricar Sau was a Catalan meteorologist born in 1913. She worked in AEMET from 1939 to 1942 only. Her name is very closely linked to her husband's, who was a renowned professor of Atmospheric Sciences at the University of Barcelona. The Spanish Weather Service honoured both of them for their work in the field of meteorology.

Cristina González Pintor was the last member from this group of pioneering Spanish meteorologists. Unlike her colleagues, who held bachelors in Science, Cristina was one of the first women architecture graduates in Spain, she never was employed as an architect. As an AEMET meteorologist, she worked in Seville and in Santander, where she was promoted as head of the centre. And in 1966, she passed her exams to obtain the highest category within the agency. Cristina González Pintor passed away in 2005.

Whereas these meteorologists were shaping the future for the science Spain, on the other side of the world, another outstanding woman was making history. Her name was ***Jean Elizabeth Laby***, and she was born in Australia in 1915. Laby grew up surrounded by science as her father was a professor at the University of Melbourne. He used to take his daughters to the laboratories at the university, and teach them physics. Hence, it was no unusual that Jean Laby, who had grown up loving physics and maths, decided to dedicate her life to them. After graduating from Melbourne Girls' Grammar, she earned a Bachelor in Physics at the University of Melbourne. After that, she obtained a position as a weather observer at the Bureau of Meteorology (the weather Agency of the Australian Government), but the Second World War truncated her plans, and she couldn't take up the post. Young Australian physicists were requested by the Government to produce optical instruments for the armed forces, and the majority of them were employed by the Optical Munitions Panel, whose chairman was coincidentally Laby's father. For this reason, there was a lack of employees at the Department of Natural Philosophy at the University of Melbourne, later Department of Physics, and Jean Laby was hired there as a part-time demonstrator in 1940. She worked at this department for more than forty years. Between 1944 and 1959, she was promoted to senior demonstrator, and during that time, she was awarded a master degree. In 1959, she became the first woman to obtain a PhD in Physics in Australia. Her research was mainly focused on the study of cosmic rays at balloon altitudes and atmospheric winds. Dr Laby was a pioneer in the study of atmospheric aerosols, ozone, and water vapour in the stratosphere, collaborating during some years in the Climatic Impact Assessment Program.

In 2009, one year after she passed away, Laby was inducted into the Victorian Honour Roll of Women. She is considered as an honorary member of the University of Melbourne and as an admirable example of a female scientist.

Anna Mani was born in India in 1918, thus she was contemporary to Dr Laby and Dr Martín Bravo. Mrs Mani was Indian, for that reason her life was very different from that of her Australian and Spanish colleagues. When Anna Mani was just a kid, Gandhi visited her hometown, and she was so impressed that from that point forward, she only wore khadi. From a very early age, Mani started to read, and at the age of twenty-one, she had already graduated with a Bachelor Science in Physics and Chemistry, and she obtained the highest honours. In 1940, she won a scholarship from the Indian Institute of Science, in Bangalore, thus beginning her scientific career. From that point until 1945, she carried out her research on spectroscopy of diamonds and rubies, writing several papers about her investigations in that field. In 1945, she submitted a PhD dissertation in spectroscopy to the Madras University in India, since she lacked a master's degree, the university denied her the PhD degree. That same year, she got a scholarship from the Indian Government to study at Imperial College London, and Mani moved to the UK, where she studied a bachelor in physics, specialising in meteorological instruments. After having obtained this second bachelor, Mani returned to her home country and joined the Indian Meteorological Department. In those days, all the weather instruments were imported to India, mainly from England. Anna Mani used her knowledge in meteorology to try to produce Indian weather instruments and make her country self-sufficient. In the sixties, she became interested in the study of ozone gas, which at that point was not a subject of research by the scientific community. Ozone gas was understood as a tracer gas to study the general atmospheric circulation, and not as a gas that in high concentrations in the atmosphere could be dangerous to human life on the Earth. It is worth briefly describing ozone gas, as it is currently understood. Ozone is a gas naturally occurring in the upper atmosphere, approximately between 15 and 30 kilometres above sea level; this layer is referred to as the ozone layer. Ozone at this altitude acts as a shield, preventing the Sun's ultraviolet radiation from reaching the Earth's surface. Direct contact with ozone with people or animals is damaging. The ozone is a shield which protects humans and the biosphere. But the ozone in the atmosphere is not always beneficial for life. High concentrations of this gas in the lower atmosphere can cause harmful effects on the health of people and animals. Furthermore, ozone does not occur naturally in the troposphere; it comes from the human's industrial activity. Mani developed the first Indian ozonesonde and published several articles about the ozone gas in the atmosphere. She dedicated a large part of her life to the study of the atmosphere.

Edith Elizabeth Farkas was born in 1921 in Hungary. She is best known for being the first woman to work at the Meteorological Service of New Zealand (MetService - Te Ratonga Tirorangi). During the Second World War, Farkas and her family had to flee across Europe from Hungary. Finally, in 1949, with the end of the war, they emigrated to the other side of the world, New Zealand, where they were hosted as Hungarian refugees. Despite Farkas holding Hungarian university degrees, her qualifications were not recognised in New Zealand, and she had to return to university. What is even more impressive about Farkas, is that she had to learn English when she arrived in her new country, because she had no formal training in this language. Despite this drawback, she was able to obtain a Master degree and a job just a few years later. In 1951, she began her professional career as a meteorologist at the MetService, where she worked for more

than thirty-five years until she retired. Like her contemporary colleague Anna Mani, Farkas's research was focused on the study of atmospheric ozone gas. She conducted world-leading ozone monitoring investigations for over thirty years. In the sixties, her research was focused on the measurement of total ozone, particularly with the Dobson ozone spectrophotometer. In 1975, Farkas set foot on the Antarctic ice as the first Hungarian woman and the first female member of the MetService to do so, and she was one of the first women to study Antarctica. Upon her retirement, she received the Metservice Henry Hill Award, recognising her dedication and enthusiasm.

If we continue with this trip through the history of meteorology, we find the surname Simpson, that the reader might know because of the Saffir–Simpson hurricane scale. This scale was defined by the engineer Herbert Saffir and the meteorologist Robert Simpson, who at the time was director of the United States National Hurricane Center. Despite the great achievements of Robert Simpson in the field of atmospheric science, this surname also must be remembered because of his wife: ***Joanne Simpson***, née Joanne Malkus, born Joanne Gerould. She was born in Boston, Massachusetts, in 1923. From childhood on, she was fascinated by clouds; still, when she entered the University of Chicago, her specialization was in astrophysics. She never dedicated her life to the study of the stars, because the Second World War changed her plans (the reader may have noticed that throughout this preface, WWII has already truncated many schemes of life). Simpson had studied courses in meteorology; hence she was called by the government to be a teacher in the training of aviation cadets of the United States army. Like Simpson, another fifty women were required to teach meteorology, and they had to carry out this job during the war. But unfortunately, at the end of the military conflict, the majority of them did not continue teaching meteorology. After the war, Joanne Simpson continued her career at university. First, she completed a Masters degree and a course on tropical meteorology, whilst at the same time, she battled to get student loans. Simpson wanted to enrol in a PhD program in meteorology, and despite no woman having obtained one before, she found a suitable advisor and started her PhD studies. Some decades later, when her name was widely known, Simpson told an interviewer that she had received some adverse reaction from professors over the fact that a woman had been enrolled on a PhD in Meteorology.

"*They told me it was totally inappropriate for a woman to be a meteorologist. You would have to work night shifts, leaving the airport in the middle of the night. You would have to fly in airplanes to do research. You'd have to do all kinds of things women can't do.*"
In the same interview, she said that the renowned meteorologist Carl Gustav Rossby had said that no woman would have ever obtained a PhD in meteorology. If she got it, it was going to be impossible for her to find a job as a meteorologis (parts of this interview are recounted in (Barbara Joan Zeitz 2016)). Who knows how Simpson overcame the many obstacles she encountered during her PhD journey: the refusal of scholarships, the hostility of their male colleagues, and the general thought that her PhD topic was not serious scientific research, or as Rossby said: "Clouds are a good subject for a little girl to study". But despite all the impediments, in 1949, Simpson finished her studies, becoming the first woman in the United States to hold a PhD in Meteorology. Unfortunately, the predictions made by Rossby, before Simpson starting her PhD became true. She was never hired as a meteorologist, instead, she dedicated her life to academia. Even at the university, she had to fight hard to get her job. Early in her career, she was an Assistant Professor at the Illinois Institute of Technology, and later she worked as a researcher at the Woods Hole Oceanographic Institution. During these years, she developed

an innovative model of cumulus clouds, considered as the first cloud model. Her discoveries were very significant since she proved the importance of cumulus clouds in driving atmospheric currents in the tropics. In the late 1950s, Simpson in collaboration with her PhD advisor, Herbert Riehl, proposed a hypothesis of tropical convection termed as "Hot Towers", this name referred to tropical cumulonimbus clouds Simpson & Riehl (1964). Simpson and her colleagues give an explanation for some tropical cumulonimbus that can reach the top of the troposphere. They demonstrated that a high amount of water vapour releases a large amount of latent heat when it condenses into liquid. The large amounts of latent heat make the cumulonimbus rise to higher levels of the troposphere. They referred to them as "hot" because of the large amount of latent heat that motivated the rising. Before that discovery, the mechanism driving atmospheric Hadley cells was poorly understood. And even after Simpson's finding, it took a long time to be completely accepted by the scientific community. During her 40s and 50s, Simpson conducted several research projects, and in 1960 she became a Full Professor at the University of California Los Angeles. Simpson has authored over 190 articles in peer-reviewed journals, primarily on the subject of meteorology. A useful review of Simpon's achievements in science is given in Houze (2003) and Tao et al. (2003). She worked for some years at NOAA and for more than twenty years at NASA, and before retiring, she held the position of Chief Scientist for Meteorology at the institution. . Dr Joanne Simpson has received several prestigious awards and recognitions of her career. In 2002 she was awarded the prestigious International Meteorological Organization Prize, becoming the first woman to receive it.

At this point, the reader might be wondering about the ethnic, racial and cultural variety of the scientists as mentioned earlier. The gender gap has become apparent during the later paragraphs, but we do not want to put aside the race or ethnicity gender gap, because it has been the cause of gross injustices even in science. The first evidence of racial inequality is that all the women we have been talking about, except for Anna Mani, were white. Sadly, this fact did not change much as history progressed, and the majority of the scientists of this preface are white. For this reason, it is essential to pay particular attention to minorities that have had to fight doubly hard: because of their gender and ethnicity. Born in 1928, ***June Esther Bacon-Bercey*** was a passionate meteorologist supporter of minorities and women. Among the many professional achievements made by June, the following should be highlighted. She was one the firsts African-American woman to deliver the weather on television, she is believed to be the first African-American woman in obtaining a degree in atmospheric sciences, and she is definitely the first one in doing so at UCLA (University of California, Los Angeles) in 1954.
But let's start by telling her story from the early beginning of her working life. After graduating in meteorology, Bacon-Bercey moved to Washington, D.C., where she worked at the National Oceanic and Atmospheric Administration's (NOAA) National Weather Service as a weather analyst and forecaster until 1959. That same year she accepted a position at the Atomic Energy Commission as a senior adviser. Still, she got back very quickly to the atmospheric field, at the beginning of the sixties she rejoined NOAA as a radar meteorologist in the New York offices.
By the end of the same decade a new door opened to June: she was offered a position in a Washington TV channel as a meteorologist, still she did not deliver weather forecasts on air. But a year later, after having been hired, June became an broadcast meteorologist. Several years later, in an interview, she said that she was hesitant to appear on air since she thought she risked losing her credibility as a meteorologist. She was afraid of being just considered a pretty face presenting the weather information, like many other journalists or presenters. It is not known how

she was seen by the viewers, but it is clear that her colleagues really appreciate her knowledge and passion. June was so good at the job and extremely talented, she eventually became chief meteorologist, and in 1972 she was awarded the American Meteorological Society's seal of approval for excellence in television weather casting, thus becoming the first woman and the first African-American to get this award. Beginning in 1979, Bacon-Bercey spent nearly ten years as the chief administrator for Television Weather Activities at NOAA. In 1989, she retired from government service, but she continued to be involved in educational activities related to atmospheric sciences. The best illustration of her commitment and wish to help women and minorities was the scholarship she created in collaboration with AGU for women studying atmospheric sciences. She was the main founder of this scholarship, and she was able to do it thanks to winning a TV game show in 1977. She used part of her winnings to endow the AGU scholarship.

In addition to the scientists mentioned above, the pages of the atmospheric science history have also been written by more recent figures such as Sylvia Alice Earle, Margaret Hamilton, Eugenia Kalnay, Marta Estrada Mirayes, Inez Fung, Julia Mary Slingo, Kathryn Sullivan, Pilar Sanjurjo, Katharine Hayhoe, and a long etcetera. Despite the growing amount of female atmospheric scientists, when we started our research, we realised it was not going to be straightforward to collect information about them. We were able to find out who these scientists with leading contributions to meteorology were. Still, for many other women, with minor contributions, it was tough to find information or even reconstruct their professional careers. We fear that we were not able to discover them all, because, in the majority of the cases, their stories were shamefully neglected by history. Regardless of the magnitude of their findings, there is less information about female scientists than about their male colleagues. This is because, as with many collectives, women's contributions to science are underrepresented in history books, linked to their male colleagues' achievements or even banished to obscurity. For all these reasons, collective efforts must be made to reconstruct and remember their contributions to meteorology, and in general to science.

USC
UNIVERSIDADE
DE SANTIAGO
DE COMPOSTELA

Chapter 1

Introduction and State of the Art

In recent times the present and future of our world's climate have become a serious and alarming issue. Unfortunately, climate change is a topic that has been heavily politicised. Besides being a widespread subject matter for the scientific community, it has also been used as an instrument by political parties. They have employed this topic as a political weapon for their own interests, becoming on several occasions the centre of attention of the international media and public opinion. For this reason, it is impossible to mention climate change without it being considered a controversial topic.
In this thesis, we accept the theory which states that the ongoing accelerated climate change is caused by anthropogenic activity of the last decades. Our reason for adopting this position is not related to politics but to the fact that the overwhelming majority of the scientific community accepts and supports this scientific theory. We kindly ask not to use any argument given in this thesis as a political instrument to accept or deny climate change.

Before continuing with the main topics of this thesis, it is necessary to give some information about global climate change as it is understood nowadays by the scientific community, as well as about the potential hazards that it might involve. The climate change is the rapid variation in the atmosphere, geosphere and hydrosphere due to the anthropogenic activity of the last centuries. This non-natural process started with the Industrial Revolution at the beginning of the XVIII century. The damage that would be caused to our environment was not known at that time, only with passage of time did the severe effect become apparent.
The causes of this process are mainly related to the increase in greenhouse gases in the atmosphere and the uncontrolled waste of the Earth's natural resources. Due to this irresponsible activity, the planet Earth has suffered an overall warming trend that has progressed since the early 20th century. The effects of climate change have been observed in the form of an increase of the air temperatures, an increment of the occurrence of severe weather phenomena, and an intensification of the water cycle. This is a feedback process, and their effects are also seen in the hydrosphere. The variation of the salinity of the oceans, the loss of the polar ice caps and a rise in sea levels are the main consequences of climate change.

Based on the preceding pieces of evidence, it is undeniable that climate change is happening, and that is one of the biggest crises facing the whole of humanity. For this reason, the study of the weather and climate is of great importance. This thesis presents research on the European climate in recent decades. We hope this analysis helps to understand the climate in these areas better, thus mitigating the impact of possible future changes and avoiding the occurrence of extreme episodes.

1.1 The Water Cycle: Precipitation and Evapotranspiration

Planet Earth is known as the "Blue Planet" because 71% of the Earth's surface is covered with water. Life, as we know, may not exist without water's contribution, since it plays crucial roles in many parts of our lives. Since water is an essential resource to sustain life, the role played by the water in climate is fundamental, and it has been the subject of a large number of studies. Still, there is plenty of room to improve our knowledge about the behaviour and contribution of the water cycle in the past, present and future climate. For this reason, this thesis is focused on the tcontribution of water to the climatic system. The water cycle is the movement and change of the different states of the Earth's water, and the transfer of this water between the atmosphere, the land and the sea. The hydrological cycle embraces all the different states of the water on Earth, and the different roles that they play. The water contained in the atmosphere, approximately 90% comes from the oceans, lakes and open water bodies (Gimeno, Drumond, Nieto, Trigo & Stohl 2010). In the context of climate change, an intensification of the water cycle movement is expected (Huntington 2006). For this reason, extensive knowledge of the hydrologic cycle and its potential future alterations is of great relevance.
The overall hydrological cycle can be summarised in the evaporation of water at one place and the precipitation elsewhere, and all the processes happening in between to these molecules (Gimeno et al. 2012). The principal components of the water cycle are illustrated in Figure 1.1. Precipitation, evaporation, transpiration, groundwater storage, ice, snow, glaciers, surface runoff, streamflow and volcanic steam are the main reservoirs of the hydrological cycle. The atmosphere contains only a small proportion of the total global water. However, this small percentage of water plays a crucial role within the hydrological cycle by connecting the oceans, lakes, rivers and groundwater water storage. The global distribution of the water cycle is as follows: 97.2% is ocean water, 2.15% corresponds to glaciers and other ice, 0.61% is groundwater, 0.009% is freshwater from lakes, 0.008% is from inland seas, 0.005% is of soil moisture, 0.001% is water of the atmosphere and a 0.0001% is water from rivers. Only 2.5% of the total global water is freshwater, and of this 0.22% is the atmospheric component.

Among all the different components of the global water cycle, in this thesis, we pay particular attention to the precipitation and evapotranspiration (ET), and their linkage. Precipitation falling over the continents has great importance in the hydrological cycle, and it results from moisture of different origins (Brubaker et al. (1993), Trenberth (1999), Gimeno et al. (2012), Van der Ent (2014)). The precipitation of advective origin results from external atmospheric moisture. The internal contribution of the rain comes from the local flux of water vapour coming from the local ET within the considered region. Finally, the humidity already present in the atmosphere of the study area also contributes to precipitation. This last component tends to be neglected because the average residence time of a water molecule in the atmosphere is 8-10 days approximately before it condenses and falls to the Earth as precipitation (Numaguti (1999), Van der Ent & Savenije (2011), Van Der Ent & Tuinenburg (2017)). This global mean residence time is different over land than in the ocean, where it is about five days.
The Weather Meteorological Organization (WMO), the governing body of the global meteorological scientific community, defines evapotranspiration as "the water vapour produced from the watershed as a result of the growth of plants in the watershed". ET is a collective term that embraces physical evaporation from surfaces (E) and biological transpiration (T) (Seneviratne et al. 2006). Evaporation is the process through which water, in liquid or solid form, becomes atmospheric water vapour, and this can include water from bare soil, lakes,

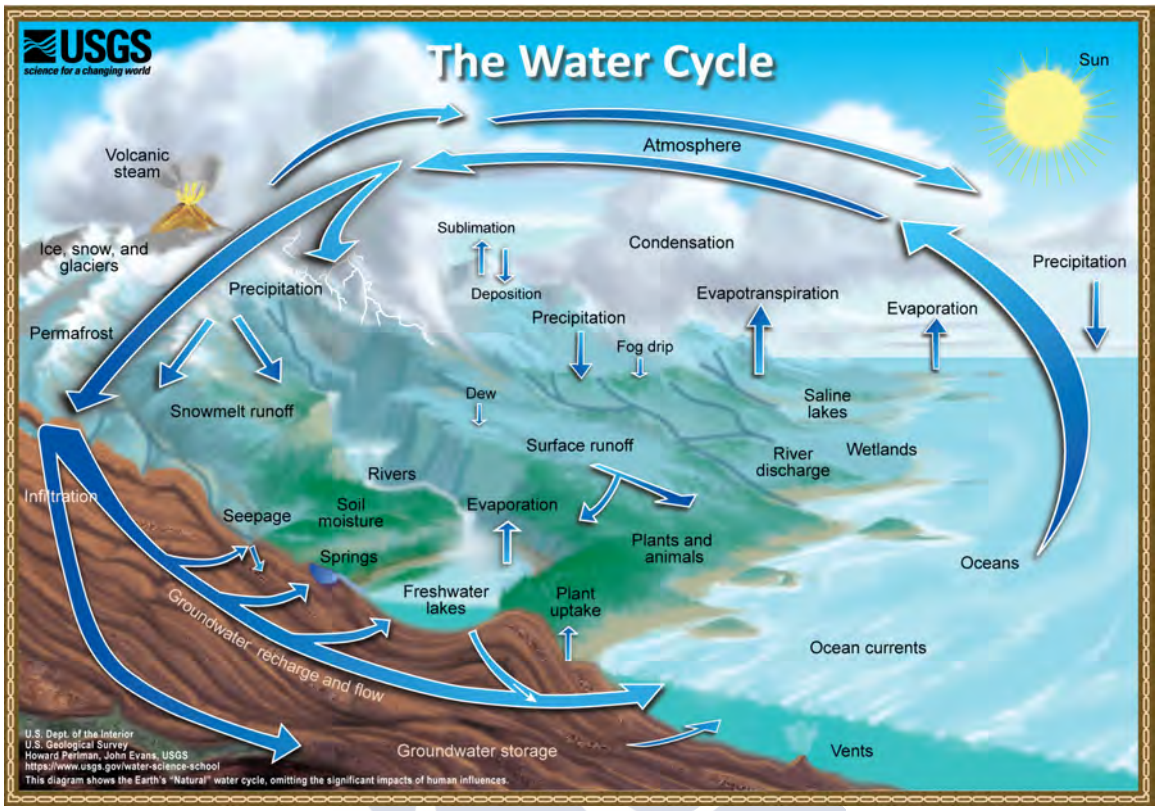

Figure 1.1: The natural water cycle. Figure adapted from US Geological Service website.

rivers, and vegetative surfaces. Transpiration is the phase conversion from liquid water to water vapour within the leaves of the plants. Transpiration and evaporation can be separated. Transpiration accounts for 39% of the ET contribution to precipitation, whereas the remaining 61% is from evaporation Schlesinger & Jasechko (2014). Still, much uncertainty exists about the contribution of ET to precipitation dynamics, and large amounts of literature theorising its role in the hydrological cycle have been published.

Every change caused by natural or anthropogenic force will cause modifications in the ET, thus in the precipitation. One of the most important features of the hydrological cycle is that evaporation always exceeds precipitation over oceans, and the opposite happens over land. This cycle can be completed when this precipitation is transported through rivers and groundwater storage to the oceans. Until the late 1950s, some studies surprisingly neglected the contribution of ET to precipitation (McDonald 1962), but at present, extensive research has shown that ET and precipitation share a feedback mechanism, varying spatially and temporally, depending on the synoptic conditions and location (Brubaker et al. (1993), Schär et al. (1999), Bisselink & Dolman (2008), Bisselink & Dolman (2009) ,Seneviratne et al. (2010)).

Although there are many theories on the nature of the feedback between ET and precipitation, there is still a need to improve the understanding of these two constituents of the water cycle.

1.2 Water Recycling

Estimating the contribution of local evapotranspiration fluxes to precipitation in a selected region is a longstanding problem in meteorology. One way to quantify the relationship between evapotranspiration and precipitation is through the study of the physical process named precipitation recycling, or water recycling. This concept has been debated for many decades (Brubaker et al. (1993), Eltahir & Bras (1994), Eltahir & Bras (1996), Savenije (1995), Seneviratne et al. (2006), Van der Ent et al. (2010)), and refers to the contribution of local ET fluxes to precipitation in a selected area.
Water recycling can be defined as the water that evapotranspirates within a specified control volume and falls as precipitation in the same volume (Brubaker et al. 1993). It is considered as a measure of the degree of control that ET has on the climate, and it plays an essential role in the water cycle of the continental areas. In this thesis, we undertake a detailed study of precipitation recycling in some particular areas of the Northern Hemisphere through various methodologies.

The intensity of the recycling mechanism is mathematically quantified by a term named recycling ratio. It measures the fraction of the precipitation over a given area and time period that originates from ET within the same area (Brubaker et al. (1993), Savenije (1995), Eltahir & Bras (1996), Trenberth (1999), Van der Ent et al. (2010), Gimeno, Drumond, Nieto, Trigo & Stohl (2010), Gimeno et al. (2012), Rios-Entenza & Miguez-Macho (2014)). It is regarded as a good indicator of the interaction between ET fluxes and precipitation and thus of land surface-atmosphere feedbacks. Still, it should be considered as an index or a diagnostic measure rather than a physical value (Koster et al. (1986), Trenberth (1999), Bosilovich & Schubert (2001)). As recycling ratio is distinctive of equilibrium status, it should not be used as a forecasting method (Eltahir & Bras 1996).

The value of the recycling ratio depends on the region's size (Savenije (1995), Eltahir & Bras (1996), Brubaker et al. (1993), Dominguez et al. (2006),Dirmeyer & Brubaker (2006), Bisselink & Dolman (2008)), on the geographical location, temporal scale, season or in the amount of precipitation in the study area (Eltahir & Bras 1996). It is immediately evident that the recycling ratio increases if the spatial scale increases because the evaporative sources can provide more moisture to precipitation (Dominguez et al. 2006). The main limitation of the computation of the recycling ratio is precisely the strong dependence between the size of the area and the recycling rate. Several studies have demonstrated that the variation of the recycling ratio follows a logarithmic behaviour rather than linear (Dirmeyer & Brubaker (1999), Eltahir & Bras (1996), Brubaker et al. (2001), Dominguez et al. (2006), Van der Ent & Savenije (2011))

1.2.1 Review of the Recycling Computation Methods

Although there is no direct way of estimating the recycling ratio, several methods have been used to approach the study of the contribution of evapotranspiration to the regional precipitation. Integral moisture budget recycling models, Lagrangian particle dispersion models, physical analysis using isotope data or Eulerian models are the most common methodologies to perform recycling computations (see Gimeno et al. (2012), for a detailed review). It should be noted that all of these indirect methodologies suffer from limitations and assumptions. Below, we discuss the main features, advantages and disadvantages of these models.

Bulk Precipitation Recycling Models

Classic or bulk recycling precipitation models are commonly used procedures to estimate the recycling ratio. They are based mainly on a simplified model developed by (Budyko & Drozdov 1953) and described in (Budyko et al. 1974) whose fundamental principle is total water content conservation. Budyko's model is a one-dimensional recycling model, but it can be applied to a two-dimensional domain. As is the case of the pioneering Budyko's model, analytical models resolve two equations of conservation of vapour mass for the advected and evapotranspired fractions of moisture in the atmosphere.
These models rely on various simplifying, but strong assumptions that can give rise to vague or inaccurate results. The three common assumptions made in bulk precipitation models are the following: the use of time-averaged moisture fluxes, the neglect of the atmospheric storage term and the well-mixed assumption (Burde & Zangvil 2001). In some particular cases, they also consider the moisture flux parallel to the boundaries of the region. The first simplification supposes a constant ET and precipitation in time and space; this can be quite acceptable to ET, but not to the rain, which is very non-homogeneous. These models have been criticised for their use of monthly mean data in estimating moisture flux entering the domain, which does not capture the diurnal and synoptic variability (Fitzmaurice 2007). Undoubtedly the most robust hypothesis is the well-mixed assumption. It implies that the particles of advected and evaporated moisture have the same probability of precipitating. Stated in another way: water from evaporation contributes uniformly throughout the atmospheric column.
Despite all the drawbacks of the classic models, they have the advantage of being rather mathematically simple, and they only use a small number of input parameters (Gimeno et al. 2012). Hence they are computationally efficient and gain speed in calculation.
By making modifications or generalizations on the Budyko model, different authors have described the analytical modelling of the recycling processes in a variety of ways (Brubaker et al. (1993), Eltahir & Bras (1994), Trenberth (1999), Schär et al. (1999), Burde & Zangvil (2001), Bosilovich (2002), Dominguez et al. (2006), Rios-Entenza & Miguez-Macho (2014)). Since in this thesis three bulk precipitation recycling models are employed (Eltahir & Bras (1994), Schär et al. (1999), Dominguez et al. (2006)), a detailed explanation of these methodologies, their underlying mathematical formulas, and the assumptions on which they rely, are given in Section 3.2.

Analysis of Isotope Data

The origin of moisture that contributes to precipitation can be assessed by using techniques based on isotope analyses. The isotopic composition of hydrogen, oxygen, deuterium and O^{18} existing in the states of water have different chemical and physical properties. If the isotope data is measured, they provide information about the origin of the moisture that feeds precipitation, thus allowing to compute the recycling ratio (Gimeno et al. 2012).

Lagrangian Methods

Lagrangian particle dispersion models have been widely used to investigate the moisture source regions within the hydrological cycle. These methods simulate the trajectories of particles or water molecules by tracing air motion backwards in time, intending to identify the evaporative sources of vapour contributing to precipitation and describing the shipping of the moisture

through the atmosphere.

A review of the multiple uses in which the Lagrangian methods have been applied is given in the following paragraph. The method of the quasi-entropic back trajectory of Dirmeyer & Brubaker (1999) can be considered the first Lagrangian moisture source diagnostic. It is an algorithm that combined with a surface fluxes model can determine the regional sources of precipitation and therefore provide estimates of the recycling rate. This approach takes as initial conditions: wind and water vapour from NCEP re-analyses; and evaporation and precipitation observations. Reale et al. (2001) employs the water vapour back-trajectory technique developed by Dirmeyer & Brubaker (1999) together with a surface flux method. In their research, they demonstrate the significant contribution of sub-tropical hurricanes occurring in the Atlantic to the moisture of Mediterranean floodings in autumn 1998. Brubaker et al. (2001) extends the methodology of Dirmeyer & Brubaker (1999) to a more prolonged period, to provide a climatology of the moisture pathways. In 2007, Dirmeyer and Brubaker published a methodology (Dirmeyer & Brubaker 2006) based on the original mathematical formalism described in Dirmeyer & Brubaker (1999), and using the same climatologies calculations as in Brubaker et al. (2001). However, this Dirmeyer and Brubaker back trajectory calculation suffers from some shortcomings. The model relies on the well-mixed assumption, meaning the amount of moisture throughout the atmospheric column is estimated to be the same at all levels. Also, the algorithm does not take into account the phase changes of the water through their pathway. Conversely, this method has a low computational cost. Stohl et al. (2004) and Stohl & James (2004) illustrates an extreme precipitation event using a backward trajectory modelling of water vapour transport based on a study developed by James et al. (2004). This model uses the Lagrangian particle dispersion model FLEXPART (Stohl et al. 1998). They analyse the sources and paths of the moisture that contributed to some devastating floods which occurred in summer 2002 in Central and Southern Europe. Among the main handicaps of this method, we must mention the inability to separate precipitation and evaporation and not taking into account ice or liquid water. Multiple subsequent studies make use of the Lagrangian Particle Dispersion model (James et al. 2004). The most significant publications are listed below. An accurate model based on the pioneer model is applied in the Sahel (Nieto et al. 2006), Iceland (Nieto et al. 2007), in the Orinoco River Basin and South America (Nieto et al. 2008). The same Lagrangian 3-dimensional FLEXPART model is used to investigate the primary sources of moisture for Central Brazil (Drumond et al. 2008) and the North-West of the Iberian Peninsula (Drumond et al. 2011). Gimeno, Nieto, Trigo, Vicente-Serrano & López-Moreno (2010) use the same Lagrangian methodology in a climatic study to identify the atmospheric water vapour sources that contribute to the moisture in the air column over the Iberian Peninsula. Brioude et al. (2013) uses an output of a regional meteorological model (Weather Research and Forecasting model (Skamarock & Klemp 2008)) as the input of the Lagrangian particle dispersion model FLEXPART. More recently, Keune & Miralles (2019) discover that a significant contribution of the summer precipitation over European watersheds depends on the moisture supplied from other watersheds, via the use of the Lagrangian particle dispersion model FLEXPART.

As stated in the study of Brioude et al. (2013), Lagrangian methods have been applied in multiple uses. They have provided valuable guidance to a better understanding of extreme precipitation events, to establish climatologies of moisture source-sink relationships (Brubaker et al. 2001), to reproduce the pathways of air pollution dispersion of anthropogenic origin (Bahreini et al. 2009) and as forecasting tools (Stohl et al. 2004). With regard to the spatial scale, Lagrangian methods have been employed to simulate atmospheric transport at both global

(James et al. (2004), Gimeno, Drumond, Nieto, Trigo & Stohl (2010)) and regional scales (Stohl et al. (1998), Nieto et al. (2006), Durán-Quesada et al. (2010)). Furthermore, the analysis of the moisture transport in a Lagrangian framework also allows us to perform computations of the recycling ratio (as in Brubaker et al. (2001), Stohl et al. (2004), Stohl & James (2004), Nieto et al. (2006), Nieto et al. (2007)).

Among the advantages of the Lagrangian models the following should be noted: a low computational cost, a good representation of the moisture paths from the sources, and a precise simulation of atmospheric plumes (Rastigejev et al. 2010). The improvements of these methods over analytical models are the following. In Lagrangian models, the computations of the atmospheric variables are not averaged in space and time, they can follow the movement of the air parcels through the atmosphere, and that it is not necessary to define a source region, because the particles are followed over time.

Conversely, there are some drawbacks related to the use of Lagrangian models. As stated in the study of Gimeno, Drumond, Nieto, Trigo & Stohl (2010), evaporation and precipitation are not separable (Stohl et al. 2004). This model and Dirmeyer & Brubaker (1999) share some disadvantages. Both of them rely on the well-mixed assumption, meaning the amount of moisture throughout the atmospheric column is estimated to be the same at all levels. Also, they do not take into account the phase changes of the water in its trajectory around the hydrological cycle.

Eulerian Methods

There are other techniques named Eulerian Online Moisture Tracer Models for investigating the relationship between precipitation and evapotranspiration. Moisture tagging is based on the concept of following or tracing water from its surficial source through space and phase transitions until it precipitates or leaves the model domain.

The so-called Off-Line Eulerian Methods use Global Circulation Models to estimate the fate of the precipitation, thus accurately representing the recycling on a large scale (Van der Ent et al. (2010), Van der Ent (2014)). Nevertheless, in small areas, they are not able to depict recycling patterns. Unlike the analytical recycling calculations, these methods are capable of giving the statistical distribution of moisture origin. Among them, we highlight the studies of Yoshimura et al. (2004) that develop an off-line one-layer Eulerian moisture tracking model or Vautard et al. (2013) with a two-dimension moisture tracking model. This latter case assumes the atmosphere is well-mixed in the vertical coordinate.

Online Eulerian Methods or Water Vapour Tracer techniques (WVT) are more complex and are operated at a higher computational cost than the off-line methods. The abbreviation WVT is slightly inaccurate because the term refers to all the states of water in the atmosphere, and not only to moisture. Online methods have been widely employed in the literature (e.g. Numaguti (1999), Bosilovich (2002), Sodemann et al. (2009), Knoche & Kunstmann (2013), Wei et al. (2015)). This is because moisture tagging is the most physically realistic method for investigating the relationship between precipitation and evapotranspiration. It is based on the concept of following or tracing a marked amount of water from a specific surface source through different atmospheric processes and through space and time until it precipitates or leaves the model domain. Mathematically, this means that the moisture coming from a source area is treated as a new moisture species, and it undertakes all physical processes in the water cycle, such as advection, diffusion, convective processes and cloud microphysics mirroring full moisture but without interfering with it. To get these new moisture species, a moisture tagging technique

is coupled or embedded with a meteorological model. We called the moisture tagged in these models Water Vapour Tracers (WVT). This technique is considered to be very realistic because it enables the tracer to exactly behave in the same way as the moisture in the meteorological model. The fact that WVT are embedded in the atmospheric model could be a disadvantage, on account of its high computational cost and that a reanalysis cannot be used.
WVT are implemented in Global Circulation Models (Koster et al. (1986), Numaguti (1999), Bosilovich (2002)) and in Regional Circulation Models (Sodemann et al. (2009), Knoche & Kunstmann (2013), Miguez-Macho et al. (2013), Wei et al. (2015)). Koster et al. (1986) and Jossaume (1986) implemented for the first time a tagging technique in two different Global Circulation Models (GCMs). The following studies were then applied in Antarctica (Koster et al. 1992), in the Sahel (Druyan & Koster 1989) and Greenland (Charles et al. 1994). Numaguti (1999) implemented a tagging algorithm in an atmospheric General Circulation Model focusing their study on the Eurasian continent. Besides that, in their study, they were able to ascertain the age of the molecule. Werner et al. (2001) modelled the isotopic composition of the polar precipitation with a tagging technique. To demonstrate that the well-mixed assumption employed in analytical models was a source of error in precipitation recycling calculus, Bosilovich (2002) used an online WVT method, in the same way as Gößling & Reick (2013). To analyse the vertical distribution of the moisture tracers in the atmospheric column Bosilovich (2002) applied WVT over North America, and Bosilovich et al. (2003) employed this latter technique to study the North American monsoon. Sodemann et al. (2009) made use of for the first time a regional climate model with tracking capabilities to analyse the contribution of moisture to some extreme events, and this implementation was followed by many others. Knoche & Kunstmann (2013) implemented in a regional climate model MM5 a fully three-dimensional evaporation tagging mechanism that enables them to follow the molecule through space and phase transitions.

Water vapour tracers are considered a more physically realistic technique than analytical or even Lagrangian methods, as they enable the tagged moisture to behave precisely in the same way as moisture. Nevertheless, the fact that the method runs coupled within an atmospheric model can be a disadvantage, since the results depend on the accuracy of the meteorological model used. Furthermore, the method has to be applied before running the model, and this also implies a high computational cost. Besides, this methodology cannot be applied to reanalysis. In the majority of the models, the land surface hydrology is not accurate, or the topography is not well represented and nor are coastal features; thus this may affect the estimations of evaporation, and hence the recycling results. Although global models give us a planetary resolution, regional models better represent complex topographies; therefore they are more exact in calculating recycling ratios in limited areas.

In this thesis, we employ a moisture tagging capability embedded in the atmospheric model Weather Research and Forecast. This tool, developed by Miguez-Macho et al. (2013) and Insua-Costa & Miguez-Macho (2018), is integrated into the WRF model used in Chapters 4, 5 and 6 by the Prof. Dr Gonzalo Miguez-Macho. This Water Vapour Tracers Method (hereafter referred as WVTM) can be used to tag the water vapour from oceanic or terrestrial sources, so evaporation can be tracked until it leaves the model domain or returns to the land surface as precipitation. WVTM allow us to trace moisture which evaporates from any tagged region. The main features of this tool experimentally are described in Section 3.3.

1.2.2 Indirect Recycling or Amplification Processes

Recycling ratio is an entirely accurate way to determine the influence of the evaporation in the precipitation. Nevertheless, to carry out a comprehensive study of the impact of evapotranspiration fluxes in the local rainfall it is advantageous to employ more methodologies Seneviratne et al. (2010).
ET fluxes constitute a source to contribute to the increase of the amount of precipitation in a region. But also, they have a direct impact on the thermal structure of the lower atmosphere by enhancing convection. This influence contributes to the improvement of the efficiency of convective precipitation processes.
The first contribution from ET to rainfall is water recycling, also referred to as "direct mechanism" or "direct coupling". It is defined as the linear contribution of local evapotranspiration fluxes to precipitation. The second contribution is known in the literature as "amplification processes", "indirect mechanism", "local coupling" or "indirect recycling" Schär et al. (1999). Amplification refers to the non-linear contribution of local ET fluxes to precipitation. It originates from advection that becomes rainfall as a result of the effect of land-atmosphere interactions on the thermodynamic structure of the lower atmosphere. In summary, ET fluxes determine the intensity of land-atmosphere coupling and the relevance of recycling or precipitation amplification processes in the local hydrology cycle. Hence, soil-precipitation feedback relies on two possible physical mechanisms: amplification and recycling. A representation of these two components is depicted in Figure 1.2. The recycling mechanism states that the exceeding precipitation over wet soils has as a main supplier the evapotranspiration over the same region. In contrast, in the amplification mechanism, the surplus of the rain comes from atmospheric transport of water, still, the efficiency of precipitation is controlled by the soil Schär et al. (1999).

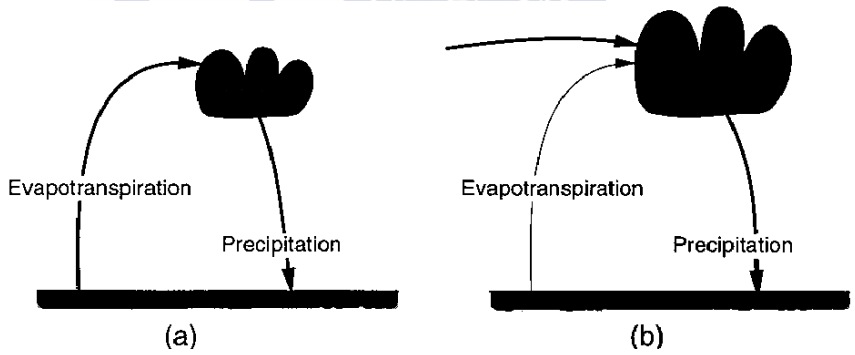

Figure 1.2: Scheme of the two physical mechanisms that contribute to soil precipitation feedback: (a) recycling and (b) amplification. Figure adapted from Schär et al. (1999)

Amplification alters the thermodynamic structure of the lower atmosphere by promoting convection and modifying the regional circulation. The primary effect of this atmospheric phenomenon is the incorporation of the advected moisture from outside the region as a source of extra precipitation. Consequently, being added to the rainfall originated from the local ET (Schär et al. 1999). Amplification or indirect mechanisms can be very relevant even tending to predominate over recycling or direct effects ((Eltahir 1998), (Schär et al. 1999), (Alfieri et al. 2008), (Seneviratne et al. 2010), (Goessling & Reick 2011), (Decker 2015)).

The contribution of direct and indirect mechanisms in increasing rainfall can be assessed, but separating these two processes is not straightforward since they are strongly linked. The scientific community has investigated the topic of amplification processes, several researchers investigating the amplification mechanism have employed procedures in which the evapotranspiration fluxes are altered, as a way to assessthe impact of the ET fluxes on the regional precipitation ((Beljaars et al. 1996*a*),Dirmeyer & Brubaker (1999), Seneviratne et al. (2006), Seneviratne et al. (2010), Rios-Entenza & Miguez-Macho (2014), Decker (2015)). They altered the ET fluxes, directly or through changes in the humidity of the soil of the meteorological models, with the aim of assesing the response of the water cycle. For example, Schär et al. (1999) carry out a study in which the soil humidity is doubled and suppressed and the effects of these on atmospheric forcings such as evapotranspiration, precipitation, temperature or even radiation fluxes.
In this thesis, we employ a method to separate recycling and amplification and be able to study the soil-precipitation feedback. The mathematical procedure of this technique is described in Section 3.4, and in Chapter 5 is employed to analyse the effects of amplification on the precipitation in a study over the Iberian Peninsula during springtime.

1.3 The Role of Groundwater

The water beneath the ground is a crucial variable controlling many processes in the climate system. In this section, we try to explain and understand what the groundwater does for the water cycle and the climate. To this end, we revise and discuss the physical features underlying groundwater dynamics and its interactions with the land-atmosphere.
Groundwater is the volume of water beneath the Earth's surface. It is contained in the pores and cracks of the soil, and the sand and rocks. This natural storage of underground water is continuously moving and is capable of interacting with the water in the atmosphere; for this reason, groundwater plays an essential role in the hydrological cycle. In contrast to the residence time of the water in the atmosphere, which barely reaches eight days, the length of time water spends in the ground is far higher it may remain a total of 1400 years below the surface (Shiklomanov & Rodda 2004).
The geographical distribution of groundwater depends on the structure of the Earth's crust, but also on other parameters as infiltration, evaporation or atmospheric influence through the precipitation. The geographical distribution of the groundwater has been widely studied. Still, the vertical distribution under the surface is more challenging to comprehend, and it has always been a somewhat controversial field of study.
One of groundwater's main features is that it has a critical buffering effect in the soil. During wet periods or humid conditions, it receives a surplus of water and acts as a sink. In dry conditions, groundwater serves as a source by supplying water through capillary rise or as a source for streams, big rivers, lakes and wetlands (Fan et al. 2007).

Groundwater is a precious and scarce resource, and it is used as a source of water supply worldwide. Among its uses, we highlight; as drinking water for human consumption and irrigation of crops. Much of the world's food is produced thanks to irrigated agriculture. Also, many plants species and animals depend upon underground water, and it is necessary for several industrial processes. Owing to population growth and the rapid economic development of the last fifty years, the demand for groundwater has increased in enormous proportions, and sadly, the use of the groundwater is not sustainably managed by humanity. This diminishing of water and groundwater supplies drives scientists' concern about the future of the water supplies. For this reason, a high amount of literature placing more emphasis on groundwater analysis has emerged in the last decades. Still, there are a lack of studies focusing their attention on groundwater processes. A recent study (de Graaf et al. 2019) forecasts that excessive groundwater pumping due to human activities may lead to substantial decreases in the levels of groundwater and losses of groundwater from its storage. Among the implications of a drop in the level of groundwater, the most worrying is the river flow decreasing or even drying up, the water temperatures changing, and the contribution of humidity to the atmosphere decreasing. These may directly affect whole ecosystems and humans.

In response to the question raised right at the beginning of the page, we can summarise the main functions of groundwater as the following: to redistribute soil water in the subterranean spaces, to sustain streamflow in humid climates, to absorb receding streams in arid climates, to sustain wetlands and temporarily hold wet-period infiltration, and later supply dry-period evapotranspiration.

1.3.1 The Water Table and Soil Moisture

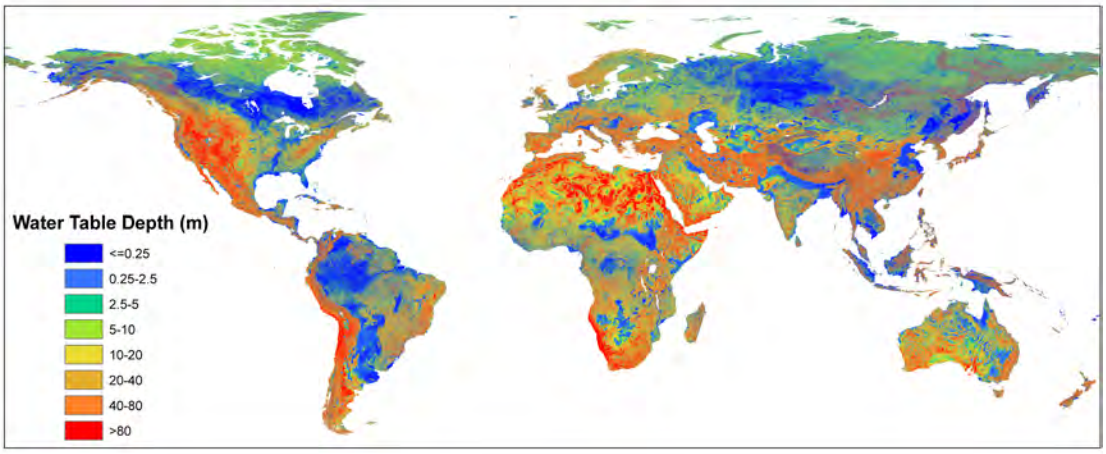

Figure 1.3: Representation of simulated global water table depth in metres. Figure adapted from Fan et al. (2013).

The water table (WT) also termed as groundwater table or phreatic level is an undulating surface that limits the zones where the soil is saturated with water and the zones where it is not (Fan et al. 2013). Above the water table, the soil is not saturated and below it is saturated. Water contained in the saturated zone is transported as groundwater flow, discharging into the seas or rivers. The ground receives seepage water from rivers and lakes, and the land provides water to rivers and streams as subsurface runoff water.
The water table depth (WTD) is considered as the leading indicator of the coupling between the ground and the atmosphere. It is also a good measure of how much memory the long timescales of variation of groundwater can induce in the moisture contained in the soil (Martínez-de la Torre & Miguez-Macho 2014).
The WTD is not constant over time, and its fluctuations may be due to many reasons. It varies depending on the season of the year, or even from year to year. For example, in some midlatitude areas, a rising of the WTD is prevalent during springtime owing to the melting of the accumulated snow during winter. Whilst, in dry summertimes, when the atmospheric demand is higher, the WTD falls. The WTD is dependent on precipitation regimes. The WTD varies due to fluctuations through capillary rise or drainage. Owing to the daily evapotranspiration and the precipitation cycle, WTD suffers diurnal fluctuations in shallow groundwater levels (Gribovszki et al. 2010).
The geographical situation influences the WTD, in areas near to water sources such as streams, lakes beds and wetlands, the WTD is shallow, and it is deep in mountain ranges. The water table can be relatively shallow over large regions of the continents. Hence, in some areas, the phreatic level can be located less than one metre beneath the land surface or at more than eighty metres down.

The groundwater is connected to the land surface through different interactions, which take higher relevance in the areas with a shallower water table and water-limited environments. The

interactions can be vertical fluxes through the WT surface or horizontal fluxes, giving rise to water redistribution through gravity-driven lateral transport.

The humidity stored in the unsaturated zone of the ground is usually defined as soil moisture (Hillel (1998), Seneviratne et al. (2010)). The land surface limits the unsaturated zone at the top, and the water table at the bottom, the pores are filled partially with air and partially with water (Ríos Entenza n.d.). In regions where the groundwater table is shallow, soil moisture is connected to the water table or even considered part of it (Fan et al. (2007), Miguez-Macho et al. (2008), Martínez-de la Torre & Miguez-Macho (2014)).
The soil moisture–atmosphere feedback effects play an essential role in land energy and water balances and thus in the whole evolution of the climate. The direct contribution of soil moisture to atmospheric processes and vice versa has been demonstrated in the literature (Beljaars et al. (1996*a*), Seneviratne et al. (2006), Seneviratne et al. (2010), Orth & Seneviratne (2012), Hagemann & Stacke (2015)). Mainly, precipitation and temperature are the atmospheric forcings whose link to soil moisture have drawn extensive attention. The soil moisture governs the contribution of precipitation to soil infiltration or runoff. The wetness somewhat controls the land surface temperature via its effect on latent or sensible heat fluxes (Castillo et al. 2015).
The role of topography in controlling soil moisture is highly relevant, just like for the water table (Liu et al. 2012). The influence of a deep water table in soil moisture is not significant. However, a shallow water table impedes the soil moisture drainage during wet periods, thus perpetuating the effect of rain for a long time (Fan & Miguez-Macho 2010). Despite their coupling, soil moisture presents longer persistence in time in comparison to atmospheric forcings.

There are some regions of the globe, where the soil moisture memory contribution is more significant to the state and temporal variations of the climate. For this reason, it is important to have an accurately represented soil moisture in the land surface models to represent the soil moisture memory and thus improve the accuracy of climate predictions (Hagemann & Stacke 2015).

1.3.2 A Short Review of the Land Surface Models

Land Surface Models (LSMs) represent land-atmosphere interactions by simulating the water and energy exchanges at the atmosphere-soil connecting surface (Maxwell & Miller (2005), Decker (2015)). LSMs are a key link between atmospheric models and hydrological models (Boone et al. 2004). Below we detail some of the widely employed LSMs. We describe the evolution of the LSMs from simplified schemes to sophisticated models which include the groundwater dynamics and which accurately describe the water table dynamics, that can be coupled to atmospheric models or not. For a detailed review of land surface models see (Yang 2004).

The first global climate models employed as LSM a simple parameterisation or bucket model that worked as the surface boundary condition (Manabe et al. (1965), Maxwell & Miller (2005)). Its name comes from considering the soil as a water container with a fixed capacity. The bucket is filled with precipitation and emptied with ET, and the runoff is regarded as an oversupply. These models do not take into account vegetation or groundwater.
That scheme was later improved by adding vegetation and snow components, which can be run offline or coupled to the atmospheric model (Dickinson (1986), Maxwell & Miller (2005)). Literature refers to these schemes and models as Biosphere atmosphere transfer scheme (BATS) or simple biosphere (SiB) models. Although these schemes can be coupled to atmospheric

models, they only have one dimension in the vertical direction. Thus they are not considering horizontal interactions. Also, different vegetation types are not considered, and there are only three land components (soil, snow and vegetation).

However, those LSMs do not accurately represent the WT. Calculating the WTD is a very lengthy and challenging process since there are still not enough measures taken in some areas of the globe. Some recent LSMs have included a realistic representation of the water table (Fan et al. (2007), Gestal-Souto (2010), Fan et al. (2013), Martínez-de la Torre & Miguez-Macho (2014), Martinez et al. (2016), Quintana-Seguí et al. (2019)). Fan et al. (2013) provides an accurate representation of a simulated global water table depth which is depicted in Figure 1.3.

As the water cycle may be understood as a fully coupled system between the land and the atmosphere, with complex interactions between them, the LSMs might be coupled to the atmospheric model. Thanks to this, the water balance would be better closed, the atmospheric forcings over regions with shallow WT would be more realistic, and the contribution of the soil water and energy fluxes would give rise to more accurate temperatures and precipitations. In this thesis, we make use of an LSM coupled to a regional meteorological model to study the role of groundwater in the atmospheric processes. This LSM termed as LEAFHYDRO is thoroughly described in Section 3.5 and results are given in Chapter 6.

1.4 Climates in the Areas of Study

1.4.1 Iberian Peninsula Climate

In the present thesis, we have chosen two different extratropical geographical locations in the Northern Hemisphere. One of them is the Iberian Peninsula (hereafter IP) located in the extreme southwest corner of Europe, approximately between 36° and 43°N and 6.5° and 9.5°W. IP covers mainland Spain and Portugal, Andorra, small areas of France and the British overseas territory of Gibraltar. IP is surrounded by the Atlantic Ocean and the Mediterranean Sea. Approximately 1.660 kilometres of coastline is covered by the Mediterranean and 1.653 kilometres by the Atlantic. It is connected to the European continent by a range of mountains named the Pyrenees, which forms a natural border between IP and France. The south of the IP is separated from the African country Morocco by the Straits of Gibraltar. This narrow strait separates the European and the African continent by 14.3km of oceanic waters. IP has an approximate area of 750 km^2 and enormous geographic complexity, with mountain ranges surrounding high plateaus in the middle of the Peninsula. IP topography is shown in Figure 3.1.

Climatic settings owing to the orography

In general, IP has two dominant climate types, the Oceanic and Mediterranean. Nevertheless, due to its uneven relief and unique geographic situation, IP has significant climatic variability, where other subtypes of climates can be found. This variability, together with the latitudinal differences between the north and the south of the IP gives rises to different temperatures or rainfall amounts across the Peninsula (Castro et al. 2005).
The Köppen-Geiger classification system defines the climate on account of the average monthly values of precipitation and air temperature. There are other methodologies to identify the different observed climates, but this is the most widely used classification to study the climate. Based on the Köpeen classification, Iberia is divided into four climatic sub-regions. Type B (dry climate), type C (temperate climate) and in some small areas type D (cold climate) and type D (polar climate) (Chazarra 2012).
Following the Köpen classification, we find the following climatologies in the IP. Two dry desert types BWh (hot desert) and BWk (cold desert) climate type (dry desert climates) are found in southeast Iberia; particularly in the provinces of Almeria, Murcia and Alicante; where the minimum values of Iberian precipitation occur. There are another two dry climate subclasses, BSh (hot steppe) and BSk (cold steppe) in the southeast of the Peninsula,the Ebro Valley, the Southern Plateau region and in some small areas of the south interior; in particular, Extremadura or Baixo Alentejo.
Temperate climates are prevalent in the IP. Csa (temperate with dry or hot summer) covers most of Iberia, and it is mainly located in the Southern Central Plateau region and the Mediterranean coastal area. Csb type (temperate with dry or mild summer) is found in the northeast of the IP, the west coast of mainland Portugal and some mountain regions within the Peninsula. Cfa (temperate with no dry season and hot summer) is located in the northeast of the Peninsula, within an area of medium-altitude which surrounds the Pyrenees and the Iberian mountains. In some mountain ranges such as the Cantabrian Mountain, the Iberian mountains, the Pyrenees and also the Northern Central Plateau region, the prevailing climate is Cfb (temperate with no dry season and mild summer). Although to a minor extent, there are some areas where the climate is classified as type D. In particular in higher altitudes of the Cantabrian Mountains,

in the Iberian Mountain rRange, the Central Ranges, Sierra Nevada or the higher elevations of the Pyrenees. Also, a subtype corresponding to polar climate, more precisely tundra, is found in small areas of the highest altitudes of the Central Pyrenees (Chazarra 2012). Regarding the temperatures but also other climate variables, IP is the geographical location where the European Atlantic and the Mediterranean climate converge. Our area of interest is southeastern Iberia. It is a semi-arid region where the influence of the Mediterranean sea is quite strong; thus, the climate is Csa according to Köppen classification. Summertime is the drier period of the year, and during these months the highest average temperatures above 22° are registered.

Iberian Precipitation Regime

Due to its complex orography and geographic situation, the precipitation regime of the Iberian Peninsula is characterised by a strong seasonal and interannual variability (Esteban-Parra et al. (1998), Serrano et al. (1999),Trigo & DaCamara (2000), Trigo et al. (2004), Muñoz-Díaz & Rodrigo (2004), Cardoso et al. (2013), Rios-Entenza et al. (2014)). The annual average rainfall shows considerable spatial variability, except for the north and northeast mountains, where the precipitation amount remains almost constant throughout the year Rodriguez-Puebla et al. (1998). The main reasons for this variability are the oceanic influence and a complicated orography. Nevertheless, other factors impact the annual rainfall of the IP, like the influence of the recycling processes.

The Iberian Peninsula is highly influenced by the synoptic frontal systems approaching from the Atlantic Ocean, especially in late autumn and winter; and by the Azores High in summer (Lana & Burgueno 2000). Due to the intensity of the westerly winter circulation, together with the global dynamics of the atmosphere at mid-latitudes, the northern façade of IP is considered one of the wettest areas in mainland Europe. The highest annual rainfall amounts are located in north-eastern Continental Portugal, in particular the Gerês mountains (in Portuguese: Serra do Gêres), in the northeast of Navarra and some areas of southwestern Galicia. In these latter areas, rainfall reaches the highest of all Iberia with a mean annual precipitation of 2800 mm (Cardoso et al. (2013), Chazarra (2012)). This evidence was confirmed by the meteorological observational network, property of the regional weather centre MeteoGalicia, these are located throughout the Galician territory. This observational data provided by MeteoGalicia indicates that the average total precipitation is approximately 2800 mm a year, indicating that the model data is realistic.

As relating to the topography, the estuaries and valleys of the big rivers (Douro, Tagus, Guadiana and Guadalquivir) draining into the Atlantic Ocean bring a significant amount of humidity into the Peninsula. At the same time, the Baetic and the Iberian Systems block the entrance of moisture from the Ocean acting as a wall. Further up to the north, the Ebro basin facilitates the entrance of humidity coming from the Mediterranean Sea.

The Mediterranean area is barely influenced by Atlantic frontal systems and humidity coming from the Ocean, and so the yearly mean precipitation is less than in the Northwest. The most significant contribution to rainfall in this region is from mesoscale convective systems. These flash floods tend to occur in early autumn, and they are the result of high Mediterranean sea surface temperatures, among other climatic contributions (Martín et al. 2007). These sudden events frequently give rise to an amount of precipitation of up to 300mm a day. However, in the southern façade of the Mediterranean Sea, particularly in the provinces of Almería, Murcia and Alicante, the average annual rainfall barely reaches 300mm. In the surrounding areas of Cabo de Gata (southeast of Spain), precipitation is less than 200mm a year (Chazarra 2012). In

some places of the Peninsula (like in the Ebro basin or southeastern Iberia), there is a shadowing effect in the precipitation due to the influence of the mountain ranges (Rodriguez-Puebla et al. 1998). This effect results in smaller rainfall amounts than in other areas, or even in periods of more than 90 days with zero precipitation recorded. Despite these differences, the annual mean precipitation is heterogeneously distributed across the Peninsula (Quintana-Seguí et al. 2019).
Meanwhile, the seasonal variability may be due to the influence of sources like the Atlantic Ocean and the Mediterranean Sea, the intricate orography or even the latitude, the interannual variability does not have an easy explanation. The interannual variability is quite strong all across the Peninsula, the monthly average precipitation varies between years, except for the northern mountain ranges, where there are some areas with a polar climate, and the rainfall remains constant during the whole year. Some studies point out the significant influence of the North Atlantic Oscillation (this weather phenomenon is briefly explained in Section 1.4.2) in the winter rainfall regime of western Iberia (Trigo & DaCamara 2000). To a lesser extent, it is modulated by other scale atmospheric modes such as the East Atlantic Oscillation, the Southern Oscillation Index and the Scandinavian Pattern (Rodriguez-Puebla et al. (1998), Rios-Entenza & Miguez-Macho (2014)).
The IP has a notable precipitation seasonality, which is more intense in southern areas and less relevant in the northeast of the Peninsula. On the whole, maximum of precipitation occurs in late autumn and winter, from October to March, due to the strong western advection that brings milder and wetter weather and intense winds. The most significant precipitation values are reached in December in the north or northwest of IP, and the lowest amounts are found in December in the southeast of Spain. In summer, quasi-stationary cyclones are dominant over Iberia and tend to overheat land masses giving rise to little precipitation. July is the driest month in Iberia, the precipitation barely reaches 5 mm/month in areas of the south of Spain (Andalusia, southern Extremadura, Murcia, and southern Valencia) or Portugal (Baixo Alentejo and Algarve) (Chazarra 2012). The highest values of precipitation observed in July stand at around 150 mm a month, and are found in the northeast mountains or in the Basque Country.
As mentioned above, rainfall has a maximum in winter in the Atlantic coastal areas and early autumn on Mediterranean shore, due to external maritime moisture advection. Also, there is a distinctive peak in inland Iberia during springtime, unrelated to ocean influence. In some areas of the North Plateau, there is a relative maximum peak, and towards the interior eastern and northeastern regions, this peak becomes an absolute value during the course of the year (Ríos Entenza n.d.).
Iberia is a zone in between Atlantic wet climate and Mediterranean dry climate, in these transition zones, land-atmosphere interactions tend to be more intense than in others. For this reason, ET fluxes have an essential role. This, together with the fact that inland Iberia is a semiarid region, where changes in the soil moisture control the regime rainfall, makes the ET fluxes the main contributor to the precipitation (Castro et al. 2005). Several studies have proved that this characteristic springtime peak is due to the intensification of land-atmosphere interactions (Ríos Entenza (n.d.), Rios-Entenza & Miguez-Macho (2014), Rios-Entenza et al. (2014)).
Some studies have demonstrated that under conditions of weak moisture transport and high convective precipitation, recycling processes are intensified (Trenberth (1999), Bosilovich (2002), Dominguez et al. (2008), Rios-Entenza & Miguez-Macho (2014)). To some extent, this is what occurrs over IP during springtime; the enhancement of the evapotranspiration fluxes give rise to high recycling ratios in the interior areas. However, the subsequent enhancement of local and mesoscale convective regimes in the interior regions represents a necessary, but not

sufficient, condition for high recycling values to take place. The availability of soil moisture constitutes the second requirement to trigger the recycling mechanism. It is undeniable that there is a clear linkage between terrestrial sources of moisture and the springtime precipitation peak. ET fluxes promote the intensification of the hydrological cycle. Thus a significant percentage of the precipitation in the springtime is due to evapotranspiration, which means that recycling processes have great importance in this area during late spring.

As already pointed out in Section 1.3, the influence of ET fluxes and soil moisture in the rainfall regime are very relevant, especially in arid and water-stressed areas. Such is the case of the interior of the Iberian Peninsula, where there are large regions with a shallow water table (Gestal-Souto (2010), Martínez-de la Torre & Miguez-Macho (2014)). If the water table is close to the Earth's surface, it enhances the contribution of evapotranspiration fluxes and surface water in the precipitation regime (Miguez-Macho et al. (2008), Jiang et al. (2009)). In the main river valleys of Iberia, such as the Ebro, the gravity-driven lateral groundwater flow and river sipping represent an additional source to infiltration, and this gives rise to positive groundwater fluxes that contribute to the ET demands and consequently enhances precipitation.

Climate Change in the Iberian Peninsula

As a result of the Earth's climate change, both temperatures and rainfall variability are expected to be altered in every region of the planet, including in the Iberian Peninsula. The intensification of the water cycle, due to the increase in greenhouse gases in the atmosphere, is expected to lead to an augmentation of rainfall regimes. But these changes are not going to be symmetric, in some areas they are expected to be more intense than in others (Rios-Entenza et al. 2014). There are some particular places, considered as climate change "hotspots", where significant changes in climate are projected. Among these climate hotspots, we highlight deltas of Africa and Asia, glacier and snowpack dependent river basins of South Asia, and semi-arid regions, like for example, the Mediterranean area (De Souza et al. 2015). On the Mediterranean shore of the IP, the projections of the future climate suggest a decrease in precipitation, especially in the warm season (Giorgi & Lionello 2008), a rise of the sea surface temperature, and warming-enhanced evaporation. As a consequence of these processes, models predict a 20% decrease in the land surface water availability, including a reduction of the river runoff Mariotti et al. (2008). The decline of the available moisture will affect the rainfall averages over land, thus giving rise to a reduction of the recycling contribution to precipitation Rios-Entenza et al. (2014). The Mediterranean area is expected to be an especially vulnerable region to global change, where long periods of high temperatures will lead to an increase in the frequency of severe drought (Giorgi & Lionello 2008).

In Chapter 4 and Chapter 5, we focus our study on the Iberian Peninsula. But, the Iberian climate is not the overall focus of our research. The reason behind this choice is the peak of precipitation in inland Iberia during May, which is associated with an intensification of the ET fluxes. We believe that the enhancement of the ET fluxes will help us to understand some other characteristics of the climatic system Rios-Entenza et al. (2014).

1.4.2 European Climate

In Chapter 6, we focus our research on the role of the land-atmosphere interactions in the climate of the European continent. To carry out this study, we perform some numerical simulations with a coupled land-atmospheric model, covering a significant part of Europe, including the whole Mediterranean area and a substantial portion of the Atlantic Ocean. For this reason, a summary of the leading climate features of Europe is provided here.
Europe is located in the Northern Hemisphere, and it is the second smallest continent in the world; it can be considered as the western peninsula of the supercontinent Eurasia. The combination of the mountain ranges such as the Alps and the Carpathians, or high plateaus and the lowlands like the Central European Highland, and extensive coastal areas make it a place of intricate orography.

The scientific community widely accepts that global warming-induced by human activity is happening. The whole planet is warming up, and the middle latitudes, where the European continent is located, are also affected (IPCC (2007), Pachauri et al. (2014), Hoegh-Guldberg et al. (2018)). A warmer climate in Europe has contributed to more severe droughts, longer fire seasons, and to an intensification of the water cycle, that has led to an increase of the occurrence of heavy precipitation (Groisman et al. 2005)). Among the most severe weather events, we highlight the heatwaves which occurred in summer 2003, 2010, 2018 and 2019 and the floods in the summers of 2002 and 2005.
Also, the increase of the atmosphere greenhouse gas concentrations due to anthropogenic activity, such as water vapour (H2O), carbon dioxide (CO2) or chlorofluorocarbons (CFCs), leads to a rise of the global temperatures. These increases are being considered as triggers of extreme weather events. The increment of greenhouse gases leads to an intensification of the interannual variability in Central Europe (Schär et al. (2004), Seneviratne et al. (2006)).
Below we detail the European rainfall regime and the aforementioned dangerous heatwaves and droughts which have occurred in the last few decades.

Rainfall Regime in Central Europe

The North Atlantic Oscillation (NAO) is an atmospheric phenomenon dominating large-scale atmospheric circulation over the Atlantic-Europe sector. It is based on the fluctuations of the sea level pressure differences between the northern low-pressure system located approximately over Iceland and the southern subtropical high pressure situated over the Azores Islands. The NAO index is defined as the north-south surface sea-level pressure difference between the Icelandic Low and the Azores High. This north-south dipole of pressure anomalies has a positive and a negative value depending on location and intensity (Castro-Díez et al. 2002).
The NAO's positive phase occurs when both the subtropical high and the sub-polar low are stronger than usual, then the gradient pressure between these two systems becomes higher. This positive index results in a stronger Atlantic jet stream, and consequently in more frequent and intense storms coming from the Atlantic Ocean to northern Europe, and an increase of the precipitations. Also, a positive NAO tends to be associated with below-average precipitation and decreased storminess in Southern Europe. If the Azores high and the Iceland low are weaker than usual, the index NAO is negative, and the gradient pressure is smaller. With this situation, the Atlantic jet stream has a west-to-east orientation, thus the winter storms are weaker and have less impact on northern Europe. On the contrary, a negative NAO gives rise to more storms and precipitation and warmer than average temperatures in southern Europe. Additionally, a

negative index brings moist air into the Mediterranean area.
The NAO has interannual and inter-seasonal variability; also, it can maintain a positive or negative phase during long periods. A positive NAO index is prevalent in winter and negative in summer. Thus the NAO tends to be more pronounced in intensity and area coverage during the Northern hemisphere winter (Wang et al. (2010)). And the NAO effect on European precipitations and temperatures is supposed to be lower in summer. Several studies have revealed the NAO is one of the most important sources of climate variability in Central Europe (Barnston & Livezey (1987), Castro-Díez et al. (2002)).

Across the Iberian Peninsula, France, Central Europe and Eastern Europe, the atmospheric circulation is predominantly from the west; even in summer when the North Atlantic jet stream is less intense than in winter. The precipitation regime in Central Europe has its maximum in winter, mainly due to the NAO and the jet stream influence. Thereupon the precipitation during this period is mostly from advective origin. The influence of the orography is also very significant in the rainfall regime in Europe. The combination of the complex terrain, with high mountain chains and big river valleys, and the large circulation atmospheric phenomena such as the jet stream and the NAO are two of the most influential factors to the precipitation distribution.

However, neither the orography or the large circulation atmospheric phenomena can explain the peak of precipitation in Central and Eastern Europe in the summertime. Furthermore, record-breaking rainfall amounts and intensities were observed in 2002, 2005 and 2013, causing severe flooding events. In 2002, a heavy rainfall episode occurred in Central Europe. The torrential rains began on August 10th and continued for five days, causing the major river systems to burst their banks and dams to overflow. The river Danube as it flows through Austria together with the River Moldau in the Czech Republic and the River Elba in Germany caused many deaths. It destroyed towns and villages, provoking significant economic losses.
The explanation of the summertime precipitation peak can be found in the contribution of the ET to the rainfall regime, that is to say in an intensification of the recycling processes (Christensen & Christensen (2003), Ulbrich et al. (2003), James et al. (2004), Pal et al. (2004)). Furthermore, various studies, among which we highlight Van der Ent et al. (2010), have demonstrated the crucial role of land-atmosphere interactions in the occurrence probability of severe meteorological events. Both the recycling processes and the distribution in the soil wetness have significant implications in the precipitation regime in the summertime.
The European precipitation regime is also affected by other components of the climatic system which are usually not considered. The sea surface temperature (SST) of the Mediterranean influences not only the precipitation of the Mediterranean basin but also the rainfall in Central Europe (Volosciuk et al. (2016), Pastor et al. (2019)). High Mediterranean SSTs are expected due to climate change, thus leading to an increase of the ET fluxes and the atmospheric moisture transport, with a backlash on Central European rainfall. It has been demonstrated that the Mediterranean SSTs contributed to the Elbe flooding in 2002 (Pastor et al. 2019).

Heatwaves in Europe

The global temperature increase is a hot topic in climate science because the increasing temperatures due to anthropogenic activity are adversely affecting the planet Earth and the whole of humanity. Furthermore, future climate forecasts for temperatures are not encouraging either, predicting a rise of temperatures all over the world.
As outlined in the previous section, Europe has been struck by devastating meteorological events in recent decades, such as the floods which occurred in summer 2002 or 2005. As in

the case of heavy rainfalls, the occurrence of extreme heatwaves in Europe has increased in the previous years, summertime: 2003, 2006,2010, 2018 and 2019. This can be seen in Figure 1.4. In summer 2002, a record-breaking heatwave affected the whole European continent, but the impacts were more significant in France and Central Europe (Schär et al. (2004), Stott et al. (2004), García-Herrera et al. (2010)). Some years later, in summer 2010, another heatwave broke temperature records across Europe, particularly in Russia.

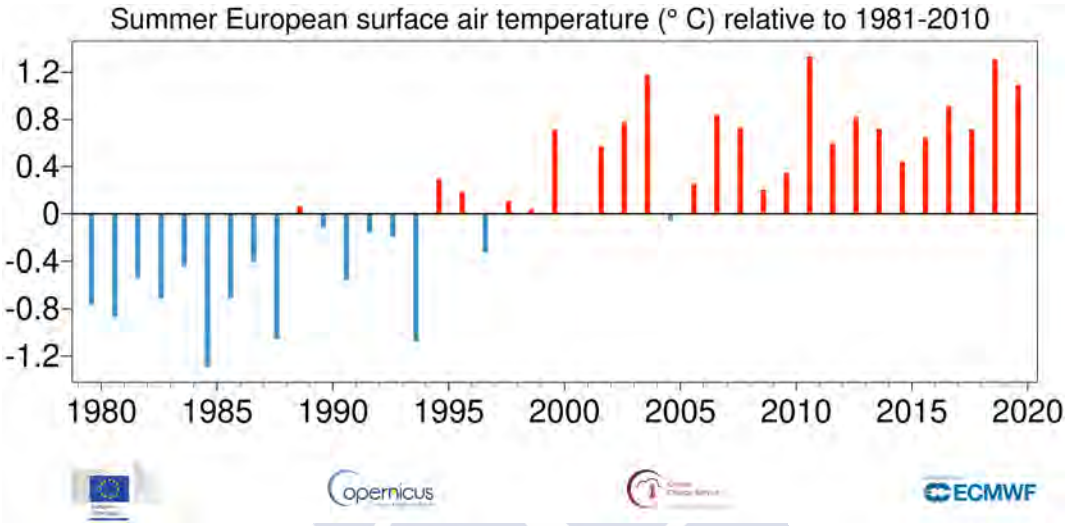

Figure 1.4: Summer European surface air temperature relative to 1981-2010. Image obtained from the official website of European Centre for Medium-Range Weather Forecasts (ECMWF) `https://www.ecmwf.int/`.

For a fuller understanding of the increase of the frequency of heatwaves, let's quickly undertake a review of the climatic system triggers that may have led to them. The phenomenon of the increase of the Earth's average temperature, also known as global warming, has given rise to an increment of the atmospheric demand. This, consequently, results in a more considerable amount of water vapour concentration in the atmosphere. Furthermore, due to the increase of incident solar radiation, evapotranspiration amounts to the atmosphere have enhanced. All these processes are connected between each other, leading to a feedback mechanism between them. During heatwaves, the presence of clear skies is quite common, further increasing temperatures. Besides, dry soil conditions result in less evapotranspiration, which ordinarily cools the ground. All these processes are linked in a cyclical chain that gives rise to the heatwave.
However, the contributing factors that give rise to this climatic risk are not entirely understood. Some studies suggest that the high temperatures reached in summer 2003 were enhanced by the anomalous conditions of SST and soil moisture in the previous seasons. Others have stressed that the reasons for the occurrence of these events were only related to the chaotic nature of the atmosphere itself, that perpetuate a blocking pattern system for several days, advecting warm air from North Africa. What is true is that the heatwaves are expected to become more common toward the end of the century in Europe (Miralles et al. 2014).

We are continually using the term heatwave, but it is essential to emphasise that this concept is not the same as extreme temperatures. A heatwave is commonly defined as a period of three or more days where maximum temperatures exceed the heatwave temperature threshold. That threshold is set differently by each national meteorological agency all around the world.

The Spanish national weather service, AEMET (Agencia Estatal de Meteorología), declares a heatwave when three conditions are met. The period lasts at least three days in a row, temperatures are beyond the 95th percentile value of the daily maximum temperature time series in summertime (July and August) in 1971-2000, and these thresholds must be exceeded by at least 10% of the governmental weather stations in the reference area. The United Kingdom's national weather service, Met Office, considers the same period but they define the temperature threshold depending on the daily maximum temperature in each UK county. Meanwhile, Australia's official weather forecasts and weather radar, Bureau of Meteorology, establishes that a heatwave occurs when both daytime and night-time temperatures are unusually high during three or more days. Finally, the World Meteorological Organization defines a heatwave as a length of five or more consecutive days of heat exceeding the average maximum temperature of the area by 5° Celsius.
To put it in simpler terms, a heatwave is a prolonged period of extreme heat and depends on the regional agency that describes it.
The increase of frequency and intensity of heatwaves should be taken seriously since this type of weather phenomena comes at the cost of a higher number of lives than any other weather hazard on the European continent. They also have tremendous economic and social impacts.

1.5 Climate modelling

Humanity has been attempting to predict and understand the weather for millennia. However, only since the middle of the 19th century, is it possible to predict the atmospheric conditions by reproducing the behaviour of the climate system mathematically. This advance was brought about by the emergence of climate models. It has to be underlined that nowadays, the study of climate and the development of physics models go hand in hand. Because of this, it is essential to keep improving meteorological models, especially in the context of climate change.
Climate models are a set of mathematical equations that simulate the behaviour of different components of the climatic system. These models were first developed to predict the atmospheric conditions in a short-term period and for a given location. Later, their use was extended to study the past and future climate over long-term periods. Among the climate models, the most commonly used are atmospheric models. There are also others which are widely employed, such as oceanographic, land surface, and ice models, which can also be coupled to the atmosphere.
The equations on which the atmospheric models are based were first formulated by the Norwegian scientist Vilhelm Bjerknes in 1904. In 1922 Lewis Fry Richardson published an extraordinary book titled "Weather Prediction by Numerical Process". This manuscript is considered one of the most remarkable books on meteorology ever written.
The equations of these models can be resolved at a global scale, termed as global climate models or General Circulation Models (GCMs), and at a regional scale referred to as Regional Circulation Models (RCMs).
Regional Climate Models numerically solve the governing equations of the atmosphere in a limited spatial area (Feser et al. 2011). They are forced with initial and boundary conditions taken from GCMs or global reanalysis, and in some cases RCMs are forced with large-scale constraints in the interior (Miguez-Macho et al. 2004). RCMs can be resolved at the order of 1 or 2 kilometres through to 25 kilometres.
Carrying out simulations with a meteorological model involves a high computational cost because supercomputers with a high level of performance have to be employed. For this reason, we believe that weather forecasting constitutes the perfect union between science and technology. The main tools employed in this thesis are an atmospheric and a land surface RCM, a detailed explanation of both of these is provided in Section 3.

Since this thesis is to be published in 2020, climate models are the ultimate and best tool that we currently have to forecast the weather. For this reason, they are the primary tool of this work. Nevertheless, we are entirely aware that more precise and accurate mechanisms to predict the atmospheric conditions are still to come, and we are exploring them. Among the latest developments, artificial intelligence is the one which arouses more interest in the weather community. This advance is possible due to the use of deep learning mathematical models, artificial intelligence could learn from past datasets how to predict the future.

USC
UNIVERSIDADE
DE SANTIAGO
DE COMPOSTELA

Chapter 2

Objectives and Structure of this Thesis

Here, we present the outline and main goals of this thesis.

In Chapter 3, the tools and methodologies applied in the present thesis are described. First, a brief explanation of the main features of the regional meteorological model WRF-ARW, the principal tool employed in this thesis, is given. As well as the characteristics of the three sets of simulations carried out with the model. Three classic recycling methods are employed to perform the computations in this thesis, their description, physics and the assumptions on which they rely are given in this chapter. A water vapour tracer technique embedded in all the sets of WRF simulations is provided. Finally, the land surface model LEAFHYDRO is presented.

In Chapter 4, the results and discussion of a study carried out with the WRF model are presented. This study aims to better understand the water cycle, by using a water vapour tracer method over the Iberian Peninsula. We also intend to evaluate the temporal and spatial distribution of atmospheric moisture in the troposphere. In this chapter, the well-mixed assumption is revisited, and a comparison between the results obtained with various classical recycling methods and the tracer technique is made.

Throughout Chapter 5, we investigate amplification and recycling processes over the Iberian Peninsula. The question of what occurs to the hydrological cycle if we remove evapotranspiration is raised. Under these conditions, the response of the rainfall regime is analysed, we intend to quantify the contribution of the direct or indirect mechanism on precipitation. To accomplish these objectives, a set of simulations with the WRF model is performed.

In Chapter 6, a study with a coupled land-atmospheric model over the European continent is made. We focus our research on the land surface interactions with the atmosphere occurred via water exchanges and heat fluxes. It is intended to assessthe role of a dynamic water table in controlling soil moisture over Europe, particularly in those water-stressed areas or regions with a shallow water table. The influence of the coupled model on the atmospheric forcings, such as temperature or precipitation, is analysed.

In Chapter 7 the main findings of this thesis are presented.

Finally, in the Appendix, an extended summary of the present thesis is provided. The language in which this summary was written is Galician, one of the official languages of the University of Santiago de Compostela.

USC
UNIVERSIDADE
DE SANTIAGO
DE COMPOSTELA

Chapter 3

Methodology

Throughout this chapter, the different tools and methodologies employed to obtain the results of the present thesis are presented to the reader. As we have already underscore in Section 1.5, the development of the science of meteorology is linked to the improvement of climate modelling. The more the climate models are improved, the more refined weather forecasts and long-term simulations we obtain. We believe it is fundamental to keep developing these models, and for this reason, the primary tools of this thesis are an atmospheric model and a land surface model. Nowadays, the Weather Research and Forecasting (WRF) regional model is one of the most frequently used models to predict and study the behaviour of the atmosphere. A brief description of the WRF model main features is presented in this chapter; as well as, the principal features of the three sets of simulations performed with WRF.

A moisture tagging capability, hereafter referred to as Water Vapour Tracer Method (WVTM), embedded in the WRF simulations, is described in Section 3.3. This procedure was developed by Insua-Costa & Miguez-Macho (2018) and implemented in the WRF code by Prof. Dr Gonzalo Miguez Macho. Thanks to the implementation of the numerical moisture tracers in the WRF model, we can accurately study the behaviour of the moisture throughout the atmospheric column, track the humidity originating in source regions, and calculate the contribution of the ET to the precipitation in the simulated areas.

Three bulk recycling models are described in detail in Section 3.2. They are based on a model developed by Budyko & Drozdov (1953) and in some simplifying assumptions. Recycling computations are carried out with these methodologies, and the results are compared to those obtained with the WVTM. As the input of the bulk recycling models, we employ the WRF output variables derived from the set up of atmospheric simulations.

Finally, the land surface atmospheric model WRF-LEAFHYDRO is presented and described in Section 3.5. WRF-LEAFHYDRO is the result of coupling the meteorological WRF model to the land surface model LEAFHYDRO, which was developed by Fan et al. (2007) and Miguez-Macho et al. (2007). This model is run with two different configurations: one including a groundwater scheme that dynamically interacts with the atmosphere, and the other with free drainage at the bottom of the soil column.

All the numerical simulations and calculations described in this chapter were performed in the Supercomputing Center of Galicia (CESGA). The computations, weather plots, tables and further results were generated by using the programming languages Fortran and Python (mainly version 3), and other tools like CDO (Climate Data Operators) or NCO (netCDF Operator). The text of this doctoral thesis dissertation was written with the document preparation system LaTeX.

3.1 The WRF model. Setup of Numerical Experiments

The Weather Research and Forecast (WRF) Modelling System is a widely-used regional numerical weather prediction and atmospheric research tool used for both operational and research purposes, and the primary tool of this thesis.
The WRF model contains two dynamic cores: the Non-hydrostatic Mesoscale Model (NMM) core designed at the National Centers for Environmental Prediction (NCEP) and the Advanced Research WRF (ARW) core, developed in large part at the National Center for Atmospheric Research (NCAR). Each dynamic core corresponds to a set of dynamic solvers that operates on a particular grid projection, grid staggering, and vertical coordinate system. In this research, the WRF-ARW is employed. Although NCAR mostly led the development of the WRF-ARW model, its maintenance and continuous modifications are carried out by partnerships. We highlight the National Oceanic and Atmospheric Administration (NOAA), the Air Force Weather Agency (AFWA), the Federal Aviation Administration (FAA), several universities and governmental organisations from various countries. WRF model is continually being developed by their creators and by the users, which implies new WRF model versions are periodically updated with new capabilities and improved parameterisation.
The WRF regional model is an open-source numerical code based on the primitive atmospheric equations using different physic parameterisations. WRF model solves the atmospheric dynamic equations in a discrete number of points, distributed in a three-dimensional grid. It is conservative for scalar variables. The horizontal resolution of each of these grids can be from metres up to hundreds of kilometres. The horizontal grid is Arakawa-C grid, where the U and V variables are calculated in the cell side, instead of in the centre of the grid cell. The mathematical WRF equations are formulated using a terrain-following mass vertical coordinate, in which the top coordinate of the model has constant pressure. These vertical or sigma-altitude coordinates follow the contour of the land, and they do not intersect it. The WRF model allows one-way, two-way and moving nest of the domains. As WRF is a regional model, the primitive equations are solved in a limited area. The WRF model also contains a multitude of physical parameterisations, many of which can be used with both dynamic cores.
The WRF-ARW system consists of a dynamics solver, which integrates the fully compressible, non-hydrostatic Euler equations. As mentioned in 1.5 the atmospheric models that have non-hydrostatic equation solvers use the full 3D momentum equation of Navier-Stokes. This equation assumes the vertical direction is incompressible (Turton 2017).
For both operational and research purposes, WRF is usually forced with initial and boundary conditions taken from Global Circulation Models (GCMs) or global reanalysis. In some cases, WRF is forced with large-scale constraints in the interior (Miguez-Macho et al. (2004), Gómez & Miguez-Macho (2017)). Although the WRF model is usually employed to obtain real data, it offers the option of performing idealised simulations for research purposes.
The WRF code itself is mostly written in Fortran programming language (Metcalf et al. 2004), and the WRF software relies on Perl and some UNIX utilities.
For further details and extensive description of the WRF model see (Skamarock et al. 2005) and (Skamarock & Klemp 2008), and the official website of the WRF model `www.wrf-model.org`.

3.1.1 First WRF Simulations Setup

A set of ten experiments hereafter referred to as SIM-IP, were carried out with the WRF modelling system (Version 3.8.1). All the computations described in Chapter 4 are computed by using these simulations. The months of April and May from 2001 to 2010 are the simulated period. SIM-IP set is centred over the Iberian Peninsula and cover a small area of the Atlantic Ocean and the Mediterranean Sea as well. Several authors such as (Mercader et al. 2010), (Cardoso et al. 2013), (Rios-Entenza & Miguez-Macho 2014) or Soares et al. (2015) have performed simulations with the WRF model over Iberia, for this reason we conclude it is an excellent tool for the present study. The model domain setup is depicted in Figure 3.1 as used in the WRF simulations has 225x225 points and a horizontal spatial resolution of 20km. The vertical grid has 54 levels expressed in a terrain-following height coordinate. Twenty levels are below 1500 metres of altitude approximately, and the domain top at 100hPa.
Simulations are forced by atmospheric initial and lateral boundary conditions with a resolution of 1-degree by 1-degree grid operationally prepared every six hours (`http://rda.ucar.edu/datasets/ds083.2`). These files, named as FNLs, are generated by the National Centers for Environmental Prediction (NCEP) with a global numerical model, also used to create Global Forecast System (GFS). Nevertheless, the FNLs are prepared about an hour after the GFS is initialised so that more observational data can be used. Parameters include: surface pressure, sea level pressure, geopotential height, temperature, sea surface temperature, soil values, ice cover, relative humidity, u- and v- winds, vertical motion, vorticity and ozone. The archive time series is continuously extended to a near-current date. The vertical coordinates in these files are expressed in sigma coordinates.
The following physics parameterisations are used: the WSM6 cloud microphysics(Hong & Lim 2006), the Dudhia scheme for shortwave radiation (Dudhia 1989), the RRTM scheme for longwave radiation (Mlawer et al. 1997), the YSU scheme for turbulence in the Planet Boundary Layer (PBL) (Chen & Dudhia 2001*a*), the NOAH land surface model (Chen & Dudhia (2001*a*), Chen & Dudhia (2001*b*)) and surface layer scheme based on Monin-Obukhov surface layer parameterisation (Monin & Obukhov 1954). The convection parameterisations used are (Kain & Fritsch 1990) and (Kain & Fritsch 1993). These parameterisations include spectral nudging for the WRF model grid ensuring us that the large-scale circulation is well represented (Miguez-Macho et al. 2004). The parameterisations schemes were selected based on previous studies already made in the same area (Rios-Entenza & Miguez-Macho (2014), Rios-Entenza et al. (2014)). For more specific details on the parameterisations, the reader is referred to Skamarock et al. (2005).
A moisture tagging capability developed by Miguez-Macho et al. (2013) and Insua-Costa & Miguez-Macho (2018) and described in detail in Subsection 3.3 was implemented in the SIM-IP set of simulations. Prof. Dr Gonzalo Miguez Macho made the implementation of this tracer capability in the model.

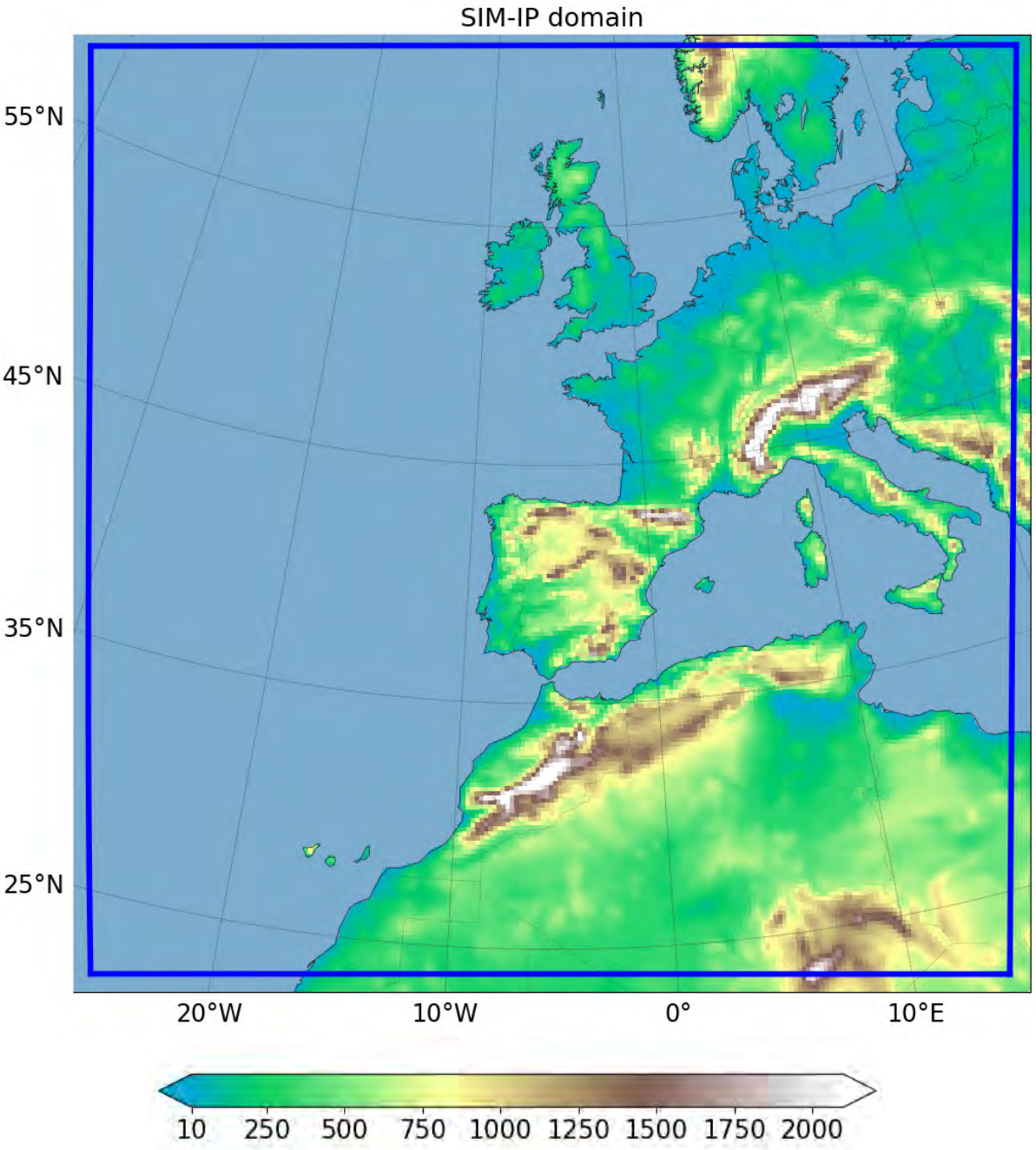

Figure 3.1: Spatial configuration of the WRF domain marked in blue lines, together with terrain height above the sea level, as used in the SIM-IP.

3.1.2 Second WRF Simulations Setup

The computations described in Chapter 5 are performed by using numerical simulations produced with the Advanced Research WRF modelling system (Version 3.4.1) over ten months of May, from May 2001 to May 2010. The set of simulations hereafter referred to as SIM-ET, are performed with two nested grids with a one-way nesting.
The parent domain has 225x225 points, and a coarse spatial resolution of 20km and the nested domain has 300x300 points and horizontal resolution of 5km, respectively named D01 and D02 in Figure 3.2. The parent domain features are the same as the domain used in SIM-IP, previously described in Section 3.1.1. The vertical coordinates in the WRF model are sigma coordinates, and for both nests, there are 27 vertical levels in the vertical coordinate.
The physics parameterisations selected are the same as in SIM-IP set of simulations: Kain-Fritsch convection (Kain & Fritsch (1990), Kain & Fritsch (1993)), WSM6 cloud microphysics (Hong & Lim 2006), RRTM scheme for longwave radiation (Mlawer et al. 1997), Dudhia scheme for shortwave radiation (Dudhia 1989), YSU scheme for turbulence in the PBL (Chen & Dudhia 2001*a*), NOAH land surface model, and Monin-Obukhov surface layer parameterisation Monin & Obukhov (1954). Convection is parameterised in the parent domain and resolved in the nested one. The nesting is one-way interacting. Parameterisations include spectral nudging for the WRF model grid. WRF runs are forced with the same atmospheric initial and lateral boundary conditions than SIM-IP. They are taken from the National Centres for Environmental Prediction (NCEP), available at the resolution of 1degree x 1degree. The nesting is one-way interacting.
A water vapour tracer technique is implemented in the WRF model to carry out the set of simulations SIM-ET (for further information of this methodology see Subsection 3.3).
The great novelty here is that in some of the WRF simulations, the evapotranspiration fluxes have been altered in Iberia. For each of ten years, from 2001 to 2010, we perform ten suites of simulations, in which ten different configurations are used. The first type of simulations consists of the default WRF control run simulation, hereafter referred to as CTL, where the land-atmosphere fluxes are normally set up. The other nine experiments also referred to as sensitivity experiments, are initialised with modified moisture distribution. In these simulations, the evapotranspiration fluxes have been gradually eliminated or doubled from the landmass of the Iberian Peninsula of the nested domain of the SIM-ET simulation setup, as seen in Figure 3.2. The suppressing of ET is done without altering the surface energy budget. Thus the water vapour is gradually removed from the land areas of both domains. The land still cools down because of ET, but the resulting water vapour is simply removed.
We have labelled each of these set of simulations depending on the ET percentage doubled or removed, and a brief explanation of the naming employed is given in Table 3.1.
Our procedure is based on a comparison between the CTL simulation and the ET altered experiments. This method was firstly used by (Schär et al. 1999). Several researchers investigating the amplification mechanism have utilised the same procedure used in SIM-ET, as a way to assessthe the impact of the ET fluxes on the regional precipitation (Beljaars et al. (1996*b*), Dirmeyer & Brubaker (1999), Seneviratne et al. (2006), Seneviratne et al. (2010), Goessling & Reick (2011), Rios-Entenza & Miguez-Macho (2014), Decker (2015)).

3.1.3 Third WRF Simulations Setup

To carry out the computations in Chapter 6, we perform a set of simulations termed as SIM-EU, with the atmospheric regional WRFV3.4.1 model (Skamarock et al. 2005) coupled to the

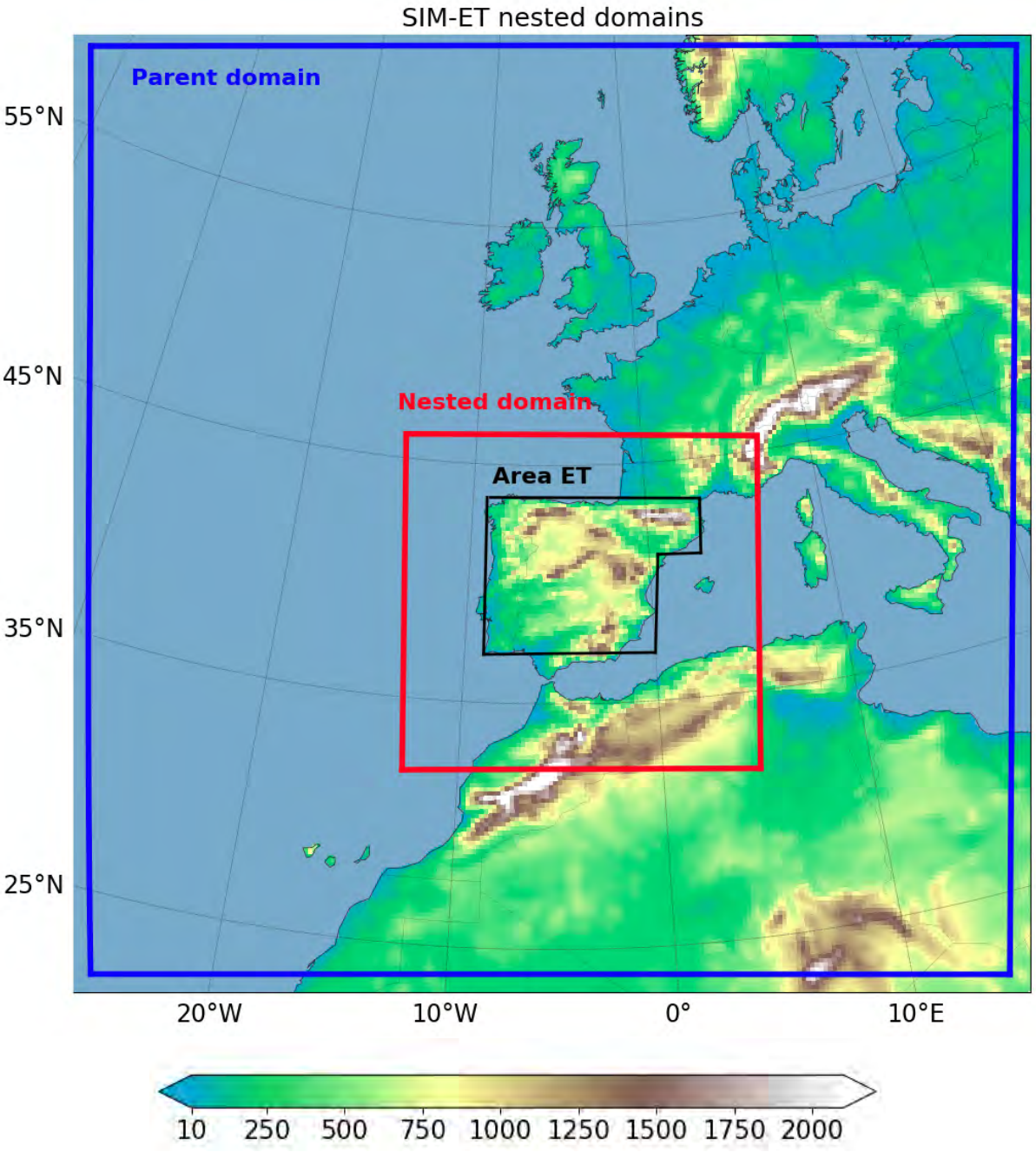

Figure 3.2: Model domains setup of the two nested domains, together with terrain height above the sea level, used in SIM-ET numerical simulation. The domains are one way nested, with a parent domain marked in blue (Parent domain) and a nested domain (Nested domain) marked in red lines. The terrestrial region marked in black lines represents the area where the ET is suppressed(Area ET).

Simulation name	Description of the control and sensitivity experiments
CTL	Control run simulation,where the land-atmosphere fluxes are normally set up.
0% ET	DRY experiment: The total ET over the land IP is removed.
15% ET	DRY experiment: Only a 15% of the original ET is maintained.
25% ET	DRY experiment: Only a 25% of the original ET is maintained.
35% ET	DRY experiment: Only a 35% of the original ET is maintained.
50% ET	DRY experiment: Only a 50% of the original ET is maintained.
65% ET	DRY experiment: Only a 65% of the original ET is maintained.
75% ET	DRY experiment: Only a 75% of the original ET is maintained.
85% ET	DRY experiment: Only a 85% of the original ET is maintained.
200% ET	WET experiment: The original ET is doubled.

Table 3.1: Terminology employed for the whole package of simulations SIM-ET, in which the ET fluxes have been altered.

LEAFHYDRO Land Surface Model (Fan et al. (2007), Miguez-Macho et al. (2007)). The LEAFHYDRO includes groundwater dynamics with a dynamic water table and river routing. The water table was validated with hundreds of observations over Europe. A detailed and technical description of the main features of LEAFHYDRO is given in Section 3.5.

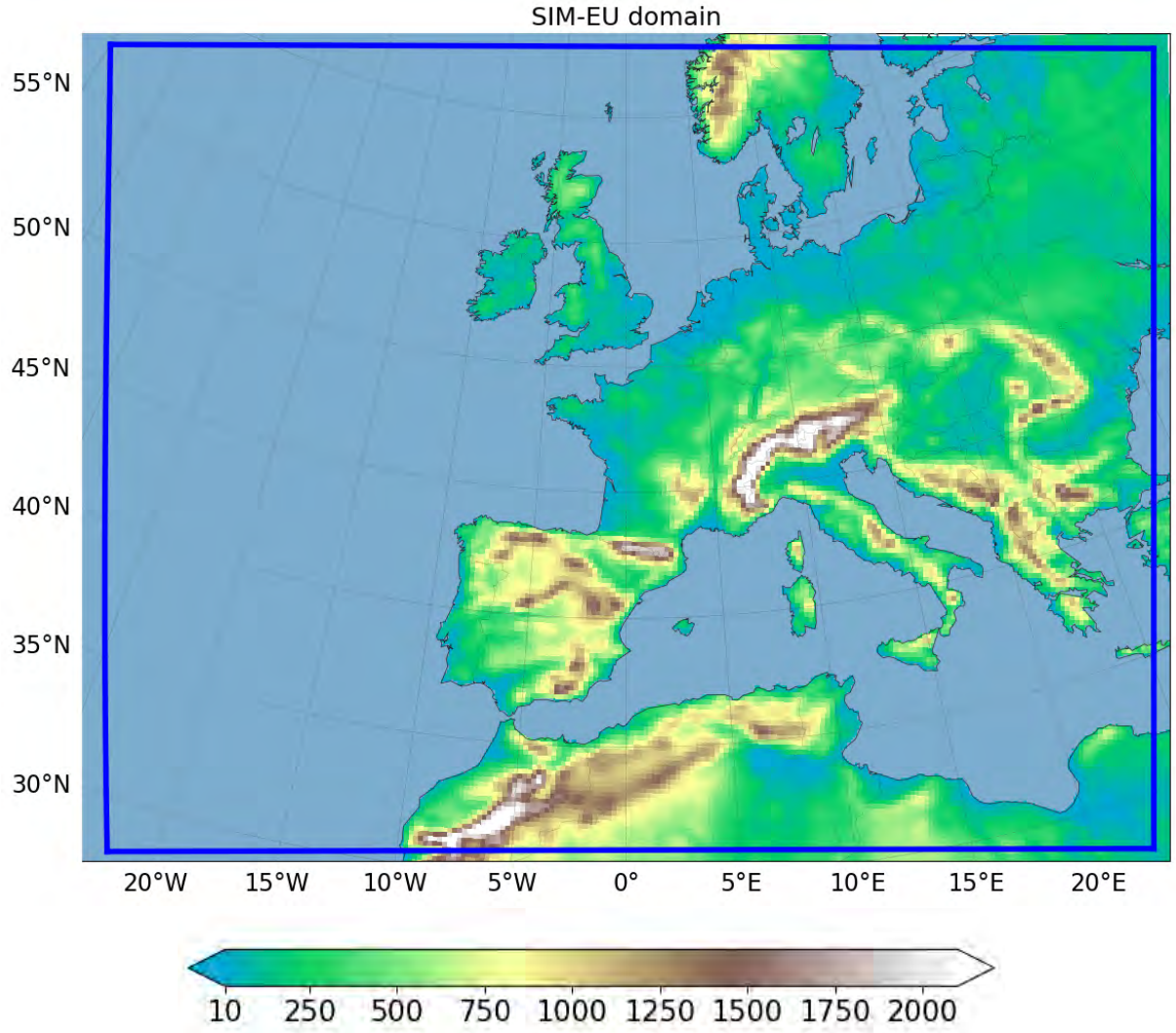

Figure 3.3: SIM-EU simulation domain marked in blue lines, and terrain height above the sea level expressed in metres.

The horizontal resolution of the atmospheric simulations conducted with the WRF-ARW is 20 km, with 250x192 points covering part of the Atlantic Ocean and most of the European continent. The vertical coordinate in the WRF model is expressed in a terrain-following height coordinate with 27 vertical levels. LEAFHYDRO simulations use the same grid as the WRF model, but it runs at a finer resolution than WRF, with a horizontal resolution of 2.5km with 2000x2000 points. Each cell of the WRF grid contains 64 cells of the LEAFHYDRO model. Atmospheric initial and boundary conditions of the WRF model are from ERA-Interim. WRF also takes soil and hydrology initial conditions from the offline run performed with the land surface model.

The LEAFHYDRO offline simulations were forced with the dataset ERA-Interim precipitation dataset produced by ECMWF for the Earth2Observe European Commission FP7 project. This is a fully global historic precipitation dataset (1979–2017) with a 3-hourly temporal and $0.1\mathrm{deg}$ spatial resolution (Beck et al. 2017), that can be taken from `http://www.gloh2o.org/`. Initial conditions for the water table are from Fan et al. (2013), a model product at 30° resolution validated with thousands of observations over Europe and the world, where soil moisture is a combination of an equilibrium profile from the water table and GFS fields.
We performed the set of simulations with the coupled model for the following years: 1995, 1996, 1997, 1998 and 2003. In each year, the period simulated is the growing season from February 1st to October 1st. We focus our study on the summertime, but the whole growing season was simulated to ensure that the spin-up time is enough to avoid cold season processes where LEAFHYDRO has difficulties.
To prevent the accumulation of biases in the soil state due to precipitation errors in the WRF simulations, we re-initialise soil conditions each year with values taken from the aforementioned offline simulations.
The WRF model was run in this study using the following physics schemes:

- Kain-Fritsch cumulus physics scheme for the convention (Kain & Fritsch (1990), Kain & Fritsch (1993)).
- WSM6 cloud microphysics scheme (Hong & Lim 2006) for the microphysics.
- Rapid Radiative Transfer Model (RRTM) longwave radiation scheme (Mlawer et al. 1997).
- Yonsei University (YSU) boundary layer scheme for turbulence in the PBL (Chen & Dudhia 2001*a*).
- Dudhia shortwave radiation scheme (Dudhia 1989).
- NOAH-MP land surface model (Chen & Dudhia (2001*a*), Chen & Dudhia (2001*b*)).

The groundwater scheme is implemented in the Noah-MP LSM. Parameterisations used include spectral nudging for the WRF model grid (Gómez & Miguez-Macho 2017).
Water vapour tracers are already implemented in the WRF model (accurately described in Section 3.3). WVTM allows us to trace water that evaporates from any selected region, tracking the origin and fate of water particles until they precipitate or are transported out of the domain. In the SIM-EU simulations tracers are activated over inland Europe.

3.2 Bulk Precipitation Recycling Models

As stated in Section 1.2.1, in this work, we employ three analytical box models. We use them to carry out recycling computations, comparing them with those obtained with the Eulerian method explained in Section 3.3.
Bulk precipitation recycling models are based on the simplified model developed by Budyko & Drozdov (1953) and described in Budyko et al. (1974), as it has previously been mentioned. The fundamental principle of this method is the conservation of the total water content over a specific region. Following the notation of Burde & Zangvil (2001) and Dominguez et al. (2006), the mathematical form of this equation is:

$$\frac{\partial W}{\partial t} + \frac{\partial (u \cdot W)}{\partial x} + \frac{\partial (v \cdot W)}{\partial y} = ET - P \tag{3.1}$$

Where W stands for the amount of water stored or precipitable water in a unit area column of air, P is referred to precipitation and ET is evapotranspiration. u , v are precipitable water weighted vertically integrated water vapour velocities in the direction x and y respectively, also termed as effective velocities. Analytical models commonly use atmospheric reanalysis data as input. In this work, we employ WRF output variables derived from the WRF-ARW simulations, which main technical features are described in Section 3.1.
The first term of the equation $\partial W/\partial t$ represents the change of the precipitable water storage in time for a particle of water vapour; the second $\partial(u \cdot W)/\partial x$ and third term $\partial(v \cdot W)/\partial y$ represent the zonal and meridional flux advection respectively. The addition of these two last terms is defined as divergence of the water vapour flux term, and it is defined as shown in Equation 3.2. This value can be calculated using the Gauss theorem if it is applied in an area.

$$\frac{\partial (u \cdot W)}{\partial x} + \frac{\partial (v \cdot W)}{\partial y} = \vec{\nabla}\vec{Q} = \frac{1}{R}\oint_S \vec{Q}\vec{n}\, dS = OUT - IN \tag{3.2}$$

Where $\vec{Q}$ is a vector of water vapour flux, S is the area of the region employed to perform the computations, $\vec{n}$ is the unit vector perpendicular to the border of the area, and OUT and IN are the flux leaving or entering the domain. As seen, the divergence term provides the amount of flux coming from the outside or the inside of the region, depending on how positive or negative is the divergence. Following the last definition of the divergence term, the equation of the conservation of water over a specific region can be redefined, as shown in Equation 3.3.

$$\frac{\partial W}{\partial t} = IN + ET - OUT - P \tag{3.3}$$

Analytical models can be classified into stationary (Eltahir & Bras (1994), Schär et al. (1999)) and non-stationary models (Dominguez et al. 2006), depending on how the time derivative of the precipitable water is considered. The stationary models like do not take into account the variations in time. Hence they are only available for monthly, seasonal or yearly timescales, while the non-stationary models provide daily or smaller timescale recycling ratios because they consider the time derivative of the precipitable water (Sánchez Altamirano 2016).
Analytical models generally provide the value of regional recycling ratio and some particular models account for the spatial variability and thus a local recycling ratio is given. This quantity is defined as the fraction of the local evaporative precipitation P_e to total precipitation $P_e(t,i,j) +$

$P_a(t,i,j)$ for a specific point (i,j) of the region and time t (Burde & Zangvil (2001), Van der Ent et al. (2010)). It varies with the position, time and size of the cells or resolution of the area studied.

$$\rho(t,i,j|S,\zeta) = \frac{P_e(t,j,i|S,\zeta)}{P_e(t,j,i|S,\zeta) + P_a(t,j,i|S,\zeta)} \tag{3.4}$$

The regional recycling ratio is dependent on time t, on the size of the region S, and the shape of the area ζ.

$$R(S,\zeta) = \frac{\int P_e(t,j,i|S,\zeta)dS}{\int (P_e(t,j,i|S,\zeta) + P_a(t,j,i|S,\zeta))dS} = \frac{\sum_{c=1}^{n}(\rho_c \cdot P_c \cdot S_c)}{\sum_{c=1}^{n} P_c \cdot S_c} \tag{3.5}$$

As we have already mentioned, the analytical models based on the Budyko's model use underlying assumptions; as new models have been developed, these assumptions have disappeared through the course of the years. The following assumptions are the most used:

- Time-averaged data is employed to estimate moisture fluxes, for example, monthly. The use of time-averaged information is not an inherent assumption to the model, but it involves it. Following Fitzmaurice (2007), there are two methods of processing the moisture flux on a monthly scale, termed as time-averaged method and accumulated method. In the first method, the moisture influx used as input to the recycling model is calculated by averaging the time-averaged vertically integrated moisture flux field. Most of the bulk recycling studies employ this technique. The second one is a much more realistic method which computes monthly moisture influx by using time-scale data. Most of the data employed to calculate the recycling methods are taken by satellite. Still, in the present thesis, we calculate the moisture influx with meteorological variables obtained from the WRF model outputs. The use of time-averaged data tend to overestimate recycling ratio values (Brubaker et al. 1993), and the variations occurring in smaller scales than monthly are not well-captured (Dirmeyer & Brubaker 2006).

- The change in atmospheric storage term is neglected. Eltahir & Bras (1994) demonstrated that at a long time-scale, for example, monthly, the change in storage of atmospheric water vapour is small compared to the atmospheric water vapour fluxes. Hence the term referred to time dependence can be dropped from the equations. Some years later, Dominguez et al. (2006) or Fitzmaurice (2007) showed that recycling ratio results might be affected by the use of this supposition, as the daily variations of moisture storage change are not taking into account.

- Finally, the major assumption made by the recycling models is that the atmosphere is well mixed. It states turbulence and convective processes, driven by sensible heat fluxes, are suppose to mix the fractions of local source of water (evapotranspired) and all other sources of water (advected) with the dry air throughout the tropospheric column (Budyko et al. (1974), Burde & Zangvil (2001)). That is, the probability of the external molecules of advective origin to be precipitated is the same as the inside of the region water vapour molecules throughout the tropospheric column. Mathematically implies that the ratio of advected water molecules in the precipitation P is the same as that in the vertically integrated atmospheric moisture W and it can be expressed as:

$$\frac{P_a}{P_e} = \frac{W_a}{W_e} \Leftrightarrow \frac{P_a}{P} = \frac{W_a}{W} \Leftrightarrow \frac{P_e}{P} = \frac{W_e}{W} \tag{3.6}$$

Where the subscript a refers to water molecules advected from outside of the domain and e to the water molecules evapotranspired within the study region. The well-mixed assumption was first employed by Budyko et al. (1974), but as recycling models improved with the increment of computational capacity, some drawbacks associated with the use of this assumption were demonstrated. For example, Koster et al. (1988) doubt the truthfulness of this assumption because it implies the ET in the lower troposphere is considered to be well mixed. Nevertheless in 1994, Eltahir & Bras (1994) still justified the use of the assumption by arguing that the convective processes perfectly mix the water vapour of the PBL, which is the area where the majority of vapour is contained. A study with a water vapour tracer method developed by Bosilovich (2002) proves that similar recycling ratios do not mean similar vertical distributions through the atmosphere because the well-mixed assumption is not able to reflect the convective processes. Other drawbacks are that the time period has to be longer than the time of boundary layer mixing (Dominguez et al. 2006) and that it can cause incorrect estimates of recycling in regions of strong shear ((Gößling & Reick 2013), (Dominguez et al. 2016)). Fitzmaurice (2007) developed a strategy to relax this assumption, but it introduces coefficients that are difficult to determine. Even though these strong modelling suppositions have been relaxed in more recent studies, the majority of the bulk recycling mo still rely on the well-mixed assumption. A more detailed explanation of the well-mixed assumption and its shortcoming can be found in Fitzmaurice (2007), Vautard et al. (2013), Gößling & Reick (2013) or Sánchez Altamirano (2016).

To bring clarity in the discussion of the recycling methodologies, we will employ three precipitation recycling models that use some of the previous assumptions, and they are explained in more detail below. These recycling models can be easily applicable to a variety of simulations and analyses already available, which constitutes a significant advantage. In the present thesis, we employ WRF outputs as inputs of the recycling models. In Section 4.5, we will compare the predictions obtained with these analytical box models to that of the proposed with Water Vapour Tracer Method (WVTM). The comparison of all the results obtained is handy to assess the accuracy of the analytical models to reproduce the real recycling values.

3.2.1 Numerical Recycling Model: Eltahir and Bras (1994)

Here, we present the 2-dimensional numerical recycling method developed by Eltahir and Brass (Eltahir & Bras (1994) and Eltahir & Bras (1996)), hereafter referred to as EBM. It is based on the principle of mass conservation (Equation 3.3) and it undertakes three of the assumptions previously explained.
EBM computes the recycling ratio in a spatially distributed grid; the study region is subdivided into multiple cells, providing a regional value (given in Equation 3.13) and so a spatial pattern of recycling over the study area. For the calculations, we employ as subdivisions the cells of the model themselves.
Since this method considers two species of water vapour molecules in the water balance equation; this equation is split in the two following expressions:

$$\frac{\partial W_a(i,j)}{\partial t} = IN_a(i,j) - OUT_a(i,j) - P_a(i,j) \tag{3.7}$$

$$\frac{\partial W_e(i,j)}{\partial t} = IN_e(i,j) + ET(i,j) - OUT_e(i,j) - P_e(i,j) \tag{3.8}$$

Where (i,j) represents each of the cells in the model domain, the subindices e and a indicates the origin of the moisture from inside or outside the region, IN represents the inward flux coming into the considered cell, OUT is the outward flux going out of the cell.
EBM applies the equation of conservation of water mass as a function of the space and time on horizontal grid cells. The time period our WRF simulations are always higher than a month. Thus the storage term can be neglected because it is much smaller than the other terms. Also, the horizontal resolution of the data employed has to be small enough to resolve significant spatial variability in evaporation and fluxes.

$$IN_a(i,j) = OUT_a(i,j) + P_a(i,j) \tag{3.9}$$

$$IN_e(i,j) + ET(i,j) = OUT_e(i,j) + P_e(i,j) \tag{3.10}$$

By employing the local recycling ratio as it is defined in Equation 3.4, and with the application of the well-mixed assumption, the previous expressions, Equation 3.9 and Equation 3.10, result in:

$$IN_a(i,j) = (1 - r(i,j)) \cdot OUT(i,j) + (1 - r(i,j)) \cdot P(i,j) \tag{3.11}$$

$$IN_e(i,j) + ET(i,j) = r(i,j) \cdot OUT(i,j) + r(i,j) \cdot P(i,j) \tag{3.12}$$

By dividing these two equations and rearranging, the local recycling ratio as it was defined by Eltahir & Bras (1994) is given in the following equation:

$$\rho_{EBM}(i,j) = \frac{IN_e(i,j) + ET(i,j)}{IN_a(i,j) + IN_e(i,j) + ET(i,j)} \tag{3.13}$$

The corresponding regional recycling value can be obtained by applying the results of Equation 3.4 to the results of the Equation 3.13.

This numerical procedure assumes the atmosphere is well mixed, and that sufficient long timescales the variation in the storage of atmospheric water vapour is small in comparison with fluxes of atmospheric water vapour, including evaporation, and thus can be neglected. Among the classic models employed in this thesis, EBM is the only method that relies on the assumption that the moisture fluxes are time-averaged. This hypothesis gives good results in regions where the fluxes are barely constant as in the Amazon region. Still, it can cause incorrect estimations of the recycling calculations in areas with variable fluxes.

With this methodology, the spatial recycling patterns tend to follow the prevailing winds of the study area. Hence these patterns tend to be very smooth. On the whole, recycling values obtained with this method are often smaller than those obtained with other bulk methods Dominguez et al. (2006).

EBM was coded in Fortran programming language and provided by its author Dr Alexandre Rios Entenza. For more information about the computational details of this method, see Appendix C of (Ríos Entenza n.d.).

3.2.2 Analytical Recycling Model: Schär et al. (1999)

One of the most straightforward manners to compute the regional recycling ratio are through the analytic integral moisture budget models, whereby the condition of a well-mixed atmosphere is applied in an integral form. In this thesis, we make use of the formula derived from the analytical method developed by Schär et al. (1999) (hereafter referred to as SCM) to perform the recycling computations. SCM is based on the equation of conservation of water over a specific region. SCM assumes that the change in atmospheric storage can be neglected and the atmosphere is fully mixed. By applying this last assumption to the Equations 3.7 and 3.8 derived from the mass conservation, we define the recycling ratio as:

$$R = \frac{P_e}{P} = \frac{OUT_e}{OUT} = \frac{\partial W_e/\partial t}{\partial W/\partial t} \tag{3.14}$$

By combining this expression of the recycling ratio with the Equations 3.7 and 3.8, we obtain:

$$(1-R)\cdot\left(\frac{\partial W}{\partial t} + P + OUT\right) = IN \tag{3.15}$$

$$R\cdot\left(\frac{\partial W}{\partial t} + P + OUT\right) = ET \tag{3.16}$$

The analytical expression of SCM to compute the regional recycling ratio is given by the Equation 3.17.

$$R_{SCM} = \frac{P_e}{P} = \frac{ET}{IN+ET} \tag{3.17}$$

Where ET and IN represent the accumulated evapotranspiration and the total input of moisture entering the boundaries of the region during the considered period. As the input of this analytical recycling model, all species of mixing ratio, velocity, pressure and precipitation from the WRF model are used.

Among the limitations of this model, we highlight that SCM does not consider the variations within the region since the terms used for the calculations are area-averaged quantities. Also, this method tends to underestimate recycling under non-parallel fluxes (Burde & Zangvil 2001), as it does not respect the direction of the moisture flux concerning the geometry of the region.

3.2.3 Dynamical Recycling Model: Dominguez et al. (2006)

In this section, we scrutinise a recent recycling model, developed by Dominguez et al. (2006) and Martinez & Dominguez (2014) and employed in some other studies (Dominguez et al. (2008), Martinez et al. (2016)). This dynamical recycling model (DRM) is a two-dimensional semi-Lagrangian analytical model derived from the Equation 3.1.
Unlike other analytical models, DRM incorporates the change in the moisture storage, represented by the first term of the conservation mass equation. So this method is applicable at a range of scales, from daily to monthly and longer. The only assumption made in this model is the atmosphere is fully mixed. By combining the expression of the well-mixed assumption and the conservation of water mass, the expression can be rewritten in terms of $(1-\rho)$ as:

$$W \cdot \frac{\partial(1-\rho)}{\partial t} + (u \cdot W) \cdot \frac{\partial(1-\rho)}{\partial x} + (u \cdot W) \cdot \frac{\partial(1-\rho)}{\partial y} = -ET \cdot (1-\rho) \tag{3.18}$$

Here, this methodology introduces a new coordinate system:

$$\chi = x - u \cdot t \tag{3.19}$$

$$\epsilon = y - v \cdot t \tag{3.20}$$

$$\tau = t \tag{3.21}$$

Where $\varepsilon(\chi, \epsilon, \tau)$, $W(\chi, \epsilon, \tau)$, $\rho_{DRM}(\chi, \epsilon, \tau)$ respectively represents evaporation, precipitable water and the local recycling ratio, along the two-dimensional trajectory $[\chi(\tau'), \epsilon(\tau')]$.
Burde & Zangvil (2001) also employed a new coordinate system, but they dropped from the equation the storage term, making for solving the differential equation more challenging. Expressing the Equation 3.18 as a function of the new coordinates, the three partial terms are noted as:

$$\frac{\partial(1-\rho)}{\partial x} = \frac{\partial(1-\rho_{DRM})}{\partial \chi} \tag{3.22}$$

$$\frac{\partial(1-\rho)}{\partial y} = \frac{\partial(1-\rho_{DRM})}{\partial \epsilon} \tag{3.23}$$

$$\frac{\partial(1-\rho)}{\partial t} = -\frac{\partial(1-\rho_{DRM})}{\partial \chi} - \frac{\partial(1-\rho_{DRM})}{\partial \epsilon} + \frac{\partial(1-\rho_{DRM})}{\partial \tau} \tag{3.24}$$

Substituting these expressions in the Formula 3.18 and solving, the local recycling ratio can be written as an ordinary differential equation:

$$\rho_{DRM}(x, y, t) = 1 - exp\left[-\int_0^{\tau} \frac{ET(\chi, \epsilon, \tau)}{W(\chi, \epsilon, \tau)} d\tau\right] \tag{3.25}$$

The local recycling ratio can quantify the ET contribution from anywhere in the whole domain, to the precipitation in a particular cell. The recycling ratio estimated with DRM depends on the shape and the size of the domain. While some analytical recycling models just let us calculate the regional recycling ratio, with DRM local recycling ratio can also be calculated. The regional recycling ratio is obtained as a sum of the Equation 3.25, in all the cells of the domain weighted by the amount of precipitation falling in each cell of a particular area.

Almost a decade later of this methodology was published, Martinez & Dominguez (2014) demonstrated that the contributions from different subregions inside the study domain could be separated. This method allows us to quantify the relative contribution from the different sources to the atmospheric moisture over a given sink region. In this thesis, we quantify the contribution of the source region marked in black lines in Figure 3.4 to the atmospheric moisture.
The numerical implementation of DRM is made by using a backward trajectory scheme, where the forward trajectory of a particle is is considered as equivalent to the backward trajectory in time. The mathematical description of this methodology is made in Merrill et al. (1986), similarly described in Equations 3.26 and 3.27, where the time step Δt is negative. This method traces the advected moisture until it leaves the domain.

$$x^{n-1} = x^n + \left(\frac{u^n + u^{n-1}}{2}\right) \cdot \Delta t \tag{3.26}$$

$$y^{n-1} = y^n + \left(\frac{y^n + y^{n-1}}{2}\right) \cdot \Delta t \tag{3.27}$$

Because the calculations are done along back-trajectories, we use as input data one additional month in the past. As the input of the DRM, we use the WRF outputs. Particularly, we make use of total precipitation, evapotranspiration, zonal and meridional winds and precipitable water (expressed in S.I units). DRM does not contemplate movements of flux between the cells contained in the domain, meaning each cell shall be considered as an isolated region, where a value of evaporation precipitation water is given.
The programming code of the DRM used in this thesis was kindly provided by their creators Prof Dr Francina Dominguez and Dr Alejo Martinez and adapted by the authors of this thesis.

3.3 Water Vapour Tracers Method (WVTM)

A recent moisture tracking technique embedded in the atmospheric regional model WRF-ARW referred to as Water Vapour Tracer Method (WVTM), is employed in our research. This method has been recently incorporated into the regional atmospheric model WRF-ARW (Miguez-Macho et al. 2013) and thoroughly validated (Insua-Costa & Miguez-Macho 2018), and employed in various studies (Ríos Entenza (n.d.), Dominguez et al. (2016), Insua-Costa & Miguez-Macho (2018)). This moisture tracer capability has been incorporated in all the experimental setups of WRF simulations employed in this thesis by Prof. Dr Gonzalo Miguez Macho.

Moisture tagging is based on the concept of following or tracing the water from its surface source through space and the phase transitions, describing all physical processes of the water cycle until it precipitates or leaves the model domain. Moisture tagging mathematically means that a second numerical formulation of the atmospheric cycle is added to the model, in which the moisture coming from a source area is treated as a new moisture species (or several, one for each hydrometeor considered in the simulation). This tracer moisture undertakes all physical processes in the water cycle, such as advection, diffusion, convection and cloud microphysics mirroring full moisture but without interfering with it. More details about the implementation of the ET-tagging algorithm are given in Insua-Costa & Miguez-Macho (2018).

At the beginning of the simulation, there is no tagged moisture in the domain; the formation of this tagged moisture starts with evapotranspiration processes over a selected area. As simulation advances, this moisture enters the lower levels of the atmosphere and ascends through the PBL and beyond. All water tagged species are followed along in the atmosphere until they leave the domain through the lateral boundaries or precipitate. At every grid cell, precipitation with origin in moisture from the tagged area is explicitly distinguished from rain derived from other moisture. The tagged moisture can leave the study region at the lateral boundaries through outflow if this tagged water return from outside of the domain is not taken into account with regard to recycled precipitation. Since the method is embedded in the WRF model, the tracer analysis is only as real as are the processes in WRF. Currently, numerical atmospheric models are regarded as the best existing tool to predict the evolution of the climate system; hence we consider WVTM as a reliable technique for recycling computations. To get the aforementioned new moisture species and thus track the tagged water pathways through the atmosphere, some of the original WRF model parameterisations were modified.

It is important to point out that among all the parameterisations that can be selected in the WRF model, the implementation of the WVTM is just available to some WRF parameterisations. The authors have selected the following parameterisations: WSM6 cloud microphysics scheme (Hong & Lim 2006); YSU scheme for turbulence in the PBL (Chen & Dudhia 2001*a*); Kain-Fritsch convection (Kain & Fritsch (1990) and Kain & Fritsch (1993)) although they can be used at the convective-resolving scale; NOAH land surface model is used (Chen & Dudhia (2001*a*), Chen & Dudhia (2001*b*)); the Rapid Radiative Transfer Model (RRTM) (Mlawer et al. 1997); Dudhia schemes for short and long radiation (Dudhia 1989). The tracer scheme, as applied to the cloud microphysics, assumes the moisture of all origins is well mixed within one model layer and in each grid cell.

These parameterisations were modified by adding a second numerical formulation of the atmospheric cycle in the WRF model, and thus we obtain six new moisture species named tracers in the output of the WRF model. These new prognostic variables represent the tagged moisture species corresponding to the six original mixing ratios in the WRF model. Their

names, definition and units, as shown in the WRF code, of these new three-dimensional mixing ratios are shown in Table 3.2. These tracers mimic the evolution of all the water species but do not interfere with their full moisture counterparts.

Short Name	Description and Units and Dimensions
TRQFX	Upward tracer moisture flux at the surface ($^{kg}/_{m^2 \cdot s}$)
TR_RAINNC	Accumulated total strat. precipitation from tracer moisture (mm)
TR_SNOWNC	Accumulated total snow and ice from tracer moisture (mm)
TR_GRAUPELNC	Accumulated total graupel from tracer moisture (mm)
TR_RAINC	Accumulated total cumulus precipitation from tracer moisture (mm)
TR_THUM_U_PHY_DT	Tracer total humidity * x-wind component * dt ($kgkg - 1m$)
TR_THUM_V_PHY_DT	Tracer total humidity * y-wind component * dt ($kgkg - 1m$)
tr_qv	Tracer mixing ratio for water vapour from ET ($^{kg}/_{kg}$)
tr_qc	Tracer mixing ratio for cloud water from ET ($^{kg}/_{kg}$)
tr_qr	Tracer mixing ratio for rain water from ET ($^{kg}/_{kg}$)
tr_qi	Tracer mixing ratio for ice from ET ($^{kg}/_{kg}$)
tr_qs	Tracer mixing ratio for snow from ET ($^{kg}/_{kg}$)
tr_qg	Tracer mixing ratio for graupel from ET ($^{kg}/_{kg}$)
tr_qh	Tracer mixing ratio for hail from ET ($^{kg}/_{kg}$)

Table 3.2: Name, definition and units of the tracer variables as seen in the WRF code.

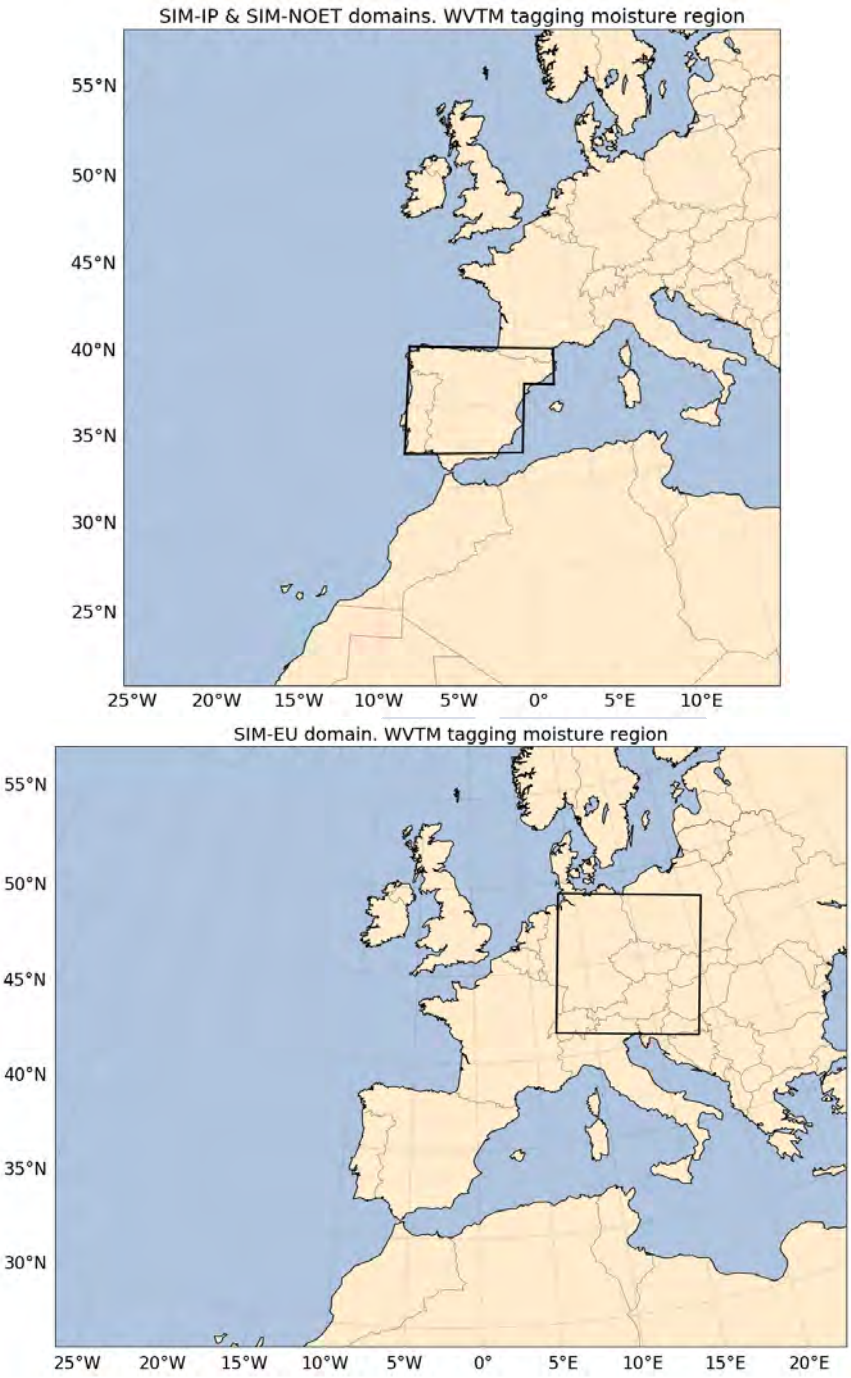

Figure 3.4: Simulated domains and WVTM moisture tagging areas marked in black lines, for the Iberian Peninsula and SIM-IP and SIM-ET experiments (upper figure) and for Europe and SIM-EU experiment (figure below).

WVTM provides a detailed three-dimensional picture of moisture sources in selected regions. Humidity can be tagged in 3D or 2D moisture sources. As for tagging water source areas, we have defined two 2D sources, both of them corresponding to terrestrial regions. The landmass of the IP marked in black lines in Figure 3.4 a is defined as a tagged region in both SIM-IP and SIM-ET experiments. And, we have selected as tagging region for the SIM-EU set of simulations, the land area framed with black lines is shown in Figure 3.4 b.

Computations with the WVTM

Recycling ratio

The implementation of the moisture tracers in the WRF model constitutes a very realistic method to describe the atmospheric processes since these tracers replicate the same equations than their counterparts. Hence, we consider WVTM an accurate method to estimate the contribution of the recycling processes in any study region. We have already defined in Section 1.2, moisture or precipitation recycling ratio as a diagnostic measure employed to quantify the percentage of precipitation falling in an area which originates from evaporation within the same region. The mathematical definition of the process commonly referred to as precipitation recycling in the literature is given in Equation 3.28 as it is described in Burde & Zangvil (2001), Van der Ent et al. (2010), Gimeno et al. (2012), Van der Ent (2014) and Rios-Entenza & Miguez-Macho (2014). As in the case of the analytical models, this mathematical term is referred to as local recycling ratio.

$$\rho_{WVTM}(i,j,\Delta t|A,\varepsilon) = \frac{P_{tagged}(i,j,\Delta t|A,\varepsilon)}{P_{tot}(i,j,\Delta t|A,\varepsilon)} \tag{3.28}$$

Where $\rho_{WVTM}(i,j,\Delta t)$ is the recycling precipitation depending on time Δt and defined in each cell of the WRF domain, where the case-study region has an area size A and a shape ε. $P_{tot}(i,j,\Delta t)$ refers to the contributions of the precipitation from internal origin and the precipitation derived from moisture advected into the region. While $P_{tagged}(i,j,\Delta t|A,\varepsilon)$ is the precipitation coming from the tagged area that falls in the point (i,j) .

$$R_{WVTM}(\Delta t|A,\varepsilon) = \frac{\sum_{i,j}\rho_{WVTM}(i,j,\Delta t|A,\varepsilon)\cdot P_{tot}(i,j,\Delta t|A,\varepsilon)\cdot \Delta A(i,j)}{\sum_{i,j}P_{tot}(i,j,\Delta t)\cdot \Delta A(i,j)} \tag{3.29}$$

$R_{WVTM}(i,j,\Delta t)$ is defined as the regional recycling ratio averaged over the selected tagged area as in Dominguez et al. (2006).

Column-integrated moisture ratio

The column-integrated water vapour or precipitable water (IWV) is an essential parameter in climate science. The AMS (American Meteorological Society) defines this term as the amount of water potentially available of the atmosphere for precipitation, usually measured in the tropospheric column.
Mathematically, if $q(p)$ is the total mixing ratio at the pressure level p, then the precipitable water IWV contained in an atmospheric column between the pressures P_1 and P_2 is given by the following Equation 3.30. Where ρ represents the density of water and g is the acceleration of gravity.

$$IWV = \frac{1}{\rho \cdot g} \int_{P_1}^{P_2} q \cdot dP \tag{3.30}$$

In this thesis, we have adapted the computation of integrated water vapour to the available mixing ratios in the WRF outputs, both the default mixing ratios and the new tracer mixing ratios. Thus, we have defined the following three equations (Eq. 3.31, Eq. 3.33, Eq. 3.32) based on the column-integrated water vapour definition.

Column-integrated condensed moisture

$$IWV_{cond} = \frac{1}{\rho \cdot g} \int_{P_{low}}^{P_{up}} q_{cond} \cdot dP = \frac{1}{\rho \cdot g} \int_{P_{low}}^{P_{up}} \left(q_{cloud} + q_{rain} + q_{ice} + q_{snow} + q_{graupel}\right) \cdot dP \tag{3.31}$$

Where q is the mixing ratio and the subindex $cond$ indicates that the variable is the sum of the mixing ratio corresponding to cloud water (q_{cloud}), rain (q_{rain}), cloud ice (q_{ice}), snow content (q_{snow}) and graupel ($q_{graupel}$) but not the water vapour mixing ratio. Therefore, q_{cond} is the sum of the condensed original mixing ratios in the whole domain of the WRF simulation. The integral is made between the pressure levels P_{up} and P_{low}, that respectively represent the upper and the lower vertical levels.

Column-integrated tagged total moisture

$$\begin{aligned} IWV_{cond,tagged} &= \frac{1}{\rho \cdot g} \int_{P_{low}}^{P_{up}} q_{cond,tagged} \cdot dP \\ = \frac{1}{\rho \cdot g} \int_{P_{low}}^{P_{up}} &\cdot (tr\_qv + tr\_qc + tr\_qr + tr\_qi + tr\_qs + tr\_qg + +tr\_qh) \cdot dP \end{aligned} \tag{3.32}$$

Column-integrated tagged condensed moisture

$$\begin{aligned} IWV_{tot,tagged} &= \frac{1}{\rho \cdot g} \int_{P_{low}}^{P_{up}} q_{tot,tagged} \cdot dP \\ = \frac{1}{\rho \cdot g} \int_{P_{low}}^{P_{up}} &(tr\_qc + tr\_qr + tr\_qi + tr\_qs + tr\_qg + tr\_qh) \cdot dP \end{aligned} \tag{3.33}$$

The subindex $tagged$ in the mixing ratios q of the two previous equations indicates that the mixing ratio is only computed in the tagged source area. According to this definition, $q_{tot,tagged}$

is the mixing ratio of the total tagged moisture, and $q_{cond,tagged}$ is the mixing ratio of the tagged condensed moisture.
We employ these three parameters as an indicator of intense cloud and precipitation formation. These values are calculated in the same way as in Knoche & Kunstmann (2013) and allow us to know more information about the convective state of the domain.
Besides, we define the ratio between the total tagged precipitable water $IWV_{tot,tagged}$ to the total precipitable water IWV as the ratio of column integrated moisture (Eq. 3.34):

$$\rho_{IWV}(i,j) = \frac{IWV_{tot,tagged}(i,j)}{IWV(i,j)} \tag{3.34}$$

The domain average of the regional recycling rates is referred to as regional recycling precipitable water:

$$R_{IWV}(\Delta t) = \frac{\sum_{i,j} IWV_{tot,tagged}(i,j)}{\sum_{i,j} IWV(i,j)} \tag{3.35}$$

By doing the quotient between both regional ratios obtained through WVTM and the computation of the moisture in the column, we employ the parameter termed as local recycling efficiency and already defined in Dominguez et al. (2016):

$$eff = \frac{R_{WVTM}(\Delta t|A,\varepsilon)}{R_{IWV}(\Delta t)} \tag{3.36}$$

Values of moistening efficiency depict the efficiency or ability to transform available atmospheric moisture into precipitation.

3.4 Relative Change in Precipitation

In the two previous Sections 3.2 and 3.3, various methodologies to study the recycling processes have been described. But, it is necessary to complete the research with the analysis of the amplification processes, as highlighted above in Section 1.2.2. For that purpose, we make use of a mathematical procedure that allows us to assess the impact of the amplification on precipitation.
The relative change in precipitation is a new parameter defined in Rios-Entenza & Miguez-Macho (2014), and mathematically described in the Equation 3.37 as follows:

$$\rho * (i, j, \Delta t) = \frac{P_{CTL}(i, j, \Delta t) - P_{ET-altered}(i, j, \Delta t)}{P_{CTL}(i, j, \Delta t)} \tag{3.37}$$

- $P_{CTL}(i, j, \Delta t)$ - Total precipitation given for each grid cell (i, j) of the study domain and for each instant of time Δt. The subindex CTL refers to the name control simulation, since this precipitation is obtained from a simulation in which the ET fluxes are normally set up. This model simulation is defined in Section 3.1.2 as "CTL".

- $P_{ET-altered}(i, j, \Delta t)$ - Total precipitation in a grid cell and time, stemming from several simulations where the ET fluxes are gradually altered, being increased or reduced. The name of the simulations are given in Table 3.1)

- $\rho * (i, j, \Delta t)$ - A regional magnitude computed in each cell grid to calculate the relative change in the precipitation of the control simulation and the simulations in which the ET is modified.

This procedure is based on calculating the variation in the precipitation of various experiments with different physics on the soil. In some of them, the ET fluxes have been totally or partially removed in a delimited area of the simulation, and in others, the humidity has been doubled. Finally, a standard experiment termed as control. We calculate the relative change in precipitation comparing the wet or dry simulations with the control experiment. We calculate the relative change in precipitation by comparison of control simulations to model experiments where ET is disabled or increased over the land to more explicitly assess the impact of local water fluxes on precipitation dynamics.
This parameter can be directly compared with the regional recycling ratio obtained through WVTM (Equation 3.28). Analogously to the regional WVTM recycling ratio, a regional relative change of the precipitation $R*$ can be defined as:

$$R* = \frac{\int_S [P_{CTL}(i, j, \Delta t) - P_{ET-altered}(i, j, \Delta t)] \cdot dS}{\int_S P_{CTL}(i, j, \Delta t) \cdot dS} \tag{3.38}$$

3.5 WRF-LEAFHYDRO Land-Atmospheric Model

Because it is fundamental not to consider the atmosphere and the land surface as isolated systems, but as a whole entity, numerous studies have highlighted the importance of the soil-atmospheric linkage, as well as, the need to improve the land surface models and coupled them to atmospheric models. As stated in Section 1.3, groundwater reservoir is usually neglected in LSMs, considering that the water cycle is closed. To eliminate the shortcomings owed to these hypotheses, recent LSMs have implemented groundwater dynamics parameterisations.
In this thesis, a coupled land-atmospheric model termed as WRF-LEAFHYDRO, which incorporates the groundwater scheme, is employed to generate a set of simulations referred to as WRF-EU. These set-up of simulations are explained in Section 3.1.3, and we use them to perform the computations of Chapter 6. LEAFHYDRO main features are presented and described here below.

3.5.1 LEAFHYDRO Land Surface Model

Land Ecosystem-Atmosphere Feedback (LEAF) is the land surface scheme implemented in the climate model the Regional Atmosphere Modelling System, or RAMS (see `http://rams.atmos.colostate.edu/`). LEAF-2 was versioned by Walko et al. (2000) from its very first version. Fan et al. (2007) and Miguez-Macho et al. (2007) describes the formulation of the modifications made in the LEAF-2 LSM, later termed as LEAFHYDRO.
The major innovation in this land surface model is that it incorporates a scheme that includes the groundwater and the rivers-lakes reservoir. The LEAFHYDRO Land Surface Model groundwater parameterisation simulates the WTD at every gridpoint of the model with or without aquifer. It calculates water fluxes and humidities, resolving several vertical soil layers of variable depth.
The dynamic water table of the LEAFHYDRO groundwater scheme couples the soil-vegetation and surface water with the groundwater, and fluctuates depending on the various two-way fluxes listed and explained below.

- The first interaction is a two-way vertical water flux that links the saturated or water table and the unsaturated zones or soil. These fluxes are gravitational drain flux and the capillary fluxes, and Darcy's law is used to represent the resulting net flux.

  Depending on the soil wetness and the atmospheric demand, the flux can be downwards, causing the water table to rise, or upwards, causing the water table to deepen.

- The second interaction is a two-way horizontal flux or lateral groundwater flow between the groundwater and the rivers.

  The horizontal or lateral fluxes represent the lateral groundwater flow between the adjacent grid cells and its eight neighbouring cells. Darcy's law computes lateral fluxes with the Dupuit–Forchheimer approximation.

- The third is the lateral groundwater flow within the saturated zone or groundwater-streams exchange.

  Also, the LEAFHYDRO incorporates a river routing scheme. This river routing transforms the generated runoff into streamflow.

  This model does not simulate human processes, such as irrigation or dams.

Water Table Dynamics in the LEAFHYDRO

1. **Mass balance in groundwater storage**

   The mass balance of the dynamic groundwater reservoir in a LEAFHYDRO cell is given by the Equation 3.39.

$$\frac{dS_g}{dt} = \Delta x \cdot \Delta y \cdot R + \sum_{1}^{8}(Q_n - Q_r) \tag{3.39}$$

   S_g - Groundwater storage in a model column (m^3).

   $\Delta x \cdot \Delta y$ - Horizontal resolution of the model (m^2).

   R -Net recharge or the flux between the unsaturated soil and the groundwater (m/s).

   Q_n - Lateral flow from or to the neighbour model grid cell (m^3/s).

   Q_r - Discharge to rivers or groundwater-streams exchange (m^3/s).

   All fluxes are assumed to be positive when incoming the groundwater reservoir and negative when outgoing.

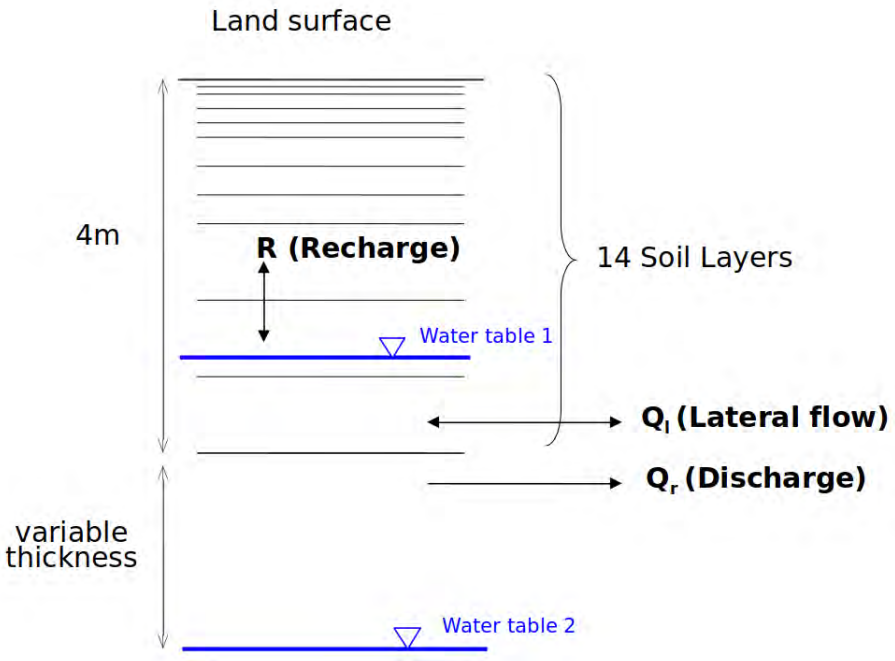

Figure 3.5: Cross section view of the land surface and the mass balance components. Figure adapted from (Miguez-Macho et al. 2016)

2. **Darcy's law for lateral groundwater flow**

$$Q_n = w \cdot \left(\frac{\int_{WTDn}^{\inf} K_n \cdot dz + \int_{WTD}^{\inf} K \cdot dz}{2} \right) \cdot \left(\frac{h_n - h}{s} \right) \tag{3.40}$$

Q_n - Lateral flow.

w - Width of flow cross section.

k_n - Conductivity.

Second term of the equation - Transmitivity.

Third term of the equation - Head difference divided by distance.

3. **Darcy's law for groundwater - river exchange**

$$Q_r = (h - Z_{rb}) \cdot \left(\frac{K_{rb}}{b_{rb}} \right) \cdot \left(W_r \sum L_r \right) \tag{3.41}$$

(a) **River flow routing from cell to cell to the ocean**

$$Q_s = \frac{S_s}{K_s} \tag{3.42}$$

(b) **Mass balance in surface water storage**

$$\frac{dS_g}{dt} = Q_n + Q_r + \sum_{i=1}^{7} I_n - Q_s \tag{3.43}$$

The land surface and soil layers formulation is thoroughly explained in Miguez-Macho et al. (2008) and Martínez-de la Torre & Miguez-Macho (2019). LEAFHYDRO main features have been thoroughly described in Fan et al. (2007) and Miguez-Macho et al. (2007), and the model is employed in many studies (Gestal-Souto (2010), Miguez-Macho & Fan (2012), Martínez-de la Torre & Miguez-Macho (2019), Martínez-de la Torre & Miguez-Macho (2014),Quintana-Seguí et al. (2019)).

3.5.2 Coupling LEAFHYDRO to WRF

In this thesis, we use the soil-vegetation-hydrology model LEAFHYDRO coupled with the WRF model. The initial conditions for soil hydrology of the WRF model are obtained from some off-line simulations carried out with the LEAFHYDRO.
The LEAFHYDRO simulations are performed for the same grid than the one used in the WRF experiments. The set of simulations resulting from running WRF-LEAFHYDRO have 20 km of resolution in the atmosphere and 2.5 km of horizontal resolution in the soil, which allows each cell in the WRF grid to exactly encompass 64 cells of the LEAFHYDRO grid.
The WRF-LEAFHYDRO model is run with two different configurations: one including the groundwater parameterisation and termed as Water Table simulation (WT simulation); and the other with free drainage at the bottom of the soil column, named as Free Drainage simulation (FD simulation). To clarify this explanation see Table 3.3.

Configurations	Description
WT simulation	This set of simulations includes the LEAFHYDRO groundwater scheme. In which the water table depth behaves as the bottom boundary condition, interacting with the soil and rivers.
FD simulation	These simulations use the free-drainage approach as a boundary condition at the bottom of the soil column (4 m). In which the soil water surplus can drain out of the land column and the water drained out of the lowest layer is no longer available.

Table 3.3: WRF-LEAFHYDRO configurations

By comparing the results obtained with both configurations of the WRF-LEAFHYDRO model (FD simulations and WT simulations), we intend to prove that by introducing a water table parameterisation we get a more accurate representation of the soil hydrology.

USC
UNIVERSIDADE
DE SANTIAGO
DE COMPOSTELA

USC
UNIVERSIDADE
DE SANTIAGO
DE COMPOSTELA

Chapter 4

A Study with a Water Vapour Tracer Method

Evapotranspiration fluxes determine the intensity of land-atmosphere coupling and the relevance of recycling processes in the local hydrology cycle. In this chapter, we focus on the study of the terrestrial ET contribution to precipitation in the Iberian Peninsula. Through the study of the recycling processes, we intend to show how the moisture is distributed throughout the atmospheric column and the simulated period. That is to say; a better picture of the regional water cycle is obtained. This study is carried out on the Iberian Peninsula since many researchers have studied its climate.

We make use of various sets of WRF simulations previously described in Section 3.1.1 and referred to as SIM-IP. Our collection of simulations covers the months of April and May from 2001 to 2010. The first simulated month of each year is considered as a spin-up period and the second simulated month is used to perform the computations.
We employ an Eulerian moisture tagging technique embedded in the WRF model. This technique allows us to track the water molecules paths in a particular region and thus to better understand the distribution of the moisture throughout the atmospheric column and its temporal evolution. Presently, the use of a moisture tagging technique constitutes the most accurate procedure to compute the recycling calculations. We evaluate the interannual variability in the study domain with the use of these moisture tracers by analysing the recycling processes in the local hydrology cycle. We also study the contribution of ET at different altitudes throughout the atmospheric column and with different synoptic situations. Based on the model simulation results, we make use of three analytical recycling methods, thoroughly described in Section 3.2. These methods are based on some strong assumptions, among which we highlight the supposition that moisture from local ET is not often well-mixed throughout the atmospheric column. We use the analytical recycling models to carry out recycling computations over the IP and compare their results with those obtained with WVTM.

The structure of this chapter is as follows. A detailed vertical analysis of the vertical moisture distribution and spatial distribution is made in Section 4.1 and Section 4.2. A spatial and temporal analysis of the precipitation and recycling ratio over the IP is presented in Section 4.3 and Section 4.4. A comparison of the recycling ratios computed via WVTM and the classic recycling models is presented in Section 4.5. The final summary and discussion of the significant results of this study are presented in Section 4.6.

4.1 Vertical Structure of the Tagged Moisture Field

In Figure 4.1, we depict four instances of the temporal evolution of the tracer water vapour mixing ratio together with the horizontal wind, in April and May of 2004. This new species is activated in the tagged region marked in black in Figure 3.4. For each instance of time, we obtain different amounts of tracer moisture. The upper left figure represents the beginning of the simulation when there is no tagged moisture in the modelled region. As the simulation advances, humidity originating from the tagging source area enters the atmosphere as tagged water vapour, then it is transported and dispersed horizontally through the domain. In general, the water tagged content is the highest close to the source region and decreases with distance depending on wind intensity and wind shear. The moisture is tracked until it precipitates or leaves the domain due to the outgoing flux.

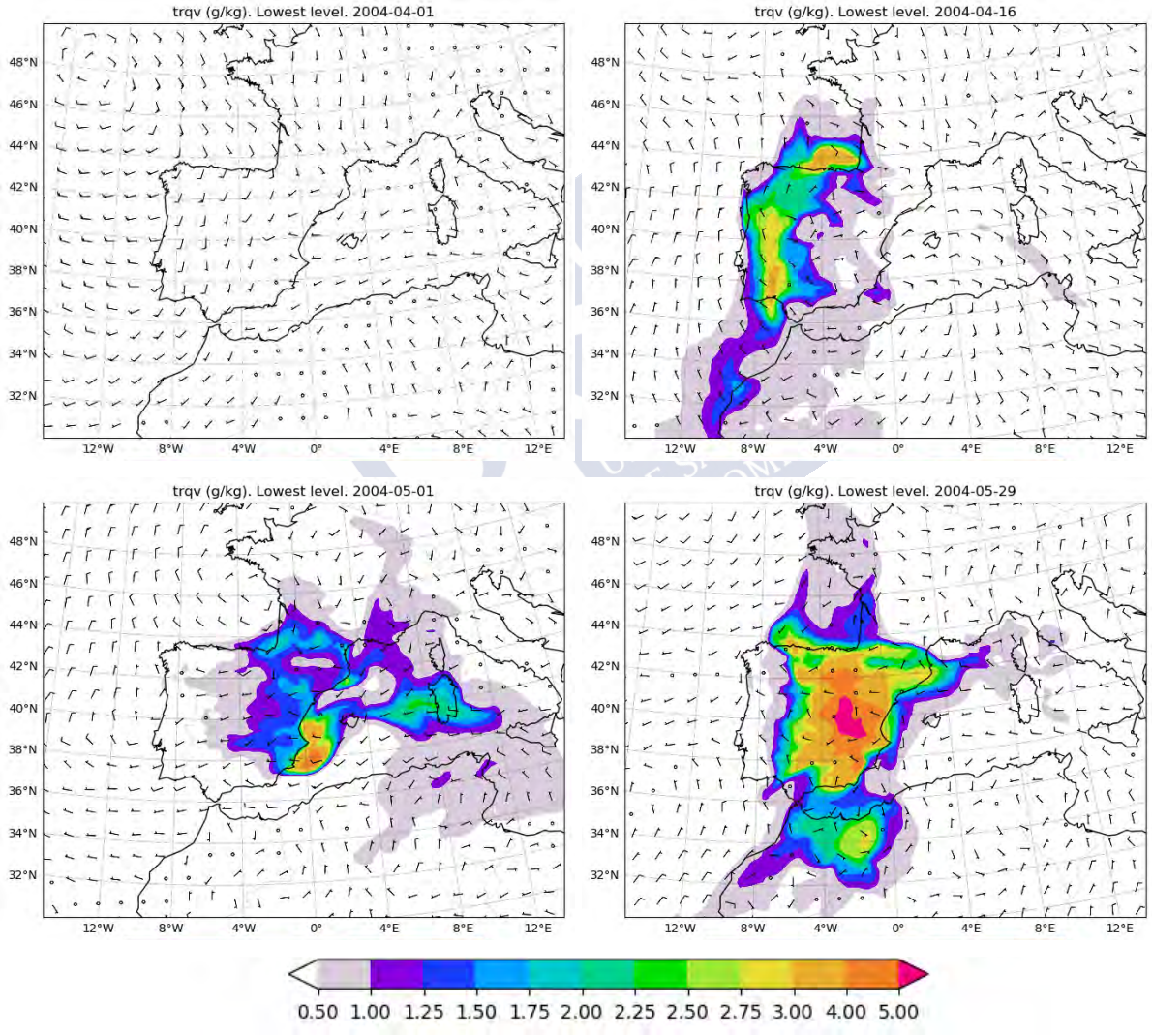

Figure 4.1: Tracer mixing ratio of water vapour together with the horizontal winds both in the lowest level of the atmosphere, in four different days of the simulation of Spring 2004.

We have shown the horizontal distribution of the tagged moisture is not uniform alongside the simulated period, but neither is the moisture evenly spread throughout the atmospheric column. Now, to illustrate the variety of the vertical and horizontal evolution of the tagged moisture, Figure 4.2 depicts the transport and spreading of the tagged vapour in two days with different synoptic situations. The upper figure shows the 28th May 2001, a day with light winds and weak wind shear over the IP. In contrast, the lower figure corresponds to 4th May 2010, depicting an intense atmospheric circulation, and consequently a high wind speed. As seen in both cases, the evolution of the tagged humidity is governed by the horizontal variations of the west-east and south-north wind components. In the first case, high concentrations of tracer moisture remain over the tagged region and surroundings, as a result of the weakened circulation, and only some amounts of this local vapour are carried away by the winds toward North Africa. However, in 2010, a significant proportion of moisture is blown to the south by the intense cyclonic flow around the low-pressure system east of the IP. With this northern wind situation, the fraction of local moisture is tiny in the north leeward half of the IP, and it gradually increases as the flow traverses the source regions towards the south. The vapour reaches North Africa, particularly the Atlas Mountains, a mountain chain covering part of Algeria and Morocco. By combining the fact that the Atlas Mountains are acting as a natural barrier to the tagged moisture, and the winds are predominantly from the north-west, the higher amounts of tagged vapour are found in this mountain chain. But also, following the wind directions moisture is blown to the interior of the European Continent, and analogously with the Atlas Mountains, moisture encounters the Alps as an obstacle. In the vertical cross-section of the tagged moisture ratio, in both cases, the percentage of moisture coming from the tagged region diminishes as the elevation from the land surface increases. The majority of the tagged vapour remains in the planet boundary layer, with the higher values near the surface. Whereas, there is barely enough water content in the upper atmosphere, approximately at 80 km. However, there are some remarkable differences between both cases. A large percentage of moisture over the IP comes from land ET (over 50 %) in the case of 2001, but it remains mostly within the planetary boundary layer, and it is not mixed aloft. The second case in 2010 is an example of when moisture originating from local ET is far from being well-mixed, even in the boundary layer. The vertical distribution of this local moisture is quite complex due to the wind shear and circulation associated with the nearby cyclonic centre. Furthermore, because of the intense advection, the fraction of local moisture at low levels is very small, and there are areas in the east of the IP where this fraction even increases with height. The moisture tagged distribution is managed by wind direction, and as wind speed increases with height, water vapour is moved. It can indeed be said that the most effective mechanism to lift the moisture humidity coming from the tagged regions is cumulonimbus convection systems.

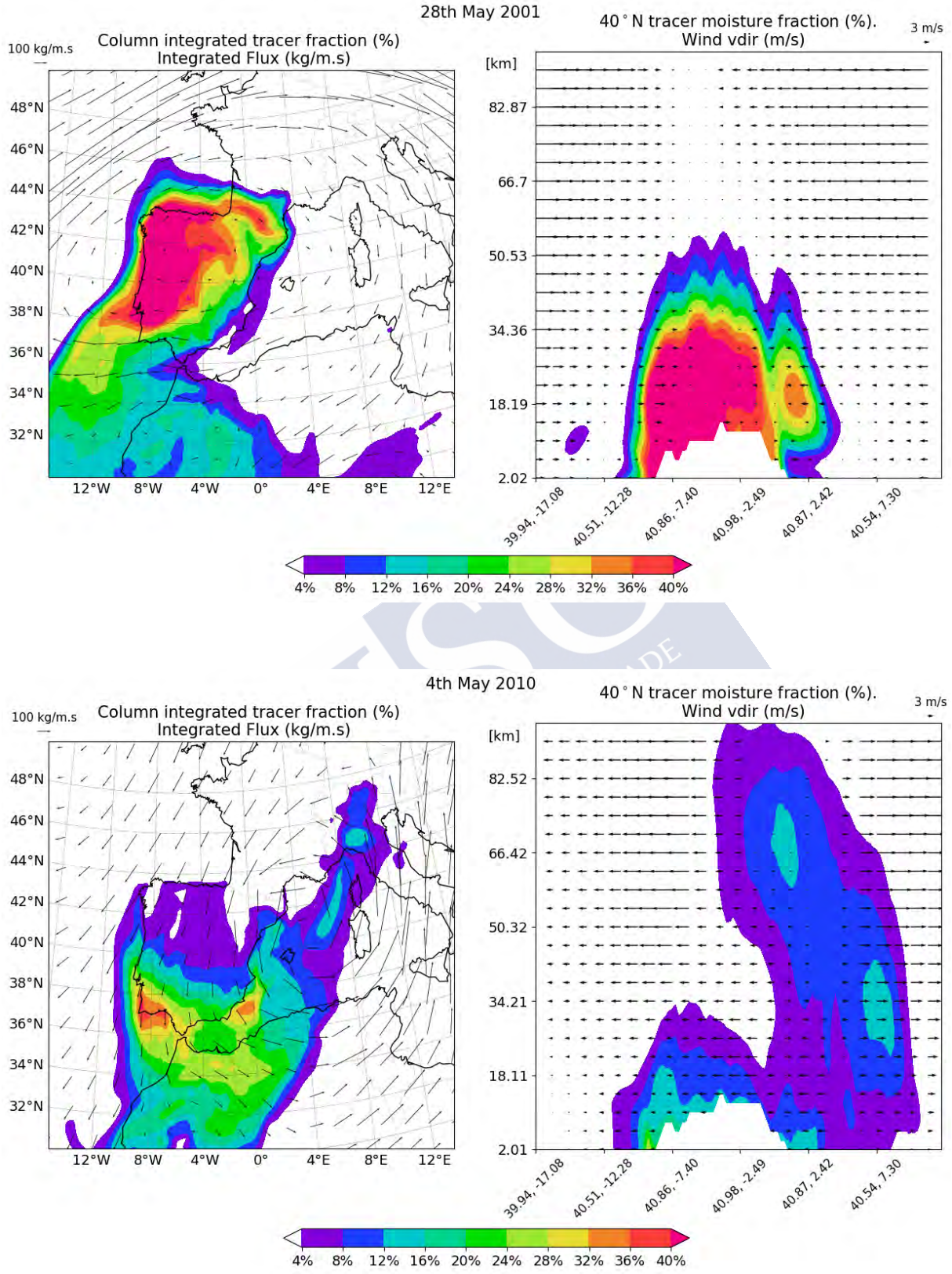

Figure 4.2: Column integrated tracer fraction in the lower level of the atmopshere together with integrated flux in the atmospheric column (in the pannels in the left). Vertical cross-section in $40N$ of the ratio between tracer moisture and moisture coming from the tagged region and vertical wind component (pannels in the right).

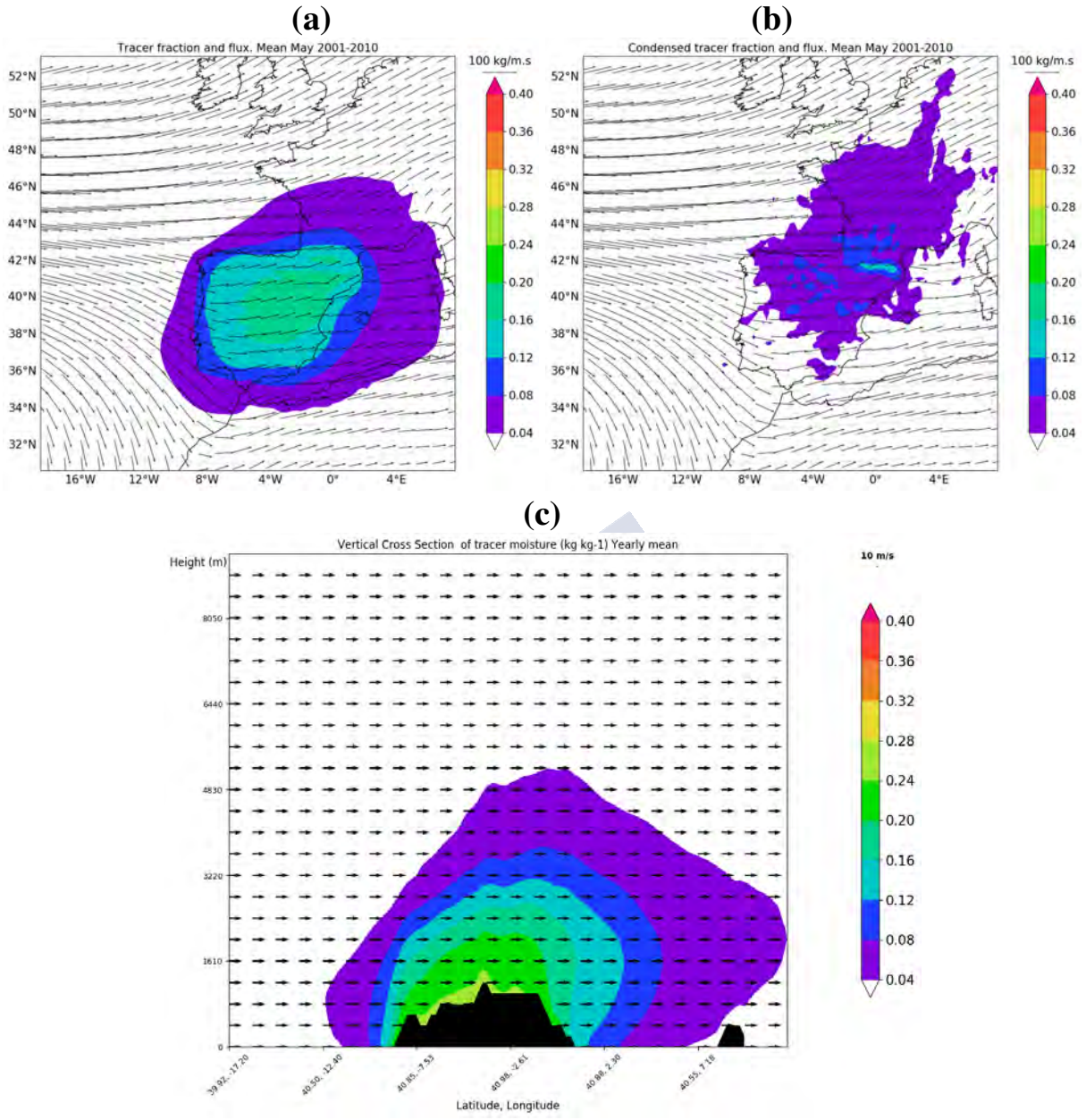

Figure 4.3: Fraction of the column-integrated tagged moisture (upper right) and fraction of the column-integrated condensed tagged moisture (upper left) together with the integrated flux. Cross-section at 40ºN of the fraction of humidity from tracers over the IP (g/kg) with a cross-section of the vertical winds. All averaged over May 2001-2010

A closer inspection of the vertical moisture distribution is given in Figure 4.3. The column-integrated tracer moisture fraction for May averaged over ten years is depicted in Figure 4.3 a. Overall, as expected, the concentrations of moisture tend to be higher the closer to the source area (the IP), decreasing with distance. The total column integrated tracer condensate in Figure 4.3 b shows, however, a very different spatial pattern. Clouds originating from ET are formed when moisture is lifted, either by forced or free convection. The ascent mechanism is usually associated with low-pressure systems travelling west from the Atlantic Ocean; hence the

tracer condensate follows the predominant south-west wind flux direction toward the interior of Europe. Very little of the condensate is from local sources upwind, in the southeastern half of the IP, even when water vapour from ET is generally in significant concentrations there The vertical cross-section at 40ºN (Fig. 4.3 c) shows that on average the tagged moisture (which is mostly water vapour) stays in the boundary layer, with its concentration gradually decreasing with distance from the surficial source, and is thus not uniformly distributed throughout the atmospheric column.
The analyses of Figure 4.2 and Figure 4.3 suggests that moisture from evapotranspiration sources is not often well mixed vertically in the atmosphere, and in particular the moisture involved in precipitation processes (the condensate) can travel considerable distances from its source.

4.2 Daily Moisture Cycle

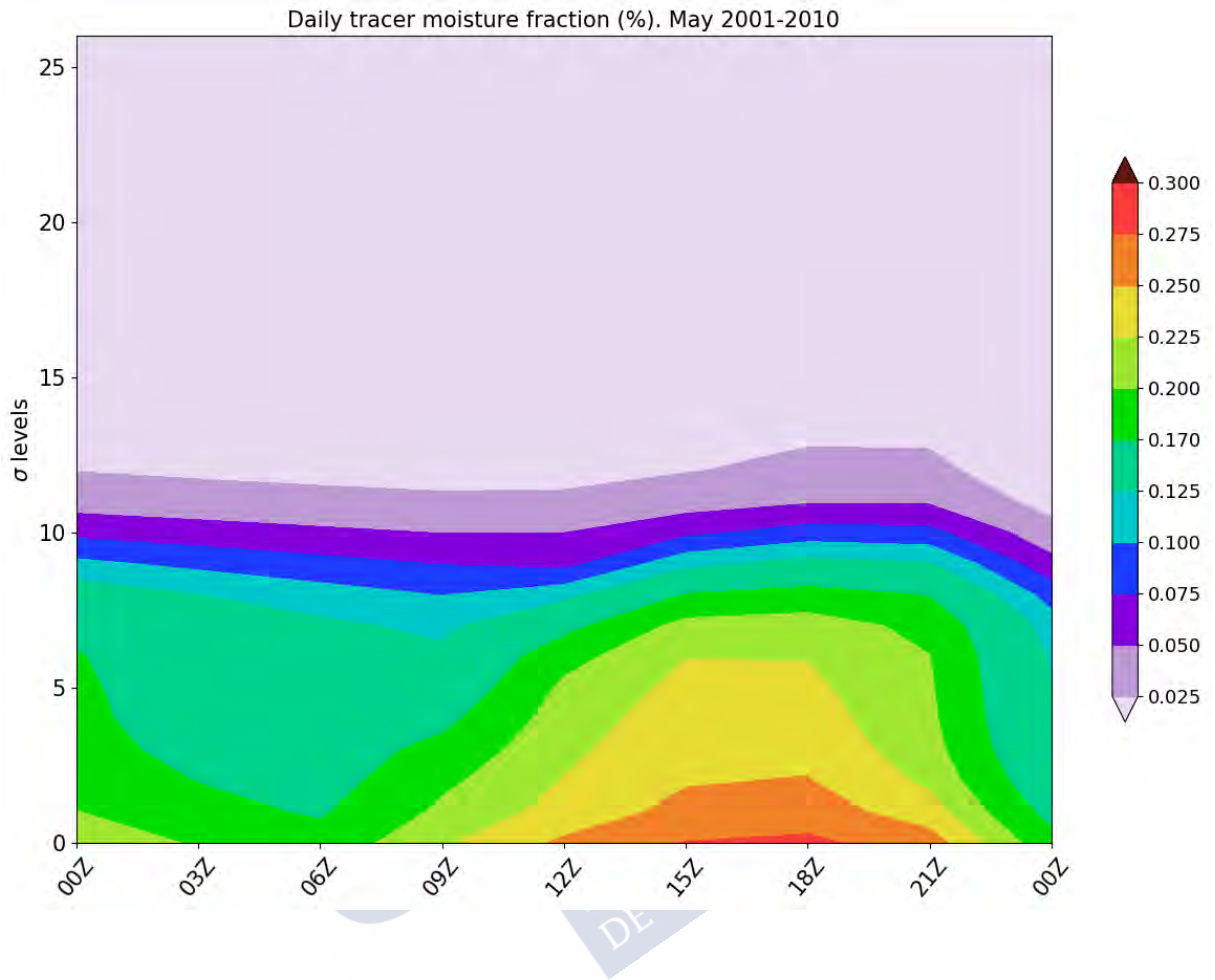

Figure 4.4: Mean daily cycle tracer moisture fraction, area averaged over the IP in May 2001-2010. The scale of the vertical axis is expressed in sigma levels.

Figure 4.4 depicts the daily cycle of the vertical distribution of tracer moisture fraction (solar time and local UTC time coincide in the IP), averaged over the entire source region (the IP) and the ten simulated years. The non-uniform transport and spreading of the moisture alongside the atmospheric column are reflected in this figure. The tracer moisture fraction varies from the lowest levels, where the highest values of moisture are found, to the higher levels, where there is barely any moisture content.

All the atmospheric forcings undergo significant changes in the PBL during the day, as is the case of the tracer humidity. The variations of the fraction humidity are mostly due to the day-night differences of evaporation. After dawn (around 06:00Z), surface heating develops a shallow convective mixed layer, which increases slowly throughout the morning until the midday hours, when the nocturnal stable layer is completely disintegrated. The fraction of humidity runs the same course, starting to increase at approximately 06:00Z through to the midday hours. The higher amounts of moisture are found during the central hours of the day, from 12:00Z until 15:00Z, corresponding to the hours of direct sun radiation. During the afternoon, a warmed ground facilitates a better mixture of the air in the PBL. During the night, after this convective

mix has occurred, the PBL is stable due to the surface longwave cooling. The radiative cooling is more intense near the surface and promotes static stability, and a shallow temperature inversion occurs. Owing to these conditions, the PBL is well mixed in the course of the night until next morning, when ET starts to increase again.
Turbulent fluxes lift this surface moisture and mix it within the PBL, creating a vertical profile where tracer fraction decreases with height during the day. It only becomes well-mixed during night hours, when the surface moisture input is minimal. It is well mixed in the PBL from the late afternoon until the early morning. The Figure 4.4 shows that local ET moisture over the source region is generally not well distributed throughout the column, not even in the PBL.

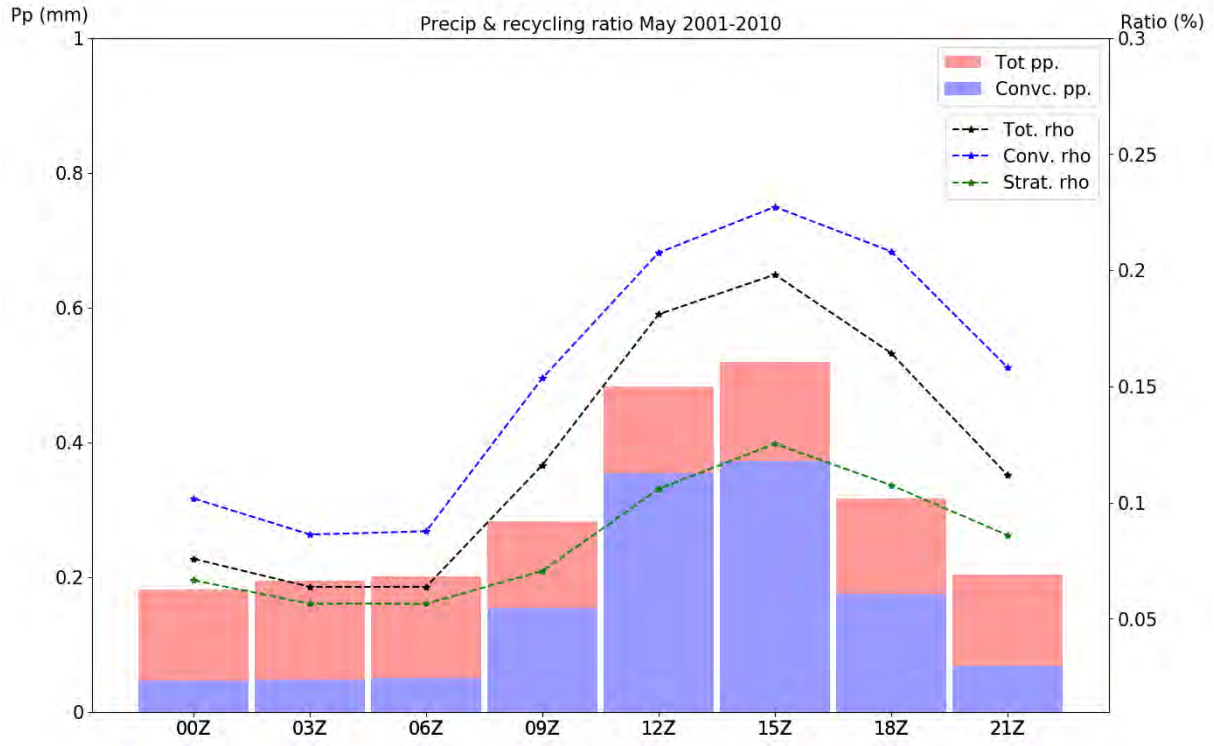

Figure 4.5: Mean daily cycle of precipitation and recycling ratio calculated through WVTM, area averaged over the IP in May 2001-2010.

The diurnal cycle of recycling ratio and precipitation are represented in Figure 4.5, also averaged over the entire source region (the IP) and the years simulated. We compute three recycling ratios, the total recycling ratio "Tot. rho" plus "Conv. rho" and "Strat. rho", representing the contribution of ET to convective and stratiform precipitation, respectively.
Recycling is stronger in the early afternoon, with rho reaching a maximum average value of 0.2, corresponding with the time where the fraction of ET moisture in the PBL is also at peak, and drastically decreasing in night time hours, when the lower atmosphere is less enriched in moisture from surface ET.
This intensification of recycling during the daytime occurs for total, as well as for convective and stratiform precipitation. Precipitation dynamics also affect the recycling ratio, which has much higher values for free convection than for stratiform or forced convection. In free convection, moisture is lifted vertically from the surface, precisely where ET moisture is more abundant,

and the precipitation originating in the ascent can still retain a significant contribution from this local surface moisture. In forced convection, for example along a front, the lifting tends to be more oblique, and advection from remote sources is usually stronger; hence the role of local sources diminishes.
Three hourly total precipitation is also shown in bars in Figure 4.5, separated into its convective (blue) and stratiform (red) components. Convective precipitation presents a marked daily cycle with higher values in the early afternoon, as convection in the spring is triggered most often during this timeframe in the IP, the result of instability rising from surface heating under a still cold air volume above. In contrast, stratiform precipitation does not have a preferential time of occurrence, and its frequency remains constant throughout the day. The daily cycle of convection is reflected in the time evolution of total precipitation, which also peaks in the early afternoon. Since the largest share of rainfall during midday is convective and the recycling ratio is much higher for convection than for stratiform precipitation, the total recycling ratio presents an enhanced daily cycle, looking more like that of convective precipitation during the day. Conversely, during night-time most rain is stratiform; thus the total recycling ratio is reduced and follows the value for this precipitation type.

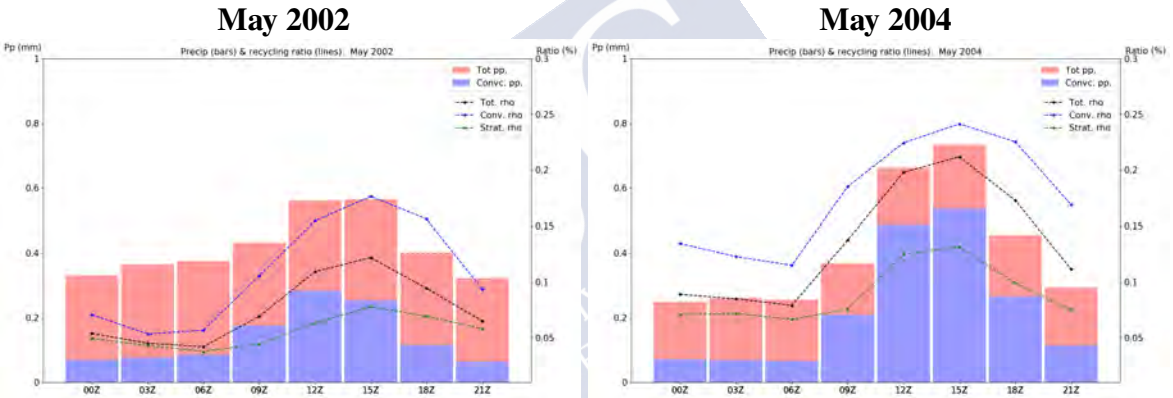

Figure 4.6: Daily cycle of precipitation and recycling ratio calculated through WVTM, area averaged over the IP for the years 2002 and 2004.

This clear relationship between recycling and convection is also shown in Figure 4.2, with the representation of two years with very different synoptic situations. In 2002 the precipitation is mostly from stratiform origin, while the convective precipitation is weak in 2004. As displayed in Table 4.1, the external moisture advection is strong in 2002 and weaker in 2004. The combination between a convective precipitation and a weak external moisture flux give rise to high recycling ratios, whilst the strong influx and stratiform precipitation motivates smaller recycling ratios. In both cases, precipitation shows again higher values at midday and in the early afternoon, due to convective events.

4.3 Precipitation and Recycling Interannual Variability

Monthly recycling processes take greater or less relevance depending on the atmospheric conditions, as we have already demonstrated in Figure 4.2 for the years 2002 and 2004. For a further discussion of the interannual variability, we have selected some representative case studies from the span of the ten years simulated. In Figure 4.7 are depicted the daily total precipitation (red bars) and daily convective precipitation (blue bars) for the six years considered. The black lines depict the local recycling ratio (Eq. 3.4), and the red lines show the daily ratio of column integrated moisture. Both computed using the Equations 3.29 and 3.34. To get information about the efficiency of conversion of available moisture into precipitation, mean efficiency (Eq. 3.36) is reported in each title.

In the first instance, we show May 2001. The highest daily precipitation value never exceeds 7 mm/day, and as indicated in Table 4.1, the average daily total precipitation value is 2.60 mm/day. The average convective precipitation is 1.56 mm/day, and so 60% of the precipitation is from convective origin. The vigorous convective situation, combined with a weak moisture flux entering the study region, is responsible for a recycling ratio of 16.14%, which is the highest in the span of the ten years simulated. The average daily recycling ratio has to be considered as a rough indicator of the recycling processes. In this particular year, the daily recycling values are triggered by the last five days of the month (due to the lack of precipitation). Therefore the high recycling rate of the month may be mainly due to these days.

The second case is May 2002, when approximately 70% of daily rainfall is principally from frontal or stratiform origin. The convective precipitation barely reaches 1.56 mm/day as opposed to a 3.35 mm/day of the total rainfall. The moisture advection is rather strong, with an average of 31.28 mm/day according to Table 4.1. Due to this vigorous zonal circulation and the large percentage of stratiform precipitation, the recycling ratio obtained is the lowest in the numerical series of ten years; on average just 8.5% of the total precipitation comes from local ET. Therefore the primary available source of precipitation is from advected moisture.

In contrast to 2002, the moisture influx advected from the Atlantic is considerably weaker in May of 2004, it barely reaches 22.61 mm/day. The daily contribution of convective precipitation to overall precipitation is higher than the stratiform contribution, especially in the second half of May. But the average proportion of convection to precipitation is still higher in May 2001; for this reason, the recycling ratio is not as high as in 2004.

May 2006 is the driest year of the measured decade, with a rainfall contribution of just 1.21 mm/day. Except for the first seven days of May, most of the precipitation is convective. The average moisture influx entering the domain is the highest in the ten years, reaching 33.12 mm per day; thus the recycling ratio in this month is not among the highest values across the span of the ten years.

May 2008 is one of the wettest years in the recorded decade, the total precipitation reaches 4.8 mm/day over the tagged region. The abundant moisture supply is responsible for the large precipitation amounts, with the instability favoured by the cold air aloft associated to the cut off of low systems in the area, observed to be frequent during this particular month. On average recycling explains 11.63% of the effect of evapotranspiration fluxes on precipitation in 2008, the remaining rain is due to the frontal contribution. The weakest moisture advection occurs during May 2010, obtaining a value of 13.56 mm/day.

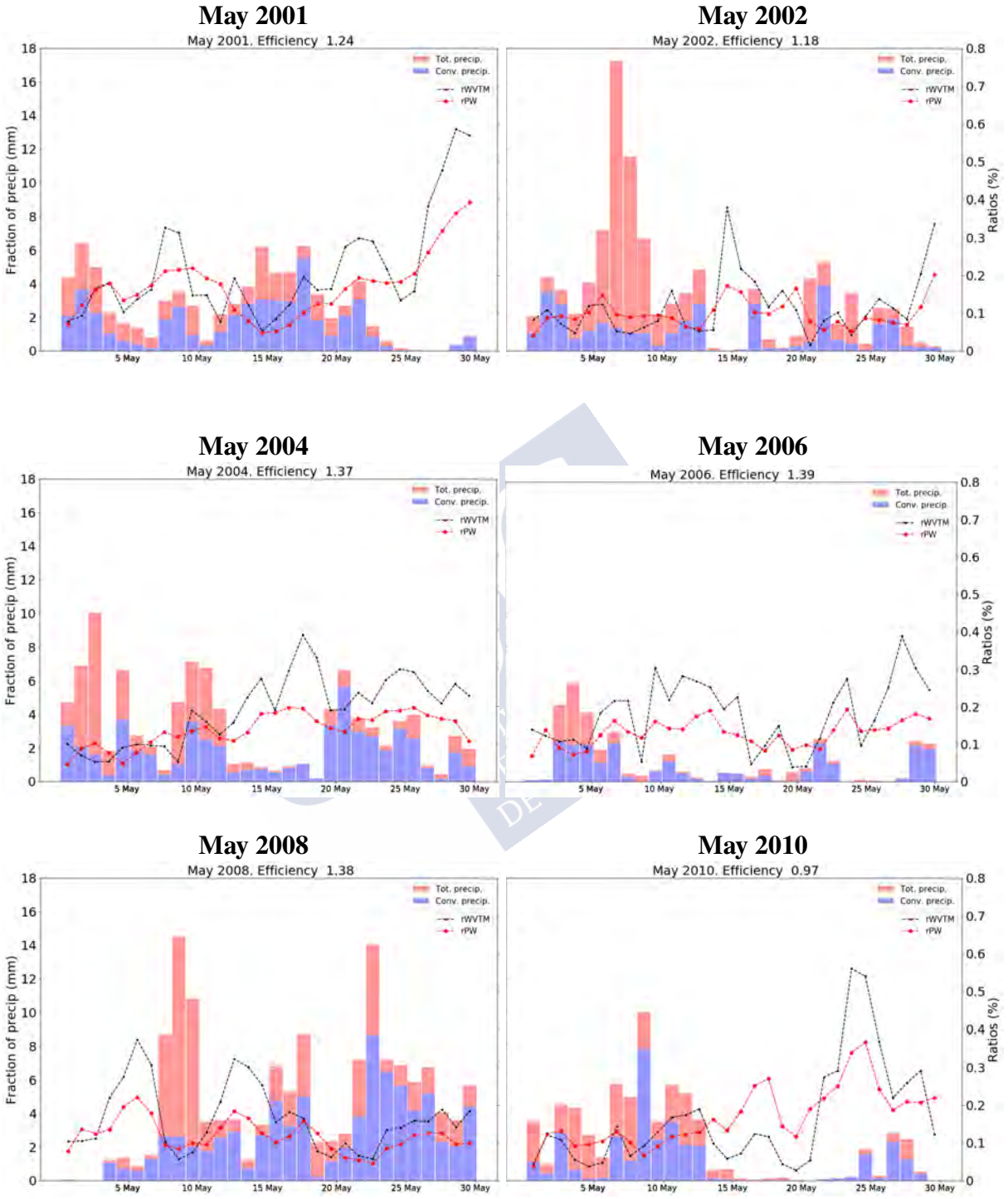

Figure 4.7: Daily convective and total precipitation (bars) and daily regional recycling ratio from WVTM (lines) throughout May 2001, 2002, 2004, 2006, 2008 and 2010. Mean efficiency is reported in each title.

Years	Totpp (mm/d)	Ppc (mm/d)	ET (mm/d)	INFLUX (mm/d)	R_{WVTM} (%)	Eff
2001	2.60	1.56	2.56	24.04	16.14	1.24
2002	3.35	1.12	2.40	31.28	8.52	1.18
2003	1.74	0.71	2.66	21.50	14.58	1.24
2004	3.28	1.82	2.55	22.61	13.22	1.37
2005	1.58	1.02	2.34	32.75	12.17	1.06
2006	1.21	0.77	2.49	33.12	13.92	1.39
2007	2.69	1.62	2.74	22.73	12.44	1.23
2008	4.80	2.69	2.42	32.50	11.63	1.38
2009	1.24	0.80	2.45	31.20	14.03	1.25
2010	2.22	1.12	2.75	13.56	14.02	0.97
Mean	2.25	1.21	2.53	25.66	12.90	1.22

Table 4.1: Total precipitation (Totpp), convective precipitation (Ppc), evapotranspiration (ET), external moisture flux (INFLUX) entering into the tagged region, daily values expressed in mm per day. Regional recycling ratio (R_{WVTM}) expressed as a percentage. Efficiency of conversion (Eff) adimensional. These values are calculated for the tagged region and for May 2001 to 2010 and the multiannual average.

Evapotranspiration fluxes have a high impact on precipitation amounts by increasing the low-level instability of the atmospheric column. Values of daily evapotranspiration are quite similar in the time series, ranging between 2.34 to 2.75 mm/day. Nevertheless, it is clear that the more available the ET is, the more convective the synoptic situation is. That is the case for May 2010.

The values of efficiency calculated through the Equation 3.36 are displayed in Table 4.1 and also reported in each title of Figure 4.7. The use of the parameter of efficiency is twofold. First, to evaluate the ability of conversion of the available atmospheric moisture into precipitation. Second, to demonstrate that the regional recycling ratio and the ratio of precipitable water are not equal. If this were true, the atmosphere would be well mixed. All the values obtained are above one, except for the year 2010 when 0.97 is obtained. The efficiency reveals the convective

state of the atmosphere, the more convective the synoptic situation is, the higher the efficiency is. Such is the case of 2004 or 2008 when the efficiency reaches 1.37 and 1.38 respectively. In this chapter, we will compare the results obtained with the local recycling ratio through the WVTM with various analytical recycling methods based on the well-mixed assumption. If the well-mixed assumption is correct, the recycling ratios obtained through the WVTM and the rate of precipitable water should be equal. As seen in Figure 4.7 these daily ratios are quite similar throughout the month but still, they are not equal.

Therefore, the most obvious finding to emerge from Section 4.3 is that a close relationship exists between convection and recycling. Still, other variables are directly linked to the recycling processes, like ET and moisture advection. With high proportions of convective precipitation, recycling ratio values tend to increase. A weak moisture advection or high amounts of ET also give rise to longer values of recycling. Analogously, a strong external moisture flux means lower values of the recycling ratio.

4.4 Spatial Distribution of the Moisture

Some studies (Seneviratne et al. (2006), Rios-Entenza et al. (2014)) have demonstrated that the relationship between ET and precipitation shows spatial variability, depending on the regional climate regime. The most common way to quantify this relationship over a specific region is by computing the recycling ratio. In this section, we intend to show this relationship by using the method of moisture tracers in the Iberian Peninsula. Figures 4.8, 4.9, 4.10, and 4.11 display the ratio computed through WVTM during the span of the ten-year simulation, together with the average pattern of vertically integrated moisture flux for the same period. Also, the monthly total precipitation for each month is depicted in the same figure and the multiannual average for precipitation and recycling ratio.

The recycling ratio varies from year to year even more than the interannual variability in May's precipitation for the period 2001-2010. There is no clear relationship between the pattern of the monthly recycling ratio and that of total rainfall (neither is there, with its convective or stratiform components, not shown). The direction and amplitude of the mean moisture flux do not seem to correlate strongly with the pattern and intensity of recycling either, at least not every year. In accordance with Table 4.1, the regional recycling ratio does not have wide variations throughout the time series, only varying from 8.52% to 16.14%. Nevertheless in Figures 4.8, 4.9, 4.10, and 4.11 , the local recycling ratio presents spatial variations across the Spanish and Portuguese territory.

In 2001, the recycling processes are more significant than any other year. Obtaining recycling rates higher than 26% in the northern half and the east-south of the Iberian Peninsula, but also values not lower than 8% in the remaining territory. The moisture flux, with westward direction, is particularly weak in the north and interior of the study area; indicating the large-scale moisture supply, from the Atlantic Ocean, for the most part, is much diminished. A similar situation occurs during 2003 when the moisture influx to the interior of the Peninsula is debilitated. Thus the recycling ratio is high in this area. Therefore, considering these two years, we conclude that under a weak synoptic forcing, the recycling contribution is predominant in large interior regions. On the contrary, recycling has reduced importance in 2002 and 2008. In both years, the recycling ratio barely reaches 20% in the area of the Pyrenees. In the particular situation of 2002, there are large areas of the Peninsula where the recycling rate is lower than 10%. These small ratios coincide with an intense zonal circulation coming from the Atlantic Ocean and high moisture flux values due to the strong advection.

Figure 4.11 displays the pattern of the multiannual average of recycling ratio and vertically integrated moisture flux for May 2001-2010. Moisture flux is mathematically averaged as coming from westerlies. Thus the recycling ratio tends to be higher in eastern Iberia, and a small percentage of moisture is blown to the Mediterranean Sea and North Africa. Rates exceeding 8% are found throughout most of the interior, eastern and north-eastern Iberia. Nevertheless, in north-east Iberia and the Pyrenees, ratios are close to 20%. There is a small area in south-east Iberia, where the recycling processes acquire relevance.

Recycling ratio varies year to year due to the interannual variability in May 2001-2010. WVTM recycling ratios are strongly linked to the mean moisture flux, and the spatial distribution of the moisture follows the direction of the prevailing flux. In general, recycling shows larger values when there are more convection and weaker moisture advection, while low recycling ratios are associated with stratiform precipitation, this type of rain in the IP is usually from Atlantic fronts.

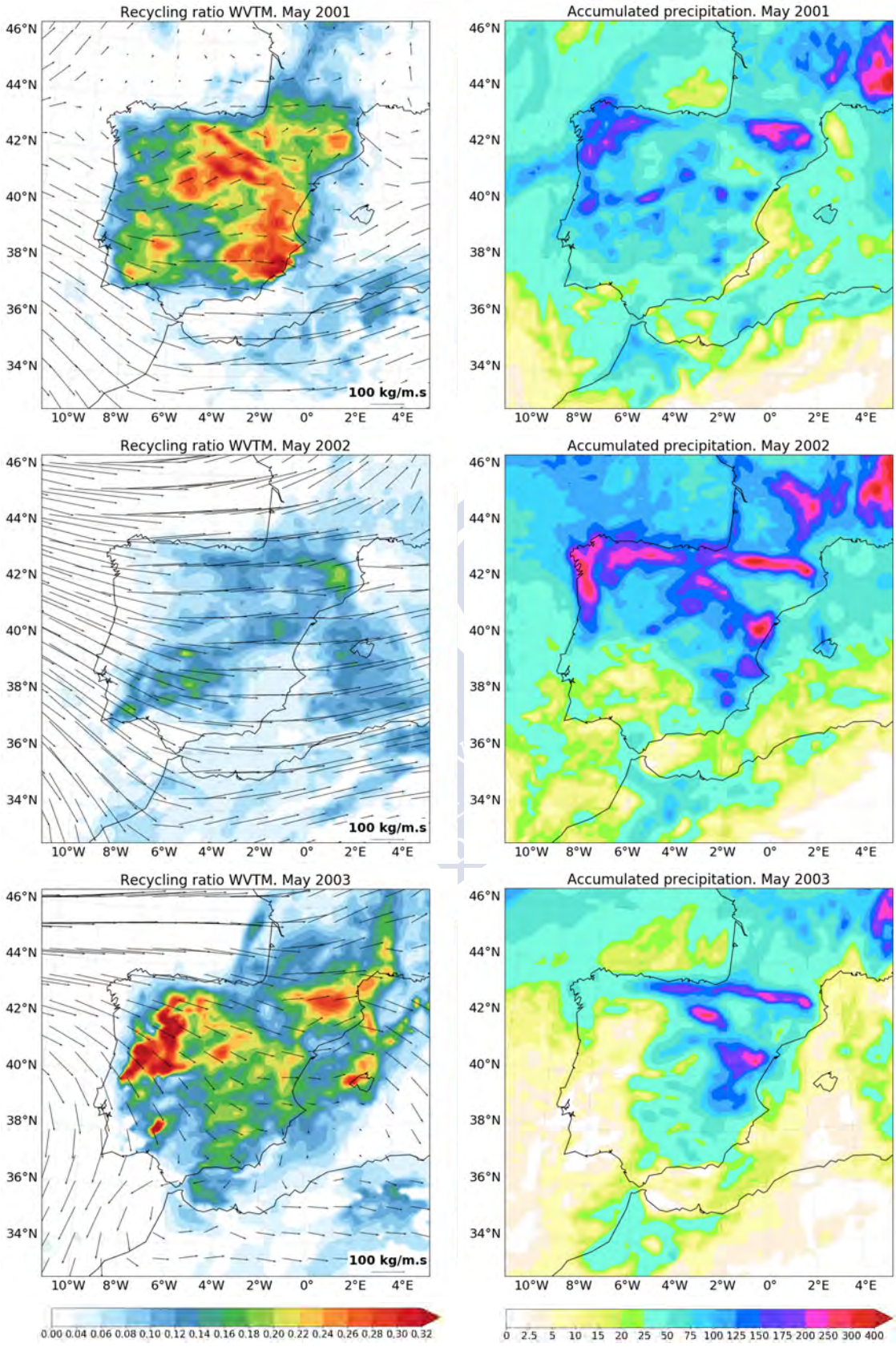

Figure 4.8: Spatial distribution of the local recycling ratio computed by WVTM, together with the average pattern of vertically integrated moisture flux (kg /ms) (left). Monthly accumulated precipitation (right). Both calculated in the parent domain for the years 2001, 2002 and 2003.

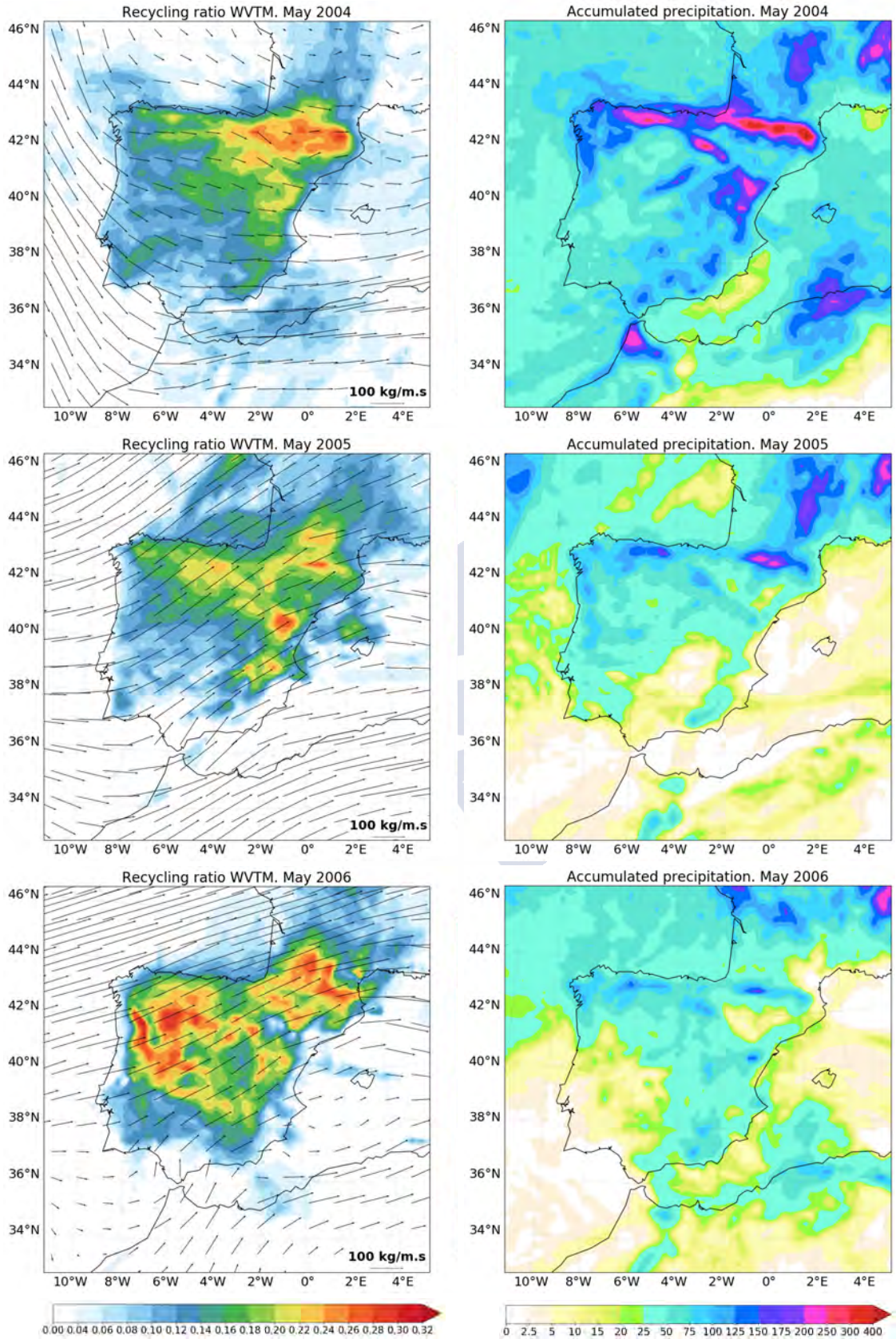

Figure 4.9: Spatial distribution of the local recycling ratio computed by WVTM, together with the average pattern of vertically integrated moisture flux (kg /ms) (left). Monthly accumulated precipitation (right). Both calculated in the parent domain for the years 2004, 2005 and 2006.

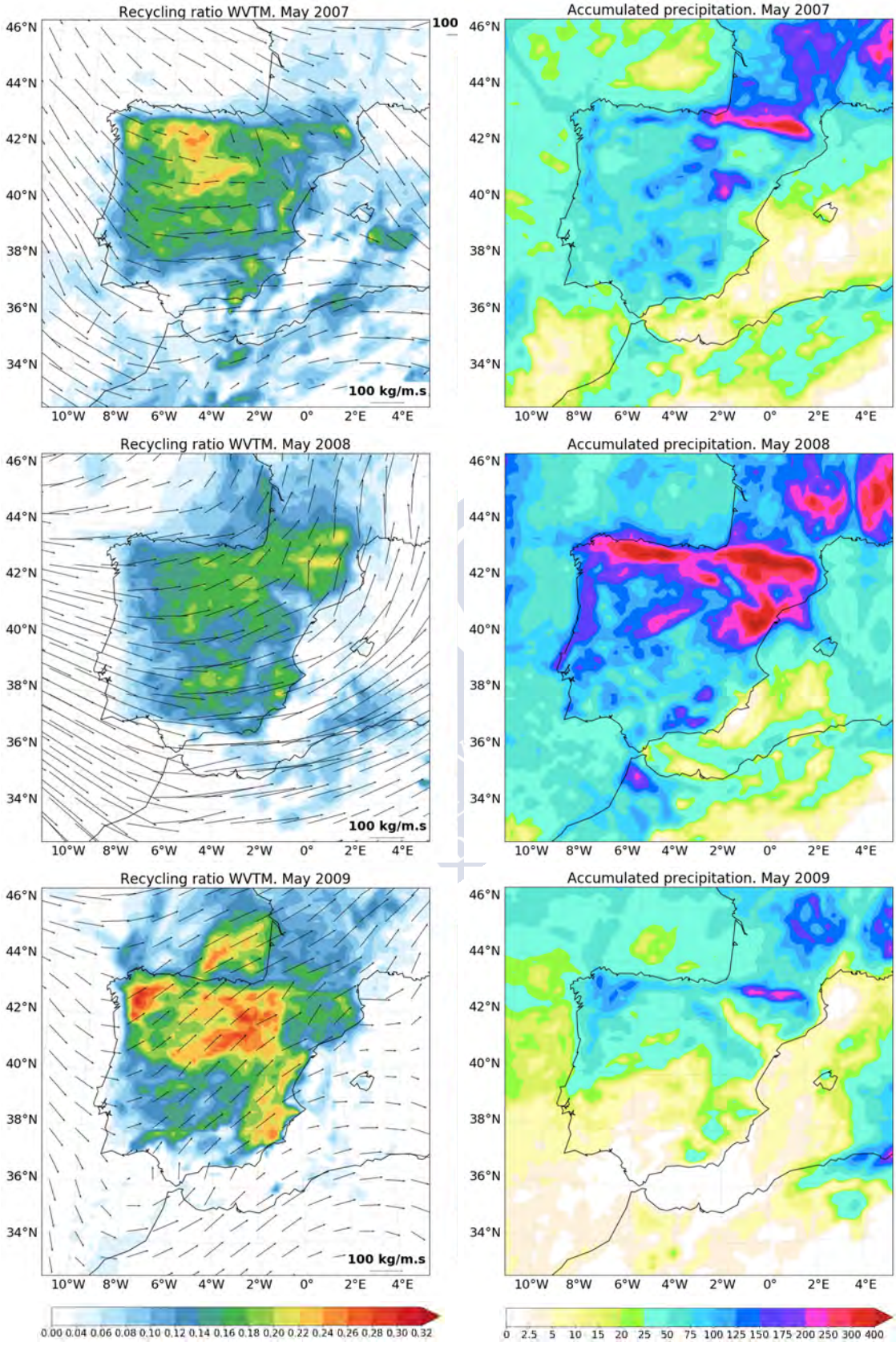

Figure 4.10: Spatial distribution of the local recycling ratio computed by WVTM, together with the average pattern of vertically integrated moisture flux (kg /ms) (left). Monthly accumulated precipitation (right). Both calculated in the parent domain for the years 2007, 2008 and 2009.

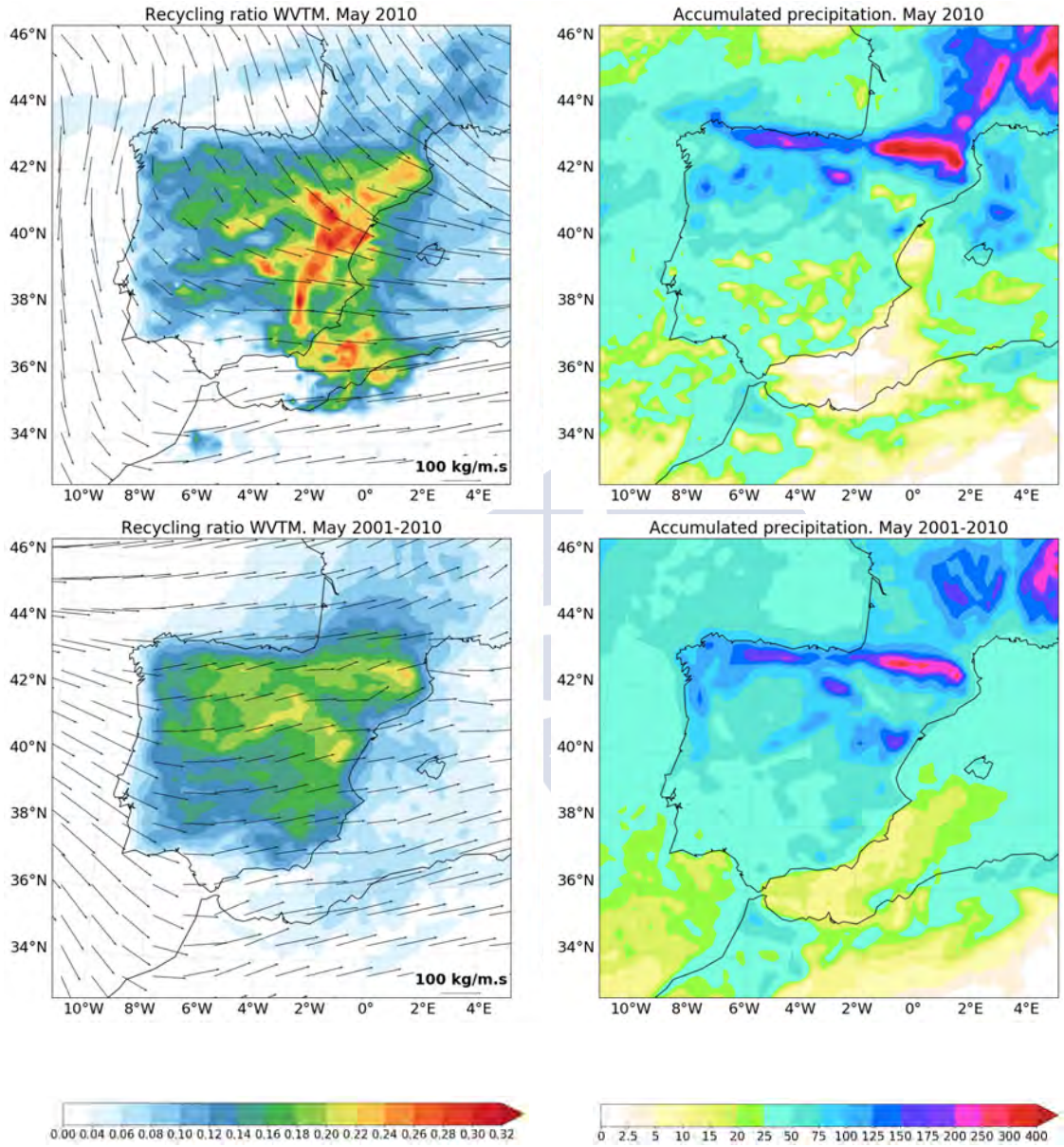

Figure 4.11: Spatial distribution of the local recycling ratio computed by WVTM, together with the average pattern of vertically integrated moisture flux (kg /ms) (left). Monthly accumulated precipitation (right). Both calculated in the parent domain for the years 2010 and the average of the span of ten years.

In Section 1.4.1, we have underscored the essential role of ET in springtime rainfall in inland Iberia. There are some areas of the interior of the Peninsula, where the peak of precipitation in spring can not be explained without considering the ET influence. In Figures 4.8, 4.9, 4.10, 4.11, the highest amounts of precipitation are found in the mountainous regions of the Pyrenees. In some years, when the precipitation is mainly from Atlantic origin, such as 2002, a maximum occurs in the north and north-west Iberia. Values of accumulated precipitation larger than 100 mm are seen in the interior northeast in every figure. These results are consistent with the springtime peak often found in the climatological observations of the precipitation in this area in May.

As can be seen in the representation of the recycling ratio calculated through WVTM and the accumulated rainfall, the spatial patterns of these variables are not equal, presenting significant differences. The recycling ratio barely reaches 6% in western Iberia, and in years with high moisture advection, such as 2002, this ratio is close to zero. This means that the contribution of the tagged moisture in these areas is insignificant. Whereas, in central and north-east Iberia, the recycling ratio presents the highest recycling values. For example, in 2001, the maximum values of precipitation are found in north-west Iberia and the Pyrenees, but the highest recycling amounts are located in central and east Iberia. The same happens in May 2010, when the ratio in the eastern façade of the Peninsula is larger than 30%, while the maximum of rainfall is found in the north. The multiannual average of the recycling ratio for the span of the ten years shows the highest values in mountain ranges (the Pyrenees, the Iberian System and the Central System), coinciding with the maximum amounts of precipitation. There are some areas, such as the Central Plateau or the western Atlantic coast, where the recycling does not match the precipitation.

4.5 Comparison between WVTM and Bulk Recycling Models

In Section 3.2, we introduce three analytical recycling models, widely employed in literature : a numerical recycling method (EBM) developed by Eltahir and Brass (Eltahir & Bras 1994), an analytical recycling method (SCM) developed by Schär et al. (1999) and a dynamical recycling model (DRM) developed by Dominguez et al. (2006).
As previously mentioned, classical recycling models based on water budget calculations are often used to obtain recycling ratios, as an indicator of land-atmosphere coupling, because these integral moisture budget methods are the easiest way to compute moisture fractions. Nevertheless, strong assumptions are often invoked in such models. The common assumption to all of them is the well-mixed atmosphere assumption, which states that most of the moisture in the air coming from ET is contained within the planetary boundary layer, where turbulent processes efficiently mix the dry air with water vapour coming from different sources. In contrast, WVTM does not need to make any suppositions, and the tracer analysis made through the WVTM is as realistic as processes in WRF. In this section, we intend to prove that this is a strong assumption and it can cause incorrect estimations of the recycling ratios. To test this, we compare the results of the WVTM, with those obtained with the classical recycling models.

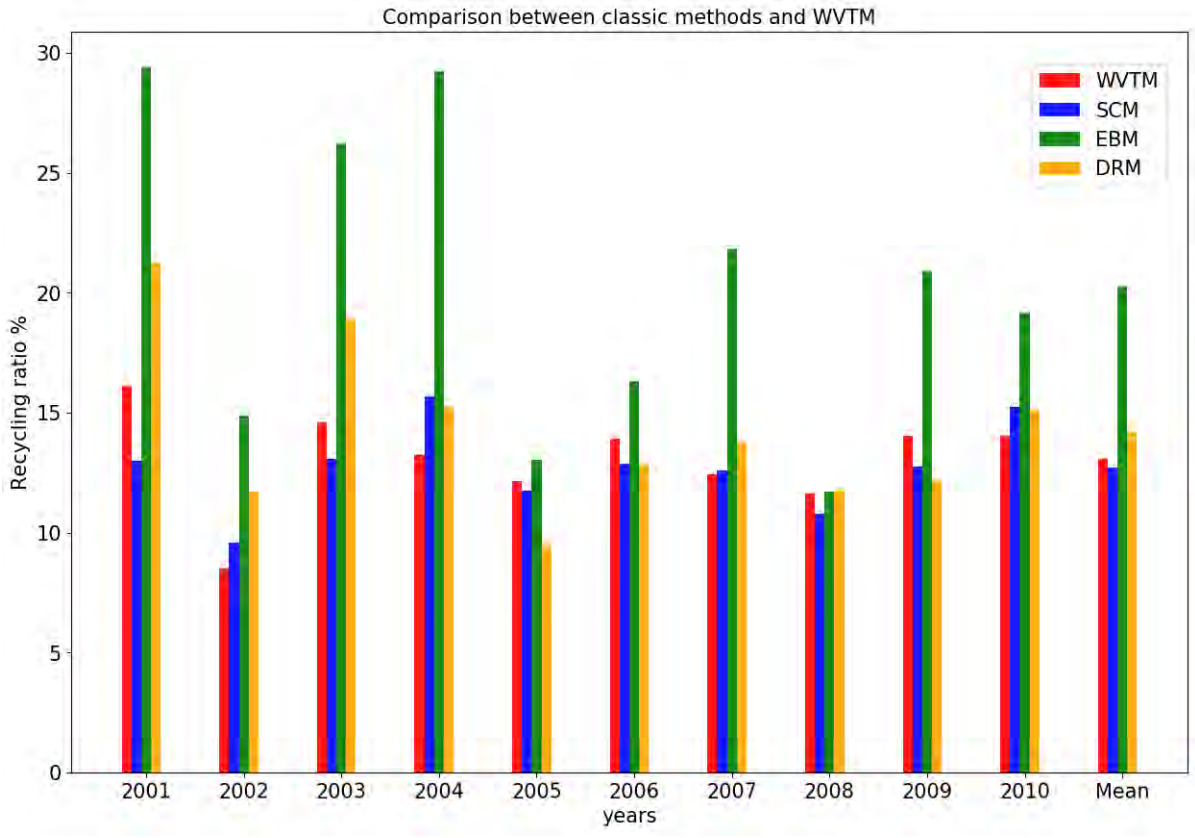

Figure 4.12: Monthly regional recycling ratio computed via WVTM (red), SCM (blue), EBM (green), and DRM (yellow) in May 2001-2010 and, multiannual average.

As has already been seen, recycling ratios obtained with WVTM barely range from a low 8.52% in 2002 to a high of 16.14% in 2001. In consonance with the synoptic situation, the highest recycling ratios through WVTM are obtained in 2001, 2003 and 2010; while the lower values are in 2002 and 2008. According to WVTM, 13.07% of the rainfall over the IP for May 2001-2010 is due to recycling processes.
Monthly regional recycling ratios corresponding to SCM remain almost constant from year to year, ranging from 9.58% to roughly 15.67%. The lowest value is obtained in 2002 with the WVTM, but surprisingly the highest ratio is achieved in 2004. The multiannual average obtained with this methodology is 12.73%. Mathematically, SCM is more straightforward than either EBM or DRM, and it provides lower values than those calculated through WVTM. But both the multiannual mean and the values obtained year to year, are in closer proximity to the WVTM results.
A more detailed procedure to compute the recycling ratio, providing not only a regional value but also a spatial recycling pattern is EBM. This model requires the time scale to be long enough (e.g. one month, as in our case) so that the change in precipitable water is much smaller than all of the other contributions and it can be neglected. EBM presents higher values than WVTM for the whole time series, and it also overestimates interannual recycling, with a percentage of 20.27%, almost 7% higher than the one obtained with WVTM.
Among the three analytical methods, the most sophisticated and recent is DRM. This model only relies on the well-mixed assumption, and it does not make any other supposition. DRM gives us regional and local recycling ratios, but also the daily variations of this parameter. DRM results vary from 11.71% to 21.27%, with an average of 14.25%. In general, these values are a bit larger than those resulting from WVTM, but they are very close to them, and the average only differs 1%.
All the models, except for DRM, provide the lowest recycling ratios in May 2002 followed by May 2008, in both years the precipitation is mainly stratiform, and moisture advection is high. This influx is particularly intense in 2002, and this is reflected in the recycling ratio. We expect that years with weak moisture influx, high values of ET and thus high convection, give rise to significant recycling rates. Thus whenever these conditions are met, WVTM presents high rates in 2001, followed by 2003, 2009 and 2010. The highest rate is also obtained in 2001 by DRM and EBM. In spite of this, this latter model overestimates the results. Nevertheless, SCM presents the most significant value in 2004, when the proportion of convective precipitation in front of total rainfall is lower than in 2001, but the average moisture influx is slightly higher. In relation to EBM, the highest values of recycling rate are obtained in 2001 and 2002, as in the case of the WVTM results. But in 2009, when the moisture influx is very low, and a relatively high ratio is expected, EBM gives a very low recycling ratio. Finally, if we take a closer look at the DRM ratios, it can be seen that as in the case of EBM, this methodology is not able to reproduce the interannual variability. The lowest value of recycling ratio is obtained in 2005 when despite having a strong moisture influx, the percentage of convection is above 60% of the precipitation. According to this analysis, we suggest that after WVTM, SCM is the most accurate methodology to calculate the average recycling ratio, but still it is somewhat dependent on the value of average influx entering the study area. Whereas DRM and EBM can not reflect the interannual variability.

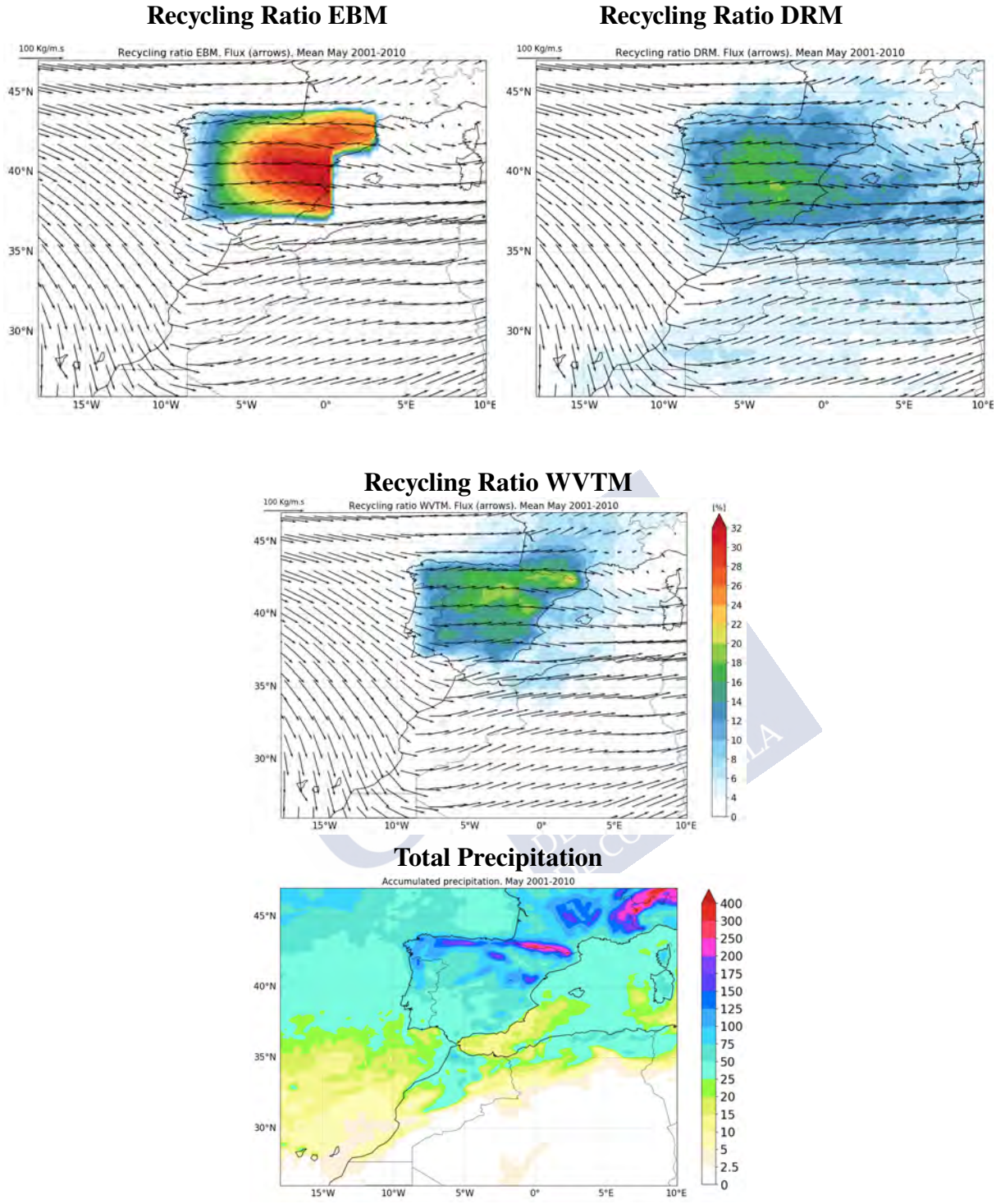

Figure 4.13: Spatial distribution of the multiannual average (May 2001 to May 2010) of the EBM, DRM and WVTM recycling ratio, together with the average flux for the same period. Average total precipitation (May 2001 to May 2010). The colorbar for the three recycling ratios is situated on the right of the figure corresponding to Recycling ratio WVTM . All the figures are represented in a regular projection.

Now that we have carefully analysed the average values, we move forward to the comparison of the average spatial variability of the recycling patterns calculated through the DRM, EBM and WVTM. The spatial pattern of the multiannual average of the recycling ratio calculated with EBM, DRM, and WVTM together with the mean moisture flux integrated throughout the column is represented in Figure 4.13, as well as the multiannual mean total precipitation.
In the case of recycling calculated through WVTM, the further evolution of the tagged moisture is governed by the horizontal winds, and the same applies to those recycling spatial patterns obtained through EBM and DRM. Nevertheless, the majority of the humidity of local origin calculated through WVTM stays within the Iberian Peninsula, and the recycling ratio from WVTM is influenced by the total precipitation and consequently by the regional orography. In contrast, the corresponding pattern from EBM is smoother and highly related to the large-scale moisture flux. Maximum values obtained with WVTM never exceed 22%, even in the northern Iberia's high mountain ranges, where the precipitation is the highest in May.
DRM allows us to do an estimation of the fraction of moisture on each grid cell of the modelled region that originated as evaporation from the tagged area, obtaining the spatial pattern of the recycling. The average obtained through DRM is more uniformly spread throughout the Peninsula, than with WVTM. Moisture reaches the interior of the European continent, and is also blown to the Mediterranean sea and North Africa. The maximum recycling rates are found in central and east Iberia, following the prevailing winds, and they are under 20%. In spite of this, their average values are similar, WVTM and DRM present different spatial distributions, with a more realistic pattern obtained through WVTM. The most significant amounts from WVTM are found in northern Iberia's high mountain ranges, whereas those derived from DRM are located over central-eastern Iberia.
Whereas recycling ratio patterns obtained with WVTM are heterogeneous, and their values are distributed over the northern half of the Iberian Peninsula; recycling patterns obtained with EBM present a smoother distribution, with the higher values concentrated in the east of Iberia. The smoothness of the spatial patterns of EBM ratios is directly linked to the fact that the mean moisture flux employed in the computation of the recycling is constant throughout the analysed time period. EBM assumes that a recycling ratio is constant throughout the month, and to perform, the computations mean moisture fluxes are employed. These two factors could be influential on the smoothness of spatial patterns of the EBM local recycling ratios.
DRM is much more realistic than EBM, and it is capable of reflecting the daily variations, but still, it is not able to capture the dynamics associated with wind shear (Huancui Hu, 2014). EBM and DRM may be considered as an approach to studying only the intensity - i.e. the spatial average- of recycling since they are not able to reproduce the detailed recycling spatial pattern with accuracy. WVTM reproduces the behaviour of the moisture better since it can follow the trajectories of the water molecules, reproducing the spatial details of the recycling mechanism.

DRM is much more realistic than EBM, and it is capable of reflecting the daily variations, but still, it is not able to capture the dynamics associated with wind shear (Hu & Dominguez 2015). EBM and DRM may be considered as an approach to studying only the intensity - i.e. the spatial average - of recycling since they are not able to reproduce the detailed recycling spatial pattern with accuracy. WVTM better reproduces the behaviour of moisture since it can follow the trajectories of the water molecules, reproducing the spatial details of a recycling mechanism.

If the classic recycling models were as realistic as WVTM, they would be able to reflect daily variations in recycling. Among the three analytical methods, the only one which is capable of doing that is DRM. A comparison of the daily evolution of the ratios obtained through WVTM, and DRM is depicted in Figure 4.14 for the years 2001, 2004 and 2008. As seen in the previous discussion, the synoptic situation of these three months is entirely different. While the convection is very high and the influx is very low in 2001, the precipitation is mostly stratiform, and the influx is strong in 2008. For May 2004 the influx is still weak, but the convection is lower than in 2001 mainly due to the ET available. Thus the recycling processes take less importance than in the first instance.

Daily ratios obtained through DRM are in close proximity with those obtained with WVTM. At the beginning of May 2001, the rate is higher when it is calculated through DRM, coinciding with weak horizontal winds over the IP. As the month advances WVTM is capable of reflecting the variations in atmospheric conditions, particularly those days with intense convection, for example from 13th to 18th of May. A similar situation occurs in May 2004, when the precipitation is mostly convective from the 10th to the 20th, and the ratios obtained through DRM are much lower than WVTM. In 2008, when the precipitation is of frontal origin, both ratios do not differ all that much, but still, DRM does not show the daily fluctuations of the influx and precipitation. The daily area-averaged rate of rainfall from the tagged region to total rainfall for May 2001, 2004 and 2008 reveals that in general, DRM tends to underestimate the moisture coming from the labelled area. Meanwhile, WVTM reflects the convective situations when recycling processes gain relevance.

Additionally, Dominguez et al. (2016) conclude that the underestimation of the recycling may be due to the well-mixed assumption, which seems to be critical in terrestrial areas. As our tagged region is inland Iberia, we include the underestimation of the recycling ratios in our area with the same assumption. The same study states that there is a link between the strong vertical shear with the fact that DRM incorrectly back tracks the moisture.

In addition to the regional recycling ratios, discussed above, some daily regional recycling ratios calculated through WVTM and DRM are shown in Figure 4.15, thus allowing to account for the spatial variability. As seen in these figures, patterns obtained through DRM are quite unrealistic, and they follow the prevailing winds. The highest recycling values are not obtained in the tagged source region, as the moisture is blown to the Mediterranean Sea and North Africa, and in the first case to the Atlantic Sea. Nevertheless, the percentage of moisture is higher for the whole domain through DRM than through WVTM. According to WVTM, the majority of the moisture evapotranspired in the Peninsula stays in this same area, or in close proximity.

From the current comparison, we conclude that analytical methods should be considered as an approach to studying the intensity of recycling since they are not able to reflect the variations year to year. In convective years and with more significant evapotranspiration, WVTM presents higher values of local recycling ratio, however recycling ratios obtained with SCM and EBM do not reflect these synoptic situations. This overestimation or underestimation may be due to the well-mixed assumption, that is not able to realistically reproduce the behaviour of the troposphere over land regions (Dominguez et al. 2016). Also, neither EBM nor DRM are capable of reproducing the spatial recycling pattern with accuracy. Among the advantages of the analytical recycling models over WVTM, we highlight their computational simplicity that makes for faster and easier computations. We suggest that WVTM illustrates the behaviour of the moisture better than any other method since it can follow the trajectories of the water molecules, thus better reproducing the spatial details of the recycling mechanism.

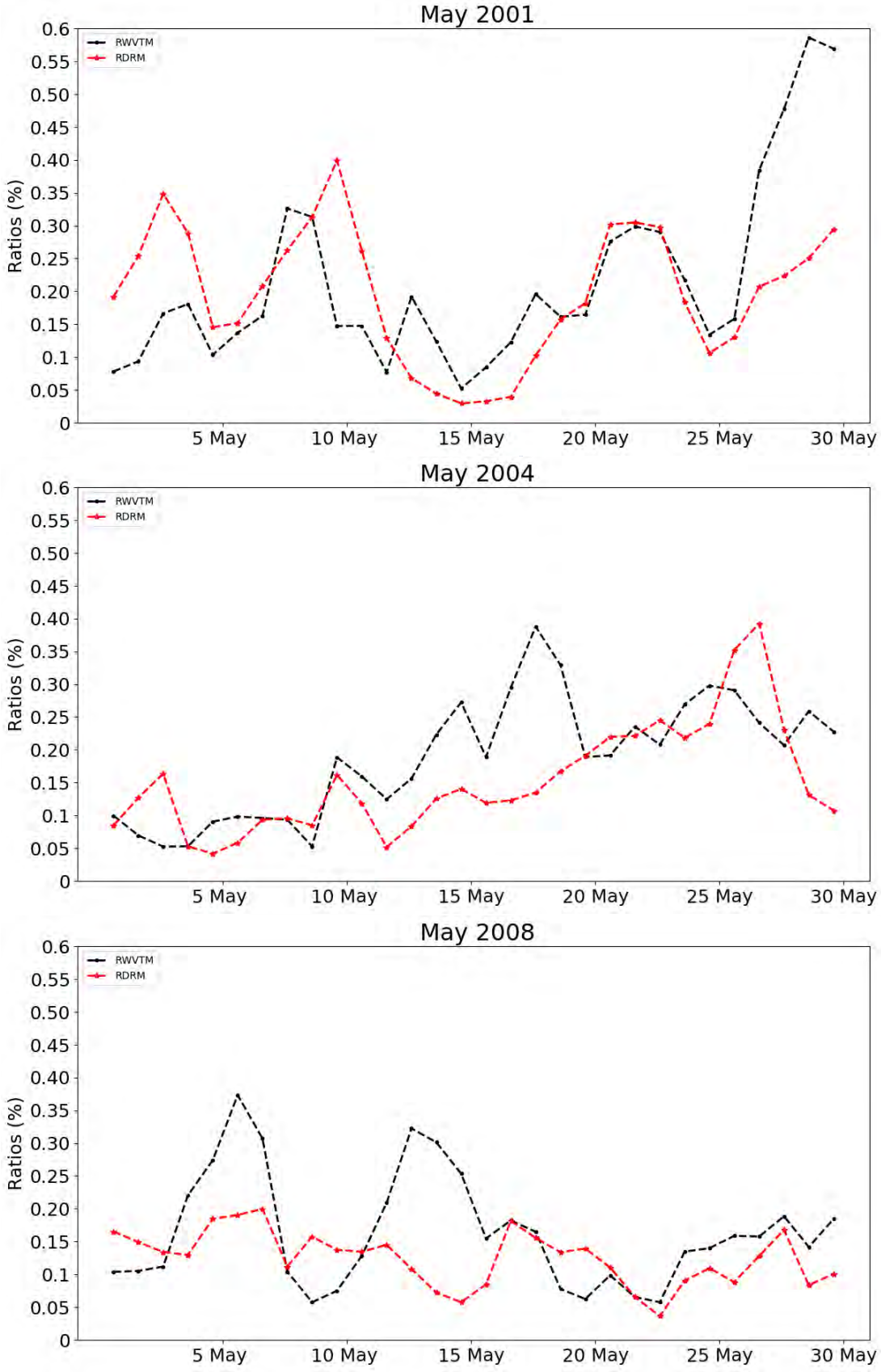

Figure 4.14: Daily WVTM climatological ratio of tracer precipitation to total precipitation (black) and DRM climatological ratio (red) for May 2001, 2004 and 2008.

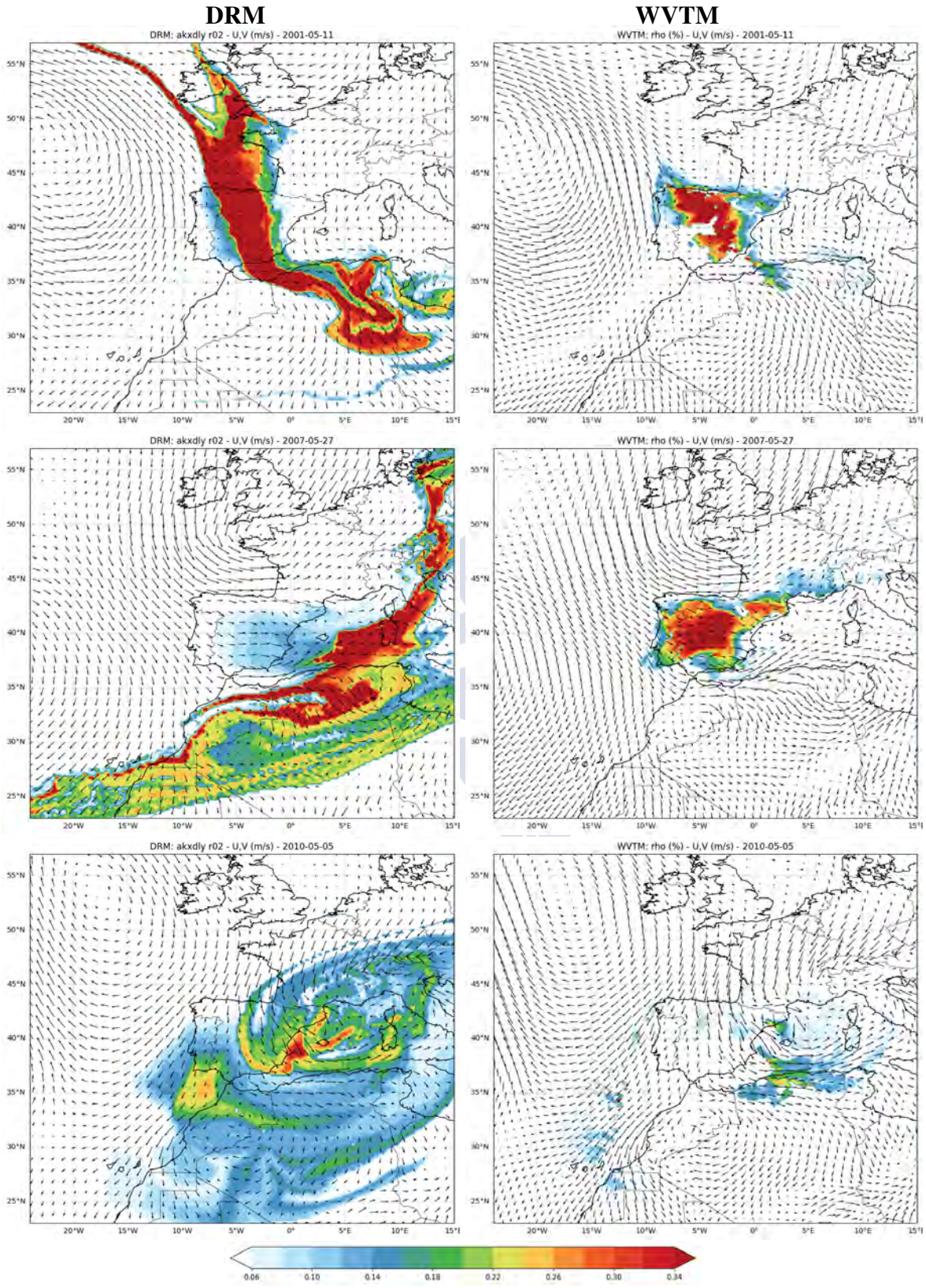

Figure 4.15: Daily recycling ratio computed through DRM (left) and WVTM (right) for three different days in 2001, 2007 and 2010, together with the daily wind pattern.

4.6 Conclusions Chapter 4

The objective of this chapter is twofold. First, to evaluate the atmospheric vertical and horizontal distribution of the moisture via using a WVTM, to better understand the water cycle, as well as to demonstrate that the well-mixed assumption suffers from inaccuracies. The second aim of this work is to pinpoint the classic recycling methods' deficiencies by comparing their results with those obtained with WVTM.
To do so, simulations with the WRF regional atmospheric model are performed over the Iberian Peninsula, during Springtime 2001-2010. A Water Vapour Tracer Method (WVTM) is incorporated in the regional climate model. This moisture tagging capability allows us to track the trajectories described by the water molecules from a source area, which in this study corresponds to the inland Iberian Peninsula, and thus provide a three-dimensional picture of the moisture pathways. WVTM opens up to the possibility of evaluating the atmospheric vertical and horizontal distribution of the moisture coming from the tagging area. Based on the model simulation results, we use three analytical recycling methods and the WVTM to carry out recycling computations over the IP and compare results among these different techniques.
As described in Section 3.2, the classic recycling methods are based on some strong assumptions; among them, we highlight the well-mixed assumption, that states that the atmosphere is well-mixed throughout the column.

The results of this investigation show that the horizontal and vertical winds govern tagged moisture evolution and that neither the horizontal distribution of the tagged moisture is uniform alongside the simulated period nor is the humidity evenly spread throughout the column. The vertical distribution of moisture tracers is analysed, confirming that humidity from ET can reach upper levels of atmospheric column decreasing with distance from the lower levels. In those atmospheric situations, in which the circulation and the wind shear are weak, moisture tends to remain over the source region. Whereas, as a result of strong circulation, the local vapour can be carried away by the winds, travelling over large distances, only being stopped by orographic barriers. Furthermore, these distances may increase if the moisture is involved in condensate precipitation processes. We conclude that the well-mixed assumption is not applicable in some particular situations when the convection is not strong enough to perfectly mix the moisture, or under conditions of strong wind shear, the advection of humidity is different in each level of the troposphere. These results, however, are not consistent with the supposition that moisture from evapotranspiration sources is always well-mixed vertically in the atmosphere.
Furthermore, the non-uniform distribution of the moisture throughout the column is also seen in the daily evolution. Tracer moisture stays mostly within the PBL, and the marked daily cycle of ET and turbulent mixing in these lower layers is reflected in its vertical distribution. The local ET moisture is only well-mixed during night hours, from the late afternoon after convective mixing has occurred through to the next morning when ET increases again, but not during the day when the increasing upward moisture flux promotes atmospheric instability.
The findings of our research suggest that a direct link may exist between recycling and convection. Convective precipitation presents higher values from midday until early afternoon when it decreases, and daily recycling values are most abundant in the afternoon when moisture from local ET is higher. Besides, we have proven that other atmospheric forcings are linked to the recycling processes, such as evapotranspiration fluxes and advected moisture. The more convective the precipitation, the higher the recycling ratio. Weak moisture advection, enhanced evapotranspiration fluxes, or even strong external moisture fluxes give rise to low recycling

ratios. The recycling ratio varies spatially and temporally, depending on synoptics and location. Our results suggest that about 13% of local precipitation come from recycling, while only approximately 8% of precipitable water is from local sources.
One of the mainstays of the traditional recycling models is the well-mixed assumption, but they also have other drawbacks. SCM does not consider variations within the study region and assumes that precipitation is constant. As well as DRM, EBM shows the spatial recycling pattern, but it considers that the moisture flux entering in the tagged area remains constant during the whole simulated period. DRM is more realistic than the other classic methods, being able to reflect the daily variations of the recycling ratio, but it still relies on the well-mixed assumption. This research has shown that EBM tends to overestimate recycling values while SCM and DRM underestimate them. In general, the interannual variations in recycling ratios are not well captured by the classical models. WVTM does not suffer from some of the shortcomings of simple analytical models to estimate moisture sources, because it does not need to make any suppositions, and the tracer analysis made through WVTM is as realistic as all the physical processes in WRF.

However, if one would like to thoroughly investigate the impact of the locally evapotranspired moisture on the regional precipitation regime, assessing the intensity of the recycling mechanism, through the computation of the recycling ratio, may not be sufficient. Interestingly, this is not only due to the dependence of the recycling ratio on the size and shape of the study region. On the contrary, the main reason lies in the following critical fact: apart from moistening the lower atmosphere, the evapotranspired humidity increases its thermodynamic instability thus favouring the development of convective cells and the subsequent precipitation of convective nature. This indirect effect of the ET fluxes is known in the literature as the amplification mechanism. In the following chapter, we carry out a study of this mechanism over the IP (the same study region as in the present chapter), to complete the analysis of the recycling processes.

USC
UNIVERSIDADE
DE SANTIAGO
DE COMPOSTELA

USC
UNIVERSIDADE
DE SANTIAGO
DE COMPOSTELA

Chapter 5

A Study of the Amplification Processes in the Iberian Peninsula

Evapotranspiration fluxes determine the intensity of land-atmosphere coupling in the local hydrology cycle. In the last part of Chapter 4, we have studied in depth the importance of recycling processes in the spring precipitation regime of the Iberian Peninsula via various methodologies. Chapter 5 can be seen as a continuation of the research carried out in the previous chapter. Our area of study is the Iberian Peninsula, and the time analysed is the month of May. In this period the precipitation peaks in some regions of Iberia, due to the contribution of the evapotranspiration fluxes. We now focus our research on the role of the non-linear contribution of ET fluxes to precipitation, also referred to in the literature as amplification or indirect mechanism. Amplification originates from advection that becomes rainfall as a result of the effect of land-atmosphere interactions on the thermodynamic structure of the lower atmosphere. As stated before, assessing the intensity of the recycling mechanism, through the computation of the recycling ratio, may not be enough to fully comprehend the impact of the ET fluxes on the rainfall regime. This is mainly due to some inherent limitations of the recycling ratio. One of them is the dependency between the rate and the size and shape of the region. The other is that the recycling ratio is associated with the direct effect of ET fluxes, that add more humidity to the lower levels of the atmosphere. In contrast, the thermodynamic instability related to the increase of moisture is neglected by this diagnostic measure. Therefore, amplification is the indirect contribution, and water recycling is considered as the linear contribution of local ET fluxes to rainfall. With the study of both of these processes, extensive knowledge of humidity contribution to precipitation is obtained. Separating amplification and recycling mechanisms is not straightforward, as they are linked. Nevertheless, the contribution of direct and indirect mechanisms in increasing rainfall can be assessed through various methodologies. Here, we employ a mathematical technique previously explained in Section 3.4, that allows us to make an estimate of the contribution of each process to precipitation. This method is conducted by calculating the relative change in the rain between a control run simulation of the WRF model and a suite of WRF simulations or sensitivity experiments, where the ET fluxes are partially or totally removed, or duplicated. The simulations are carried out with the WRF model and explained in Subsection 3.1.2. The alteration of the ET is made without affecting the energy surface budget. The land still cools down because of ET, but the resulting water vapour is removed.

5.1 The Impact of ET Fluxes in Spring Precipitation

5.1.1 Precipitation interannual Variability

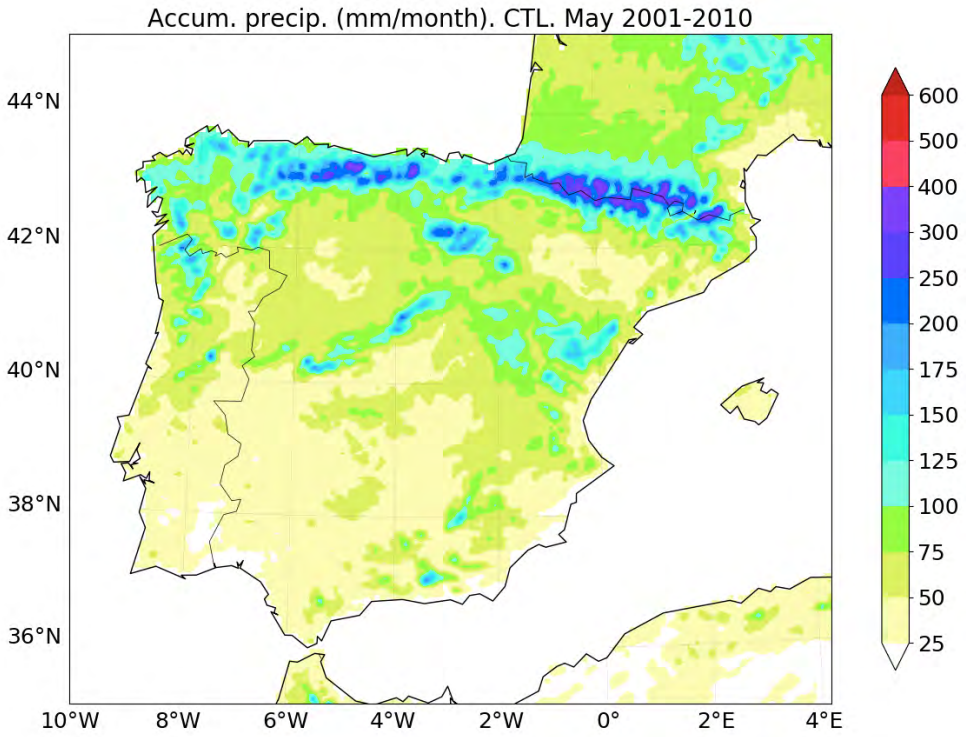

Figure 5.1: Mean of accumulated precipitation (mm/month) over the Iberian Peninsula computed for the control simulation (CTL) in the nested domain.

In this section, we show the rainfall amounts obtained from the set of simulations SIM-ET, whose technical specifications are given in Section 3.1. In these experiments, the evapotranspiration fluxes have been altered, thus affecting the precipitation. We refer to the simulations as CTL when the ET fluxes are in default set up, DRY when the moisture is gradually or totally removed from the soil and WET when it is doubled. WET and DRY experiments are initialised with modified soil wetness but identical to CTL in terms of the lateral boundary forcing.

It is essential to bear in mind the climatological mean precipitation for the CTL simulation (see Figure 5.1), thus giving us a more graphic idea of the usual amounts of rainfall during May.

The maximum precipitation obtained over land mass Iberia is located in the high mountain ranges of the northern half of the Peninsula. In the Pyrenees and Cantabrian mountains, rainfall ranges from 150 mm/month in lower elevations to nearly 300 mm/month in high areas. Precipitation ranges in value from 100 to 175 mm/month in the Galician massif, because Atlantic fronts have a significant influence in this area. Because of the orographic precipitation, these values are also found in the Central System, Denian range and the Baetic Mountains in the south, In the Central Plateau, springtime precipitation is somewhere between 25 and 100 mm/month, as well as the Southern and Sub-southern Plateaus. In the main river basins such as the Ebro, Guadalquivir, Guadiana and Tajo, precipitation never exceeds 50 mm/month. There is a small area in the

south-east of the Peninsula, located between the Baetic Mountain Range and Jucar and Segura Basin, where rainfall peaks to 75 or 100 mm/month in May.
Observed annual rainfall presents a maximum throughout the interior of the Iberian Peninsula, specifically in the east and north-east in springtime (Rodriguez-Puebla et al. 1998). This peak is not linked to the orographic rainfall and neither to the precipitation of Atlantic origin, but to the role of surface water fluxes, that is to say to the intensification of the recycling processes (Rios-Entenza & Miguez-Macho (2014), Rios-Entenza et al. (2014)).

In light of this, we compare the precipitation obtained from the CTL experiment with the sensitivity experiments DRY and WET. We analyse the results obtained from those suites of simulations 0%ET, 15%ET, 25%ET, 35%ET, 50%ET, 65%ET, 75%ET, and 85%ET in which the ET is partially removed and 200%ET in which the ET is doubled. It is worth stressing that the numbers in the previous sentence indicate the percentage of evapotranspiration removed or added. All these modifications are made over land, and so the precipitation in the sea in the plots is masked. In these sensitivity experiments, the vapour flux is being removed from the system, and thus it does not moisten the lower levels of the atmosphere. Still, the energy absorbed at the surface is converted into latent heat flux (evaporation), and the surface is being cooled down, allowing us to evaluate the effect of modifying the moisture fluxes avoiding the thermal impact on atmospheric stability of warm soil.
In Figures 5.2, 5.3 and 5.4, the differences between the climatological mean of the precipitations obtained from the CTL simulations and the DRY or WET experiments are shown. As expected, the spatial patterns of precipitation in the DRY and WET experiments are similar to the ones obtained in the CTL simulation. As the percentage of ET removed increases, the precipitation differences between the CTL and the DRY experiments become more significant, and the same applies for the difference between CTL and WET experiments, in which the differences are substantial.
On the Iberian Peninsula, there is barely precipitation in the southern half, and thus the precipitation differences are not expected to be high. However, in the northern half, significant differences between 0%ET and CTL simulations are found, especially towards the east, coinciding with the high mountain ranges. The same applies to the 15%ET and 25%ET, although the contrasts with the CTL simulation are smaller than with the 0%ET simulation. As the percentage of ET altered becomes smaller, the differences diminish. And finally, for the analysis of 75%ET and 85%ET simulation, the most considerable differences do not reach values of accumulated precipitation of 25 mm/month. These results suggest the system's response to the ET alteration presents an approximately linear behaviour since the reductions in precipitation are proportional to the decrease of evapotranspiration fluxes.

In the north-east and some areas of the interior of the Iberian Peninsula, the peak of precipitation can only be explained apropos the recycling processes, that is the direct effect that adds new moisture to the atmosphere. We know that the more convection there is, the higher the peak becomes. The amplification processes are linked to the increase of the thermodynamic instability of the atmospheric column. This gives rise to more frequent development of convective cells, thus to the enhancing of the regional circulation that produces more convective rainfall. If the total of the ET is eliminated, these areas where the peak is mainly due to the convection present higher differences with the CTL simulation. The accumulated rainfall of the simulation where the ET fluxes are doubled presents a proportional increase with regards to the ET increase. The more ET available, the more intense are the convective processes because the thermodynamic instability has expanded by adding moisture in the low levels of the atmosphere.

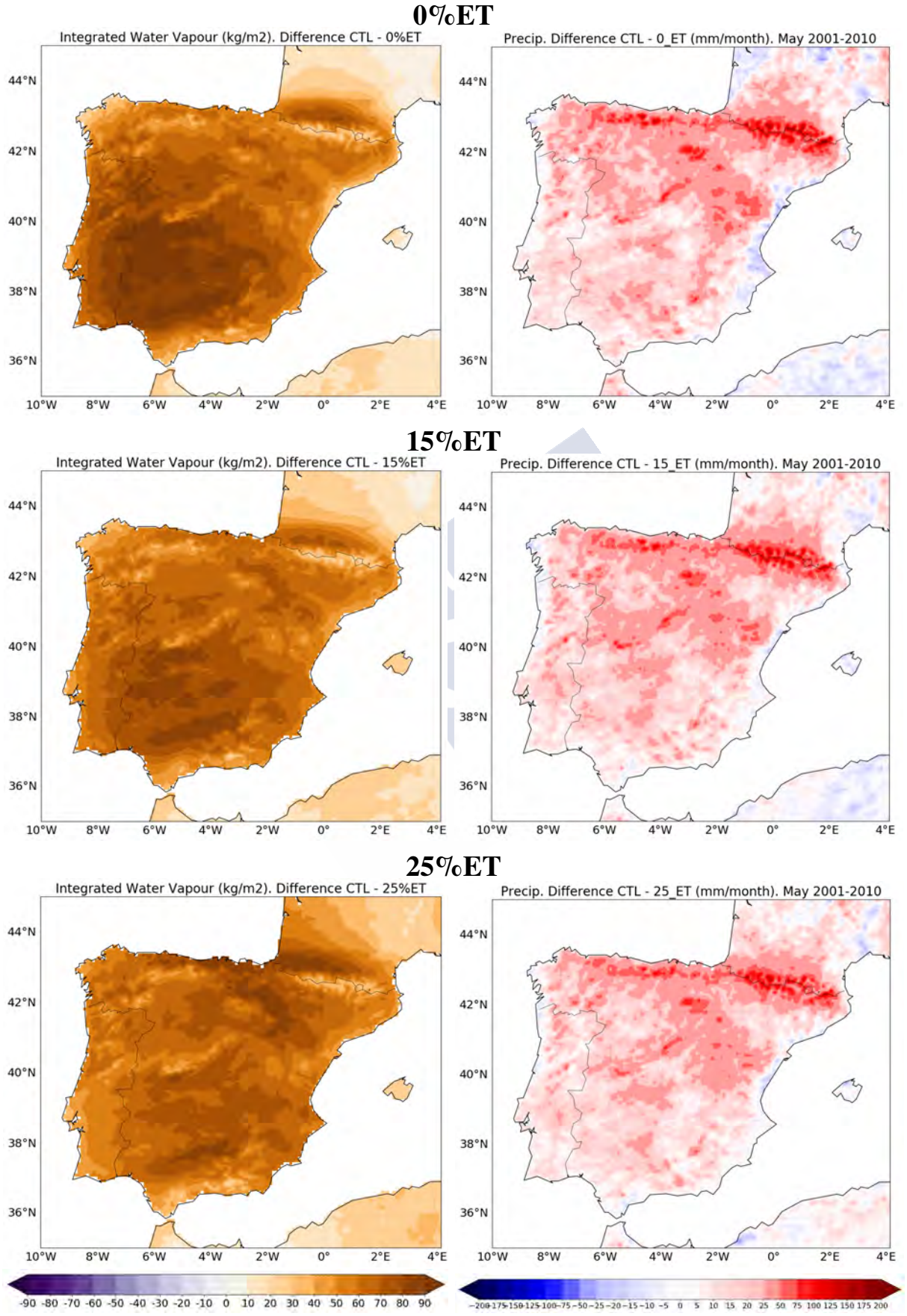

Figure 5.2: Climatological difference between integrated water vapour and precipitation.

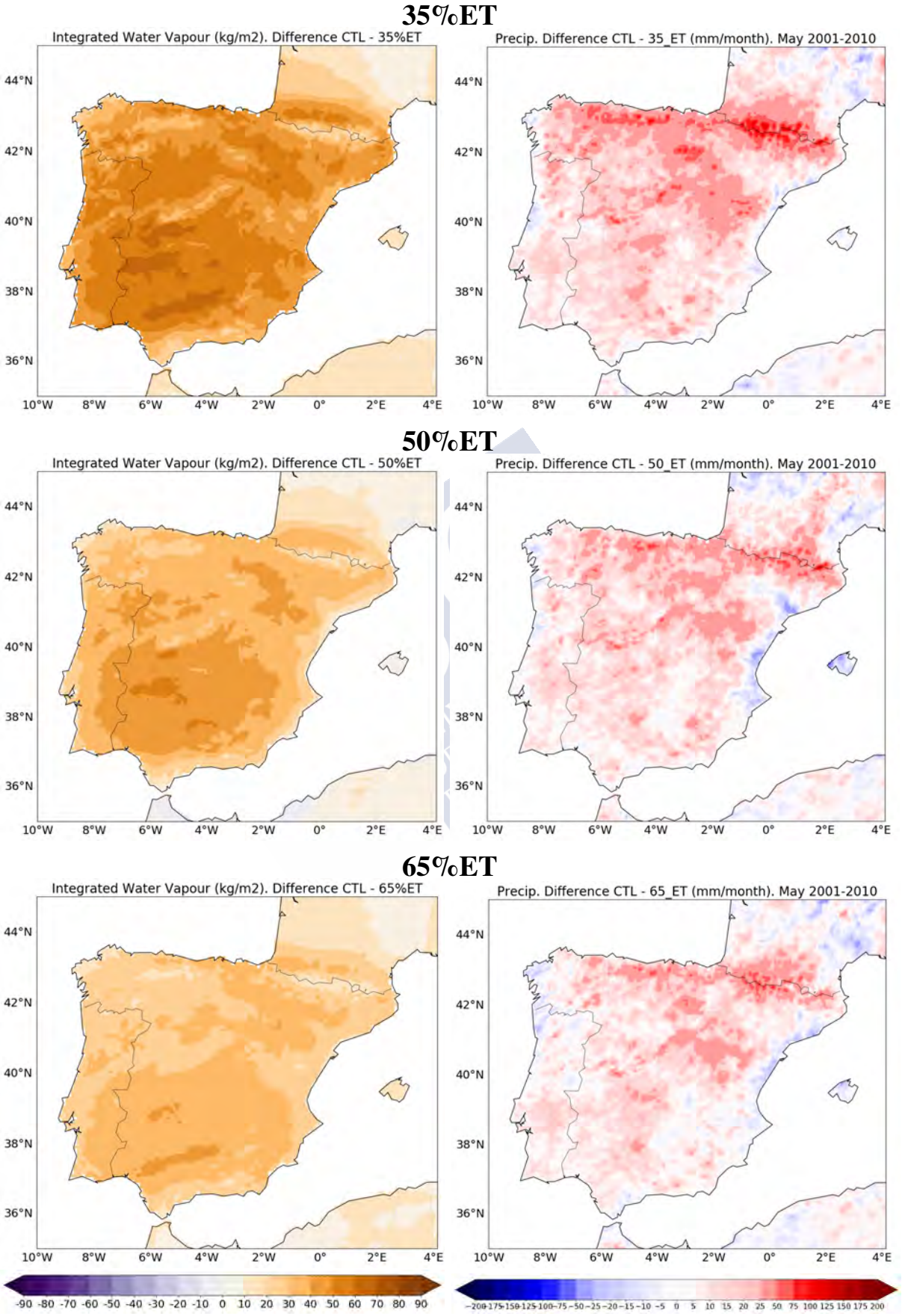

Figure 5.3: Climatological difference between integrated water vapour and precipitation.

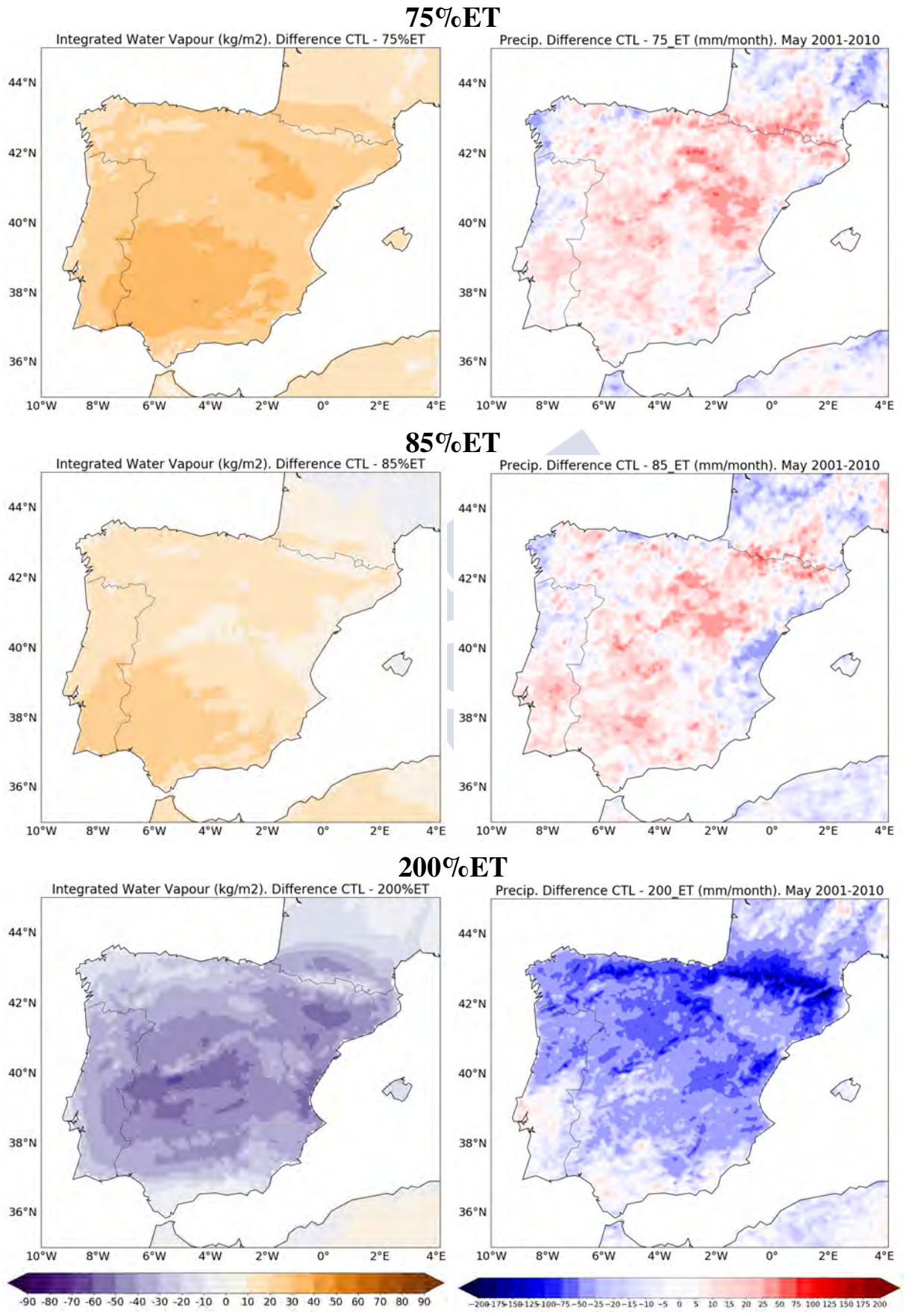

Figure 5.4: Climatological difference between integrated water vapour and precipitation.

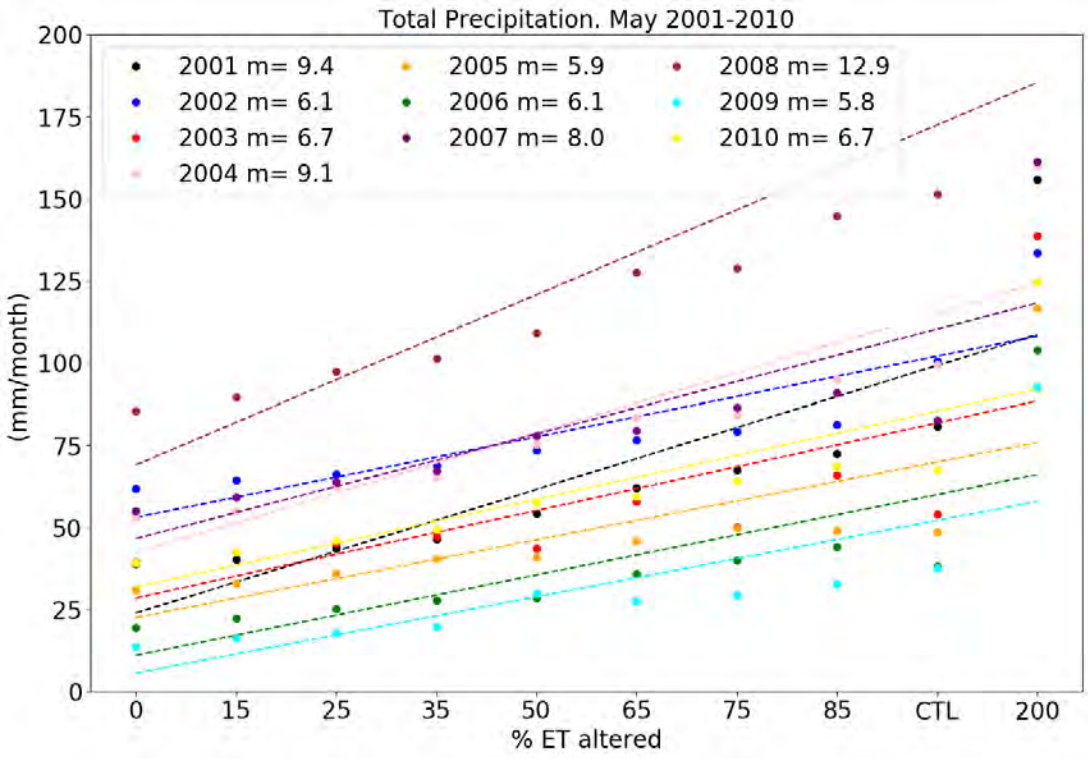

Figure 5.5: Average of total precipitation (mm/month) over the Iberian Peninsula computed for different percentages of ET reduction in the parent domain.

The interannual variability of the control precipitation has been analysed in the previous chapter, in Section 4.3. Here, we complete that investigation through the study of the precipitation variability when the ET fluxes are altered. In Figure 5.5, the average of total precipitation over the Iberian Peninsula for the different percentages of ET reductions and the CTL simulations are depicted. The decrease of total precipitation when ET fluxes are gradually removed is approximately linear, thus indicating that there is a direct relationship between precipitation and moisture fluxes. Regarding the interannual variability, the rainiest month of the climatological series is May 2008, when the CTL experiment presents average spatial values of more than 125 mm/month. As seen in the previous chapter, during May 2008, the moisture flux entering the domain is the strongest of all the years, reaching 33.50 mm/day, and the precipitation is mainly of convective origin. Under these atmospheric conditions, the outcome of a recycling ratio of less than 12% is not surprising. The angle of the line corresponding to the year 2008 is the steepest amongst all of the years, indicating that altering the ET fluxes has a linear and robust effect on the decreasing of convective precipitation. In May 2001 and May 2004, the precipitation is mostly convective, and thus the figures obtained present high values. Whereas, in May 2002 or May 2005, when the precipitation is mostly from external origin, the slope shows less pronounced values, indicating that the shock on the system is not so intense since the main contribution to precipitation are not the ET fluxes. We conclude that the behaviour of the convective rainfall relies upon the initialisation of the upward moisture fluxes in the simulation, thus suffering a marked decrease when ET is suppressed. Since the precipitation in May in Iberian Peninsula peaks due to the enhancement of the ET fluxes, we suggest that local ET plays a prominent role in the Iberian precipitation during the springtime.

5.1.2 Diurnal Cycle

To gain a thorough understanding of the effects on the climate system of altering the ET fluxes and to complete the previous analysis of precipitation, Figure 5.6 shows the daily cycle of the upward moisture flux. It also shows precipitation and recycling in the CTL, WET and DRY simulations over the Iberian Peninsula (solar time and local UTC time coincide in the IP). It should be noted that in the CTL experiments, the evapotranspiration fluxes are normally set up. In contrast, in the DRY analysis, there is no upward moisture, and in the WET experiment, the humidity has been doubled.

The aspect of the daily evolution of the ET fluxes is consistent with the technical description given in 3.1.2, since there is no moisture in the DRY experiment, while high values are obtained in the WET experiment. In both WET and CTL experiments, the ET fluxes present lower values from midnight through to the early morning, being almost constant during these hours. The arrival of the morning brings solar energy to the troposphere as shortwave radiation in the form of ultraviolet rays and visible light. As the day advances, the ET fluxes experience a rapid increase, peaking in the middle of the day and presenting the highest value at the beginning of the afternoon. ET fluxes experience a rapid decrease from the central hours of the day through the night when there is no solar light. A similar pattern is observed in the daily evolution of the total precipitation. The main reason for this behaviour lies in the contribution of the convective precipitation to total rainfall. The convective precipitation presents a marked daily cycle, while the stratiform contribution does not. Convection rises to its maximum values when ET fluxes are also at the peak, and it drastically decreases in night time hours, when the lower atmosphere is less enriched with moisture from surface ET.

Lastly, panel (d) of Figure 5.6 shows the daily evolution of the regional recycling ratio computed via WVTM. As expected, the WET experiment presents the higher rates, followed by the CTL simulation and the DRY analysis, in which there is no recycling. It has been demonstrated in Chapter 4, a link between the daily convection and the recycling processes exists. Recycling is much stronger in the early afternoon, coinciding with the time when convection peaks, but also when ET is the highest.

(a) Evapotranspiration

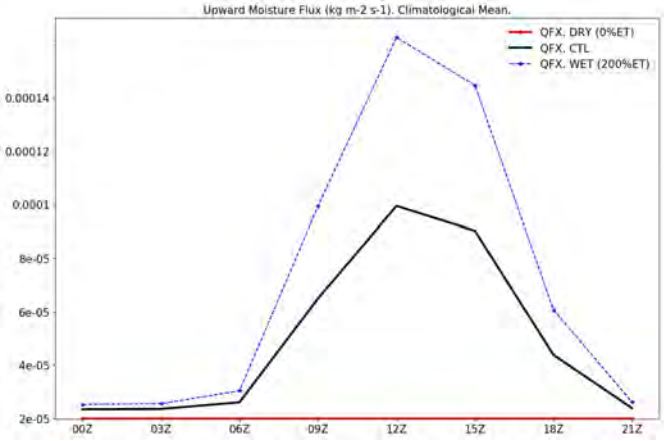

(b) Total Precipitation

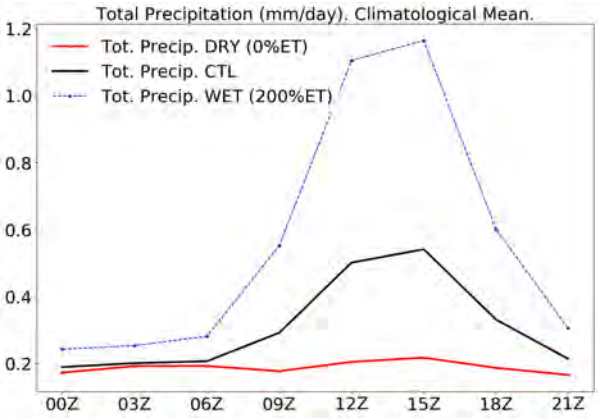

(c) Convective Precipitation

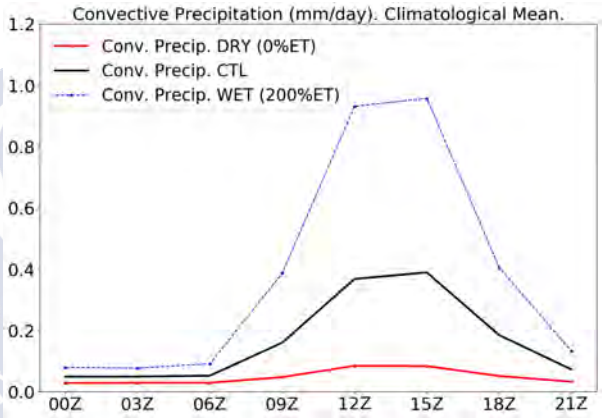

(d) Recycling Ratio via WVTM

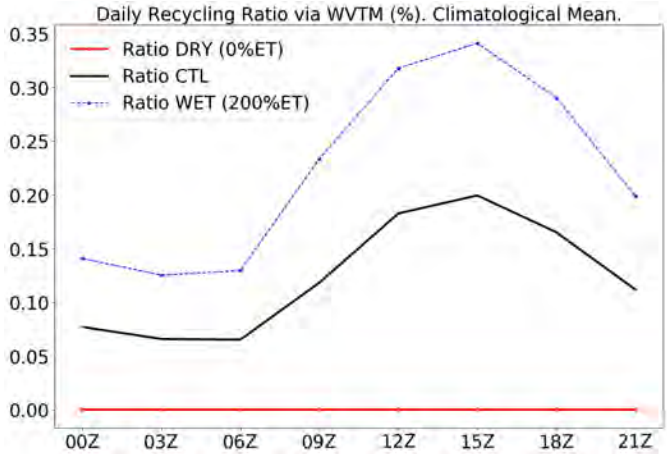

Figure 5.6: Climatological daily cycle, area-averaged over the Iberian Peninsula. Panel (a) shows evapotranspiration fluxes, panel (b) and (c) show total and convective precipitation respectively, and panel (d) shows recycling ratio computed through WVTM. Blue lines represent the WET experiment, black lines represent the CTL simulation, and red lines depict the DRY experiment.

5.2 Recycling or Amplification of Precipitation Dynamics

In Section 5.1, we have seen that the response of the system shows an approximately linear behaviour, with similar reductions in ET and precipitation. Since precipitation recycling is not sufficient to quantify the local precipitation regime, throughout this section, we intend to study the contributions of recycling and amplification, to rainfall via the computation of the amplification.
In addition to the recycling ratio calculated via WVTM, here, we compute the experimental rate of the relative change in precipitation. Both ratios allow us to estimate the role of ET fluxes in precipitation dynamics by comparing them.
As seen in Figure 5.7, both the local relative change in precipitation and the recycling are not uniform over inland Iberia. The recycling contribution has the highest values in the eastern regions and the inner north. This recycling pattern is mainly due to the direction of the prevailing humidity fluxes together with the orography. Whereas the amplification processes seem to be more relevant, presenting percentages of local relative change in precipitation of barely 70%. Still, their pattern is very noisy and does not show a clear spatial distribution.

Recycling is on average about a third of the total impact, while the amplification processes are responsible for the remaining two thirds. These results suggest that the effect of ET on precipitation is largely via indirect or amplification mechanisms, such as the increasing of moist static instability in the column, conducting to stronger or new convection development. The primary source of moisture for the extra precipitation induced by local ET is therefore mainly external in origin.

(a) Recycling ratio via WVTM

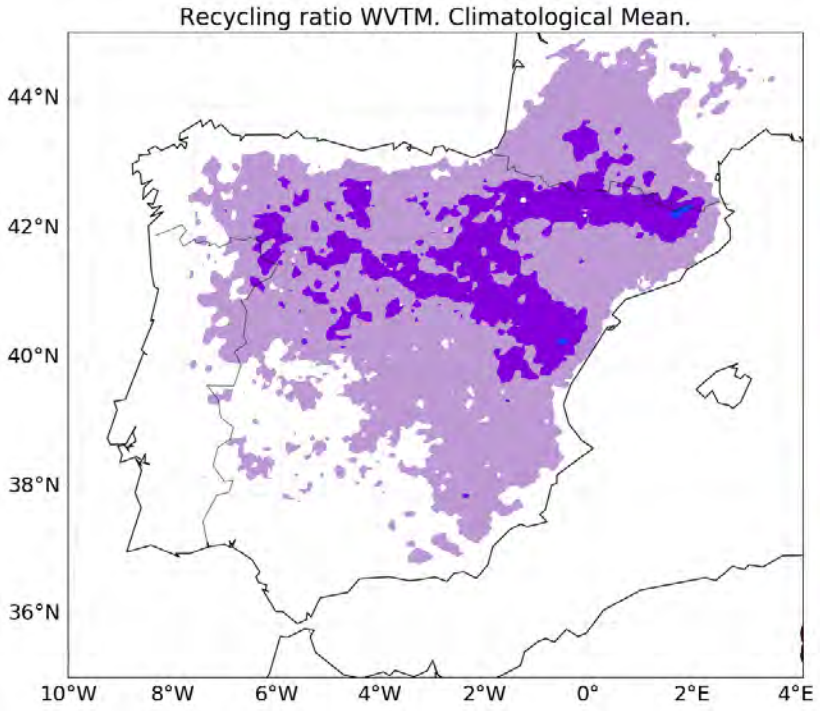

(b) Local relative change in precipitation

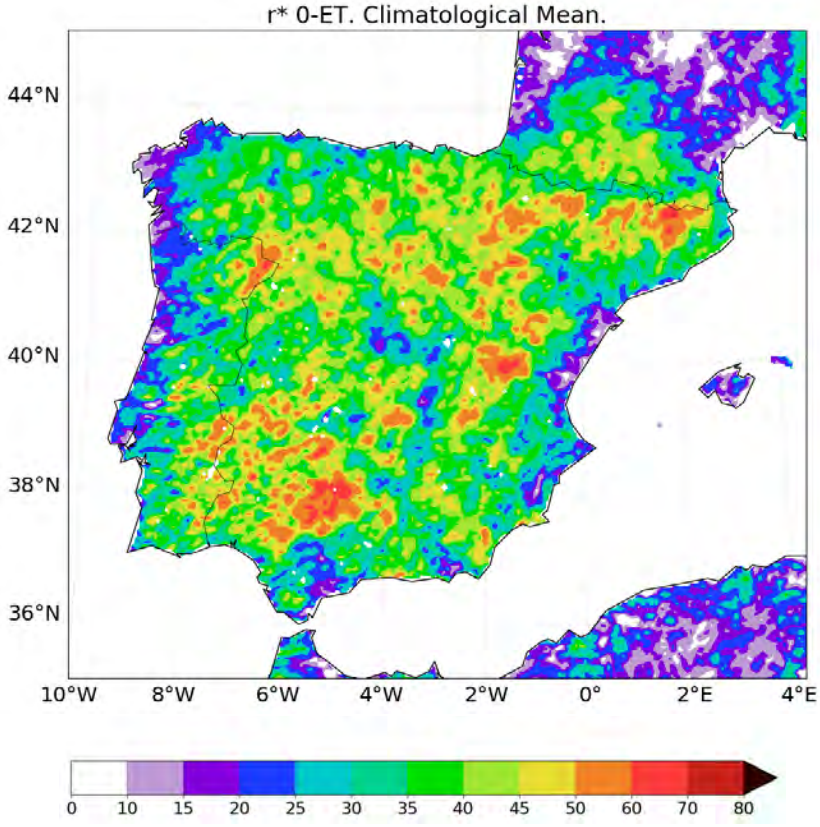

Figure 5.7: Spatial patterns of climatological means recycling ratio computed with WVTM (a) and local relative change in precipitation when ET fluxes over land are removed (b).

5.3 Conclusions Chapter 5

In the springtime, a peak of precipitation in the east and northeast of the Iberian Peninsula is often recorded. Studies have demonstrated that this maximum is not associated with the stratiform rainfall, mainly of Atlantic origin. This peak is due to the contribution of the ET fluxes, thereupon produced by an intensification of the recycling processes.
To complete the analysis of the recycling processes presented in Chapter 4 and better comprehend the amplification processes, we have carried out some experiments modifying the land-atmospheric fluxes in the open-source code of the WRF-ARW meteorological model. We have performed two types of tests, referred to as DRY or WET experimental cases. DRY experiments are composed of a set of eight simulations of ten years each, in which the water vapour flux from the ground has been gradually removed. Each set of simulations has a different percentage of upward moisture flux in the ground. WET experiments are one set of the same ten years, and for this case, we have doubled the water vapour flux in the ground. These modifications were done without altering the energy balance of the land surface, or any other feature. Finally, we have performed a set of control simulations termed as CTL, to compare them with the DRY and WET experiments.
To estimate the effect of ET fluxes on precipitation dynamics due to the direct mechanism (or water recycling), or to the indirect mechanism (or amplification) is the main objective in this chapter.

The response of the system shows a roughly linear behaviour, with similar reductions in ET and precipitation. The decrease of precipitation when ET is removed is quite significant, suggesting a prominent role of local ET in Iberian rain during springtime. By removing the ET fluxes, the shock to the system is not so intense, and the behaviour of precipitation is somewhat linear.

The results of the comparison of the recycling ratio and the relative change of the precipitation show that both processes are not uniform over inland Iberia. The recycling contribution has the highest values in the eastern regions and the inner north. Recycling is on average about one-third of the total impact, while amplification tends to predominate over recycling. About one-third of the effect on precipitation is associated with recycling, and two-thirds amplification.
Results suggest that the effect of ET on precipitation is primarily via an indirect contribution. This is due to the increase of moist static instability in the column, that leads to stronger or new convection development. The primary source of moisture for the extra precipitation induced by local ET is therefore mostly external in origin

USC
UNIVERSIDADE
DE SANTIAGO
DE COMPOSTELA

USC
UNIVERSIDADE
DE SANTIAGO
DE COMPOSTELA

Chapter 6

A Study of the European Climate with a Coupled Land-Atmospheric Model

Throughout this chapter, we investigate the climate of the European continent during recent years, paying particular attention to the summertime periods. We focus our study on the land surface interactions with the atmosphere occurring via water exchanges and heat fluxes. The focus of our research is on the influence of the groundwater reservoir on the components of the climate system, particularly in those water-stressed areas or regions with a shallow water table.

For that purpose, we employ a soil-vegetation-hydrology model termed as LEAFHYDRO coupled to the regional meteorological model WRF, which can reproduce the water table dynamics very accurately. This land surface model includes a groundwater parameterisation with a dynamic water table and river routing, and it is run in a finer resolution than the atmosphere within WRF. With this tool, we can simulate the entire water cycle, because by including the groundwater parameterisation, the soil water is redistributed in the given space, and the soil conditions are being improved. We perform a set of ten long-term simulations across five years. For each year performing two types of simulations with different configurations in the soil. The first type is termed as WT simulation, and the dynamic water table interactions are switched on, while the second type of experiment has free-drainage at the bottom of the soil column; and we refer to it as FD simulations.

The timescale of the dynamic water table variations happens more slowly than the atmospheric forcings. For example, temperature or precipitation can suffer daily or even hourly significant changes, while the daily fluctuations of the soil moisture are negligible. Still, the influence of the groundwater through evapotranspiration fluxes to the atmosphere give rise to variations in the atmospheric forcings. The presence of a water table leads to variations in the soil wetness via capillary upward fluxes and drainage, directly affecting the evapotranspiration fluxes. The role of soil moisture dynamics is very relevant in those areas with a shallow water table or water-limited regions because the groundwater in these zones has a strong influence on near-surface soil moisture distribution. In this chapter, we investigate the variations of the water table, their influence on the soil moisture variability, and the consequential impacts on land surface fluxes, near-surface temperature and precipitation, and hence, the climate.

In this chapter, a moisture tagging capability embedded in the WRF model is employed to assess the effect of ET fluxes on the European rainfall regime.

6.1 The Dynamic Water Table

6.1.1 Spatial and Seasonal Variability of the European Water Table Depth

The water table depth across the globe presents daily, seasonal, and interannual variations. The water table variability has been demonstrated with observational data across the United States soil by Fan et al. (2007).

In this section, we intend to show the spatial and temporal variations of the dynamic European Water Table resulting from the simulations of the WRF model coupled with the LEAFHYDRO model.

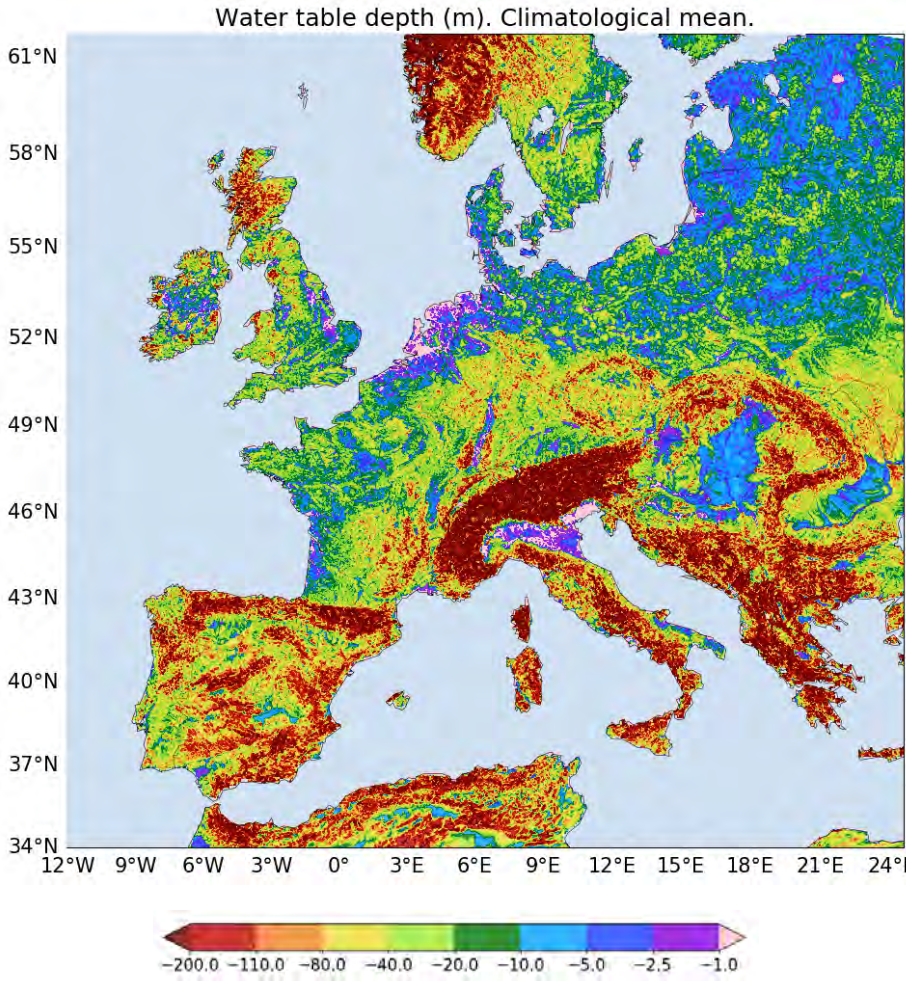

Figure 6.1: Simulated water table depth (metres below land surface). Interannual mean computed over the years 1995,1996,1997,1998 and 2003.

The depth of the simulated dynamic water table varies depending on the soil wetness and the atmospheric demand. If the vertical fluxes are downwards the WT rise, and if the vertical fluxes are upward, it leads to a deeper WT. The interannual mean over five years of the water table depth is depicted in Figure 6.1. This depth ranges from barely 1 metre to approximately 200 metres below the surface. We consider it to be a shallow water table if the depth is between 0 and 10 metres below the ground.

The shallower WTs across Europe are found in the coastal areas; the plateaus or lowlands such as the North European Plain, the Massif Central located in France or the Great Hungarian Plain situated between the Carpathian Dinaric and Balkan Mountains. The WT is also near the surface in the big river basins, such as the Danube, Loire, Rhine and Elbe.
The greatest depth of water tables are found in regions with high altitudes, such as mountain ranges or high plateaus. We highlight the Cantabrian Mountains, the Iberian mountain ranges, the Central ranges and the Pyrenees in the Iberian Peninsula. The Alps in Central Europe, the Apennines in Italy and the Dinaric Alps acting as a boundary between the Adriatic Sea and the continent. Also, the Balkan mountain range connecting Bulgaria and Serbia and the Carpathian Mountains forming an arc throughout Central and Eastern Europe. The more extended areas with deep water tables correspond to the Alps and the Balkan Peninsula.

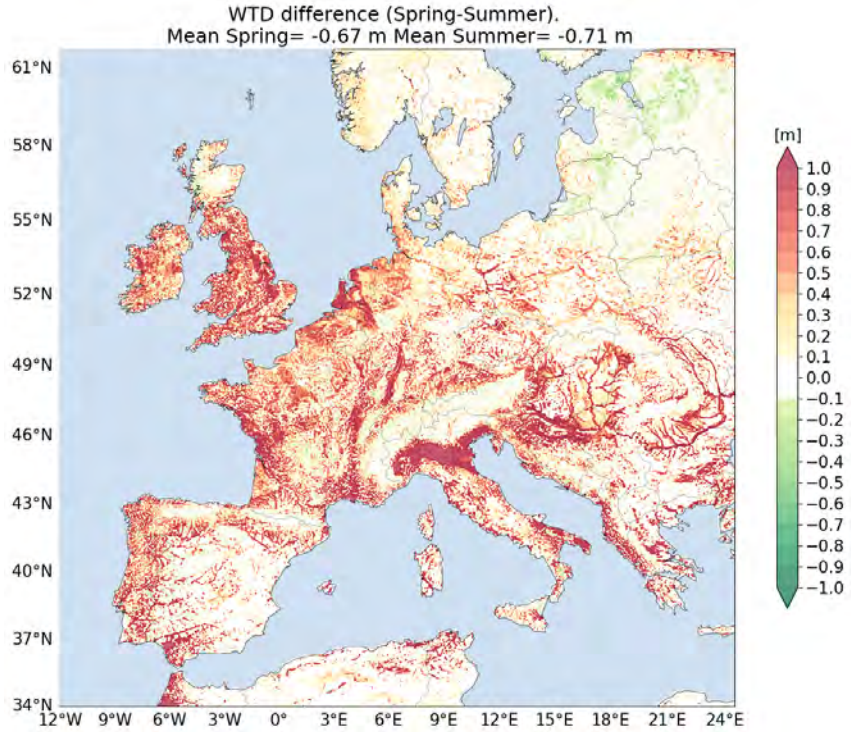

Figure 6.2: Water table depth difference between spring and summer, both seasons averaged over the years 1995,1996,1997,1998 and 2003.

The water table is dynamic, it is interacting with the climatic system, and thus it changes with time. Its timescale fluctuations are longer if they are compared with those undergone by the atmospheric forcings, the WT depth seasonal variations are seen in Figure 6.2. In springtime, the rainfall regime is more intense due to the precipitation from Atlantic origin, while in Summer the amount of rainfall contributing to increasing the groundwater storage is less, and the atmospheric demand is higher than in any other season; thus the water table deepens.
The higher differences between both seasons are found in the river valleys, especially in the Po river valley and in the lowlands. Whereas the mountain ranges and high plateaus barely suffer variations between spring and summer. In the title of the figure the average in inland Europe is reported. This average is computed only for the values of water table considered to be shallow (less than -10 metres). The spatial average computed for the springtime is -0.67 m, and -0.71 m

is obtained in the summer. Although these water table differences only range between 2 metres, the increase or decrease in a shallow area may greatly influence other elements of the climatic system, such as moisture in the soil or near-surface temperatures.

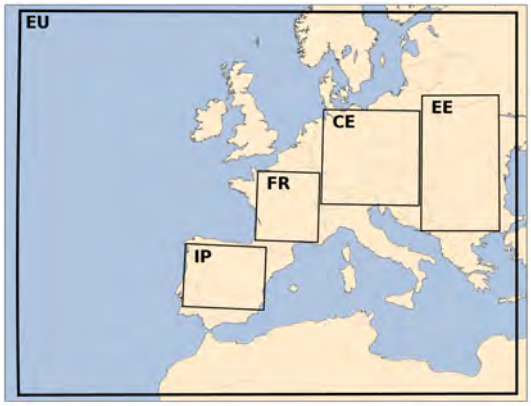

Figure 6.3: Areas marked in black lines is where the calculations are made. Iberian Peninsula (IP), France (FR), Central Europe (CE), Eastern Europe (EE).

To facilitate the study of the different regions of the European continent, we have defined four areas depicted in Figure 6.3. The region termed IP covers the Iberian Peninsula, with an area of $400 \cdot 10^3$ square kilometres. The region termed as FR covers almost France and is the smallest with a size of $350 \cdot 10^3$ square kilometres. The area termed as CE is Central Europe and it covers the Alps and part of the Danube basin, in this region are located Germany, Poland, Czech Republic, part of Switzerland, Austria and Slovakia, the area is of approximately $760 \cdot 10^3$ km^2 . The region termed as EE is Eastern Europe and it includes part of Ukraine, Romania, Serbia and Bulgaria, the Carpathian mountains, the Great Hungarian Plain and the mouth of the Danube are located within this region, its area is of approximately $510 \cdot 10^3$ square kilometres.

As seen in the previous Figure 6.2, the water table presents seasonal variability, despite having a long timescale of variation, the WT is deeper in summer than in spring. The higher WTD variations between Spring and Summer are found in the shallowest areas, with values of water table depth greater than -10 metres below the surface, such as the Great Hungarian Plain and the Valley of the Po river.

Now if we take a look at the monthly variations of the WT through several years (see Figure 6.4), an almost linear decrease from March to August is observed in the simulated WT for every year and area. In spite of this, during the Springtime (the months of March, April and May), the water table values decrease, the process is slow, and these values tend to be quite close to one another. From June to September, the decrease in the water table depth is much more rapid in every case study.

Since the percentage of shallow areas over the whole regions is given in the top of Figure 6.4, we can directly compare some of them. The size of regions IP and FR are quite similar, but while the IP region only presents a 21.66% of its total area of shallow water table, a 44.55% of the whole territory covered by the FR region is shallow. Central Europe (CE) is the biggest of the regions, almost doubling the FR region, and presenting 42.13% of the area where the water table remains above the -10 metres.

The shallowest depths are found in the CE region with values ranging from -2.5 metres below the surface in March 1995 to -3.6 in August 2003. This region covers the Alps with a deep water

table, but also the North European Plain, close to the sea which has a shallow water table.
The FR region with an area of $350 \cdot 10^3\ km^2$ presents close values to those obtained in Central Europe, the water table depth is shallow, since this region has a low height above the sea, encompassing the Massif Central and large shoreline areas. Deeper values are found in the IP region, where the maximum obtained is -3 metres below the surface. In this region, the lowland areas are surrounded by lots of mountain ranges that prevent the increase of the water table depth.
In the EE region, the WTD averages vary from -3.68 m to -5.14 m below the surface. In this area is located the Great Hungarian Plain, which is quite shallow, but it is surrounded by high mountain ranges such as the Carpathians, the Balkan and the Dynaric.

If we analyse the four regions year to year, the shallowest groundwater depths are observed during the year 1995 for the regions of France, Central and Eastern Europe. While the most profound WT is obtained in the year 2003, it is followed by the year 1996 and in France the year 1997. The deep water table in Central and Eastern Europe during 2003 might have had a direct influence on the intensity of the summer heatwave, which was one of the strongest on record.

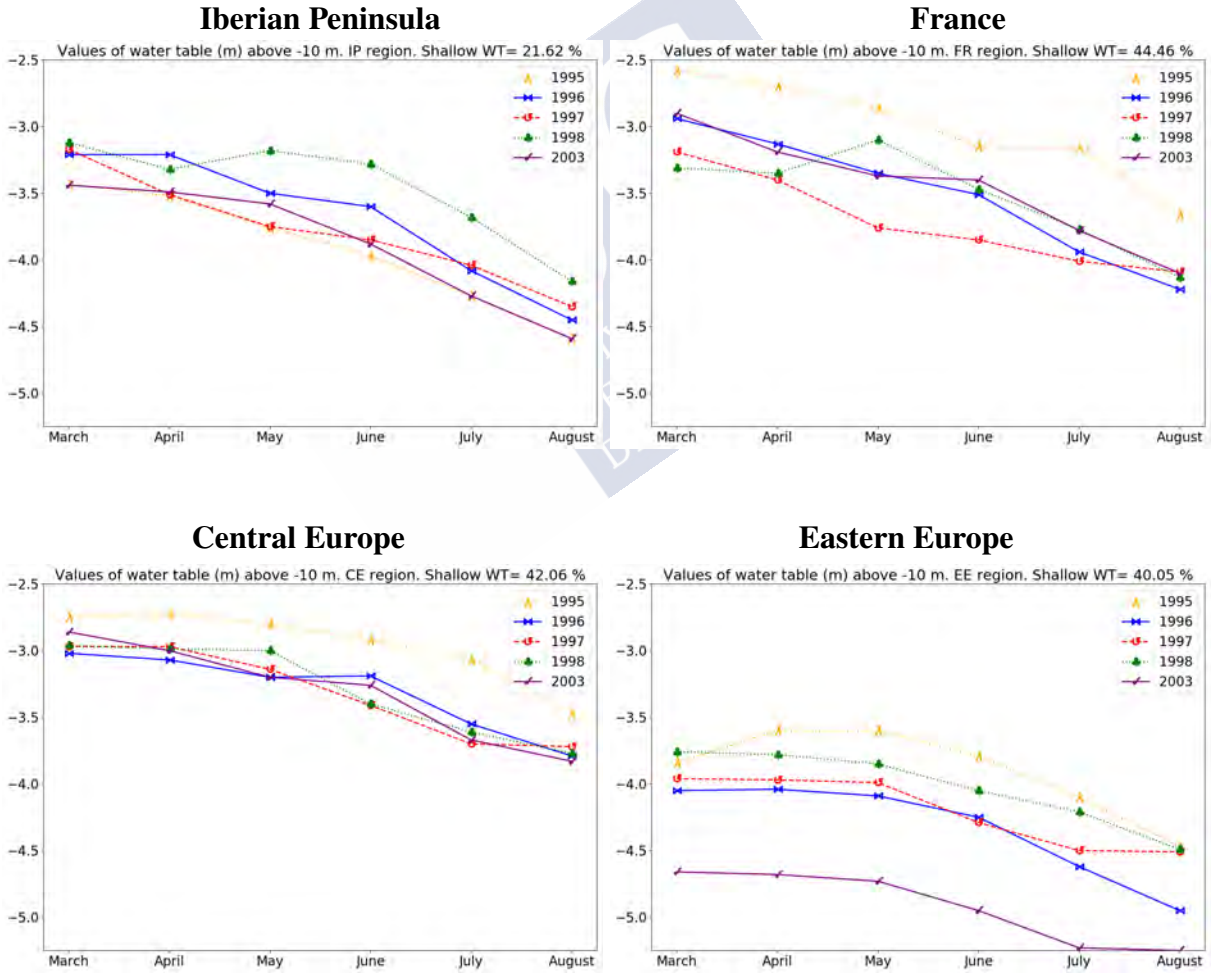

Figure 6.4: Monthly water table depth (metres below the land surface) averaged over the four regions: Iberian Peninsula (IP), France (FR), Central Europe (CE) and Eastern Europe (EE).

6.1.2 Impact of the Water Table on the Soil Wetness

As explained in Chapter 1, the humidity stored in the unsaturated zone of the ground is defined as soil moisture. This moisture is bounded at the top with the land surface and by the water table at the bottom. In some areas where the water table is shallow, the soil wetness is connected to the WT or considered part of it. In this section, the influence of the simulated water table in the soil moisture is studied, and we analyse the spatial and temporal variations of the soil moisture memory in both WT and FD simulations.
In Figure 6.5, the depth of the interannual dynamic water table in spring and summer is depicted, together with the soil wetness differences between the WT simulations and the simulations with free drainage in the soil. The presence of the simulated water table induces changes in the soil moisture; thus, the wetness presents different values in the WT simulations than in the simulations with free drainage, both in spring and summer.

The soil moisture spatial and temporal variability is mainly due to two factors, the atmospheric processes and the changes in the water table depth, which are dependent on each other. Concerning the variations in the soil wetness due to climatic conditions, moisture gradually decreases through spring until the end of the summer. This is because of increasing temperatures, and the weakness of precipitation patterns as summer draws near. It is during this time that the atmospheric demand is higher, resulting in a reduction of the soil wetness and an increment of the ET fluxes to the atmosphere.
The dynamic water table of the WT simulations exercises control over the soil moisture through the two way fluxes, the capillary fluxes and the gravitational drain flux. These variations of the soil moisture are translated to the land surface via the ET fluxes.

It may appear that the humidity differences found between WT and FD simulations are not too significant. However, since the soil moisture varies very little in comparison to the atmospheric forcings, a difference of 0.1 m^3/m^3 is considered significant. From Figure 6.5, it is clear that there is more soil moisture in the WT simulations than in the FD simulations.
The water table induces a spatial pattern in the moisture of the WT simulations. Because of this, there are differences between the values of humidity obtained in the WT and FD simulations. The similarities in the WTD and soil moisture pattern illustrate the controlling role of the water table position on the soil moisture spatial variability. While the soil moisture of the FD simulations seems to follow the different climatic conditions in each season, the soil wetness in the WT simulations follows both the WTD variations and the seasonal variability in the atmosphere.
The differences are more significant in the areas with a shallow water table and practically null in those areas with a deep water table. The marker differences are found in the areas with low elevation, such as the big river valleys (the Po Valley, the area surrounding the mouth of the Danube River), the Carpathian Basin, the North European Plain or the coastal areas (the Atlantic Coast of France, the coastal areas between the mouth of the Rhine and the Elbe Rivers). In areas like the Great Hungarian Plain or the Coastline of the North Sea, the more considerable amounts of soil moisture in the WT are due to lateral groundwater flow converging from the mountains.

In Figure 6.6, the temporal evolution of the WTD and the soil wetness over the years 1995, 1996, 1998, 1998 and 2003 is depicted for the shallowest regions, France, Central and Eastern Europe. The water table depth presents an annual cycle, and the same applies to the soil wetness. Water table becomes deeper as the growing season advances, and then again, the available soil moisture decreases due to the higher atmospheric demand. The soil moisture is almost constant or slowly falls throughout the spring, and from June to September, the WTD suffers a marked decrease. The soil moisture obtained in the WT and the FD simulations change very little from

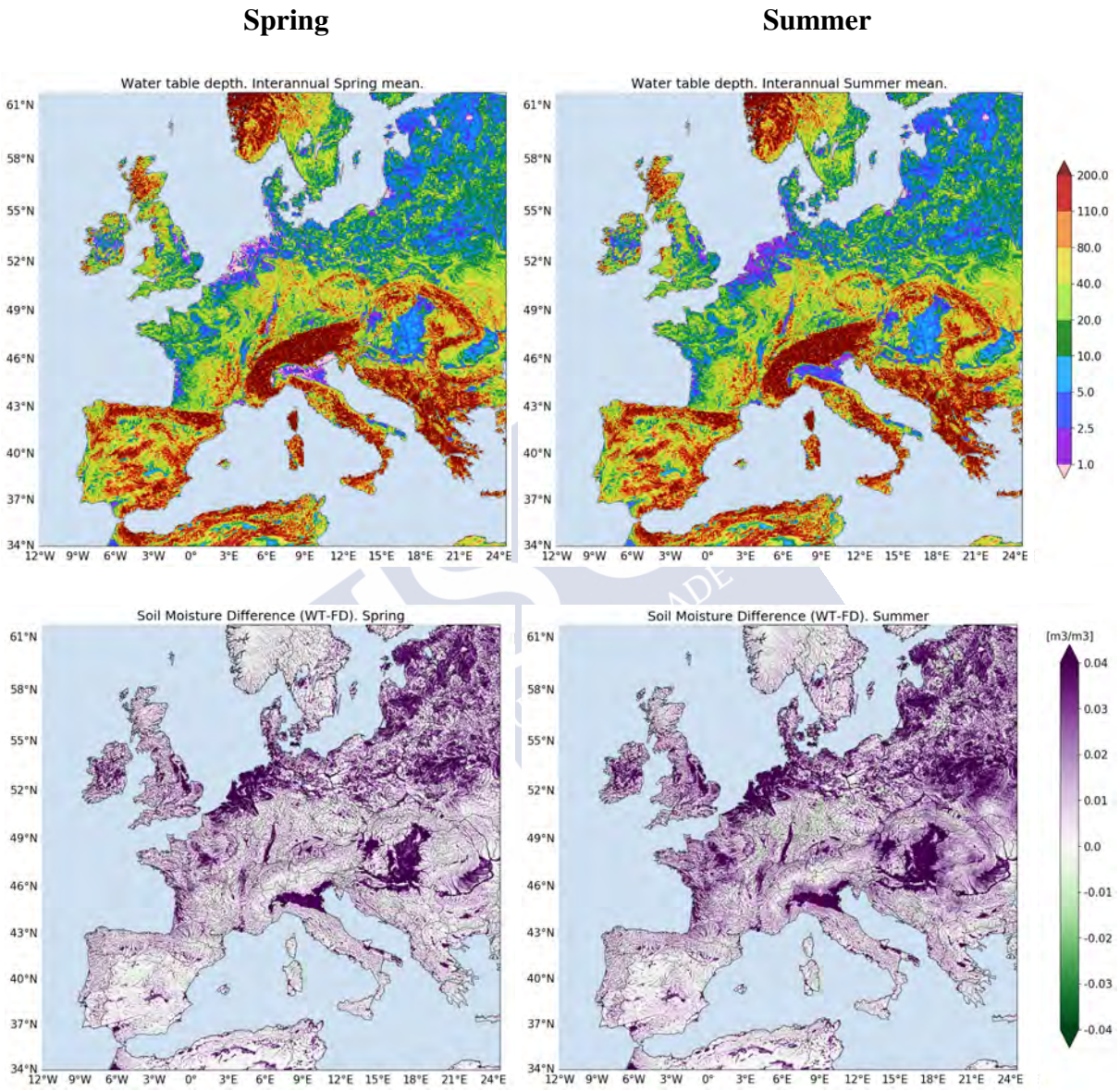

Figure 6.5: Simulated water table depth (upper). Soil moisture difference between the WT simulation and the FD simulation (down). Both computations are made in spring (left column) and summer (right column).

spring to summer, but still, the moistness below the land's surface is higher during the spring months. As seen before, there is more moisture in the WT than in the FD simulations, and the highest differences between both of them become more pronounced in the summertime, particularly in those areas with a shallow water table.

In summary, the water table in the WT simulations is influenced by the topography, but it also suffers fluctuations throughout the year due to the seasonal climatic different conditions. The atmospheric conditions and the soil water holding capacity impacts the soil wetness, but the presence of a dynamic water table affects the humidity in the soil too. The new pattern induced by the water table in the underground moisture keeps the soil wetter throughout the year, especially in those areas with a shallow water table, or during the periods of water scarcity. We conclude that the influence of a deep water table in the soil moisture is not significant, although a shallow water table impedes the soil moisture drainage during dry periods.

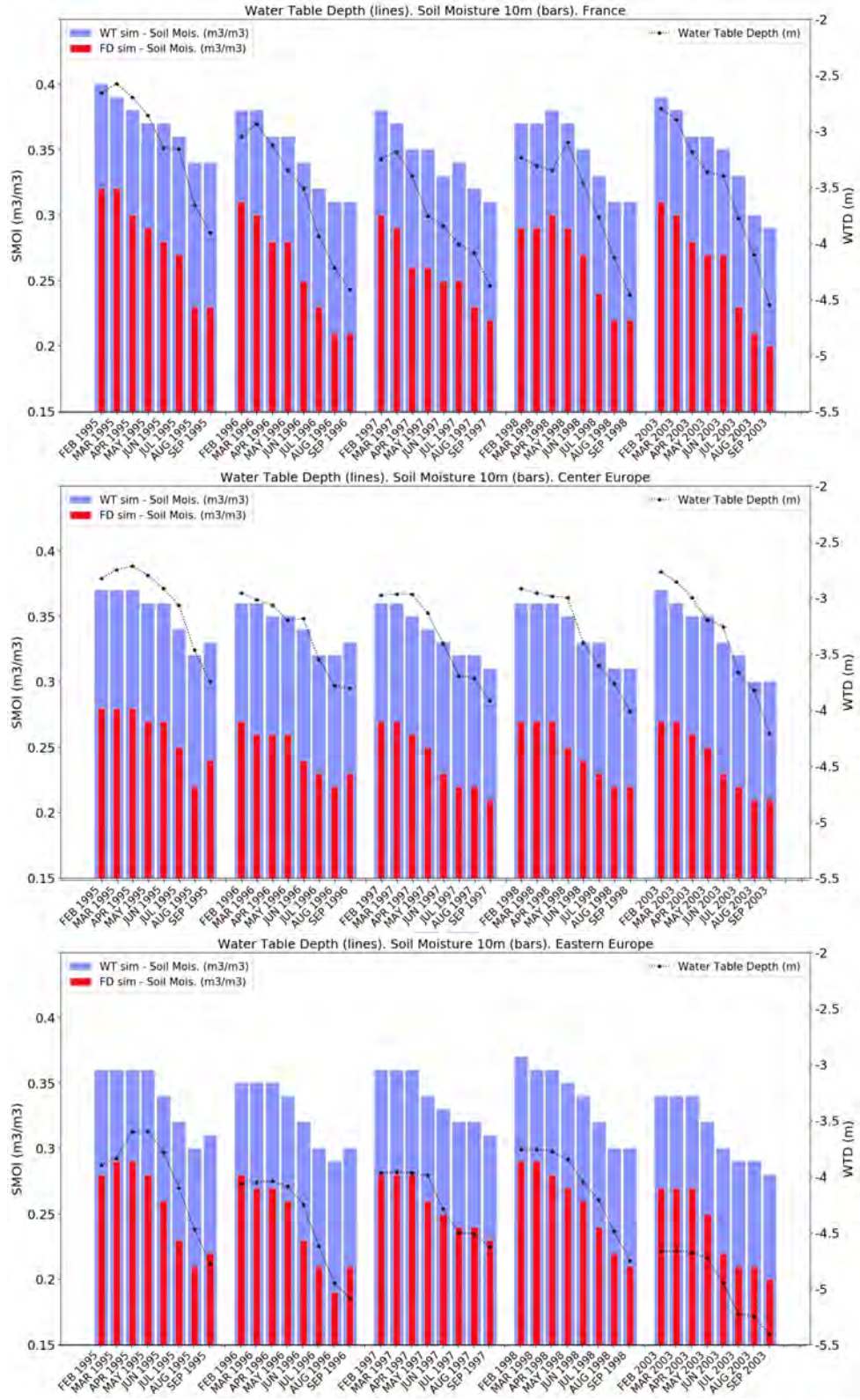

Figure 6.6: Spatial average of the monthly water table depth (black lines) and soil moisture obtained from the WT simulation (blue bars) and the FD simulation (red bars). Both the soil wetness and the water table depth are computed for the values below -10 and 0 metres below the land surface.

6.2 Influence of the Water Table on the Atmospheric Forcings

As seen in the preceding section, the presence of fluxes across the water table induce fluctuations of the water table and variations of the soil moisture. The groundwater contribution to the atmospheric forcings has been demonstrated in multiple studies (Seneviratne et al. (2006), Seneviratne et al. (2010), Orth & Seneviratne (2012), Miralles et al. (2014)) and particular attention has been paid to the influence of the soil moisture to land evapotranspiration (Gestal-Souto (2010), Martínez-de la Torre & Miguez-Macho (2014)).

Throughout this chapter, we provide various pieces of evidence of the influence of the soil moisture on the evapotranspiration fluxes, air temperatures and precipitation regime. To this end, we show the results obtained by simulating the atmospheric forcings with a dynamic water table (WT simulations) and with free drainage in the soil (FD simulations) and compare them over the years 1995,1996, 1997, 1998 and 2003 in four different regions of the European continent. The fields presented here are obtained from the coupled land-atmospheric model WRF-LEAFHYDRO. The accumulated surface evapotranspiration (SFCEVP in WRF model), the convective precipitation (RAINC in WRF model), the stratiform rain (RAINNC in WRF model) and the temperatures (T2 in WRF model) have the same vertical and horizontal resolution as the WRF model.

6.2.1 Enhanced Evapotranspiration

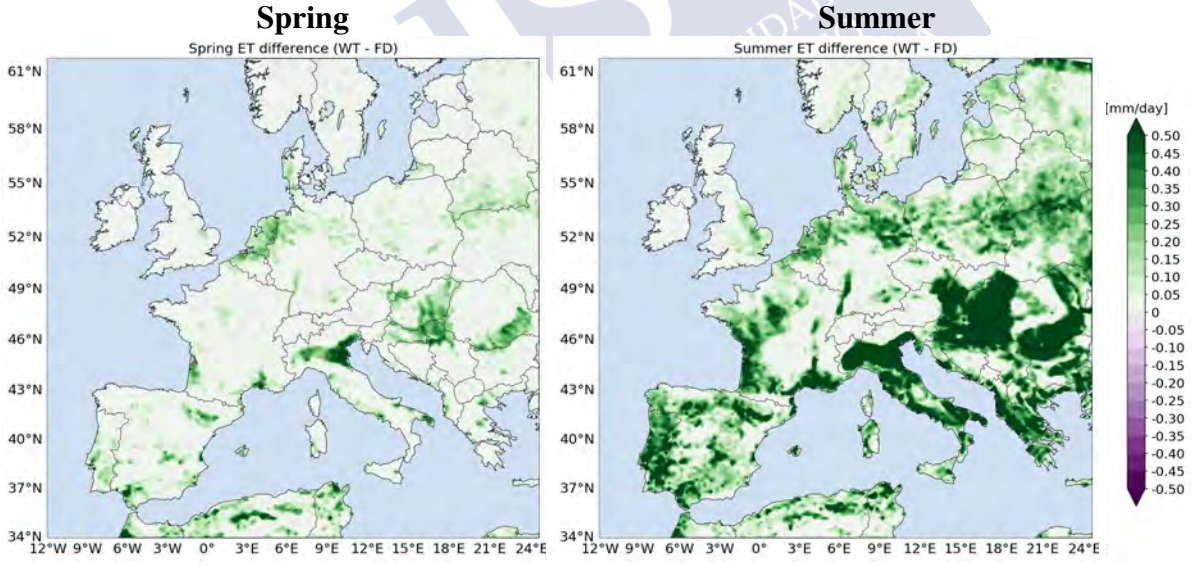

Figure 6.7: Mean spring (left) and summer (right) ET difference (mm/day) between the experiments with and without groundwater (WT - FD) for the five year simulation period.

The variations of the soil wetness lead to fluctuations in the evapotranspiration fluxes throughout the year. The soil moisture presents higher values in the WT than in the FD simulations. Besides, the soil wetness in the ground is higher during spring when the regime of precipitations is stronger, and the atmospheric demand is less. These seasonal variations can also be observed in daily evapotranspiration since this atmospheric forcing is directly affected

by the variations of the soil wetness. Figure 6.7 shows the evapotranspiration fields for spring and summer as the mean daily ET differences between the WT and the FD experiments. In the WT experiment, the soil moisture is preserved from previous periods, thus the soil is wetter. In these experiments, evapotranspiration is sustained throughout the growing season, notably in the summertime when heatwaves and droughts tend to occur. However, in the experiment with free drainage, there is less soil water, and ET partially shuts down. Hence the ET values are lower in these simulations.
Both in spring and summer, the ET follows a similar spatial pattern to the water table, yet the differences between WT and FD simulations are even more significant in summer. In summer, the ET enhancement is larger over the river basins, where groundwater flow convergence leads to intense upward flux, and over the shallow water table regions like the Great Hungarian Plain, the Atlantic coasts of France or the North European Plain. The Po valley, the Ebro valley, the North sea Germanic coastal areas, and the Great Hungarian plain are observed as enhanced ET zones every year. However, the differences are more abundant in the summertime.

The annual variations of the averaged surface evapotranspiration over the Iberian Peninsula, France, Central and Eastern Europe for the years simulated are presented in Figure 6.8.
The surface evapotranspiration increases from the beginning of the spring to the end of the spring or the beginning of summer, then falls slightly during July and August. The values of ET peak in France, Centre and Eastern Europe in June, the enhanced evapotranspiration averaged over the Iberian Peninsula presents the largest values in May. This response is because the evapotranspiration demands are the highest in springtime in larger areas of the Peninsula, as already demonstrated in Chapters 4 and 5. Whereas in Iberia, the ET barely ranges from 1.7 to 3.4 mm/day throughout the year, as we move towards the interior of the European continent, the variations become more pronounced. The region of France is directly comparable to Iberia because the size of both areas is quite similar. While in France 44.46% of the water table is shallow, the Iberian Peninsula presents a 21.62% of water table depth above -10 metres, suggesting that the role of the evapotranspiration fluxes is more critical in France. During the summertime in Central and Eastern Europe, precipitation decreases and the atmospheric demand is higher, promoting depletion of the soil moisture and an increase of evapotranspiration to the atmosphere. In both regions, the evapotranspiration reaches its maximum rates in June, suffering a progressive decline as summer advances, especially in 1995 and 2003, when the wetness in the soil is also less.

We conclude that the effects of the land-atmosphere fluxes are significant, especially in the central vast shallow water table regions of Central and Eastern Europe. We expect substantial effects on the climatic system of the enhanced ET fluxes of the WT simulations since the evapotranspiration, apart from dampening the lower levels of the atmosphere, increases its instability, thus promoting the ascent of the moisture and subsequent condensation.

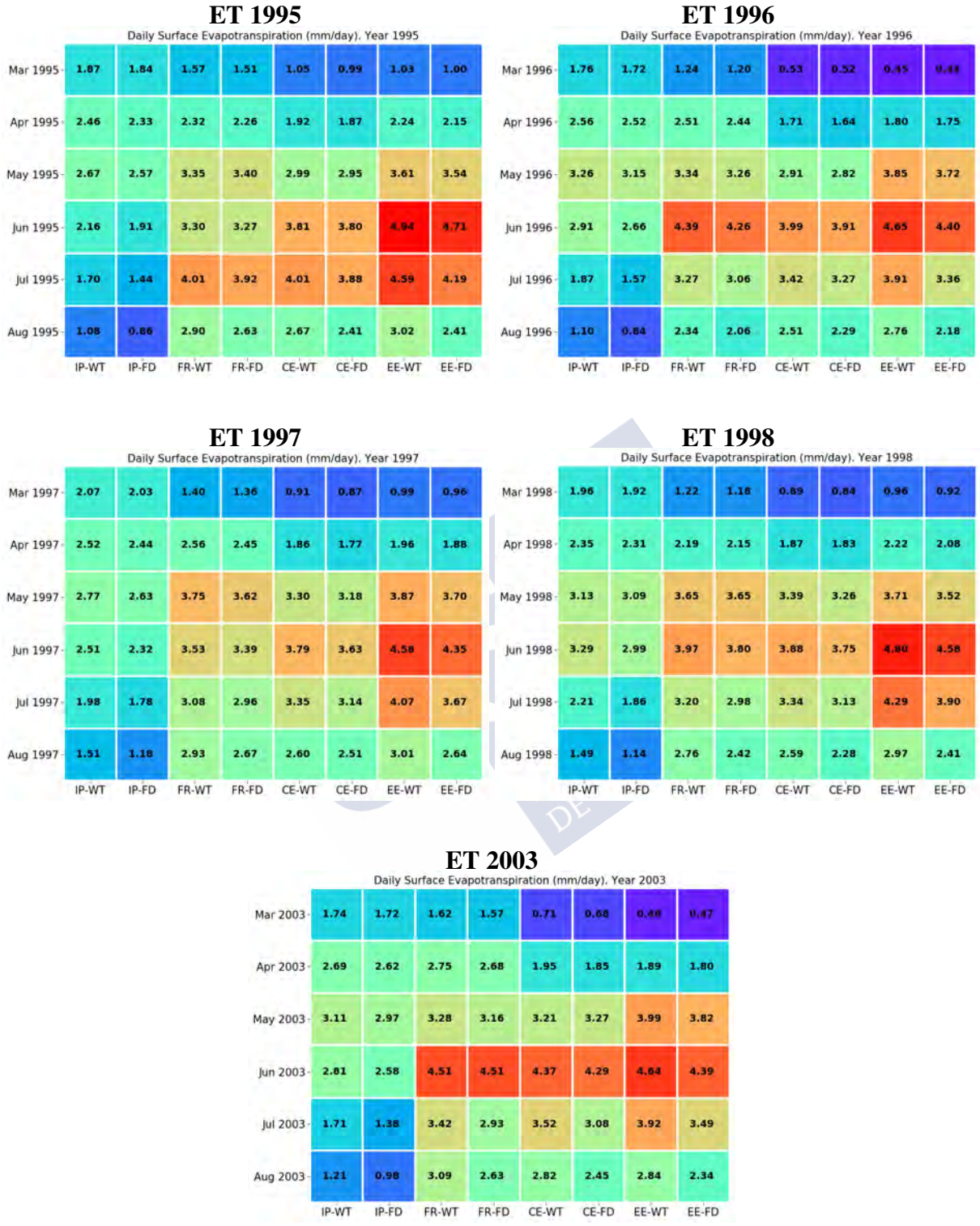

Figure 6.8: Annual variations of the daily surface evapotranspiration averaged over the Iberian Peninsula, France, Central Europe and Eastern Europe, from March to August for the 5-years simulated.

6.2.2 Effects on Temperatures

So far, it has been proven that over shallow water table regions the wetness in the soil is higher and the evapotranspiration rises. Therefore, it is clear that the introduction of a dynamic water table, like the one employed in the WT simulations, affects the behaviour of the whole climatic system. Temperatures are one of the atmospheric forcings whose link to the soil moisture and consequently to the ET fluxes have drawn lots of attention in the literature. Miralles et al. (2014) showed that under cloudy and persistent synoptic conditions, it seems very likely a depletion of the soil moisture and subsequent reduction in evaporative cooling occurs, which may further amplify air temperatures. A year later, Castillo et al. (2015) demonstrated that the wetness somewhat controls the land surface temperature via its effect on latent or sensible heat fluxes. In 2019, Martínez-de la Torre & Miguez-Macho (2019) used the land surface model LEAFHYDRO, obtaining significantly wetter soil and enhanced ET over shallow water table regions, and suggesting that groundwater might have a sizable impact on climate over the Iberian Peninsula. This section aims to evaluate the impact of the introduction of a wetter soil in the climatic system in the near-surface temperatures. To this effect, we show the temperatures obtained from the experiments with the land surface model LEAFHYDRO coupled to the regional meteorological model WRF. We hypothesise that under the conditions of wetter soils, the direct outcome is a cooling of the surface and lower levels of the troposphere, giving rise to lower temperatures in WT simulations than in the FD ones. This response of the temperatures is due to the so-called "negative water vapour feedback".

Before we get into the discussion relating to the present subject matter, we shall begin by briefly explaining the positive and negative water vapour feedback and their effects on temperatures. Climate feedback loops are a cyclical chain reaction that impacts on various atmospheric factors, making them stronger or weaker. Since these feedbacks involve variations in several components of the climate system, they are complex processes which are difficult to comprehend. Climate feedback loops are considered positive when the climatic response is accelerated, and negative when the answer is decelerated, often in an effort to stabilise the system. A positive feedback in the water vapour cycle happens when the temperatures rise, thus resulting in an increase of the water-holding capacity, and then, in turn, an increase of the amount of water vapour in the atmosphere. And if the atmosphere holds still more water vapour, the temperatures grow again, and so on until other processes stop this feedback loop. Water vapour is considered the most important natural greenhouse gas in the atmosphere, contributing more natural greenhouse effect than other greenhouse gases such as carbon dioxide and methane (Jacob (2001), Wagner et al. (2006)). The vast majority of the scientific community believes the atmospheric warming due to anthropogenic activity is directly linked to the increase of the water vapour content. Therefore, it is evident that global warming, previously explained in the opening pages of this thesis, is enhanced due to water vapour positive feedback.

Positive water vapour feedback makes sense intuitively, but there is the possibility that by adding more water vapour to the atmosphere, a negative feedback effect happens. This process occurs if more water vapour leads to an increase of the cloudiness or a decrease of the downward longwave radiation. Consequently, in both cases, the effect of adding more water vapour would be cooling the air rather than warming it. In this case, we can even refer to this phenomenon as cloud radiation feedback, since it involves cyclical feedback from the clouds and the radiation. Clouds reflect sunlight and reduce the amount of energy that reaches the Earth's surface to warm it. If the amount of solar warming decreases, then the air temperature would drop.

After having defined the concept of climate feedbacks, a question may arise to the reader:

When is a negative or positive feedback more likely to happen? We will try to solve this matter on the following pages.

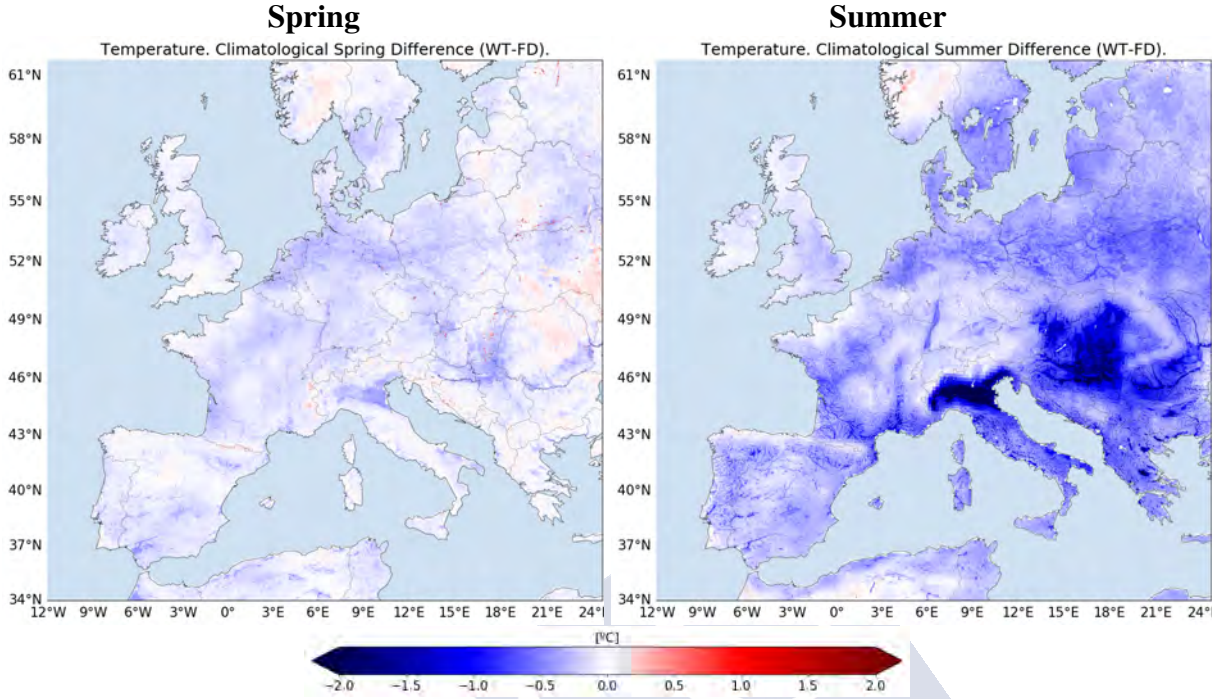

Figure 6.9: Climatological difference between air temperatures in WT and FD experiments in spring (left) and summer (right).

Turning now to the main objective of this section, we shall proceed to analyse in-depth the reaction of the temperatures of the addition of soil moisture. From the data in Figure 6.9, it is apparent that, as expected, the WT simulations in which the soil is wetter present lower climatological mean temperatures. Whereas in the FD experiments, in which the ground is drier, there is less water vapour content in the lower troposphere and temperatures are higher. Furthermore, the influence of the soil moisture on temperatures is less pronounced in spring than in summer, which means the impact of soil moisture is more significant during this period of the year when the atmospheric demand is higher. Those areas with a shallower water table present higher differences, meaning that the influence of the soil humidity of the WT simulation is essential, and it affects the atmospheric forcings. The most significant differences are found in the valley of the River Po, the Great Hungarian Plain and the coastal areas of France and Northern Europe, which are the regions with a less deep water table.

In the light of these results, we hypothesised that a process of water vapour negative feedback is happening for the set of five years. An analysis of the evolution of the temperatures throughout the seasons of our data set it is required.

In Figure 6.10, the daily mean temperature computed for spring and summer in the four case-study regions over the five years is shown. Temperatures in spring present similar values in the WT and the FD simulations, with differences that range from 0.02°C to 0.27°C. As we have previously shown, temperatures from the WT simulations are lower than those obtained in the FD simulations. Still, there are five situations in which the FD simulations present averages slightly superior to the WT simulations, however, these differences never exceed 0.09°C, and

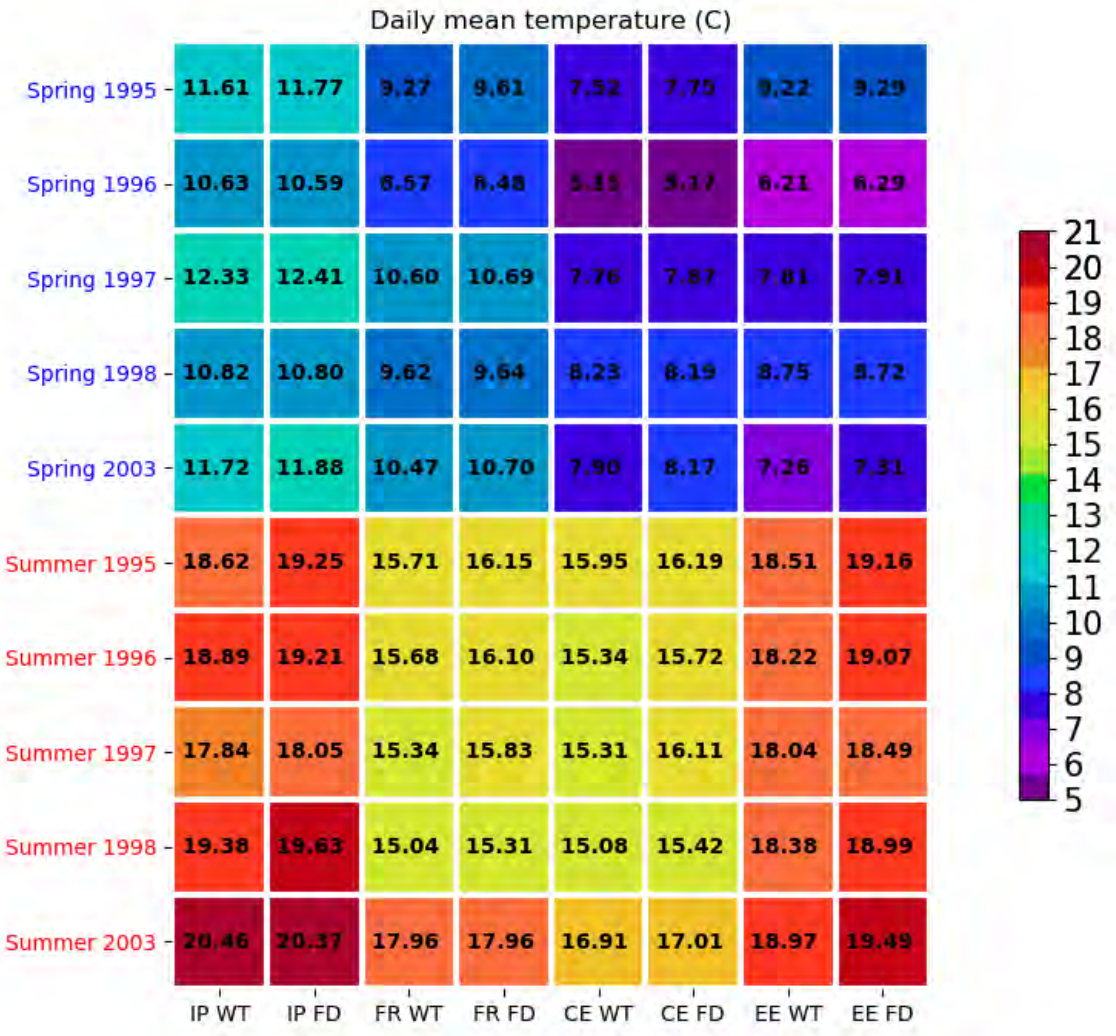

Figure 6.10: Average of the seasonal air temperatures over the five case-study regions. The abbreviation WT denotes the simulations with a dynamic water table, and FD indicates the simulation with free drainage. The abbreviations IP, FR, CE and EE refer to the regions Iberia, France, Central Europe and Eastern Europe, respectively.

we do not consider the influence of the soil wetness a driving factor on temperatures. In summer the temperatures increase for all the case studies, especially in the Iberian Peninsula and Eastern Europe, closely followed by France and Central Europe. As expected, the temperatures' differences between the WT and the FD simulations are higher in summer than in spring. In all cases, temperatures peak in the FD simulations, except in the Iberian Peninsula in summer 2003. And precisely that same season is the hottest on the record, with mean temperatures in the WT experiment of 20.46°C in the Iberian Peninsula, 17.96°C in France, 16.01°C in Central Europe and 19.97°C in Eastern Europe. The mean obtained in the wet simulations for Iberia in summer is 0.16°C higher than in the simulations with free drainage, it can be considered a significant difference. In the area of France, the temperatures are equal for both WT and FD experiments, and in Central Europe, the difference between the two experiments is the lowest of the five years.

By focussing our attention on the evolution of the temperatures over three of the summers of our climatology, we discover that the negative differences obtained in the Iberian Peninsula are also found in France and Central Europe in summer 2003 (see Figure 6.11). These negative differences between temperatures in the WT and FD simulations also appear on the Atlantic coast of the Iberian Peninsula and a small area of the United Kingdom in August 1997. These differences are less significant than those seen in summer 2003.

From previous sections, it can be observed that the soil moisture and consequently, the ET fluxes in the WT simulations increase in all the simulated years. Nevertheless, through the analysis of the temperatures in 2003, it is clear that the climatic system does not respond likewise in the rest of the years. Since this is a rather unexpected outcome, we analyse down below some atmospheric forcings related to the increase of the temperatures in summer 2003 in WT simulations.

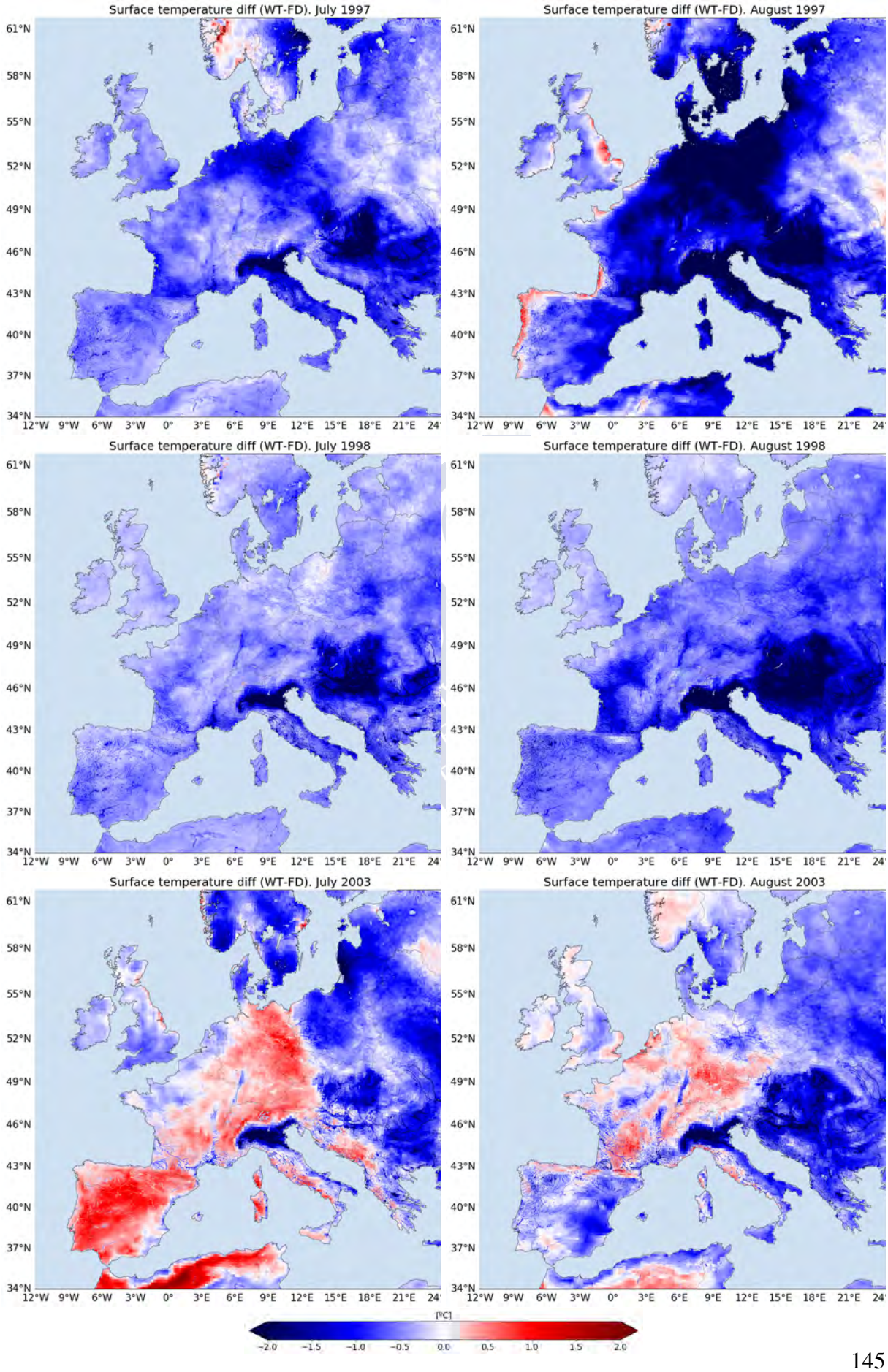

Figure 6.11: Monthly differences between temperatures in the WT and FD experiments for the months of July and August of 1997, 1988 and 2003.

2003 Summer Heatwave in Europe

It has been outlined in Chapter 1, that heatwaves have become the "new normal" in the summertime in Europe. For this reason, an in-depth study of these dangerous weather events might help us to mitigate the impact of future similar episodes, or at least to anticipate them with the implementation of more sophisticated early warning systems. The record-breaking 2003 European summer heatwave has caused rivers of ink to flow in the scientific community since the effects of this extreme event were devastating. The most dramatic and striking consequences were the high mortality rate associated with the heatwave. Nowadays, there are still numerous limitations on the methodologies to analyse the mortality owing to high temperatures; however, the vast majority of studies estimate the death toll linked to the 2003 heatwave to have been between 35000 and 40000 (Schär et al. (2004), Fischer et al. (2007), García-Herrera et al. (2010), Miralles et al. (2014)). In addition to mortality, the heatwave also caused forest fires all over Portugal, Spain and France, bad air quality, crop devastation and even shortages of potable water. In Southern and Central Europe, the socioeconomic impact of this event was huge.

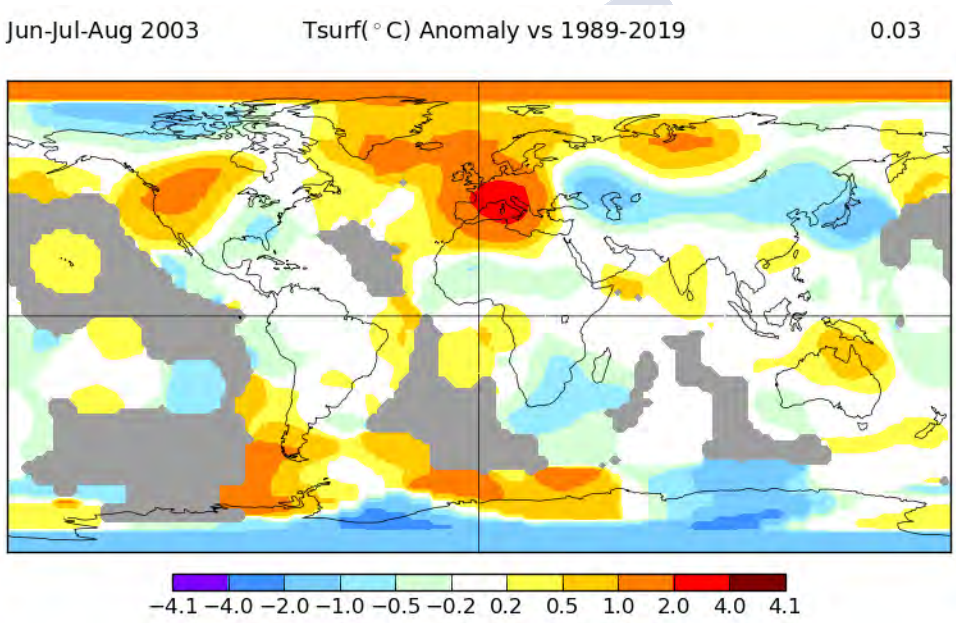

Figure 6.12: Surface air temperature anomalies during summer 2003 with respect to the period 1989-2019. Figure adapted from `http://www.giss.nasa.gov/cgi-bin/update/gistemp/`

In Figure 6.12 the temperature anomalies for summer 2003 with respect to the 1989-2919 reference period are shown, and the image was obtained from data from GISTEMP, `http://data.giss.nasa.gov/gistemp/maps/` (Hansen et al. 2001). Anomaly temperatures exceeded 3°C, in comparison to the mean for 1989-2019, across a large area of the European continent, especially France, Central Europe, Italy and Eastern Europe. These extreme temperatures were reached at the beginning of August 2003 through a combination of factors. Firstly, an atmospheric blocking system composed of a persistent anticyclone stationed above western Europe that allowed the advection of warm air from the African continent. Secondly, this situation, combined with the lack of soil moisture and high sea surface temperatures in

the Mediterranean Sea, motivated a process chain in the climatic system. A depletion of soil moisture and subsequent reduction of evaporative cooling started a cycle in which the reduced cloudiness and the increased downward radiation led to exceptionally high-temperature anomalies and prevented precipitation. In Central and Eastern Europe, these conditions were exacerbated by the lack of precipitation during the previous winter.

Here, we try to investigate the physical processes underlying the heatwave that occurred in 2003, through the comparison of the simulations with a dynamic water table and the free drainage simulations. As already shown in previous studies on the 2003 heatwave (Miralles et al. 2014), two-time windows have been defined to describe the dramatic weather event. The period between July 23rd to 31st is termed as Preheatwave, while the period between August 4th to 13th is defined as Megaheatwave. The daily average of both periods for the integrated water vapour and the downward longwave flux for both WT and FD experiments is shown in Figure 6.13 and Figure 6.14.

During the Preheatwave period, the water vapour integrated throughout the atmospheric column presents high values, especially in the northeast and the Great Hungarian Plain. Those values are even higher in the WT experiment, except for the Iberian Peninsula, where the results of FD and WT simulation show spatial patterns with significant similarity. The amounts of downward longwave radiation obtained in the FD and WT simulations are close, but still, they are slightly higher for the experiment with the dynamic water table. For both atmospheric forcings, the higher values of the WT experiment are reached in those regions in which the water table is in closer proximity to the surface, such as the Great Hungarian Plain or the North European Plain. The integrated water vapour during the Megaheatwave shows higher values in France, the River Po valley and the coastal areas of the North Sea. Once again, the water content in the atmosphere is significantly higher in the experiments with a dynamic water table than with free drainage in the soil, and the same happens in the case of the downward longwave radiation. The most striking result to emerge from these figures is the higher values obtained for the radiation fluxes of the WT experiment, particularly in the French coastal areas. We suggest that the high values obtained for both the water vapour content and longwave radiation are firmer catalysts to the increase of the temperatures during this period, and a strong positive temperature-water vapour feedback processes. These findings suggest that the long extension in time of the extreme event might be related to the strong positive feedback.

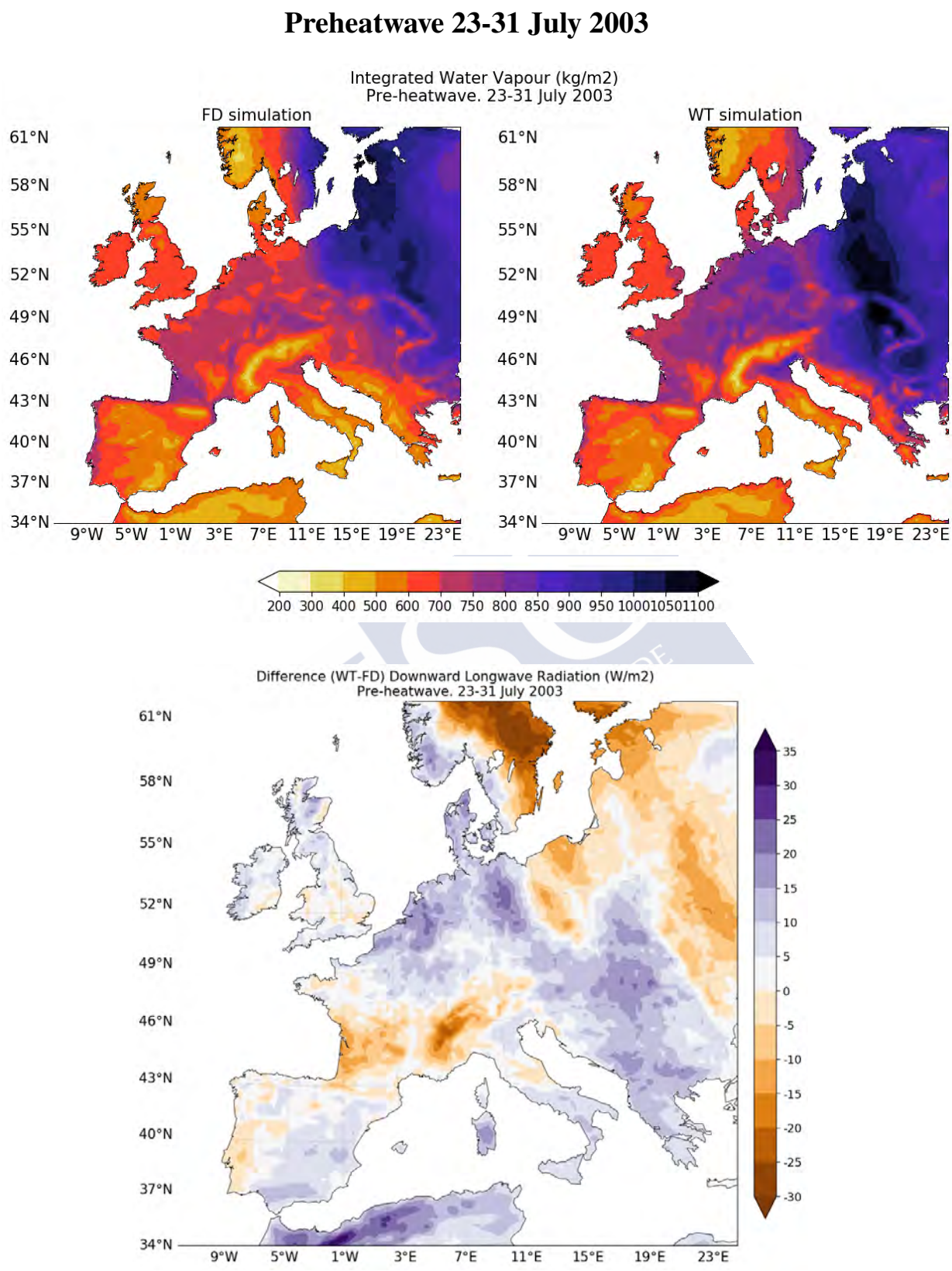

Figure 6.13: Integrated water vapour (above) and downward longwave radiation difference between the WT and the FD simulations (below). Both computed for the period corresponding to the preheatwave of summer 2003.

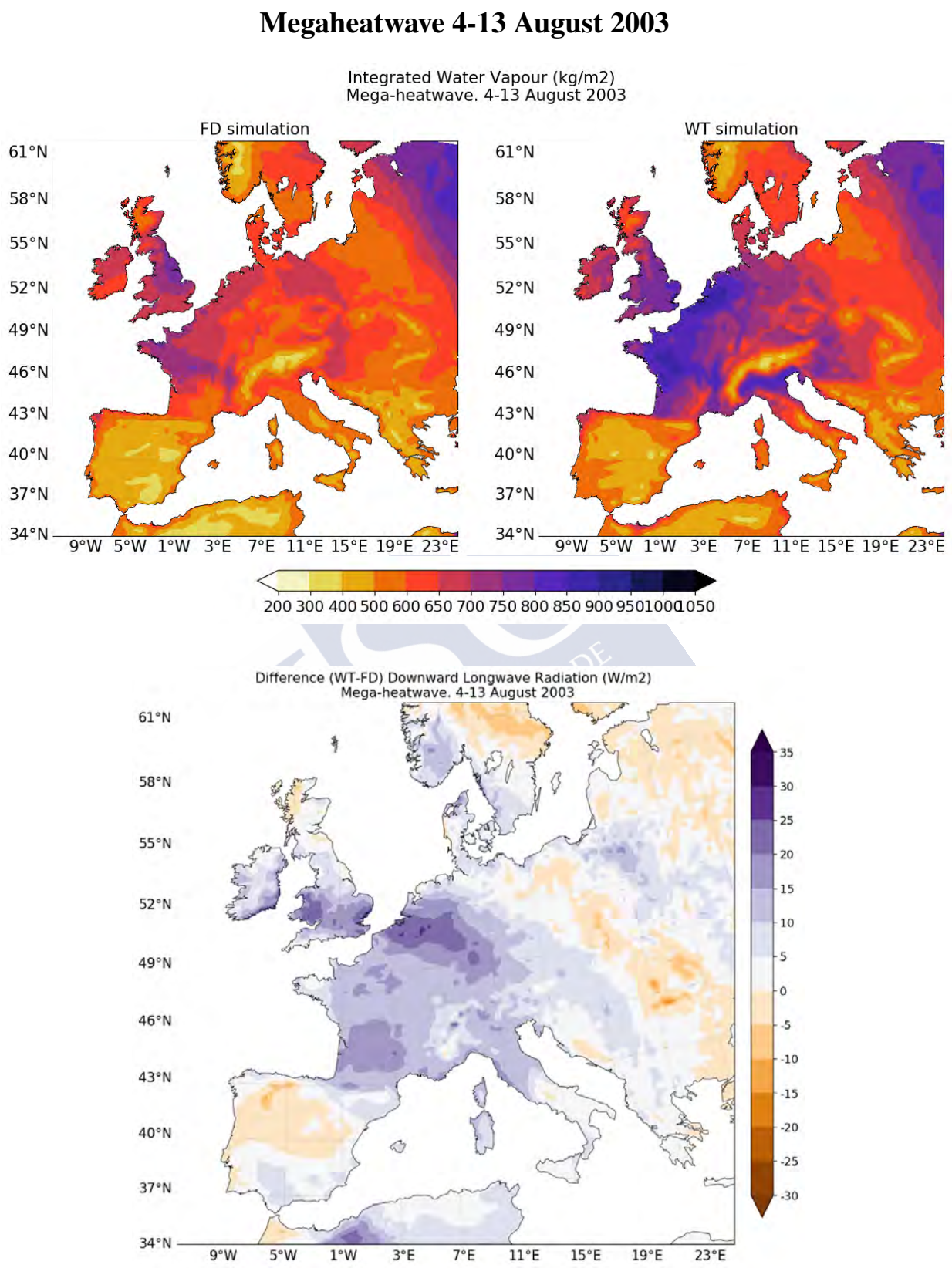

Figure 6.14: Integrated water vapour (above) downward longwave radiation difference between the simulations with the dynamic water table and with free drainage in the soil(below). Both computed for the period corresponding to the heatwave of summer 2003.

We now compare the two different responses of the climatic system to the wetter soil. For this purpose, we examine the evolution of the daily temperatures and other fluxes in France during August 1996 (Figure 6.15) and August 2003 (Figure 6.16). In the titles of both figures the temperatures averaged in France for the WT simulations and FD simulations are reported. Termed respectively, Temperature-WT and Temperature-FD.
Figure 6.15 is a representative situation of a negative temperature-water vapour feedback. Daily temperatures throughout the month are lower in the WT experiment than in the FD experiment, and the same applies for the daily evolution of the temperature, which is even more different during the day. Concerning the longwave downward fluxes, this atmospheric forcing presents similar values in the WT and FD simulations day by day. Those obtained with the WT experiments tend to be slightly superior, and the same happens for the daily evolution. In those days in which the downward radiation fluxes are high in the FD simulations, the disparities between both lines of temperatures grow wider. Since the WT simulations have more soil moisture, it is immediately evident that the water vapour content is the largest of both types of experiments, in the majority of the days. This happens in August 1996, even when the differences are not very marked. We suggest that this is a representative situation of negative feedback, since the amount of water vapour content increases. Here the cooling effect of the ET fluxes is more potent than the heating effect of the downward radiation fluxes, whose values are quite similar in both situations. Thus during this month, the temperatures obtained in the WT simulations are the lowest.
On the contrary, the temperatures resulting during the summer heatwave 2003 present the opposite behaviour. At the beginning of the month, during the Megaheatwave, temperatures of the WT simulation are higher than temperatures of the FD simulation. During all these days, the amount of precipitable water in the WT simulations is surprisingly higher, and the same applies to the downward longwave radiation. This latter, especially increases on the second and third day of the month, coinciding with a steep increase of the downward radiation. This result seems somewhat counterintuitive, because, as has been said before, it is immediately evident that an enhancement of the ET fluxes should lead to lower temperatures in the WT simulations than in the FD simulations. As is the case of the longwave radiation and precipitable water shown in Figure 6.14, those two atmospheric forcings are strikingly high, suggesting strong feedback between both of them and temperature.

The present section was designed to determine the effect of the dynamic water table on temperatures. The primary outcome of this analysis is that soil moisture is a key variable in controlling the air temperatures. A wetter soil, like those in the WT simulations, gives rise to an increase of the evapotranspiration fluxes, that means an increment of the water vapour content in the troposphere. This situation leads to two possible contrasting responses of the climatic system, that may compete between each other, a probable positive or negative feedback that can cancel one another out. In summer 2003, the blocking pattern, that enhances the advection of warm air, gives rise to an increase of the downward longwave radiation that motivates an increase of the water vapour in the atmosphere and thus a consequent rise of temperatures. We believe that beyond a specific elevated temperature, radiation is more effective in heating the atmosphere than ET fluxes in cooling it.

France August 1996. Temperature-WT=14.37°C Temperature-FD= 15.11°C

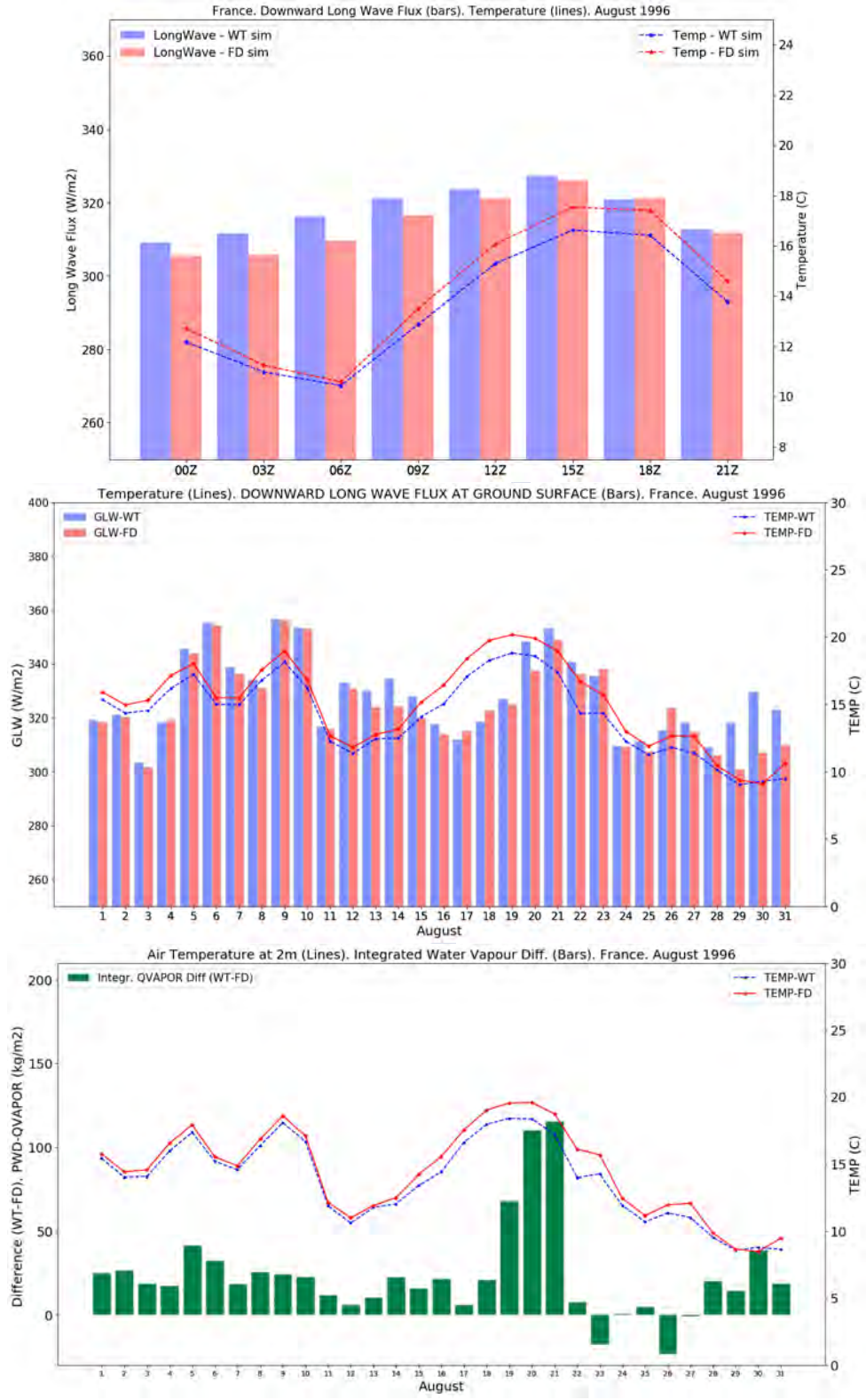

Figure 6.15: France August 1996. Daily (upper figure) and monthly (middle) evolution of the temperatures and the downward longwave radiation, monthly evolution of the temperatures together with the daily difference of the integrated water vapour (down). Colour code: WT simulations in blue, FD simulations in red and the difference (WT-FD) in green.

France August 2003. Temperature-WT=19.06°C Temperature-FD=18.94°C

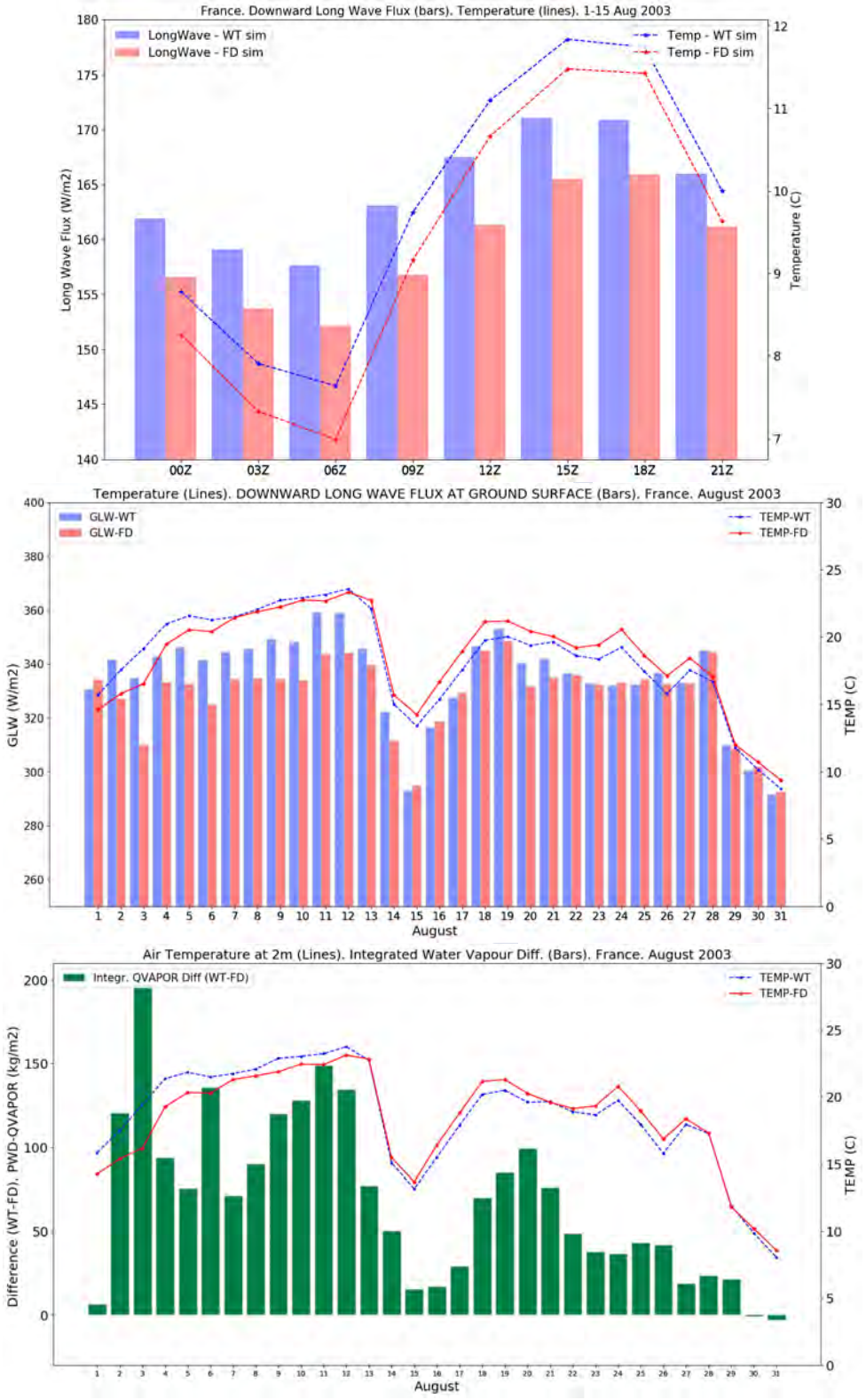

Figure 6.16: France August 2003. Daily (upper figure) and monthly (middle) evolution of the temperatures and the downward longwave radiation, monthly evolution of the temperatures together with the daily difference of the integrated water vapour (down). Colour code: WT simulations in blue, FD simulations in red and the difference (WT-FD) in green.

6.2.3 Effects on Precipitation

Forecasting precipitation accurately is a continuing concern to meteorologists. Since the atmospheric models, both global and regional, are always in continuous development, the prediction of rainfall becomes more accurate as time goes by. Precipitation presents uncertainties that make its prediction challenging. We speculate that one of the reasons leading to imprecisions on the precipitation forecast is the lack of accurate hydrology embedded in the operational weather models. We investigate the response of the European precipitation when a dynamic water table is incorporated in the regional model WRF. An increment of the precipitation is expected with wetter soils because various authors have seen this reaction before. Beljaars et al. (1996*b*) shows with an experiment with the ECMWF model when initialised with moist soil that the precipitation was higher and closer to actual observations. Almost twenty years later, Betts (2004) demonstrates that by increasing the soil moisture, more precipitation and evapotranspiration is obtained, besides showing the strong link between soil moisture and surface fluxes. Nevertheless, the land surface model employed in this research is much more complicated than a simple increase in the humidity in the soil. In our particular case, we have proven that evaporation has increased with moisture and temperatures react to the soil moistness. Their behaviour is easier to predict since they have a direct link to radiative and turbulent fluxes. Nevertheless, there is not full knowledge about how the efficiency of precipitation systems changes according to the soil.

Despite some lack of understanding, the enhancement of the evapotranspiration fluxes in the simulations with dynamic water tables makes us suppose that convective precipitation enhancement might be happening. Since precipitation is not as influenceable as other atmospheric forcings more closely linked to the soil, this enhancement might take place in those areas where the water table is close to the surface.

Figure 6.17 shows the monthly precipitation and evapotranspiration throughout the climatological series averaged over Europe. As previously seen, evapotranspiration fluxes are higher in the WT simulations (blue line) than in the FD simulations (red line). The evapotranspiration differences between both simulations become more pronounced during the months in which this variable peaks, meaning that the effect of the soil during these months is very significant.

With respect to the total and convective precipitation, the difference between the simulations with and without dynamic groundwater is much less marked than in any other atmospheric forcings. However, the rain in the WT simulations tends to be higher for both convective and total precipitation. Since the effect of the evapotranspiration fluxes on the stratiform precipitation is negligible or non-existent, the differences between both types of simulations in the total precipitation are due to the effect on the convective rain. The average is computed over the land territory of Europe, so it is representative of the overall response of the rainfall regime to a wetter soil.

Turning now to a more detailed analysis, one has to look at the evolution of the seasonal means of the convective precipitation computed for the WT and FD simulations in Iberia, France, Central and Eastern Europe in Figure 6.17. This figure more than just providing information about the influence of the soil humidity on the convective processes, also lets us have a rough idea of the annual precipitation regime in each of the case-study areas. Since Iberia and France are two regions of similar size they are directly comparable, and the same applies for Central and Eastern Europe. As we have seen in Chapter 4 and 5 in Iberia the convective precipitation peaks in springtime, and the total precipitation decreases throughout the three months of summer.

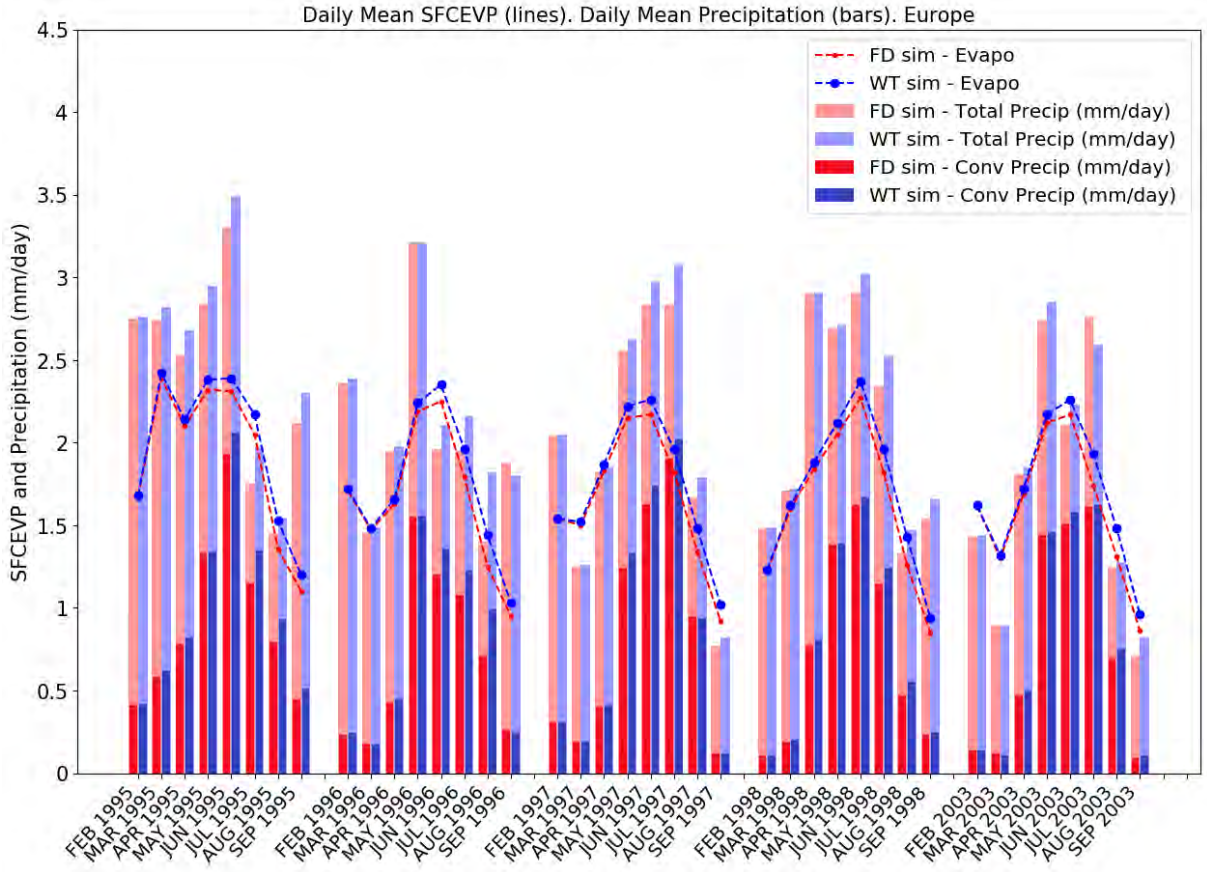

Figure 6.17: Daily mean of total and convective precipitation (bars), and evapotranspiration (lines) computed for the land area of the European continent contained in the domain of our experiment during the months of the growing season of the five years of the climatological series. The amounts in blue represent the WT experiment and the values plotted in red represent the FD experiment.

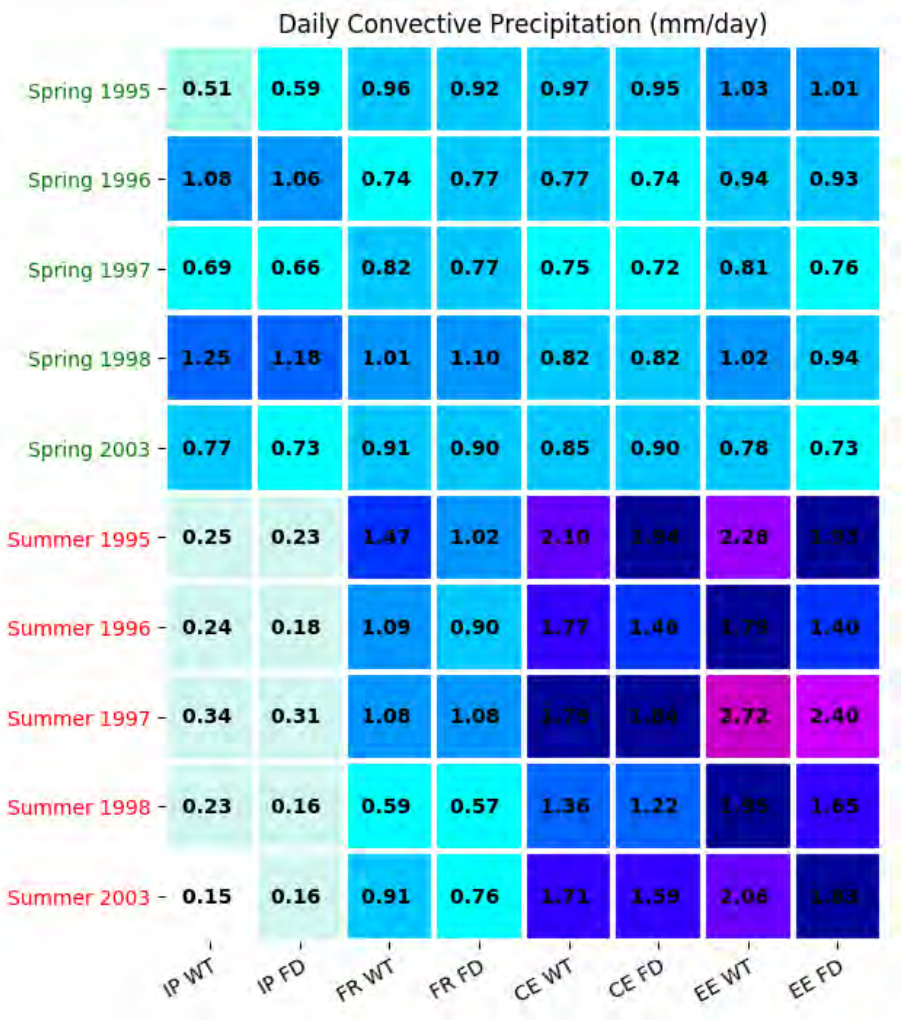

Figure 6.18: Spatial average of the seasonal convective precipitation for the Iberian Peninsula (IP), France (FR), Central Europe (CE) and Eastern Europe (EE), each of them computed with the outputs of both the WT experiment (WT) and the FD experiment (FD) over the years 1995, 1996, 1997, 1998 and 2003.

While in France, the convection is intensified in June or occasionally July, and for this reason, daily convective precipitation reaches its maximum in summer. As in the case of France and Iberia, in Central Europe, advection is an essential contributor to precipitation. But in some particular periods of the year, when moisture from advective origin diminishes, the contribution of the convective processes take specific relevance. The summertime in Central Europe presents higher values of convective precipitation than the spring, and this enhancement might be related to the local moisture recycling over the shallower areas.
The differences between the WT and FD experiments in spring are smaller than in summer when the gap is much more marked. We see that during the springtime, the behaviour of the precipitation does not show significant differences between the WT and the FD experiments since during this period, the effect of the ET fluxes has more limited significance. In contrast, the averages in summertime present more significant differences between both types of simulations. Those values are the highest for the WT simulation, confirming our initial hypotheses that a wetter soil gives rise to more convective precipitation. However, further analysis of the figure, demonstrates that the average in summer 2003 in Iberia for the WT experiment is 0.15 mm/day, which is a slightly lower amount than the 0.16 mm/day in the FD experiment.

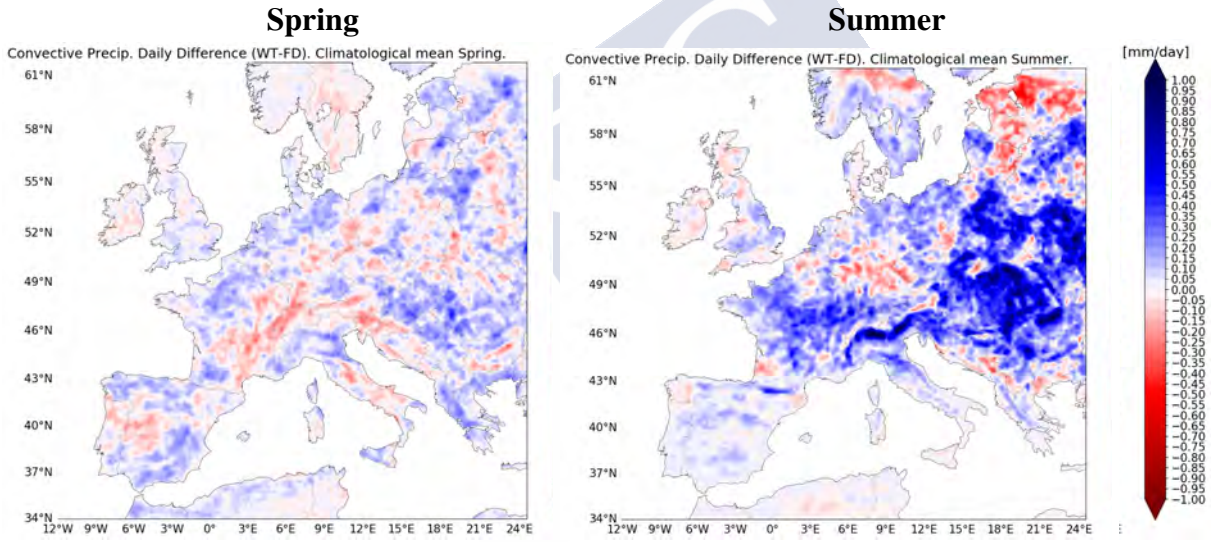

Figure 6.19: Convective precipitation daily difference between WT and FD simulations in spring (left) and summer (right), computed over the set of years 1995, 1996, 1997, 1998 and 2003.

A general picture of the differences between the climatological convective precipitation in experiments with the water table and without it is given in Figure 6.19. At first sight these figures seem a bit noisy, however general tendencies about convective precipitation can be observed.
In spring there is no clear pattern in the spatial distribution of the precipitation differences, and the differences range from -0.20 to 0.20 mm/day. Thus we conclude that the effect on the convection is negligible during this season. However, in summer, the effect of the ET fluxes on convection takes particular relevance in those areas with a shallow water table. The big blue spot located in Eastern Europe is representing a positive difference in favour of the WT experiments, showing us that in the Great Hungarian Plain, or even in the Valley of the River Po, convection increases, and these are the shallowest water table areas of our domain.
We have seen throughout this section that the effect of the water table on the convective precipitation is not as great as in other atmospheric forcings. But it should not be forgotten that

the relationship between soil and rainfall is cyclical. If the amount of precipitation increases with a wetter soil, the contribution of rain to infiltration or runoff increases too, thus improving the soil hydrology in a loop process.

Analysis with WVTM in Central Europe

As anticipated in Section 1.4.2, it is not possible to carry out a study of the summertime precipitation in Central Europe, without bearing in mind the water recycling processes, because its contribution to rainfall is very significant (Bisselink & Dolman (2008), Sodemann et al. (2009)). Nevertheless, it must be noted that the main contributor to precipitation in this area is the advective component, only in those periods when the advected moisture decreases, does the local ET take more relevance, and thus the water processes are enhanced.

To complete the study of the precipitation carried out in Section 6.2.3, here we conduct a brief analysis of the contribution of recycling in the Central Europe rainfall regime. In Figure 6.20, the evolution of the total and convective precipitation and the regional recycling ratio computed through WVTM throughout the growing season is shown. Blue lines and blue bars represent the WT experiment, while the colour red indicates the results obtained with FD simulations. Total precipitation increases from February to May, as well as convective precipitation. During May, June and July, both convective and total precipitation present their maximum values, with the highest amount in June. As summer advances convective and total precipitation decrease, and in September, the convective precipitation shows low values. The recycling ratio follows the same behaviour, increasing throughout spring and peaking in June, and then decreasing throughout summer.

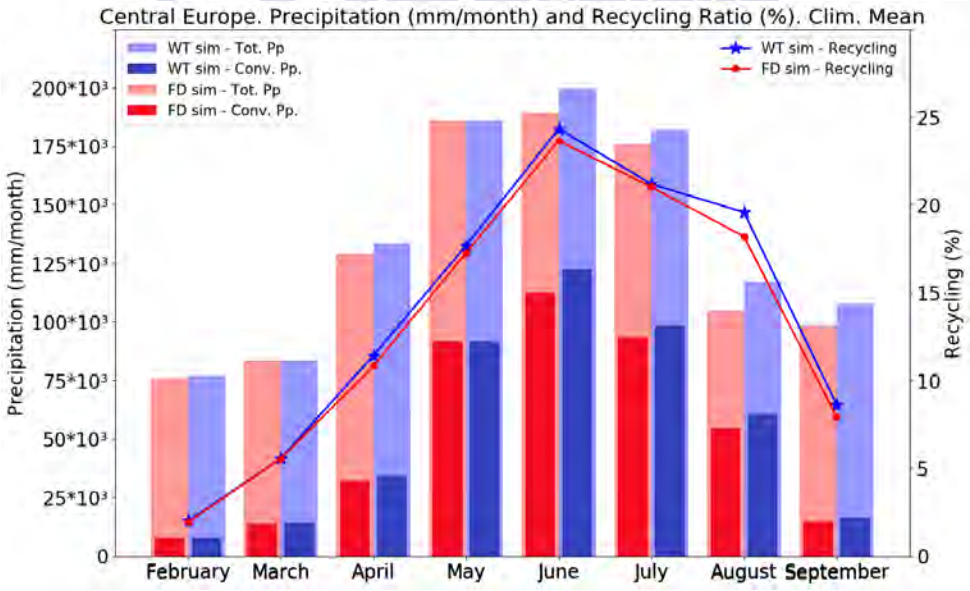

Figure 6.20: Monthly evolution of the total and convective precipitation (bars) and recycling ratio (lines) climatological mean computed over Central Europe. Colours denote: blue for WT experiment and red for FD experiment.

The high recycling ratios obtained in the CE region (see Figure 6.3) suggest that the maximum of precipitation obtained in June is directly linked to recycling processes, as the majority of the studies in that region anticipated.

Related to the differences between the WT and the FD simulations, precipitation shows prominent differences in those months when the recycling processes take more relevance, while during the rest of the growing seasons, both convective and total precipitation presents similar values. The same applies to the recycling ratios, that do not show significant differences between the WT and FD experiments. However, the rates computed with the data of the WT experiment are more significant than those values obtained in the FD simulations.

Further analysis of the recycling ratio is given in Figure 6.21, that shows the spatial pattern of the recycling ratio climatological mean together with the integrated flux for both the WT and the FD experiment. As expected, the amounts for both simulations are quite similar, with the WT simulation figures being slightly higher. The integrated flux is predominantly from westerlies, and since the orography and the flux strongly influence the recycling pattern, the maximum values of recycling are presented in the eastern region of the source tagged area.
The results of these analyses underscore the great significance of the recycling processes in the summer precipitation in Central Europe. No significant differences were found between the recycling processes in the WT and FD experiments; in spite of this, slightly higher values were observed in the simulations with the dynamic water table. Thus we suggest that water recycling is not as dependent on the water table depth as some studies presume.

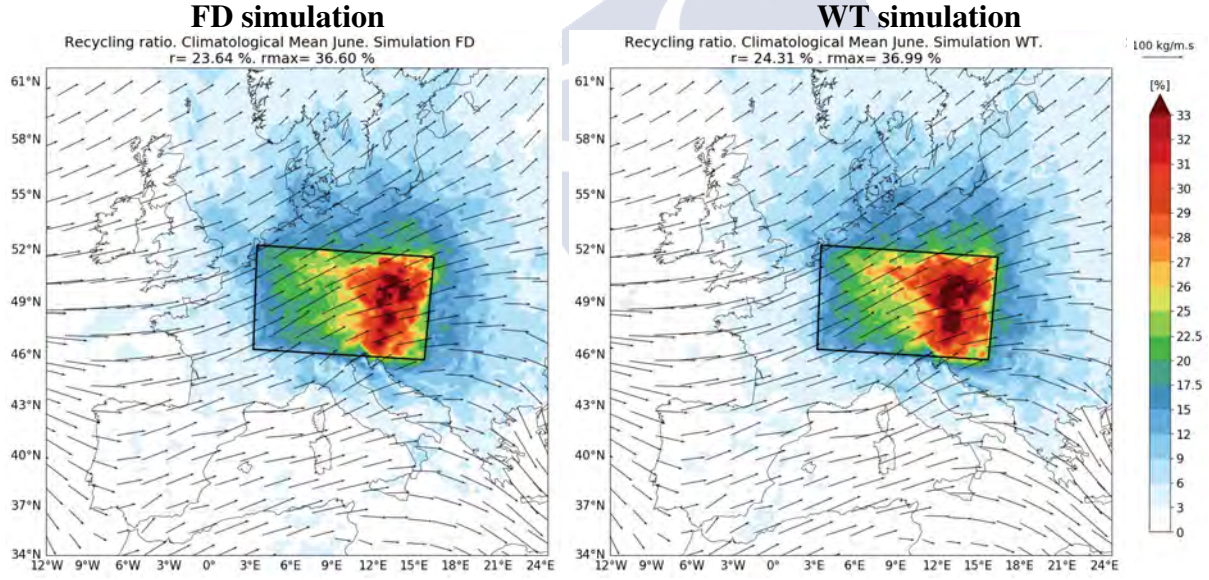

Figure 6.21: Climatological mean of the local recycling ratio computed via WVTM for the FD simulation (left) and the WT simulation (right). The source region is situated in Central Europe.

6.3 Conclusions Chapter 6

In this chapter, we have employed a fully coupled hydrology-atmospheric modelling system called LEAFHYDRO. This LSM is coupled to the well known regional meteorological model WRF-ARW. We generated two types of experiments for each of the simulated years (1995, 1996, 1997, 1998 and 2003). We refer to these two types of simulations as FD or WT experiments. The FD experiments present free drainage at the bottom of the soil column. Thus the surplus of water in the soil is no longer available since it is drained out. In the WT experiments, the land surface model incorporates a groundwater scheme, in which the water table depth is considered as soil boundary conditions, and fluctuating depending on the soil fluxes. This scheme includes the groundwater and the rivers-lakes reservoir. Hence it represents the water table very accurately. And when it is coupled to the atmospheric model WRF, the groundwater impacts on other essential components of the climatic system.

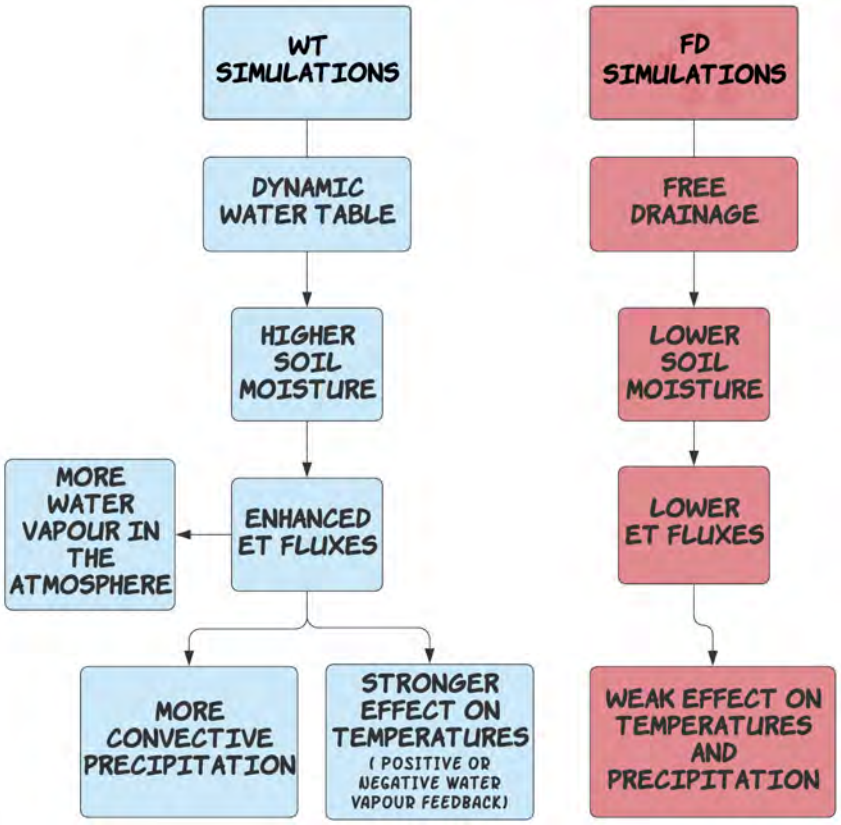

Figure 6.22: Flowchart of the influence on the climatic system of the WT and FD experiments.

The results of the research show that the groundwater induces a buffering effect on soil moisture dynamics in regions with a relatively shallow water table over long timescales. Among these regions, we highlight the plateaus or lowlands such as the North European Plain, the Massif Central located in France or the Great Hungarian Plain situated between the Carpathian Dinaric and Balkan Mountains, the coastal areas and the big river basins, like the Danube, Loire, Rhine and Elbe. As expected, the soil humidity available is most abundant in those simulations with the groundwater scheme. In summer, the soil wetness suffers a depletion, due to the combination of atmospheric demand and water scarcity.

As seen in the flowchart of Figure 6.22, in general, the values of evapotranspiration in the WT simulations are higher when compared with a simulation with LEAFHYDRO's groundwater scheme deactivated. Although we show an enhanced ET due to more soil moisture availability when considering the groundwater, the differences between WT and FD experiments are not so pronounced regarding what was expected. This is because the ET fluxes do not show a proportional increase to the adding of more soil moisture since other factors influence the ET. Hence the statement of higher soil moisture in the WT simulations presented in Figure 6.22 needs fine-tuning. On the whole, ET fluxes are better represented in the simulations with a groundwater scheme, showing slightly larger values. Only when the soil dries out completely, as happens during droughts, does the evapotranspiration become limited, because the plants are reaching their field capacity. Hence the differences between FD and WT experiments are significant because the WT simulations can maintain the ground moistened, while there is barely enough moisture in the FD simulations. In contrast, during other periods, the differences between both types of simulations are not significant, presenting differences of 10%.

A better representation of ET also implies other atmospheric forcings and processes are more realistic, such as temperatures and precipitation. The most prominent finding to emerge from the analysis of the temperatures is that contrary the expectations, two possible responses of the temperature may occur, and we refer to them as negative and positive feedback. A negative feedback is the most apparent response of the atmospheric system. It is expected to obtain the largest temperatures in the FD experiments since there is less soil humidity to moisten the troposphere, and this gives rise to atmospheric heating. This situation is the most common.
Contrary to expectations, a positive feedback could happen, and the temperatures of the WT simulations could be higher than in the FD simulations. In the WT simulations, there is more water vapour in the atmosphere. Thereupon, more longwave radiation coming from the sunlight is trapped than would naturally be, increasing the temperatures in the system. This process is a phenomenon known as the greenhouse effect. A flowchart of both possible processes is given in Figure 6.23.
One of the more significant findings to emerge from this study is that a positive feedback is happening in summer 2003. The solar energy entering the lower levels of the atmosphere in the WT simulations is lower than in the FD experiments. Whereas the integrated water vapour is much more significant in the first type of simulations. We suggest that this situation was enhanced by the presence of an atmospheric blocking pattern that remained stationary during nearly ten days, rather than due to a depletion of the soil moisture from the previous seasons.
Finally, the effect on accurate hydrology on the precipitation has shown that the convective processes seem to be enhanced in the WT simulations, giving rise to more convective rainfall and thus to more total rainfall. Also, water recycling presents slightly larger values in the WT simulations, but these last processes seem to be not affected by the water table.

By introducing a water table parameterisation, we observe that a realistic representation of the soil hydrology has a significant impact on soil moisture. Thereupon the evaporation fluxes, temperatures and precipitation are more realistic. We believe that coupled land hydrology-meteorological models are needed to improve the predictability of the atmosphere, particularly under extreme weather events, such as heatwaves.

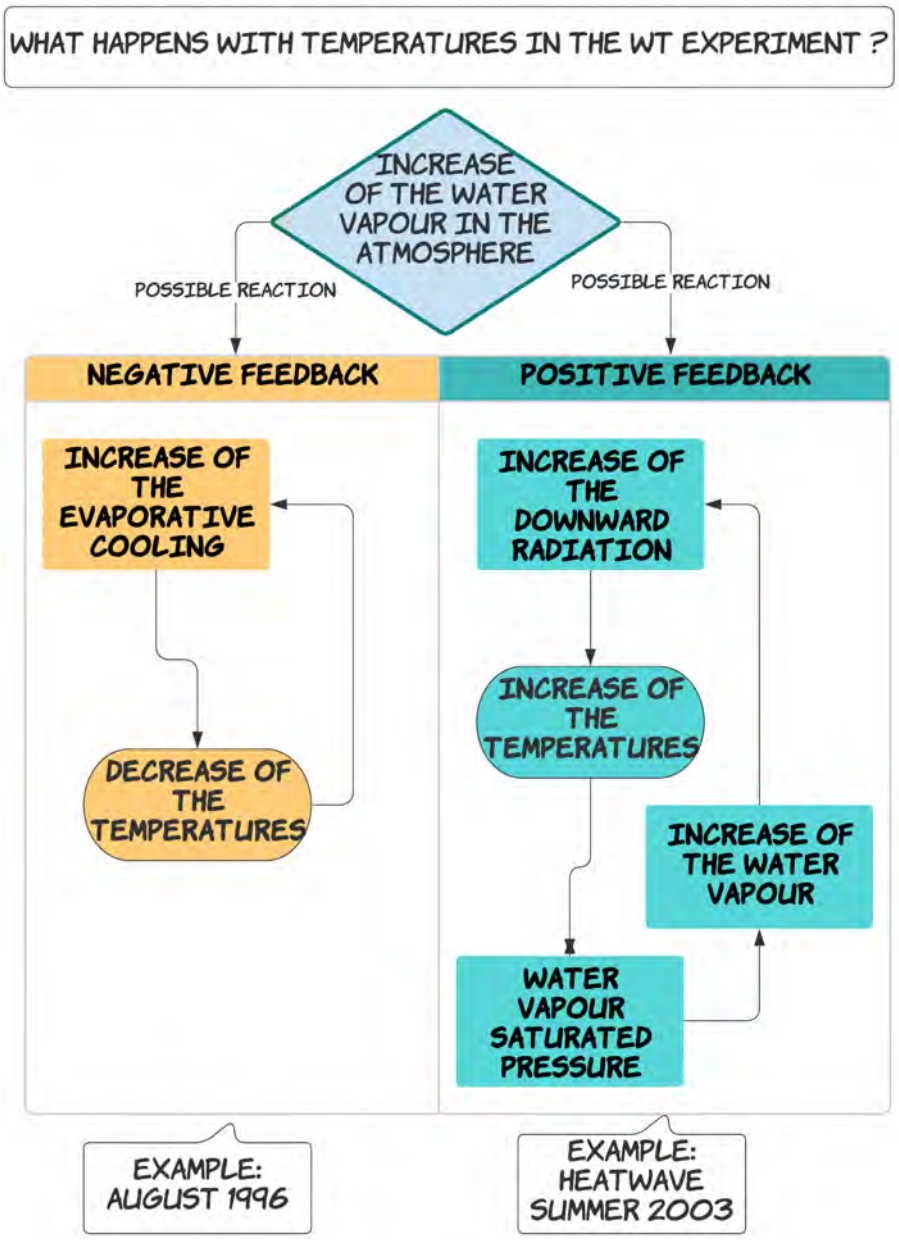

Figure 6.23: Flowchart of the temperature-water vapour feedback.

USC
UNIVERSIDADE
DE SANTIAGO
DE COMPOSTELA

Chapter 7

General Conclusions

In a context of climate change due to anthropogenic activity, the study of the atmospheric system is fundamental, especially in those areas of the globe more likely to be adversely impacted by climate variations. In this thesis, we study physical processes underlying land-atmosphere interactions, and in particular those related to evapotranspiration.
Below, we summarise the main findings and general conclusions concerning the research questions raised in this thesis.

1. The Water Vapour Tracer Method allows us to obtain a more detailed picture of the regional water cycle. We focus on investigating the spatial and temporal distribution of the moisture from local evapotranspiration. We find that it is not often uniformly mixed throughout the atmospheric column, and its concentration varies throughout the day and with the synoptic conditions. In general, it remains mostly within the boundary layer and it gets lifted into the free atmosphere by fronts or convection. Mixing ratios of ET moisture are higher close to the ground and follow a daily cycle mirroring that of the ET source. Mixed up by turbulence, ET moisture concentrations are high in the PBL during the day, especially in the late afternoon and progressively decrease overnight.

   Most of the classical recycling models assume that moisture from all origins is well-mixed in the atmospheric column. We find this not to be the general case. Thus, estimations of the recycling ratio by those classic models can present large biases. These models tend to overestimate recycling values and produce totally erroneous spatial distributions, as in the case of the Eltahir and Brass Method, or underestimate recycling ratios such as the Schär Method or the Dynamical Recycling Method. We conclude that they cannot represent precipitation recycling accurately, whereas WVTM can describe these processes more precisely. We study recycling over the Iberian Peninsula in spring, when it is more intense, and calculate the average recycling ratio to be about 13%, with values above 20% in many mountainous areas of the interior northeast.

2. To fully understand the contribution of locally evapotranspired moisture to precipitation, it should be taken into account that ET fluxes, apart from moistening the troposphere, increase convective instability. This process favours the development of convective cells and the subsequent precipitation of a convective nature. We find that about two thirds of the impact of ET fluxes on precipitation over Iberia in spring is from this indirect effect, also referred to as amplification mechanism. In contrast, the direct mechanism, where ET acts as a moisture source for rain, is responsible for the remaining third. The primary

origin of moisture for the extra precipitation induced by the effect of ET fluxes in spring is mainly non-local. ET increases moist static instability in the column, leading to stronger or extra convection development.

3. The atmosphere and the soil are tightly coupled via ET fluxes. The atmosphere changes soil conditions, but ET fluxes can also alter atmospheric conditions significantly. We employ a land surface model coupled to a meteorological model, to explore some examples of this strong coupling over Europe. The novelty of our investigation is that we employ a land surface model that includes a dynamic water table for a more accurate representation of the soil hydrology, whereby soil moisture availability is higher in areas with a shallow water table.

   We find that evapotranspiration fluxes are slightly more significant where there is more humidity in the soil, as seen in the WT simulations. This increment is not directly proportional to soil wetness; instead it is mostly related to whether ET fluxes are energy limited (no difference) or water limited (large difference). Over Europe as a whole, only in exceptional circumstances, such as extreme and prolonged droughts when most of the land becomes water limited, can significant widespread differences between WT simulations and FD simulations, be observed. In the WT experiments, precipitation is in general enhanced in its convective contribution, which is highly influenced by amplification and recycling processes. Even so, differences in precipitation amounts are not very large between simulations with and without groundwater.

   However, the response of temperatures to a more realistic soil hydrology is not straightforward. In most situations, an increment of the soil wetness causes a decrease in atmospheric temperatures. In general, when ET fluxes are enhanced, a cooling follows, and not only locally where soil moisture differences occur, but regionally. In some situations, as in the 2003 summer heatwave, the effect is the opposite, and temperatures increase with ET fluxes. This positive feedback arises due to an increment of the water vapour saturated pressure in the atmosphere; this increases the downward longwave radiation, thus inducing a 2m temperature rise. In extreme heat conditions, the greenhouse effect of a moister boundary layer during the night overruns the cooling effect of ET fluxes on the very surface in daylight hours.

A better understanding of land-atmosphere feedbacks can improve the model's representation of the land surface and help weather agencies and other governmental services to provide more accurate forecasts, and what is even more important, is to anticipate extreme or dangerous events, and mitigate their impact on human health, the environment, and the economy.

USC
UNIVERSIDADE
DE SANTIAGO
DE COMPOSTELA

USC
UNIVERSIDADE
DE SANTIAGO
DE COMPOSTELA

Summary Extended Version in Galician

Capítulo 1: Introdución e Estado da Arte

Hoxe en día, o presente e o futuro do clima mundial é un tema moi preocupante, desafortunadamente, o tema da mudanza climática está fortemente politizado. A clase política actual está a tomar os argumentos esgrimidos pola comunidade científica, e a empregalos como instrumento político no seu propio beneficio. Por esta razón é imposíbel falar de mudanza climática sen pensar nela como un asunto moi controvertido.
Neste traballo, aceptamos como válida a teoría de que está a existir unha mudanza climática debida á grande actividade antropoxénica das últimas décadas. O motivo polo que adoptamos esta postura científica non é debido a ningunha ideoloxía política, senón ao feito de que unha maioría abrumadura da comunidade científica actual apoia e demostra que a mudanza climática que está a acontecer hoxe en día é debida á acción das persoas. Pedimos ao lector que non empregue ningún argumento dado nesta tese como arma política, ben sexa para apoiar ou desmentir a mudanza climática.
Pasamos agora a facer a descrición dalgúns dos termos e conceptos que empregamos ao longo desta tese.

Ciclo Hidrolóxico

Denomínase a Terra como "planeta azul" porque o 7% da superficie terrestre está cuberta de auga. A vida como a coñecemos non existiría sen a contribución da auga, cuxo rol no clima é tamén fundamental e ten sido obxecto de infinidade de estudos. Aínda así, hai moita marxe para a mellora do noso coñecemento sobre a súa contribución no clima. Por iso, esta tese céntrase na contribución da auga ao sistema climático. O ciclo hidrolóxico é o movemento e cambio das diferentes fases da auga terrestre, e a transmisión dela entre a atmosfera, a terra e os mares ou océanos. O 90% da auga contida na atmosfera provén dos océanos, lagos e demais fontes de auga. Nun contexto de mudanza climática, espérase unha intensificación do ciclo hidrolóxico. Dentro das diferentes contribucións a este ciclo, centrámonos nesta tese na precipitación e na evapotranspiración (ET).
A precipitación que cae sobre os continentes ten unha grande importancia dentro do ciclo hidrolóxico, e provén de humidade con distintas orixes. A precipitación de orixe advectiva é a resultante da humidade atmosférica que provén do exterior da rexión analizada. A precipitación de orixe exterior á rexión de estudo provén dos fluxos locais de vapor de agua xerados pola evapotranspiración local. Finalmente, a humidade que xa está presente na rexión de estudo tamén contribúe á precipitación. A evapotranspiración ou ET é un termo que engloba a evaporación física da superficie terrestre (E) e a transpiración biolóxica (T). A evaporación é un proceso físico polo que a auga en estado líquido ou sólido pasa a vapor atmosférico. A transpiración é o

proceso de conversión de auga líquida a vapor de auga nas follas das plantas. A pesar da grande cantidade de estudos científicos que existen acerca da contribución da ET á precipitación, hai unha grande incerteza sobre isto, o cal deixa a porta aberta para continuar a súa investigación.

Reciclaxe de Humidade

Un xeito de cuantificar a relación entre a ET e a precipitación é mediante o estudo dos procesos físicos chamados reciclaxe de precipitación ou reciclaxe de humidade. Este concepto refírese á contribución dos fluxos de ET ao réxime de precipitacións dunha rexión, e pode cuantificarse matematicamente mediante a taxa de reciclaxe. Nesta tese vaise facer un estudo detallado dos procesos de reciclaxe en diferentes rexións do continente europeo e a través de varios métodos matemáticos de cálculo da taxa de reciclaxe.

O Rol das Augas Subterráneas

As augas fréaticas ou subterráneas son o conxunto de auga contido por debaixo da superficie terrestre. Ao igual que a auga que se atopa por enriba da superficie da Terra, as augas freáticas están en continuo movemento, e interactúan coas primeiras.
A distribución xeográfica das augas subterráneas ten unha grande dependencia coa estrutura da cortiza terrestre, pero tamén con parámetros como a infiltración, evaporación, ou a precipitación. A pesar de haber numerosos estudos sobre distribución xeográfica das augas fréticas, hai unha ausencia de investigacións sobre a súa distribución vertical, xa que é moito máis difícil de compreder. Unha das características máis salientábeis das augas freáticas é o efecto coador ao que dan lugar no solo. Durante períodos húmidos, cando recibe o solo recibe un exceso de auga via a actuar como un coador, mentres que nas secas actúa como proveedor de auga á atmosfera a través dos ríos, mananciais, arroios, lagos e zonas húmidas. As augas fréaticas son un ben prezado e un recurso escaso, e son empregadas como fonte mundial de suministro de auga, como auga potable para o consumo humano, para o consumo de animais e plantas, para regar os campos e en procesos industriais.
Defínese capa freática ou nivel freático ao manto subterráneo ou superficie ondulante que se limita as zonas subterráneas nas que o solo está saturado con auga coas zonas onde non o está. A auga contida na zona saturada é transportada polo fluxo das augas subterráneas ata os oceanoes, mares e ríos. A profundidade da capa frética considérse un bó indicador do acoplamento entre a terra e atmosféra. Esta medida non é constante, varía cos anos e as estacións.
A humidade contida na zona non saturada do subsolo é definida como humidade do solo, e nas rexións nas que a profundidade do nivel freático se atopa cercana á superficie, a humidade do solo é considerada parte da capa freática. Os procesos de retroalimentación entre a humidade do solo e atmosfera xogan un papel fundamental no balance de auga enerxía terrestre, e polo tanto na evolución do clima. A humidade do solo goberna a contribución da precipitación á infiltración das augas do solo ou escorrentía. A humidade do solo controla a temperatura da superficie terrestre a través do efecto dos fluxos de calor sensíbeis e latentes. A influencia de capa freática profunda na humidade do solo non é especialmente significativa. Sen embargo, una capa frética pouco profunda impide a drenaxe da humidad do solo durante os períodos húmidos, perpetuando así o efecto da chuvia. Se temos en conta isto último e o feito de que a humidade do solo ten persistencia no tempo en comparación coas condicións atmosféricas, podemos dicir que o solo garda memoria.

Capítulo 2: Obxectivos e Estrutura da Tese

A motivación experimental desta tese é a de mellorar o noso entendimento do sistema climático, a través do estudo das interaccións terra-atmosfera. Centrámonos no rol que xoga a humidade que provén dos fluxos de evapotranspiración terrestres nas condicións atmosféricas e pescudamos sobre o impacto teñen os procesos de reciclaxe de auga nalgunhas áreas do continente europeo.

Para acadar estes obxectivos emprégase como ferramenta principal o modelo meteorolóxico rexional WRF-ARW, cuxas características principais son explicadas no Capítulo 3. Nel tamén se describen tres modelos clásicos de reciclaxe de auga e unha técnica de trazadores de humidade implementada no modelo WRF. Por último, presentamos as características principais do modelo de solos LEAFHYDRO.

No Capítulo 4 presentamos a discusión e resultados dun estudo levado a cabo co modelo WRF sobre a Península Ibérica na primavera. O obxecto desta investigación é o de comprender mellor o ciclo hidrolóxico a través do uso da ferramenta dos trazadores. Tamén se avalía a distribución espacial e temporal da humidade na troposfera e se fai unha análise dos procesos de reciclaxe na rexión de estudo.

Ao longo do Capítulo 5 lévase a cabo unha investigación conxunta dos procesos de amplificación da precipitación e os procesos de reciclaxe de humidade sobre a Península Ibérica. Para iso faise un experimento co modelo WRF durante varios anos consecutivos.

No Capítulo 6 investígase o clima do continente europeo cun modelo acoplado terra-atmosfera chamado WRF-LEAFHYDRO. Centramos o noso estudo nas interaccións da superficie terrestre coa atmosfera que ocorren a través do intercambio de agua e fluxos de calor.

No Capítulo 7 preséntanse as principais conclusións desta tese.

Capítulo 3: Metodoloxía

Hoxe en día o desenvolvemento das ciencias da atmosfera está vencellado ao avance da modelización climática e, polo tanto, da supercomputación. Canto máis se melloran os modelos matemáticos do clima, máis precisas son as predicións meteorolóxicas a curto e longo prazo. Debido á importancia destes modelos e á necesidade da súa mellora, nesta tese utilizamos como ferramenta principal un modelo meteorolóxico e un modelo de solos. O empregado é o modelo rexional WRF, cuxas iniciais significan en inglés "Predición e Investigación do Tempo". O WRF é usado frecuentemente polas axencias meteorolóxicas (entre as que destacamos MeteoGalicia, a axencia meteorolóxica rexional de Galicia) e os centros de investigación. Emprégase para predicir o estado da atmosfera a curto prazo ou ben para facer estudos do clima pasado. Facemos tres tipos de experimentos co modelo WRF, cada un destes sets de simulación emprégase nun dos capítulos de resultados e teñen características diferentes. Ímonos referir a eles cos seguintes nomes:

- WRF-IP: Trátase dun conxunto de simulacións feitas co modelo WRF sobre a Península Ibérica durante todas as primaveras comprendidas entre os anos 2001 e 2010. A súa peculiaridade é que no código do modelo WRF implementouse un método de trazadores de humidade sobre o solo da península.
- WRF-ET: Este é un conxunto de experimentos feitos co WRF durante os meses de Maio de 2001 a 2010 sobre a Península Ibérica. En cada un dos anos fanse á súa vez dez

simulacións, nas que se elimina de xeito gradual a humidade do chan ou se duplica, co cal este set abrangue un total de 100 simulacións. Aquí tamén son engadidos os trazadores no chan da Península.

- WRF-EU: Neste conxunto de simulacións o WRF acóplase ao modelo de solos LEAFHYDRO, aplicado en Europa durante os meses de Febreiro a Outubro de cinco anos diferentes (1995, 1996, 1997, 1998, 2003). Para cada ano fíxose unha simulación na que se ten en conta a capa freática, á que chamaremos "WT simulation", e unha simulación na que non se teñen en conta as interaccións da capa freática coa atmosfera e, polo tanto, hai drenaxe da auga acumulada, referirémonos a ela como "FD simulation". Empregamos tamén o método de trazadores de humidade, situando a súa rexión de etiquetado en Centro Europa.

O método de trazadores de humidade usado, ao que de aquí en diante nos referiremos como WVTM, é unha técnica Euleriana de etiquetado de humidade que foi implementado no WRF polo Profesor Doutor Gonzalo Míguez Macho, director desta tese. Esta metodoloxía permite seguir a humidade dende que se evapora nunha rexión fonte ata que precipita dentro da nosa rexión de estudo ou sae dela. Tamén permite estudar a distribución da humidade na columna atmosférica e a súa evolución temporal, así como cuantificar a contribución da evapotranspiración á precipitación nas nosas áreas de estudo. O emprego dos trazadores de humidade é actualmente a metodoloxía máis precisa para analizar os procesos de reciclaxe.

Empregamos tres métodos clásicos de cálculo de reciclaxe: un modelo numérico de reciclaxe desenvolto por Eltahir & Bras (1994) e ao que nos referiremos como EBM; un modelo analítico desenvolvido por Schär et al. (1999) e chamado SCM; e un método semi-lagranxiano ou método dinámico de reciclaxe ao que nos referimos como DRM (Dominguez et al. 2006). As tres metodoloxías baséanse no modelo desenvolto por Budyko en 1953, e nalgunhas suposicións adicionais. Unha das hipóteses na que se basean todos estes modelos, e que máis controversia vai xerar, é que a humidade está ben mesturada ao longo da columna atmosférica. Con estes métodos facemos cálculos das taxas de reciclaxe sobre as rexións de estudo, e comparámolas cos resultados obtidos co WVTM. Como dato de entrada deste modelo, empréganse os arquivos xerados das simulacións feitas co WRF.

Outra das ferramentas utilizadas é un modelo de terra-atmosfera chamado WRF-LEAFHYDRO, que xurdiu de acoplar o citado modelo meteorolóxico WRF co de solo-vexetación-hidroloxía LEAFHYDRO. Ten unha parametrización de augas freáticas que representa de xeito moi preciso a capa freática e os leitos e desembocaduras dos ríos. Con ela podemos simular o ciclo hidrolóxico completo, xa que ao incluír a parametrización de augas subterráneas, a auga do solo non desaparece e redistribúese no espazo, do mesmo xeito que ocorre na realidade. O LEAFHYDRO córrese con dúas configuracións diferentes, unha incluíndo un esquema de augas freáticas (WT simulation), e outra con drenaxe libre de auga no fin da columna do solo (FD simulation).

Todas as simulacións numéricas e cálculos descritos neste capítulo fixéronse no Centro de Supercomputación de Galicia (CESGA). Os cálculos, mapas do tempo, táboas e demais resultados xéranse empregando as linguaxes de programación Fortran e Python (versión 3), e outras ferramentas como CDO ou NCO. O texto desta tese doutoral escríbese co editor de textos LaTeX.

Capítulo 4: Estudo cun Método de Trazadores de Humidade

Os obxectivos deste capítulo son varios: avaliar a distribución vertical e horizontal da humidade contida na atmosfera, para así comprender mellor o ciclo hidrolóxico; demostrar que a hipótese de que a humidade na atmosfera está ben mesturada sofre de inexactitudes; por último, analizar as desvantaxes dos métodos clásicos de cálculo de taxas de reciclaxe.

Para acadar os nosos resultados, usamos un conxunto de simulacións feitas co modelo meteorolóxico WRF descritas anteriormente e ás que nos referimos como WRF-IP. Empregamos tamén o método dos trazadores previamente implementado.

Os nosos resultados amosan unha estrutura non uniforme da humidade evaporada do solo na Península Ibérica. O vento goberna a evolución da humidade etiquetada, por iso non é uniforme a humidade ao longo da columna atmosférica, como tampouco o é por enriba do territorio da Península. A humidade proveniente da evapotranspiración decrece en altura, ao aumentar a distancia dende o chan, así como ao aumentar a distancia dende a Península. Cando a circulación atmosférica e a cizalladura son febles, a humidade tende a permanecer sobre a rexión fonte. Mentres, cando hai unha circulación intensa, a humidade é transportada polos ventos, chegando a percorrer longas distancias, só sendo parada polas barreiras orográficas. Estas distancias poden ser maiores se a humidade está relacionada con procesos de precipitación condensada. A humidade etiquetada permanece na súa meirande parte na capa límite planetaria. Nos resultados vemos como a humidade proveniente da evapotranspiración sofre unhas variacións diarias moi definidas, estando só ben mesturada durante as horas nocturnas, dende as últimas horas da tarde, cando se produce a mestura convectiva ata a seguinte mañá, cando a humidade se incrementa de novo. Pero non está ben mesturada durante o día, xa que se produce un aumento dos fluxos de humidade saíntes, que promoven a inestabilidade atmosférica. Á vista destes resultados, suxerimos que a suposición dunha atmosfera ben mesturada non pode ser certa naquelas situacións nas que a convección non é suficientemente forte, como para mesturar a ET en toda a columna atmosférica, ou naqueles casos nos que hai moita cizalladura, pois a advección de humidade será diferente en cada nivel da atmosfera. Concluímos que a suposición de atmosfera ben mesturada non é sempre válida. Os descubrimentos feitos neste capítulo suxiren que pode existir unha relación moi estreita entre a convección e a reciclaxe.

Con respecto á evolución ao longo do día, a precipitación convectiva mostra valores maiores dende a metade do día ata comezos da tardiña, decrecendo a partir dese intre. Pola súa parte, os valores de reciclaxe son maiores durante a tarde, cando a humidade proveniente da ET é maior. En xeral, vese que canto máis convectiva é a precipitación, maiores son as taxas de reciclaxe. Mentres, en situacións de advección feble de humidade, altos fluxos de evapotranspiración ou valores altos de fluxo de humidade, obtéñense taxas de reciclaxe baixas. A reciclaxe varía espacial e temporalmente, dependendo da situación sinóptica e da rexión analizada. Na Península Ibérica, preto dun 13% da precipitación local provén da reciclaxe, mentres que só aproximadamente un 8% da auga precipitable provén de fontes locais.

Fíxose unha comparación entre o método dos trazadores e os métodos clásicos de cálculo de reciclaxe. Estes últimos presentan algunhas limitacións, a máis importante é a de considerar que a humidade está ben mesturada na columna atmosférica, ademais presentan outras desvantaxes. O SCM non considera as variacións da humidade, evapotranspiración ou precipitación dentro da rexión de estudo. O EBM considera que o fluxo de humidade que entra na rexión de estudo permanece constante ao longo de todo o período analizado, e isto non é así na realidade. Tanto o EBM como o DRM presentan variacións espaciais no patrón da reciclaxe, e isto é unha avantaxe. O DRM é moito máis realista que os outros dous métodos clásicos, xa que é capaz de

reflectir as variacións da humidade día a día, pero aínda así segue a considerar que a atmosfera está ben mesturada. A nosa comparación entre o WVTM e os métodos clásicos, amosa que o EBM tende a sobrevalorar os valores de reciclaxe na Península Ibérica, mentres que o SCM e o DRM infravalóranos. En xeral, as variacións interanuais das taxas de reciclaxe non son ben reflectidas polos modelos clásicos. Pola súa parte, a análise feita polo WVTM non precisa facer suposicións, sendo tan realista como os procesos físicos do WRF.

Capítulo 5: Estudo dos Procesos de Amplificación na Península Ibérica

Para facer unha investigación exhaustiva do impacto da humidade evapotranspirada local na precipitación rexional, a análise dos procesos de reciclaxe pode non ser suficiente. Curiosamente, isto non se debe á dependencia que sofre a taxa de reciclaxe coa forma e o tamaño da rexión de estudo, senón aos denominados na literatura científica como procesos de amplificación da precipitación, mecanismo de amplificación ou efectos indirectos dos fluxos de evapotranspiración. Este mecanismo de amplificación vén dado polo comportamento da propia evapotranspiración. O certo é que ademais de humeceder a atmosfera nos seus niveis máis baixos, a humidade proveniente da ET incrementa a inestabilidade termodinámica, favorecendo así o desenvolvemento de células convectivas que á súa vez dan lugar a máis precipitación de natureza convectiva.
Neste capítulo formulámonos a seguinte pregunta "Que ocorre co ciclo hidrolóxico se eliminamos a evapotranspiración do solo?" Eliminándoa, poderemos analizar a resposta do réxime de precipitacións, e cuantificar así a contribución dos mecanismos directos (reciclaxe) ou indirectos (amplificación) á choiva. Para responder a devandita pregunta e analizar así os procesos de amplificación, levamos a cabo un estudo sobre a Península Ibérica co modelo meteorolóxico WRF, o conxunto de simulacións empregadas aquí foi descrito anteriormente e denominado WRF-ET. A resposta do sistema atmosférico amosou un comportamento case lineal, con reducións parecidas entre a precipitación e a evapotranspiración. O decrecemento das choivas cando a ET é eliminada é moi significativo, suxerindo que a ET local ten un rol moi importante no réxime de precipitacións da Península Ibérica durante a primavera.

Os resultados de comparar a taxa de reciclaxe e o cambio relativo na precipitación amosan que nin os procesos de amplificación nin os de reciclaxe son uniformes no interior da Península. A contribución dos procesos de reciclaxe é maior nas rexións do leste e nalgunhas rexións interiores do nordeste. A reciclaxe contribúe en promedio un terzo do impacto total, mentres que a amplificación ou o mecanismo indirecto contribúen os outros dous terzos, predominando sobre a reciclaxe.
Concluímos que o efecto da ET na precipitación é maiormente indirecto, debido ao incremento da inestabilidade na columna atmosférica, que dá lugar á convección máis forte ou ao desenvolvemento dunha nova convección. Concluímos que a fonte primaria da humidade para a precipitación extra na península inducida por ET local é maiormente de orixe non local.

Capítulo 6: Estudo do Clima de Europa cun Modelo Acoplado Terra-Atmosfera

Neste capítulo faise un estudo do clima de Europa co modelo acoplado terra-atmosfera WRF-LEAFHYDRO, referíndonos ao conxunto de simulacións como WRF-EU. Preténdese identificar o rol que ten a capa freática no control da humidade do solo europeo, tendo maior

interese as rexións que teñen unha capa freática superficial ou as que teñan falta de auga no solo. Analizamos tamén a influencia do modelo acoplado nos forzamentos atmosféricos, como a temperatura e a humidade. As variacións temporais da capa freática son moito máis lentas que as que pode sufrir calquera variable da atmosfera. Por exemplo, a temperatura e a precipitación poden ter cambios significativos ao longo do día, ou mesmo ao longo dun par de horas. Sen embargo, as flutuacións diarias da humidade do solo son ínfimas e por iso practicamente despreciábeis. A pesar disto, a influencia das augas subterráneas na atmosfera a través dos fluxos de evapotranspiración vai dar lugar a variacións nos forzamentos atmosféricos. Os nosos resultados amosan que a presenza da capa freática no experimento SIM-EU conleva variacións na humidade do solo, a través dos fluxos saíntes dos capilares e da drenaxe, afectando directamente os fluxos de evapotranspiración. En escalas longas de tempo, as augas subterráneas nas WT-simulation dan lugar a un "efecto coador" na humidade do solo das rexións con capa freática pouco profunda. Entre estas rexións, destacamos as mesetas e chairas como a Gran Chaira Europea, o Macizo Central localizado en Francia ou a Gran Chaira Húngara situada entre os Cárpatos, Balcáns e os Alpes Dináricos. Tamén presentan unha capa freática superficial as zonas de costa e as concas dos grandes ríos, como o Danubio, o Rin, o Elba e o Loira.

Como cabía esperar, a humidade dispoñíbel no solo é mais abundante nas simulacións que incorporan a capa freática, que nas que non a teñen. En ambos os dous tipos de experimentos, a humidade do solo diminúe no verán, debido ao incremento da demanda atmosférica, sendo moito máis acusado este decrecemento nas FD simulation. Os valores da evapotranspiración nas WT simulation son maiores que nas FD simulation debido á maior cantidade de humidade no solo no primeiro caso. Sen embargo, as diferenzas entre os dous tipos de simulacións non son tan pronunciadas como cabería esperar. Isto é debido a que os fluxos da ET non amosan un incremento proporcional ao incremento da humidade no solo, xa que outros factores entran tamén en xogo no comportamento da ET. Só cando o solo se atopa totalmente seco, como soe acontecer nas ondas de calor ou sequías, a evapotranspiración vese moi limitada, xa que as plantas chegan á súa capacidade de campo. É entón cando as diferenzas que obtemos entre a humidade do solo das WT simulation e as FD simulation son moi acusadas. Neste caso as WT simulation poden manter o solo húmido, mentres que a penas hai humidade no solo das FD simulation. Concluímos que a pesar de que as diferenzas non son moi grandes, os fluxos da ET son representados de xeito moito máis realista nas simulacións co esquema de augas freáticas, que nas simulacións con drenaxe libre.

Con respecto ás temperaturas, os resultados que emerxen da nosa análise son, contrariamente ao esperado, dúas posíbeis respostas por parte do sistema climático: pode ocorrer unha retroalimentación positiva ou unha negativa. Unha retroalimentación negativa é a resposta esperada por parte da WT simulation. Nestas simulacións hai máis humidade no solo, e polo tanto máis auga que humedeza as capas baixas da troposfera, dando lugar a un enfriamento atmosférico. Obtívose esta resposta por parte do sistema en numerosas ocasións, sendo a máis habitual. Contrariamente ao previsto, tamén pode darse unha retroalimentación positiva no sistema das WT simulation. Neste caso, un incremento do vapor de auga na atmosfera motiva máis radiación de onda longa atrapada nas capas baixas da atmosfera, isto á súa vez dará lugar a un incremento das temperaturas. Este proceso coñécese comunmente como efecto invernadoiro. A retroalimentación positiva aparece nos nosos experimentos, en concreto no verán de 2003. Crese que durante varios días deste período, este proceso foi fornecido polo bloqueo atmosférico que orixinou unha das ondas de calor máis daniñas acontecidas en Europa nas últimas décadas. Por último, estudouse a resposta das precipitacións co modelo WRF-LEAFHYDRO. Obtívose

un incremento das choivas de orixe convectiva nas WT simulation. Tamén se analizaron os procesos de reciclaxe no interior do continente europeo, comprobando que aínda que semellan non estar moi influenciados pola mellora da hidroloxía, os valores obtidos nas WT simulation son lixeiramente superiores.

Conclúese que unha representación máis realista das augas subterráneas, a través da introdución dunha parametrización de capa freática no modelo meterolóxico, ten un impacto significativo na humidade do solo e, consecuentemente, nos fluxos de evapotranspiración e, dun xeito menor, nas precipitacións e no réxime de precipitacións.

Capítulo 7: Conclusións Xerais

A continuación, pasamos a resumir as conclusións obtidas en todos os estudos levados a cabo nesta tese.

1. O Método de Trazadores de Humidade permítenos obter unha descrición en maior detalle do cicle hidrolóxico rexional. Témonos centrado na análise da distribución espacial e temporal da humidade proveniente da evapotranspiración local. Atopamos que a humidade non está sempre uniformemente mesturada ao longo da columna atmosférica, xa que as concentracións varían ao longo do día e coa situación sinóptica. Polo xeral, a humidade permance na capa límite planetaria sendo elevada na atmosfera libre polas frontes ou pola convección. En relación ao ciclo diario, as concentracións de humidade proveniente da ET mestúranse debido á turbulencia diurna e polo tanto son maiores na capa límite planetaria durante o día, especialmente nas últimas horas da tardiña, e durante a noite estes valores decrecen.

   A meirande parte dos modelos clásicos de reciclaxe supoñen que a humidade de tódalas orixes está ben mesturada ao longo da columna atmosférica. Observamos que isto non acontence sempre, e por iso as taxas de reciclaxe obtidas con estes modelos presentan erros sistemáticos. Os modelos clásicos soen sobrevalorar as taxas de reciclaxe e dar lugar a distribuscións espacias totalmente erradas, como no caso do Método de Eltahir e Brass, ou infravalorar as taxas de reciclaxe como o fan o Método de Shär or o Método dinámico de Reciclaxe. Concluímos que os modelos clásicos non poden representar de forma precisa os procesos de reciclaxe, mentres que o Método de Trazadores de Humidade sí o fai. Estudamos a reciclaxe sobre a Península Ibérica na primavera, cando é moi intensa, e obtivemos valores promedio de taxa de reciclaxe de aproximadamente o 13%, chegando ata o 20% nas rexións montañosas do noreste peninsular.

2. Para un estudo completo da contribución da humidade localmente evapotranspirada á precipitación, debemos ter presente que os fluxos da ET, ademais de humedecer a troposfera, dan lugar a maior inestabilidade convectiva. Este último proceso favorece o desenrolo de celdas convectivas e o polo tanto de precipitación de natureza convectiva. Nas nosa investigación, vimos que dous terzos do impacto dos fluxos da ET na precipitación da Península Ibérica na primavera é correspondente ao efecto indirecto ou mecanismo de amplificación, mentres que pola contra, o mecanismo directo, no que a ET actúa como fonte de humidade á chuvia, é responsábel do terzo restante. Concluímos que a fonte primaria de humidade para a precipitación extra inducida polo efecto dos fluxos da ET na primavera é maioritariamente de orixe non local. A evapotranspiración incrementa a

inestabilidade estática da humidade na columna, dando lugar ao desenrolo de convección máis forte ou convección a maiores.

3. A atmosfera e o solo atópanse estreitamente acoplados a tráves dos fluxos da evapotranspiración. A atmosfera varía o estado do solo, pero os fluxos da ET poden modificar tamén as condicións atmosféricas de xeito significativo. Aquí empregamos un modelo de solos acoplado a un modelo meteorolóxico coa fin de analizar este forte acoplamento sobre Europa. O novedoso da nosa investigación e que empregamos un modelo de solos que inclúe unha capa freática dinámica que permite representar de xeito preciso a hidroloxía do solo. Nesta nova representación do solo a dispoñibilidade de humidade do solo é maior nas áreas con capa freática pouco profunda. Nas WT simulation viuse que os fluxos da ET son lixeiramente maiores nas rexións nas que hai máis humidade no solo. Este incremento non é directamente proporcional ao aumento de humidade no solo, se non que depende de si os fluxos da ET teñen enerxía limitada ou falta de auga.

   Só en situacións excepcionais se observan diferencias entre os fluxos da ET nas WT simulation e FD simulation. Como sería o caso de secas extremas e prolongadas durante as que a meirande parte do terreo se queda se auga. Polo xeral, a contribución convectiva á precipitación presenta melloras nos experimentos con capa freática. Aínda así, as diferencias na precipitación entre a WT simulation e a FD simulation non son moi signficativos.

   Pola súa parte, a resposta das temperaturas á unha hidroloxía máis realista non é tan sinxelo de interpretar. Na meirande parte dos casos, un incremento da humidade do solo vai dar lugar a un decrecemento das temperaturas da atmósfera. isto débese a que, polo xeral, se os fluxos da ET son maiores van dar lugar a un enfriamento rexional da atmosfera. Sen embargo, vimos unha resposta contraria en algúns casos, como pode ser na onda de calor do verán de 2003. Estase producindo un efecto de retroalimentación positiva debido ao incremento do vapor de agua na atmosfera, que a súa vez deu lugar a un incremento da radiación de onda longa entrante e polo tanto a un aumento das temperaturas a dous metros.

Un maior coñecemento dos procesos de retroalimentación terra-atmosfera pode mellorar a representación dos modelos da superficie do solo e axudar ás axencias meteorolóxicas e outros servizos gobernamentais a proveer mellores predicción meterolóxicas, e o que é máis importante, a anticipar os eventos extremos e mitigar o seu impacto na saúde das persoas, no mediambiente e na economía.

USC
UNIVERSIDADE
DE SANTIAGO
DE COMPOSTELA

List of Figures

Figure 1.1: The natural water cycle 31
Figure 1.2: Scheme of the recycling and the amplification processes 37
Figure 1.3: Representation of the simulated global water table depth 40
Figure 1.4: Summer European surface air temperature 49

Figure 3.1: Spatial configuration of the SIM-IP experiment 58
Figure 3.2: Spatial configuration of the SIM-ET experiment 60
Figure 3.3: SIM-EU simulation domain 62
Figure 3.4: WVTM moisture tagging areas in the IP and Central Europe 74
Figure 3.5: Cross section view of the land surface and the mass balance components . 80

Figure 4.1: Temporal evolution of the tracer water vapour 86
Figure 4.2: Tagged water vapour and vertical cross-section of the tracer ratio 88
Figure 4.3: Integrated total tracer, integrated condensed tracer and cross section . . . 89
Figure 4.4: Mean daily cycle tracer moisture fraction 91
Figure 4.5: Mean daily cycle of precipitation and recycling ratio 92
Figure 4.6: Daily cycle of precipitation and recycling ratio in 2002 and 2004 93
Figure 4.7: Daily variations of the recycling, convective and total precipitation 95
Figure 4.8: Local recycling ratio in the IP in May 2001, 2002 and 2003 99
Figure 4.9: Local recycling ratio in the IP in May 2004, 2005 and 2005 100
Figure 4.10: Local recycling ratio in the IP in May 2007, 2008 and 2009 101
Figure 4.11: Local recycling ratio in the IP in May 2010 and multiannual mean . . . 102
Figure 4.12: Regional recycling ratio computed via WVTM, DRM, SCM and EBM . 104
Figure 4.13: Local recycling ratio computed via EBM, DRM and WVTM 106
Figure 4.14: Daily regional recycling ratios calculated via WVTM and DRM 109
Figure 4.15: Daily local recycling ratios via WVTM and DRM 110

Figure 5.1: Accumulated precipitation mean over the Iberian Peninsula 116
Figure 5.2: IWV amd precipitation difference for 0%, 15% and 25% 118
Figure 5.3: IWV amd precipitation difference for 35%, 50% and 65% 119
Figure 5.4: IWV amd precipitation difference for 75%, 85% and 200% 120
Figure 5.5: Averaged total precipitation for all the SIM-ET simulations 121
Figure 5.6: Climatological diurnal cycle 123
Figure 5.7: Local relative change in precipitation 125

Figure 6.1: Climatological water table depth 130
Figure 6.2: WTD difference between spring and summer 131

Figure 6.3: Areas in Europe used for the computations 132
Figure 6.4: Averaged monthly WTD 133
Figure 6.5: Seasonal WTD and soil moisture 135
Figure 6.6: Monthly soil moisture and WTD evolution throughout the years 137
Figure 6.7: Enhanced evapotranspiration difference in spring and summer 138
Figure 6.8: Annual variations of the daily surface evapotranspiration 140
Figure 6.9: Climatological differences of the air temperatures 142
Figure 6.10: Average of the seasonal air temperatures 143
Figure 6.11: Differences between temperatures in the WT and FD experiments . . . 145
Figure 6.12: Surface air temperatures anomalies in summer 2003 146
Figure 6.13: IWV and downward longwave radiation. Preheatwave 148
Figure 6.14: IWV and downward longwave radiation. Megaheatwave 149
Figure 6.15: Temperatures, downward radiation and IWV. 1996 151
Figure 6.16: Temperatures, downward radiation and IWV. 2003 152
Figure 6.17: Daily precipitation and evapotranspiration 154
Figure 6.18: Seasonal convective precipitation 155
Figure 6.19: Convective precipitation difference between WT and FD simulations . . 156
Figure 6.20: Precipitation and recycling ratio in Central Europe 157
Figure 6.21: Local recycling ratio in Central Europe 158
Figure 6.22: Flowchart of the influence of the WT and FD simulations 159
Figure 6.23: Flowchart of the temperature-water vapour feedback 161

List of Tables

Table 3.1: Terminology employed in the SIM-ET simulations 61
Table 3.2: Tracer variables as seen in the WRF code 73
Table 3.3: WRF-LEAFHYDRO configurations 82

Table 4.1: interannual variability over the Iberian Peninsula 96

USC
UNIVERSIDADE
DE SANTIAGO
DE COMPOSTELA

List of Acronyms

AEMET	Agencia Estatal de Meteorología (Spanish national weather service)
BOM	Bureau Of Meteorology
ET	Evapotranspiration
FD	Free Drainage
GCM	Global Climate Model
IP	Iberian Peninsula
LSM	Land Surface Model
LEAF	Land Ecosystem-Atmosphere Feedback
NWP	Numerical Weather Prediction
NAO	North Atlantic Oscillation
PBL	Planet Boundary Layer
RCM	Regional Climate Model
SST	Sea Surface Temperature
WRF	Weather Research and Forecasting model
WT	Water Table

USC
UNIVERSIDADE
DE SANTIAGO
DE COMPOSTELA

Bibliography

Alfieri, L., Claps, P., D'Odorico, P., Laio, F. & Over, T. M. (2008), 'An analysis of the soil moisture feedback on convective and stratiform precipitation', *Journal of Hydrometeorology* **9**(2), 280–291.

Bahreini, R., Ervens, B., Middlebrook, A., Warneke, C., De Gouw, J., DeCarlo, P., Jimenez, J., Brock, C., Neuman, J., Ryerson, T. et al. (2009), 'Organic aerosol formation in urban and industrial plumes near Houston and Dallas, Texas', *Journal of Geophysical Research: Atmospheres* **114**(D7).

Barbara Joan Zeitz, M. (2016), *A Thesaurus of Women from Water to Music*, iUniverse.

Barnston, A. G. & Livezey, R. E. (1987), 'Classification, seasonality and persistence of low-frequency atmospheric circulation patterns', *Monthly weather review* **115**(6), 1083–1126.

Beck, H. E., Vergopolan, N., Pan, M., Levizzani, V., Van Dijk, A. I., Weedon, G. P., Brocca, L., Pappenberger, F., Huffman, G. J. & Wood, E. F. (2017), 'Global-scale evaluation of 22 precipitation datasets using gauge observations and hydrological modeling', *Hydrology and Earth System Sciences* **21**(12), 6201.

Beljaars, A. C., Viterbo, P., Miller, M. J. & Betts, A. K. (1996*a*), 'The anomalous rainfall over the United States during July 1993: Sensitivity to land surface parameterization and soil moisture anomalies', *Monthly Weather Review* **124**(3), 362–383.

Beljaars, A. C., Viterbo, P., Miller, M. J. & Betts, A. K. (1996*b*), 'The anomalous rainfall over the United States during July 1993: Sensitivity to land surface parameterization and soil moisture anomalies', *Monthly Weather Review* **124**(3), 362–383.

Betts, A. K. (2004), 'Understanding hydrometeorology using global models', *Bulletin of the American Meteorological Society* **85**(11), 1673–1688.

Bisselink, B. & Dolman, A. (2008), 'Precipitation recycling: Moisture sources over Europe using ERA-40 data', *Journal of Hydrometeorology* **9**(5), 1073–1083.

Bisselink, B. & Dolman, A. (2009), 'Recycling of moisture in Europe: contribution of evaporation to variability in very wet and dry years.', *Hydrology & Earth System Sciences Discussions* **6**(2).

Boone, A., Habets, F., Noilhan, J., Clark, D., Dirmeyer, P., Fox, S., Gusev, Y., Haddeland, I., Koster, R., Lohmann, D. et al. (2004), 'The Rhone-aggregation land surface scheme intercomparison project: An overview', *Journal of Climate* **17**(1), 187–208.

Bosilovich, M. G. (2002), 'On the vertical distribution of local and remote sources of water for precipitation', *Meteorology and atmospheric physics* **80**(1-4), 31–41.

Bosilovich, M. G. & Schubert, S. D. (2001), 'Precipitation recycling over the central United States diagnosed from the GEOS-1 data assimilation system', *Journal of Hydrometeorology* **2**(1), 26–35.

Bosilovich, M. G., Sud, Y. C., Schubert, S. D. & Walker, G. K. (2003), 'Numerical simulation of the large-scale North American monsoon water sources', *Journal of Geophysical Research: Atmospheres* **108**(D16).

Brioude, J., Arnold, D., Stohl, A., Cassiani, M., Morton, D., Seibert, P., Angevine, W., Evan, S., Dingwell, A., Fast, J. D. et al. (2013), 'The Lagrangian particle dispersion model FLEXPART-WRF version 3.1'.

Brubaker, K. L., Dirmeyer, P. A., Sudradjat, A., Levy, B. S. & Bernal, F. (2001), 'A 36-yr climatological description of the evaporative sources of warm-season precipitation in the Mississippi River basin', *Journal of Hydrometeorology* **2**(6), 537–557.

Brubaker, K. L., Entekhabi, D. & Eagleson, P. (1993), 'Estimation of continental precipitation recycling', *Journal of Climate* **6**(6), 1077–1089.

Budyko, M. & Drozdov, O. (1953), 'Characteristics of the moisture circulation in the atmosphere', *Izv. Akad. Nauk SSSR Ser. Geogr. Geofiz* **4**, 5–14.

Budyko, M. I., Miller, D. H. & Miller, D. H. (1974), *Climate and life*, Vol. 508, Academic press New York.

Burde, G. & Zangvil, A. (2001), 'The estimation of regional precipitation recycling. Part I: Review of recycling models', *Journal of climate* **14**(12), 2497–2508.

Cardoso, R., Soares, P., Miranda, P. & Belo-Pereira, M. (2013), 'WRF high resolution simulation of Iberian mean and extreme precipitation climate', *International Journal of Climatology* **33**(11), 2591–2608.

Castillo, A., Castelli, F. & Entekhabi, D. (2015), 'Gravitational and capillary soil moisture dynamics for distributed hydrologic models'.

Castro-Díez, Y., Pozo-Vázquez, D., Rodrigo, F. & Esteban-Parra, M. (2002), 'NAO and winter temperature variability in southern Europe', *Geophysical Research Letters* **29**(8), 1–1.

Castro, M. d., Martín-Vide, J. & Alonso, S. (2005), 'El clima de España: pasado, presente y escenarios de clima para el siglo XXI'.

Charles, C., Rind, D., Jouzel, J., Koster, R. & Fairbanks, R. (1994), 'Glacial-interglacial changes in moisture sources for Greenland: Influences on the ice core record of climate', *Science* **263**(5146), 508–511.

Chazarra, A. (2012), 'Variabilidad de los climas de Köppen en la España peninsular y Baleares en el periodo 1951-2010'.

Chen, F. & Dudhia, J. (2001*a*), 'Coupling an advanced land surface–hydrology model with the Penn State–NCAR MM5 modeling system. Part I: Model implementation and sensitivity', *Monthly weather review* **129**(4), 569–585.

Chen, F. & Dudhia, J. (2001*b*), 'Coupling an advanced land surface–hydrology model with the Penn State–NCAR MM5 modeling system. Part II: Preliminary model validation', *Monthly Weather Review* **129**(4), 587–604.

Christensen, J. H. & Christensen, O. B. (2003), 'Severe summertime flooding in Europe', *Nature* **421**(6925), 805–806.

de Graaf, I. E., Gleeson, T., van Beek, L. R., Sutanudjaja, E. H. & Bierkens, M. F. (2019), 'Environmental flow limits to global groundwater pumping', *Nature* **574**(7776), 90–94.

De Souza, K., Kituyi, E., Harvey, B., Leone, M., Murali, K. S. & Ford, J. D. (2015), 'Vulnerability to climate change in three hot spots in Africa and Asia: key issues for policy-relevant adaptation and resilience-building research'.

Decker, M. (2015), 'Development and evaluation of a new soil moisture and runoff parameterization for the CABLE LSM including subgrid-scale processes', *Journal of Advances in Modeling Earth Systems* **7**(4), 1788–1809.

Dickinson, R. E. (1986), 'Biosphere/atmosphere transfer scheme (BATS) for the NCAR community climate model', *Technical report, NCAR* .

Dirmeyer, P. A. & Brubaker, K. L. (1999), 'Contrasting evaporative moisture sources during the drought of 1988 and the flood of 1993', *Journal of Geophysical Research: Atmospheres* **104**(D16), 19383–19397.

Dirmeyer, P. A. & Brubaker, K. L. (2006), 'Evidence for trends in the Northern Hemisphere water cycle', *Geophysical research letters* **33**(14).

Dominguez, F., Kumar, P., Liang, X.-Z. & Ting, M. (2006), 'Impact of atmospheric moisture storage on precipitation recycling', *Journal of climate* **19**(8), 1513–1530.

Dominguez, F., Kumar, P. & Vivoni, E. R. (2008), 'Precipitation recycling variability and ecoclimatological stability. A study using NARR data. Part II: North American monsoon region', *Journal of Climate* **21**(20), 5187–5203.

Dominguez, F., Miguez-Macho, G. & Hu, H. (2016), 'WRF with water vapor tracers: A study of moisture sources for the North American monsoon', *Journal of Hydrometeorology* **17**(7), 1915–1927.

Drumond, A., Nieto, R. & Gimeno, L. (2011), 'Sources of moisture for China and their variations during drier and wetter conditions in 2000- 2004: a Lagrangian approach', *Climate Research* **50**(2-3), 215–225.

Drumond, A., Nieto, R., Gimeno, L. & Ambrizzi, T. (2008), 'A Lagrangian identification of major sources of moisture over Central Brazil and La Plata Basin', *Journal of Geophysical Research: Atmospheres* **113**(D14).

Druyan, L. M. & Koster, R. D. (1989), 'Sources of Sahel precipitation for simulated drought and rainy seasons', *Journal of Climate* **2**(12), 1438–1446.

Dudhia, J. (1989), 'Numerical study of convection observed during the winter monsoon experiment using a mesoscale two-dimensional model', *Journal of the atmospheric sciences* .

Durán-Quesada, A. M., Gimeno, L., Amador, J. & Nieto, R. (2010), 'Moisture sources for Central America: Identification of moisture sources using a Lagrangian analysis technique', *Journal of Geophysical Research: Atmospheres* **115**(D5).

Eltahir, E. A. (1998), 'A soil moisture–rainfall feedback mechanism: 1. Theory and observations', *Water resources research* **34**(4), 765–776.

Eltahir, E. A. & Bras, R. L. (1994), 'Precipitation recycling in the Amazon basin', *Quarterly Journal of the Royal Meteorological Society* **120**(518), 861–880.

Eltahir, E. A. & Bras, R. L. (1996), 'Precipitation recycling', *Reviews of geophysics* **34**(3), 367–378.

Esteban-Parra, M., Rodrigo, F. & Castro-Diez, Y. (1998), 'Spatial and temporal patterns of precipitation in Spain for the period 1880–1992', *International Journal of Climatology: A Journal of the Royal Meteorological Society* **18**(14), 1557–1574.

Fan, Y., Li, H. & Miguez-Macho, G. (2013), 'Global patterns of groundwater table depth', *Science* **339**(6122), 940–943.

Fan, Y. & Miguez-Macho, G. (2010), 'Potential groundwater contribution to Amazon evapotranspiration', *Hydrology and Earth System Sciences* **14**(10), 2039.

Fan, Y., Miguez-Macho, G., Weaver, C. P., Walko, R. & Robock, A. (2007), 'Incorporating water table dynamics in climate modeling: 1. Water table observations and equilibrium water table simulations', *Journal of Geophysical Research: Atmospheres* **112**(D10).

Feser, F., Rockel, B., von Storch, H., Winterfeldt, J. & Zahn, M. (2011), 'Regional climate models add value to global model data: a review and selected examples', *Bulletin of the American Meteorological Society* **92**(9), 1181–1192.

Fischer, E. M., Seneviratne, S. I., Vidale, P. L., Lüthi, D. & Schär, C. (2007), 'Soil moisture–atmosphere interactions during the 2003 European summer heatwave', *Journal of Climate* **20**(20), 5081–5099.

Fitzmaurice, J. A. (2007), A critical analysis of bulk precipitation recycling models, PhD thesis, Massachusetts Institute of Technology.

Foote, E. (1856), 'Art. xxxi.–circumstances affecting the heat of the Sun's Rays', *American Journal of Science and Arts (1820-1879)* **22**(66), 382.

García-Herrera, R., Díaz, J., Trigo, R. M., Luterbacher, J. & Fischer, E. M. (2010), 'A review of the European summer heatwave of 2003', *Critical Reviews in Environmental Science and Technology* **40**(4), 267–306.

Gestal-Souto, Martinez de la Torre, R.-E. (2010), 'The role of groundwater on the Iberian climate, precipitation regime and land-atmosphere interactions', *Revista Real Academia Galega de Ciencias (In Galician)* **29**(4), 89–198.

Gimeno, L., Drumond, A., Nieto, R., Trigo, R. M. & Stohl, A. (2010), 'On the origin of continental precipitation', *Geophysical Research Letters* **37**(13).

Gimeno, L., Nieto, R., Trigo, R. M., Vicente-Serrano, S. M. & López-Moreno, J. I. (2010), 'Where does the Iberian Peninsula moisture come from? an answer based on a Lagrangian approach', *Journal of Hydrometeorology* **11**(2), 421–436.

Gimeno, L., Stohl, A., Trigo, R. M., Dominguez, F., Yoshimura, K., Yu, L., Drumond, A., Durán-Quesada, A. M. & Nieto, R. (2012), 'Oceanic and terrestrial sources of continental precipitation', *Reviews of Geophysics* **50**(4).

Giorgi, F. & Lionello, P. (2008), 'Climate change projections for the Mediterranean region', *Global and planetary change* **63**(2-3), 90–104.

Goessling, H. & Reick, C. (2011), 'What do moisture recycling estimates tell us? Exploring the extreme case of non-evaporating continents', *Hydrology and Earth System Sciences* **15**, 3217–3235.

Gómez, B. & Miguez-Macho, G. (2017), 'The impact of wave number selection and spin-up time in spectral nudging', *Quarterly Journal of the Royal Meteorological Society* **143**(705), 1772–1786.

Gößling, H. & Reick, C. H. (2013), 'On the well-mixed assumption and numerical 2-D tracing of atmospheric moisture', *Atmospheric Chemistry and Physics* **13**, 5567–5585.

Gribovszki, Z., Szilágyi, J. & Kalicz, P. (2010), 'Diurnal fluctuations in shallow groundwater levels and streamflow rates and their interpretation–A review', *Journal of Hydrology* **385**(1-4), 371–383.

Groisman, P. Y., Knight, R. W., Easterling, D. R., Karl, T. R., Hegerl, G. C. & Razuvaev, V. N. (2005), 'Trends in intense precipitation in the climate record', *Journal of climate* **18**(9), 1326–1350.

Hagemann, S. & Stacke, T. (2015), 'Impact of the soil hydrology scheme on simulated soil moisture memory', *Climate Dynamics* **44**(7-8), 1731–1750.

Hansen, J., Ruedy, R., Sato, M., Imhoff, M., Lawrence, W., Easterling, D., Peterson, T. & Karl, T. (2001), 'A closer look at United States and global surface temperature change', *Journal of Geophysical Research: Atmospheres* **106**(D20), 23947–23963.

Hillel, D. (1998), *Environmental soil physics: Fundamentals, applications, and environmental considerations*, Elsevier.

Hoegh-Guldberg, O., Jacob, D., Taylor, M., Bindi, M., Brown, S., Camilloni, I., Diedhiou, A., Djalante, R., Ebi, K. L., Engelbrecht, F. et al. (2018), Impacts of 1.5 ºc global warming on natural and human systems, IPCC.

Hong, S.-Y. & Lim, J.-O. J. (2006), 'The WRF single-moment 6-class microphysics scheme (WSM6)', *Asia-Pacific Journal of Atmospheric Sciences* **42**(2), 129–151.

Houze, R. A. (2003), From hot towers to trmm: Joanne simpson and advances in tropical convection research, *in* 'Cloud Systems, Hurricanes, and the Tropical Rainfall Measuring Mission (TRMM)', Springer, pp. 37–47.

Hu, H. & Dominguez, F. (2015), 'Evaluation of oceanic and terrestrial sources of moisture for the north american monsoon using numerical models and precipitation stable isotopes', *Journal of Hydrometeorology* **16**(1), 19–35.

Huntington, T. G. (2006), 'Evidence for intensification of the global water cycle: review and synthesis', *Journal of Hydrology* **319**(1-4), 83–95.

Insua-Costa, D. & Miguez-Macho, G. (2018), 'A new moisture tagging capability in the Weather Research and Forecasting model: formulation, validation and application to the 2014 Great Lake-effect snowstorm', *Earth System Dynamics* **9**(1), 167.

IPCC, C. C. (2007), 'The physical science basis'.

Jacob, D. (2001), 'The role of water vapour in the atmosphere. A short overview from a climate modeller's point of view', *Physics and Chemistry of the Earth, Part A: Solid Earth and Geodesy* **26**(6-8), 523–527.

James, P., Stohl, A., Spichtinger, N., Eckhardt, S. & Forster, C. (2004), 'Climatological aspects of the extreme European rainfall of August 2002 and a trajectory method for estimating the associated evaporative source regions'.

Jiang, X., Niu, G.-Y. & Yang, Z.-L. (2009), 'Impacts of vegetation and groundwater dynamics on warm season precipitation over the Central United States', *Journal of Geophysical Research: Atmospheres* **114**(D6).

Kain, J. S. & Fritsch, J. M. (1990), 'A one-dimensional entraining/detraining plume model and its application in convective parameterization', *Journal of the Atmospheric Sciences* **47**(23), 2784–2802.

Kain, J. S. & Fritsch, J. M. (1993), Convective parameterization for mesoscale models: The Kain-Fritsch scheme, *in* 'The representation of cumulus convection in numerical models', Springer, pp. 165–170.

Keune, J. & Miralles, D. (2019), 'A precipitation recycling network to assess freshwater vulnerability: Challenging the watershed convention', *Water Resources Research* **55**(11), 9947–9961.

Knoche, H. R. & Kunstmann, H. (2013), 'Tracking atmospheric water pathways by direct evaporation tagging: A case study for West Africa', *Journal of Geophysical Research: Atmospheres* **118**(22), 12–345.

Koster, R. D., Eagleson, P. S. & Broecker, W. S. (1988), 'Tracer water transport and subgrid precipitation variation within atmospheric general circulation models'.

Koster, R. D., Jouzel, J., Suozzo, R. J. & Russell, G. L. (1992), 'Origin of July Antarctic precipitation and its influence on deuterium content: a GCM analysis', *Climate Dynamics* **7**(4), 195–203.

Koster, R., Jouzel, J., Suozzo, R., Russell, G., Broecker, W., Rind, D. & Eagleson, P. (1986), 'Global sources of local precipitation as determined by the NASA/GISS GCM', *Geophysical research letters* **13**(2), 121–124.

Lana, X. & Burgueno, A. (2000), 'Some statistical characteristics of monthly and annual pluviometric irregularity for the Spanish Mediterranean coast', *Theoretical and applied Climatology* **65**(1-2), 79–97.

Liu, M., Bárdossy, A., Li, J. & Jiang, Y. (2012), 'Physically-based modeling of topographic effects on spatial evapotranspiration and soil moisture patterns through radiation and wind'.

Manabe, S., Smagorinsky, J. & Strickler, R. F. (1965), 'Simulated climatology of a general circulation model with a hydrologic cycle', *Mon. Wea. Rev* **93**(12), 769–798.

Mariotti, A., Zeng, N., Yoon, J.-H., Artale, V., Navarra, A., Alpert, P. & Li, L. Z. (2008), 'Mediterranean water cycle changes: transition to drier 21st century conditions in observations and CMIP3 simulations', *Environmental Research Letters* **3**(4), 044001.

Martín, A., Romero, R., De Luque, A., Alonso, S., Rigo, T. & Llasat, M. (2007), 'Sensitivities of a flash flood event over Catalonia: a numerical analysis', *Monthly weather review* **135**(2), 651–669.

Martínez-de la Torre, A. & Miguez-Macho, G. (2014), 'Groundwater influence on soil moisture memory and land-atmosphere interactions in the Iberian Peninsula'.

Martínez-de la Torre, A. & Miguez-Macho, G. (2019), 'Groundwater influence on soil moisture memory and land–atmosphere fluxes in the Iberian Peninsula', *Hydrology and Earth System Sciences* **23**(12), 4909–4932.

Martinez, J. A. & Dominguez, F. (2014), 'Sources of atmospheric moisture for the La Plata River basin', *Journal of Climate* **27**(17), 6737–6753.

Martinez, J. A., Dominguez, F. & Miguez-Macho, G. (2016), 'Effects of a groundwater scheme on the simulation of soil moisture and evapotranspiration over southern South America', *Journal of Hydrometeorology* **17**(11), 2941–2957.

Maxwell, R. M. & Miller, N. L. (2005), 'Development of a coupled land surface and groundwater model', *Journal of Hydrometeorology* **6**(3), 233–247.

McDonald, J. E. (1962), 'The evaporation-precipitation fallacy', *Weather* **17**(5), 168–177.

Mercader, J., Codina, B., Sairouni, A. & Cunillera, J. (2010), 'Results of the meteorological model WRF-ARW over Catalonia, using different parameterizations of convection and cloud microphysics', *Journal of Weather and Climate of the Western Mediterranean* **7**, 75–86.

Merrill, J. T., Bleck, R. & Boudra, D. (1986), 'Techniques of Lagrangian trajectory analysis in isentropic coordinates', *Monthly Weather Review* **114**(3), 571–581.

Metcalf, M., Reid, J. K. & Cohen, M. (2004), *Fortran 95/2003 Explained*, Vol. 3, Oxford University Press Oxford.

Miguez-Macho, G. & Fan, Y. (2012), 'The role of groundwater in the Amazon water cycle: 2. Influence on seasonal soil moisture and evapotranspiration', *Journal of Geophysical Research: Atmospheres* **117**(D15).

Miguez-Macho, G., Fan, Y., Weaver, Walko, R. & Robock, A. (2007), 'Incorporating water table dynamics in climate modeling: 2. Formulation, validation, and soil moisture simulation', *Journal of Geophysical Research: Atmospheres* **112**(D13).

Miguez-Macho, G., Gómez, B., Regueiro-Sanfiz, S. & Georgescu, M. (2016), The groundwater buffering effect on heatwaves and precipitation: coupled groundwater-atmosphere simulations over Europe and North America with a WRF-LEAFHYDRO system., *in* 'EGU General Assembly Conference Abstracts', Vol. 18.

Miguez-Macho, G., Li, H. & Fan, Y. (2008), 'Simulated water table and soil moisture climatology over North America', *Bulletin of the American Meteorological Society* **89**(5), 663–672.

Miguez-Macho, G., Rios-Entenza, A. & Dominguez, F. (2013), The impact of soil moisture and evapotranspiration fluxes on the spring water cycle in the Iberian Peninsula: A study with moisture tracers in WRF, *in* 'AGU Fall Meeting Abstracts'.

Miguez-Macho, G., Stenchikov, G. L. & Robock, A. (2004), 'Spectral nudging to eliminate the effects of domain position and geometry in regional climate model simulations', *Journal of Geophysical Research: Atmospheres* **109**(D13).

Miralles, D. G., Teuling, A. J., Van Heerwaarden, C. C. & De Arellano, J. V.-G. (2014), 'Mega-heatwave temperatures due to combined soil desiccation and atmospheric heat accumulation', *Nature geoscience* **7**(5), 345–349.

Mlawer, E. J., Taubman, S. J., Brown, P. D., Iacono, M. J. & Clough, S. A. (1997), 'Radiative transfer for inhomogeneous atmospheres: RRTM, a validated correlated-k model for the longwave', *Journal of Geophysical Research: Atmospheres* **102**(D14), 16663–16682.

Monin, A. S. & Obukhov, A. M. (1954), 'Basic laws of turbulent mixing in the surface layer of the atmosphere', *Contrib. Geophys. Inst. Acad. Sci. USSR* **151**(163), e187.

Muñoz-Díaz, D. & Rodrigo, F. (2004), 'Impacts of the North Atlantic Oscillation on the probability of dry and wet winters in Spain', *Climate Research* **27**(1), 33–43.

Nieto, R., Gallego, D., Trigo, R., Ribera, P. & Gimeno, L. (2008), 'Dynamic identification of moisture sources in the Orinoco basin in equatorial South America', *Hydrological sciences journal* **53**(3), 602–617.

Nieto, R., Gimeno, L., Gallego, D. & Trigo, R. (2007), 'Contributions to the moisture budget of airmasses over Iceland', *Meteorologische Zeitschrift* **16**(1), 37–44.

Nieto, R., Gimeno, L. & Trigo, R. M. (2006), 'A Lagrangian identification of major sources of Sahel moisture', *Geophysical Research Letters* **33**(18).

Numaguti, A. (1999), 'Origin and recycling processes of precipitating water over the Eurasian continent: Experiments using an atmospheric general circulation model', *Journal of Geophysical Research: Atmospheres* **104**(D2), 1957–1972.

Orth, R. & Seneviratne, S. I. (2012), 'Analysis of soil moisture memory from observations in Europe', *Journal of Geophysical Research: Atmospheres* **117**(D15).

Pachauri, R. K., Allen, M. R., Barros, V. R., Broome, J., Cramer, W., Christ, R., Church, J. A., Clarke, L., Dahe, Q., Dasgupta, P. et al. (2014), *Climate change 2014: synthesis report. Contribution of Working Groups I, II and III to the fifth assessment report of the Intergovernmental Panel on Climate Change*, Ipcc.

Pal, J. S., Giorgi, F. & Bi, X. (2004), 'Consistency of recent European summer precipitation trends and extremes with future regional climate projections', *Geophysical Research Letters* **31**(13).

Pastor, F., Valiente, J. A. & Palau, J. L. (2019), Sea surface temperature in the Mediterranean: Trends and spatial patterns (1982–2016), *in* 'Meteorology and climatology of the Mediterranean and black seas', Springer, pp. 297–309.

Quintana-Seguí, P., Barella-Ortiz, A., Regueiro-Sanfiz, S. & Miguez-Macho, G. (2019), 'The utility of land-surface model simulations to provide drought information in a water management context using global and local forcing datasets', *Water Resources Management* pp. 1–22.

Rastigejev, Y., Park, R., Brenner, M. P. & Jacob, D. J. (2010), 'Resolving intercontinental pollution plumes in global models of atmospheric transport', *Journal of Geophysical Research: Atmospheres* **115**(D2).

Reale, O., Feudale, L. & Turato, B. (2001), 'Evaporative moisture sources during a sequence of floods in the Mediterranean region', *Geophysical research letters* **28**(10), 2085–2088.

Ríos Entenza, A. (n.d.), 'Impact of land-atmosphere fluxes on the spring precipitation regime of the Iberian Peninsula'.

Rios-Entenza, A. & Miguez-Macho, G. (2014), 'Moisture recycling and the maximum of precipitation in spring in the Iberian Peninsula', *Climate dynamics* **42**(11-12), 3207–3231.

Rios-Entenza, A., Soares, P., Trigo, R., Cardoso, R. & Miguez-Macho, G. (2014), 'Precipitation recycling in the Iberian Peninsula: spatial patterns and temporal variability', *J Geophys Res atmos. doi* **10**.

Rodriguez-Puebla, C., Encinas, A., Nieto, S. & Garmendia, J. (1998), 'Spatial and temporal patterns of annual precipitation variability over the Iberian Peninsula', *International Journal of Climatology: A Journal of the Royal Meteorological Society* **18**(3), 299–316.

Sánchez Altamirano, C. (2016), 'Estimation of the precipitation recycling ratio'.

Savenije, H. H. (1995), 'Does moisture feedback affect rainfall significantly?', *Physics and Chemistry of the Earth* **20**(5-6), 507–513.

Schär, C., Lüthi, D., Beyerle, U. & Heise, E. (1999), 'The soil–precipitation feedback: A process study with a regional climate model', *Journal of Climate* **12**(3), 722–741.

Schär, C., Vidale, P. L., Lüthi, D., Frei, C., Häberli, C., Liniger, M. A. & Appenzeller, C. (2004), 'The role of increasing temperature variability in European summer heatwaves', *Nature* **427**(6972), 332–336.

Schlesinger, W. H. & Jasechko, S. (2014), 'Transpiration in the global water cycle', *Agricultural and Forest Meteorology* **189**, 115–117.

Seneviratne, S. I., Corti, T., Davin, E. L., Hirschi, M., Jaeger, E. B., Lehner, I., Orlowsky, B. & Teuling, A. J. (2010), 'Investigating soil moisture–climate interactions in a changing climate: A review', *Earth-Science Reviews* **99**(3-4), 125–161.

Seneviratne, S. I., Lüthi, D., Litschi, M. & Schär, C. (2006), 'Land–atmosphere coupling and climate change in Europe', *Nature* **443**(7108), 205–209.

Serrano, A., Mateos, V. & Garcia, J. (1999), 'Trend analysis of monthly precipitation over the Iberian Peninsula for the period 1921–1995', *Physics and Chemistry of the Earth, Part B: Hydrology, Oceans and Atmosphere* **24**(1-2), 85–90.

Shiklomanov, I. A. & Rodda, J. C. (2004), *World water resources at the beginning of the twenty-first century*, Cambridge University Press.

Simpson, J. & Riehl, H. (1964), 'Cloud structure and distributions over the tropical pacific ocean', *Atmospheric science technical paper; no. 63* .

Skamarock, W. C. & Klemp, J. B. (2008), 'A time-split nonhydrostatic atmospheric model for weather research and forecasting applications', *Journal of computational physics* **227**(7), 3465–3485.

Skamarock, W. C., Klemp, J. B., Dudhia, J., Gill, D. O., Barker, D. M., Wang, W. & Powers, J. G. (2005), A description of the advanced research WRF version 2, Technical report, National Center For Atmospheric Research Boulder Co Mesoscale and Microscale . . . .

Soares, P. M., Cardoso, R. M., Ferreira, J. J. & Miranda, P. M. (2015), 'Climate change and the Portuguese precipitation: ENSEMBLES regional climate models results', *Climate dynamics* **45**(7-8), 1771–1787.

Sodemann, H., Wernli, H. & Schwierz, C. (2009), 'Sources of water vapour contributing to the Elbe flood in August 2002—A tagging study in a mesoscale model', *Quarterly Journal of the Royal Meteorological Society: A journal of the atmospheric sciences, applied meteorology and physical oceanography* **135**(638), 205–223.

Stohl, A., Cooper, O., Damoah, R., Fehsenfeld, F., Forster, C., Hsie, E.-Y., Hübler, G., Parrish, D. & Trainer, M. (2004), 'Forecasting for a Lagrangian aircraft campaign'.

Stohl, A., Hittenberger, M. & Wotawa, G. (1998), 'Validation of the Lagrangian particle dispersion model FLEXPART against large-scale tracer experiment data', *Atmospheric Environment* **32**(24), 4245–4264.

Stohl, A. & James, P. (2004), 'A lagrangian analysis of the atmospheric branch of the global water cycle. Part I: Method description, validation, and demonstration for the August 2002 flooding in central europe', *Journal of Hydrometeorology* **5**(4), 656–678.

Stott, P. A., Stone, D. A. & Allen, M. R. (2004), 'Human contribution to the European heatwave of 2003', *Nature* **432**(7017), 610–614.

Tao, W.-K., Halverson, J., LeMons, M., Adler, R., Garstang, M., Houze, R., Pielke, R. & Woodley, W. (2003), The research of dr. joanne simpson: Fifty years investigating hurricanes, tropical clouds, and cloud systems, *in* 'Cloud Systems, Hurricanes, and the Tropical Rainfall Measuring Mission (TRMM)', Springer, pp. 1–16.

Trenberth, K. E. (1999), 'Atmospheric moisture recycling: Role of advection and local evaporation', *Journal of Climate* **12**(5), 1368–1381.

Trigo, R. M. & DaCamara, C. C. (2000), 'Circulation weather types and their influence on the precipitation regime in Portugal', *International Journal of Climatology: A Journal of the Royal Meteorological Society* **20**(13), 1559–1581.

Trigo, R. M., Pozo-Vázquez, D., Osborn, T. J., Castro-Díez, Y., Gámiz-Fortis, S. & Esteban-Parra, M. J. (2004), 'North Atlantic Oscillation influence on precipitation, river flow and water resources in the Iberian Peninsula', *International Journal of Climatology: A Journal of the Royal Meteorological Society* **24**(8), 925–944.

Turton, J. V. (2017), The spatial and temporal distribution of foehn winds on the Larsen C ice shelf, Antarctica, PhD thesis, University of Leeds.

Ulbrich, U., Brücher, T., Fink, A. H., Leckebusch, G. C., Krüger, A. & Pinto, J. G. (2003), 'The central European floods of August 2002: Part 1–Rainfall periods and flood development', *Weather* **58**(10), 371–377.

Van der Ent, R. J. (2014), 'A new view on the hydrological cycle over continents'.

Van der Ent, R. J., Savenije, H. H., Schaefli, B. & Steele-Dunne, S. C. (2010), 'Origin and fate of atmospheric moisture over continents', *Water Resources Research* **46**(9).

Van Der Ent, R. J. & Tuinenburg, O. A. (2017), 'The residence time of water in the atmosphere revisited', *Hydrology and Earth System Sciences* **21**(2), 779–790.

Van der Ent, R. & Savenije, H. (2011), 'Length and time scales of atmospheric moisture recycling', *Atmospheric Chemistry and Physics* **11**(5), 1853.

Vautard, R., Gobiet, A., Jacob, D., Belda, M., Colette, A., Déqué, M., Fernández, J., García-Díez, M., Goergen, K., Güttler, I. et al. (2013), 'The simulation of European heatwaves from an ensemble of regional climate models within the EURO-CORDEX project', *Climate Dynamics* **41**(9-10), 2555–2575.

Volosciuk, C., Maraun, D., Semenov, V. A., Tilinina, N., Gulev, S. K. & Latif, M. (2016), 'Rising mediterranean sea surface temperatures amplify extreme summer precipitation in central Europe', *Scientific reports* **6**(1), 1–7.

Wagner, T., Beirle, S., Grzegorski, M. & Platt, U. (2006), 'Global trends (1996–2003) of total column precipitable water observed by Global Ozone Monitoring Experiment (GOME) on ERS-2 and their relation to near-surface temperature', *Journal of Geophysical Research: Atmospheres* **111**(D12).

Walko, R. L., Band, L. E., Baron, J., Kittel, T. G., Lammers, R., Lee, T. J., Ojima, D., Pielke Sr, R. A., Taylor, C., Tague, C. et al. (2000), 'Coupled atmosphere–biophysics–hydrology models for environmental modeling', *Journal of applied meteorology* **39**(6), 931–944.

Wang, G., Dolman, A. & Alessandri, A. (2010), 'European summer climate modulated by NAO-related precipitation', *Hydrol. Earth Syst. Sci. Discuss* **7**(4), 5079–5097.

Wei, J., Knoche, H. R. & Kunstmann, H. (2015), 'Contribution of transpiration and evaporation to precipitation: An ET-Tagging study for the Poyang Lake region in Southeast China', *Journal of Geophysical Research: Atmospheres* **120**(14), 6845–6864.

Werner, M., Heimann, M. & Hoffmann, G. (2001), 'Isotopic composition and origin of polar precipitation in present and glacial climate simulations', *Tellus B: Chemical and Physical Meteorology* **53**(1), 53–71.

Yang, Z.-l. (2004), Modeling land surface processes in short-term weather and climate studies, *in* 'Observation, Theory And Modeling Of Atmospheric Variability: Selected Papers of Nanjing Institute of Meteorology Alumni in Commemoration of Professor Jijia Zhang', World Scientific, pp. 288–313.

Yoshimura, K., Oki, T., Ohte, N. & KANAE, S. (2004), 'Colored moisture analysis estimates of variations in 1998 Asian monsoon water sources', *Journal of the Meteorological Society of Japan. Ser. II* **82**(5), 1315–1329.

List of Related Scientific Publications

Articles in Peer-Reviewed Journals

- S. Regueiro-Sanfiz, A. Rios-Entenza, R. M. Cardoso, P. M. Matos Soares, J. Alejandro Martínez, G. Miguez-Macho. Submitted 2020.

  Evapotranspiration fluxes in the Iberian Peninsula water cycle: a recycling study with moisture tracers in WRF and comparison with classical analitical models.

- P. Quintana-Seguí, A. Barella-Ortiz, S. Regueiro-Sanfiz, G. Miguez-Macho. 2019.

  The Utility of Land Surface Model Simulations to Provide Drought Information in a Water Management Context Using Global and Local Forcing Datasets.

  Water Resources Management.

Selected Conference Abstracts

- S. Regueiro-Sanfiz, R. M. Cardoso, P. M. Matos Soares and G. Miguez-Macho. 2018.

  A study of recycling processes with moisture tracers embedded in the WRF model over the Iberian Peninsula. Comparison with classic recycling model.

  European Geoscience Union General Assembly 2018. Vienna, Austria.

- S. Regueiro Sanfiz, B. Gómez , and G. Miguez-Macho. 2017.

  The role of evapotranspiration fluxes in summertime precipitation in Central Europe: coupled groundwater-atmosphere simulations with the WRF-LEAFHYDRO system.

  European Geoscience Union General Assembly 2017. Vienna, Austria.

- S. Regueiro-Sanfiz, G. Miguez-Macho. 2016.

  The role of evapotranspiration in spring precipitation in the Iberian Peninsula: recycling or amplification or precipitation dynamics?

  8th EGU Leonardo Conference. Ourense, Spain.

- G. Miguez-Macho, B. Gómez, S. Regueiro-Sanfiz, and M. Georgescu. 2016.

  The groundwater buffering effect on heatwaves and precipitation: coupled groundwater-atmosphere simulations over Europe and North America with a WRF-LEAFHYDRO system.

  European Geoscience Union General Assembly 2016. Vienna (Austria)

USC
UNIVERSIDADE
DE SANTIAGO
DE COMPOSTELA